A CRITICAL REVIEW OF MEASUREMENT TECHNIQUES IN COASTAL HYDRAULICS

by

G.G. Smith
B.Sc (Eng) in Civil Engineering, Cape Town

A thesis submitted to the University of Cape Town
in partial fulfilment of the requirements for
the degree of Master of Science in Engineering

March 1990

Department of Civil Engineering
University of Cape Town

to my parents

DECLARATION

I, Geoffrey Grant Smith, hereby declare that this thesis is my own work and that it has not been submitted for a degree at any other university.

G.G. Smith
March 1990

SYNOPSIS

This thesis reviews measurement techniques in the field of coastal hydraulics. Techniques of wave measurement are studied in detail and the analysis of wave measurements is then dealt with. Particular attention is paid to the analysis of one-dimensional wave energy spectra. Two computer programs were adapted for use on a microcomputer for the analysis of these spectra by the autocorrelation and the Fast Fourier Transform techniques. Experiments were conducted to determine the effect of input parameters on the analysed spectrum; the sensitivity of the one-dimensional wave energy spectrum to the number of data points, the sampling interval, and the maximum lag number (for autocorrelation analysis), is illustrated. Guidelines and examples are included for the selection of appropriate parameters.

Current measurement is reviewed, including Eulerian, Lagrangian, remote-sensing and profiling techniques. Finally, sediment measurement is reviewed, with emphasis on tracer techniques, point sampling and sensing techniques, and nearshore profiling techniques.

Pertinent findings in this thesis are summarised as follows:

(i) Wave measurement at a single point is a well researched field; the Waverider buoy is particularly practical and effective.

(ii) Spectral analysis is a practical means of obtaining several useful wave parameters.

(iii) HF radar is effective for comprehensive current and wave measurements; it is likely to be the measurement technique of the future.

(iv) Eulerian current measurement near the sea surface is extremely problematic.

(v) Quantitative sediment tracer studies are unreliable; however useful qualitative information can be obtained.

(vi) A very effective point measurement technique uses the Streamer Trap, whereby the sediment transport rate is measured directly, and many of the common problems of sampling are overcome.

(vii) There are several effective techniques of nearshore profiling; however all are adversely affected by high surf conditions.

ACKNOWLEDGEMENTS

I would like to thank my supervisor, Professor F A Kilner, head of the Department of Civil Engineering, University of Cape Town, for his guidance during the period of this study.

My grateful thanks to Mrs V Atkinson, for typing this thesis in its entirety.

A word of thanks to Dr F A Shillington of the Department of Oceanography, for his assistance regarding the Fourier analysis of wave records.

My thanks also to various division members of the Earth, Marine and Atmospheric Science and Technology of the C.S.I.R., who furnished me with valuable information, especially Messrs A van Tonder, L W Coetzee, W Botes and A C van Wyk.

My thanks are due to the staff of the Department of Civil Engineering, for general assistance during the period of the study.

Finally, I would like to thank my housemates for their moral support.

TABLE OF CONTENTS

LIST OF TABLES

LIST OF FIGURES

NOMENCLATURE

A	Amplitude of a wave component
B	Breadth of a mobile layer of sand in the surf zone
C	Wave celerity, i.e. phase velocity; alternatively, concentration of tracer sand
d	Water depth; or the depth of a mobile sand layer
f	Wave frequency; $f = 1/T$
f_d	The Doppler frequency
f_N	Nyquist frequency
Δf	Resolution bandwidth
G_k	The raw (unsmoothed) estimate of the energy spectrum (i.e. energy density)
$G(f)$	Spectral density function defined for non-negative frequencies only
$\hat{G}_k$	The smoothed spectral estimate corresponding to the central frequency of the adjacent frequency bands averaged
h	The constant time interval between digitised samples of the wave record
$H_{1/3}$	The significant wave height
H_s	The significant wave height, same as $H_{1/3}$
H_{10}	Average height of highest 10 percent of all waves for a given time period
H_1	Average height of highest 1 percent of all waves for a given time period
H_{rms}	The root mean square wave height
H_{max}	The most probable value of the highest wave in some specific interval of time
H_{mo}	The significant wave height, calculated from the wave energy spectrum
H_b	Design breaker height

Im	The imaginary part of the Fourier coefficient, X(k)
j	The symbol of complex notation, indicating the imaginary part of a complex quantity
k	Harmonic number; or the index for the computed set of discrete frequency components of the DFT
K	Subsurface pressure response factor
L	Wavelength of ocean wave; alternatively, the number of adjacent spectral estimates that are averaged
m	Maximum lag number
n	The time sample index used in the discrete Fourier transform
N	The number of samples of the wave record being considered for spectral analysis
Q	The flow rate of sediment
r	The lag number
Re	The real part of the Fourier coefficient, X(k)
R(rh)	The estimate of the autocorrelation function at lag number r
$R(\tau)$	The autocorrelation function
S(f)	Spectral density function defined for both positive and negative frequencies (two-sided)
T	Wave period; or the length of a wave record
T_z	The zero-upcrossing period
$T_{mo,2}$	The zero-upcrossing period, calculated from the wave energy spectrum
$T_{1/3}$	The period corresponding to the significant wave (of height $H_{1/3}$)
T_c	The crest period
V	The advection rate of the sand; alternatively, current velocity
v	Number of degrees of freedom
w	Specific weight of sea water

$X(k)$	The set of Fourier coefficients obtained by the DFT, each coefficient having a real and an imaginary part
$\|X(k)\|$	Magnitude of the Fourier coefficient, $X(k)$
$x(n)$	The discrete set of water surface elevation samples from the wave record
λ	Radio wavelength
ϵ	The spectral width parameter
ρ	The bulk density of a sediment

INTRODUCTION

Coastal hydraulics is a sub-branch of hydraulics, restricted to a study of the action of water within that part of the sea extending a few kilometres from the shoreline. This thesis is concerned with measurements associated with this action of water.

The objectives of this thesis are to explore various types of measurement, in order to determine:

(i) The principle of operation of measuring instruments.
(ii) The techniques of obtaining measurements.
(iii) The methods of analysis and interpretation of measured data.

In order to evaluate various types of measurement, particular attention is given to the accuracy, and the advantages and disadvantages of techniques.

Measurement techniques which are relevant to coastal engineering are primarily dealt with; measurements relevant to offshore ocean engineering are also briefly mentioned. Emphasis is placed on coastal structures, and other coastal engineering applications; measurements in physical hydraulic models are excluded.

Since wave forces are the largest to impinge on coastal structures, a large part of this thesis focuses on waves: Chapter 1 deals with the measurement of waves, and chapter 2 covers the analysis and interpretation of wave measurements.

Currents are important to engineers for two main reasons:

(a) they cause forces on structures
(b) they cause the movement of ships, and of materials such as sediment, and pollutants.

Thus, measurements of current velocities, and of current circulation patterns, are important to coastal engineers; this is dealt with in Chapter 3.

Various types of sediment measurement assist coastal engineers in the quantification of sediment transport. This facilitates the solving of problems of sediment erosion and accretion. Thus, chapter 4 deals with the relevant sediment measurements.

CHAPTER 1 - WAVE MEASUREMENT

1.1 INTRODUCTION

The main object of measuring the fluctuating ocean surface elevation is to obtain a wave record, such as that in Figure 1.1, or the equivalent time series. These records are generally about 20 minutes long, and are often taken simultaneously with measurements for synoptic weather maps, i.e. at 00h00, 06h00, 12h00 and 18h00 G.M.T. It will be shown in Chapter 2 that, from a wave record, the wave energy spectrum can be analysed (Fig. 1.2), to yield useful information for coastal engineering.

Wave direction information is also used by coastal engineers. The direction of dominant, easily visible wave trains in the ocean can be measured in a direct fashion. Alternatively, a more detailed directional distribution of waves is to be found in the directional wave energy spectrum, which is a two-dimensional graphical plot of the occurrence of wave energy in the component frequencies and directions of ocean waves (Fig. 1.3). This is generally analysed from measured time series of three hydrodynamic properties of waves.

This chapter investigates various techniques of wave measurement. Particular attention is given to the principle of operation of wave measuring instruments, their advantages and disadvantages, their accuracy, techniques of measurement and problems encountered. In addition, some attention is paid to the interpretation of measurements, excluding the analysis of wave records, which is covered in detail in Chapter 2.

The types of wave measurement are categorized, mainly according to the location of measuring instruments in relation to the sea surface, as follows:

(i) Wave measurement with fixed surface instruments.
(ii) Wave measurement with subsurface instruments.
(iii) Wave measurement with floating surface instruments.
(iv) The measurement of wave direction.
(v) Wave measurement from above the surface.

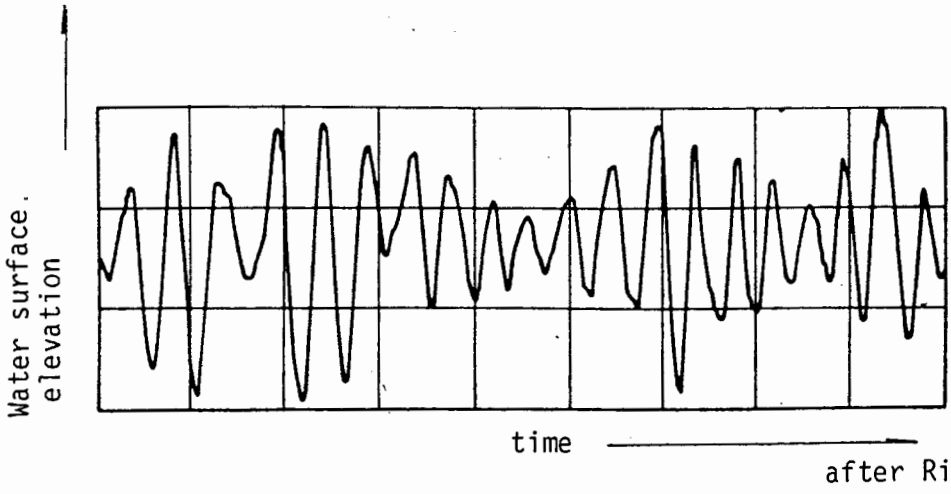

after Ribe and Russin (1974)

Figure 1.1 : A wave record.

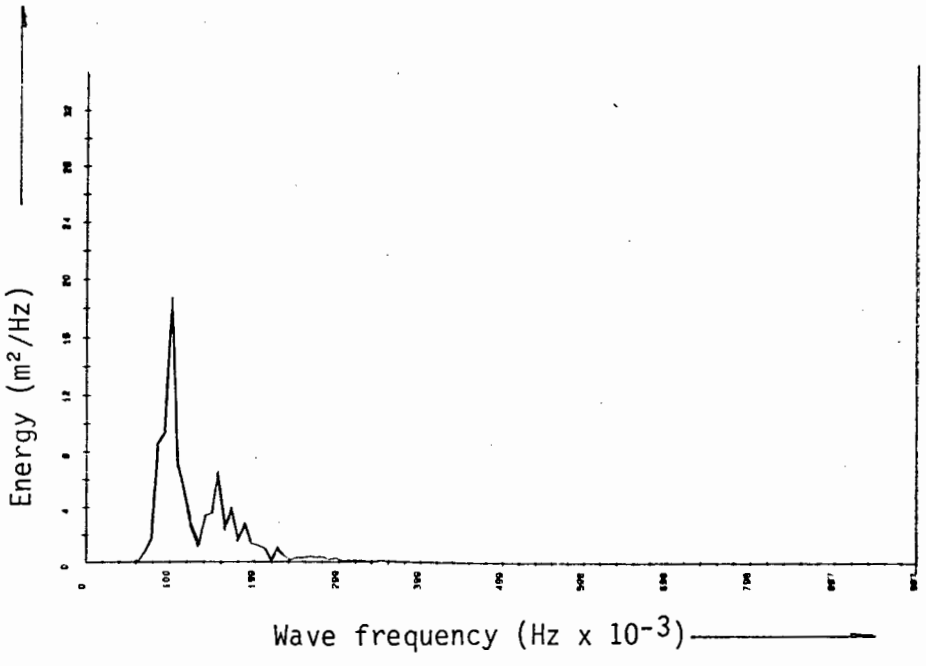

Figure 1.2 : A one-dimensional wave energy spectrum, analysed from wave measurements taken at Slangkop on the South African coast.

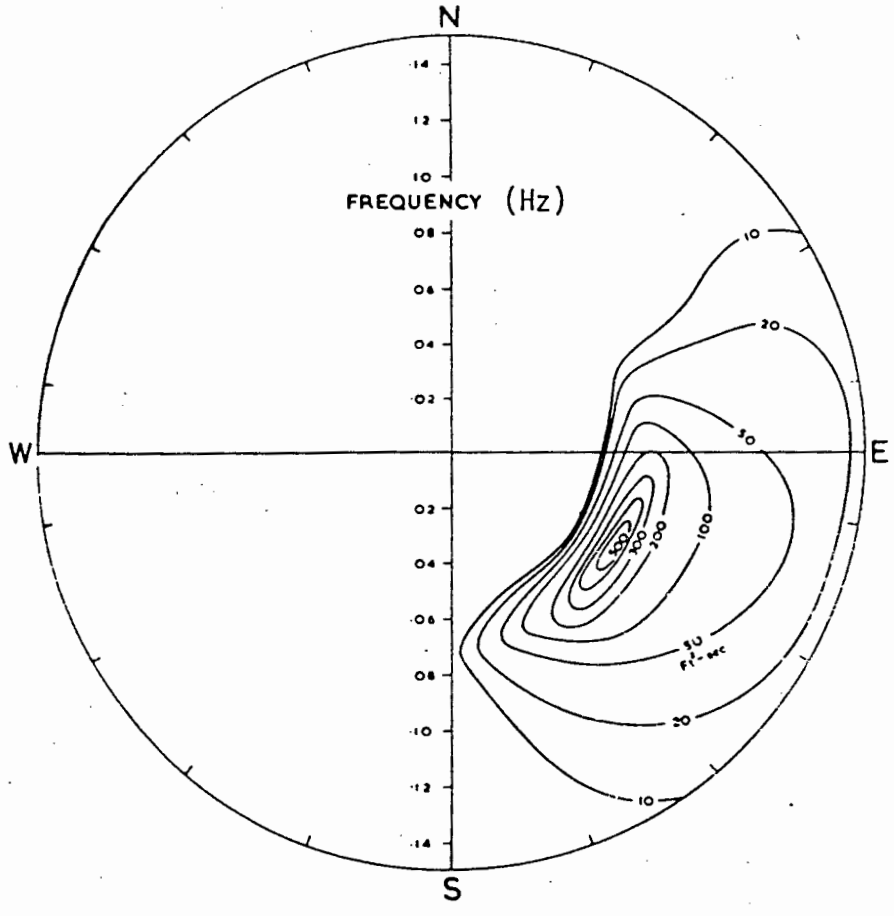

Figure 1.3 : The directional wave energy spectrum. The contours show the occurrence of wave energy.

after Cartwright (1961)

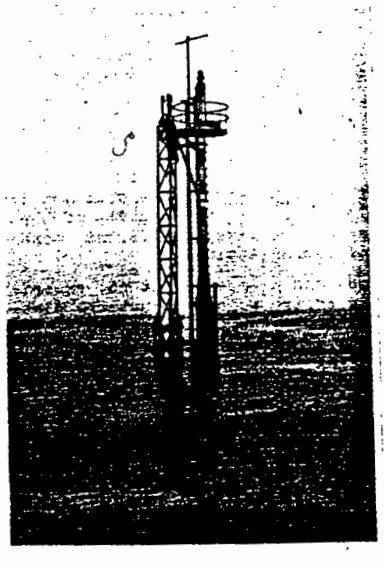

Figure 1.4 : Structure for wave measurement.

Pilon (1974)

1.2 WAVE MEASUREMENT WITH FIXED SURFACE INSTRUMENTS

This type of instrument is generally longitudinal. It is usually mounted vertically through the water surface, on stationary structures such as piers, drilling platforms, or structures specially constructed (e.g. Fig 1.4). Waves are usually measured by recording changing phenomena (such as changing electrical properties) as the water level fluctuates along the gauge length.

The types of fixed surface instruments described here include the float-type gauge, wave staffs, and an acoustic type of gauge.

1.2.1 The float-type gauge

This gauge comprises a float in a perforated tube, mounted vertically through the water surface. The float movement due to wave action is recorded by a stylus arm, through a mechanical connection. The result is a plot of water surface elevation versus time (Fig. 1.1). An example of a float-type wave gauge is the Wemelsfelder gauge (This was used in feasibility studies for the water-cooled Koeberg nuclear power station near Cape Town).

Unfortunately, this gauge is very susceptible to fouling by marine growth. Therefore, electrically operated wave staffs, which generally endure longer periods without maintenance, are more often used.

1.2.2 Wave staffs

As the water level fluctuates along the length of wave staffs, electrical properties (e.g. resistance) change. These changing electrical properties can be recorded (e.g. on magnetic tape or with a pen recorder), or transmitted to a shore station for recording, to yield a wave record.

Unfortunately, wave staffs have the following disadvantages:

(1) Corrosion of metal parts.

(2) Errors in wave measurement caused by films of water adhering to the gauge.

(3) Errors in wave measurement due to wave run-up.(i.e. water from waves washing up on the instrument). This may vary with the direction of wave approach, depending on the symmetry and the mounting arrangement of the gauge.

(4) The destruction of electronic devices by lightning.

(5) Damage from collisions with floating objects.

In spite of these disadvantages, if used carefully, wave staffs provide accuracy sufficient for most engineering purposes.

1.2.2.1 Step-resistance wave staffs

Since sea water is a good conductor, it can be used as a connecting link between electrical contact points. Thus a number of insulated resistors can be connected to uniformly spaced contact points, which are exposed to the sea on a wave staff; fluctuating water level can cause the inclusion or exclusion of these resistors in an electrical circuit. If a constant voltage is supplied to such a circuit, the output current measured will be related to the water surface elevation. Basic step-resistance gauges include a series type and a parallel type.

(a) The series-type step-resistance wave gauge:
This type of gauge is ideal for use in fresh water. Fig. 1.5 illustrates the circuit diagram of a series-type gauge used by C.E.R.C.(i.e. The Coastal Engineering Reasearch Centre of the U.S. Army Corps of Engineers). A constant d.c. voltage is supplied to the gauge. Resistors which are insulated (by epoxy resin in the C.E.R.C.

gauge), are connected in series. The junctions between resistors are connected to metal contact points exposed to the water, generally at a spacing of approximately 50 mm. As the water surface rises due to wave action, the resistors which are connected to submerged contact points are short-circuited, causing an increase in current, related to the number of contact points below the surface. (this relationship is linear if appropriate resistance values are selected). The effect is reversed when the water level falls again. The output current drives the stylus of a strip-chart pen recorder, to yield a wave record. Williams (1969, pp 16-20) presents details of the fabrication of this type of gauge.

(b) The parallel-type step-resistance wave gauge:

The parallel-type gauge is ideal for use in salt water. The circuit diagram is illustrated in Fig. 1.6. One end of each resistor is connected to a contact point, the other being connected to the gauge voltage supply (via a transformer unit). The sea water will serve as a current path between the contact points and a ground rod. As the contact points are submerged by rising water, the resistors are added, in parallel, to the circuit. The values of these resistors are selected so that the current flowing in the gauge is directly proportional to the number of contacts submerged. As in the series gauge, the current drives a motor, which moves to record wave height versus time (a wave record). Williams (1969, p 34) describes the fabrication of this type of gauge.

(c) Common problems with basic step-resistance gauges:

Errors in wave measurement can occur, due to a thin film of water clinging to the gauge after a wave has passed. This film acts as a leakage path for electric current, particularly if the values of the resistances are high compared to the water film resistance. Since the step-resistance gauge is made up of discrete contact points, the wave record it produces is a step function. The occurrence of current leakage is evident when this step function becomes smoothed.

Current leakage can be reduced by using a coating of a silicon compound, which causes water to form separate droplets instead of a film. In addition, the configuration of the contact points affects

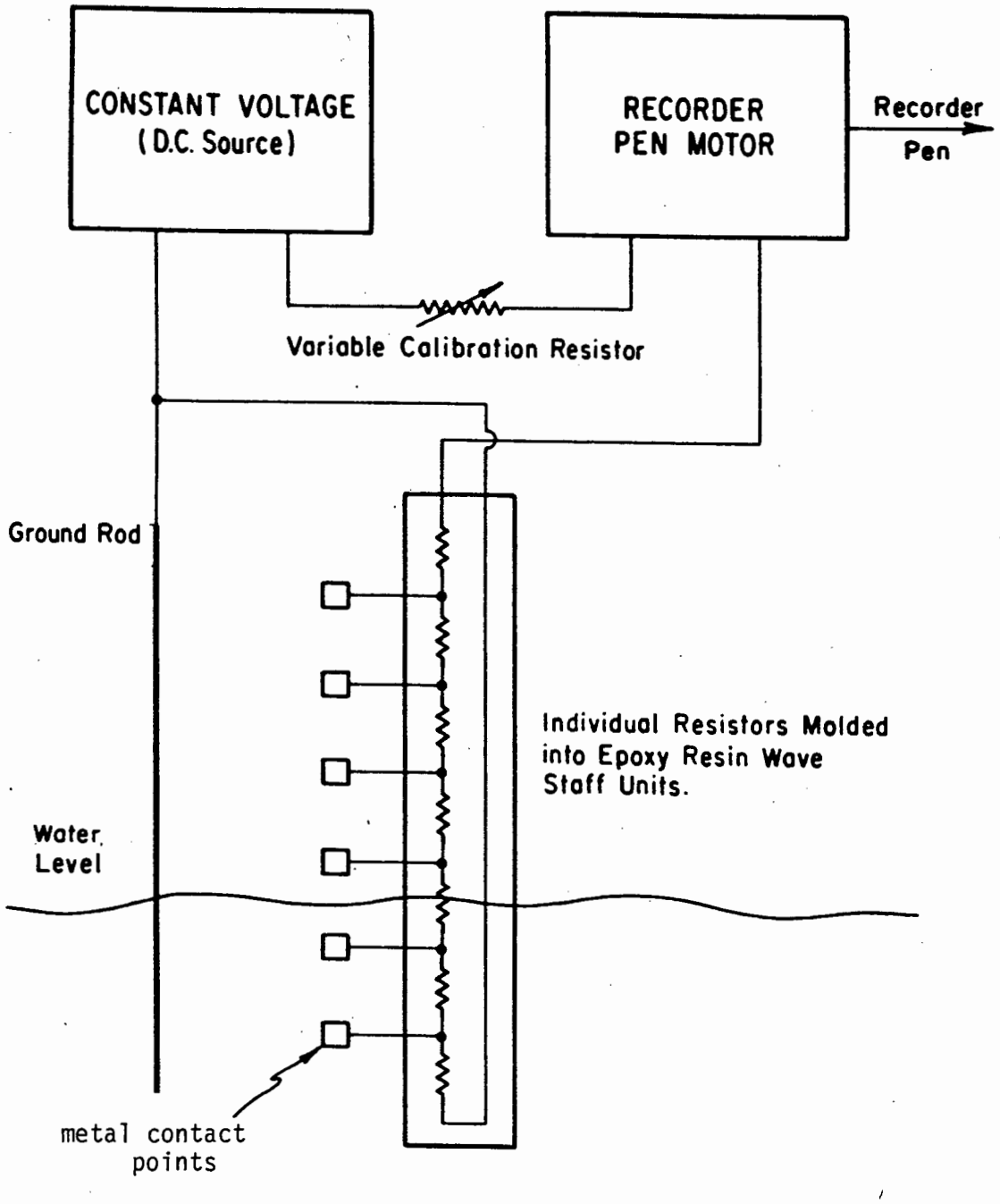

Figure 1.5 : Circuit diagram for a series-type step-resistance wave gauge.

after Williams (1969)

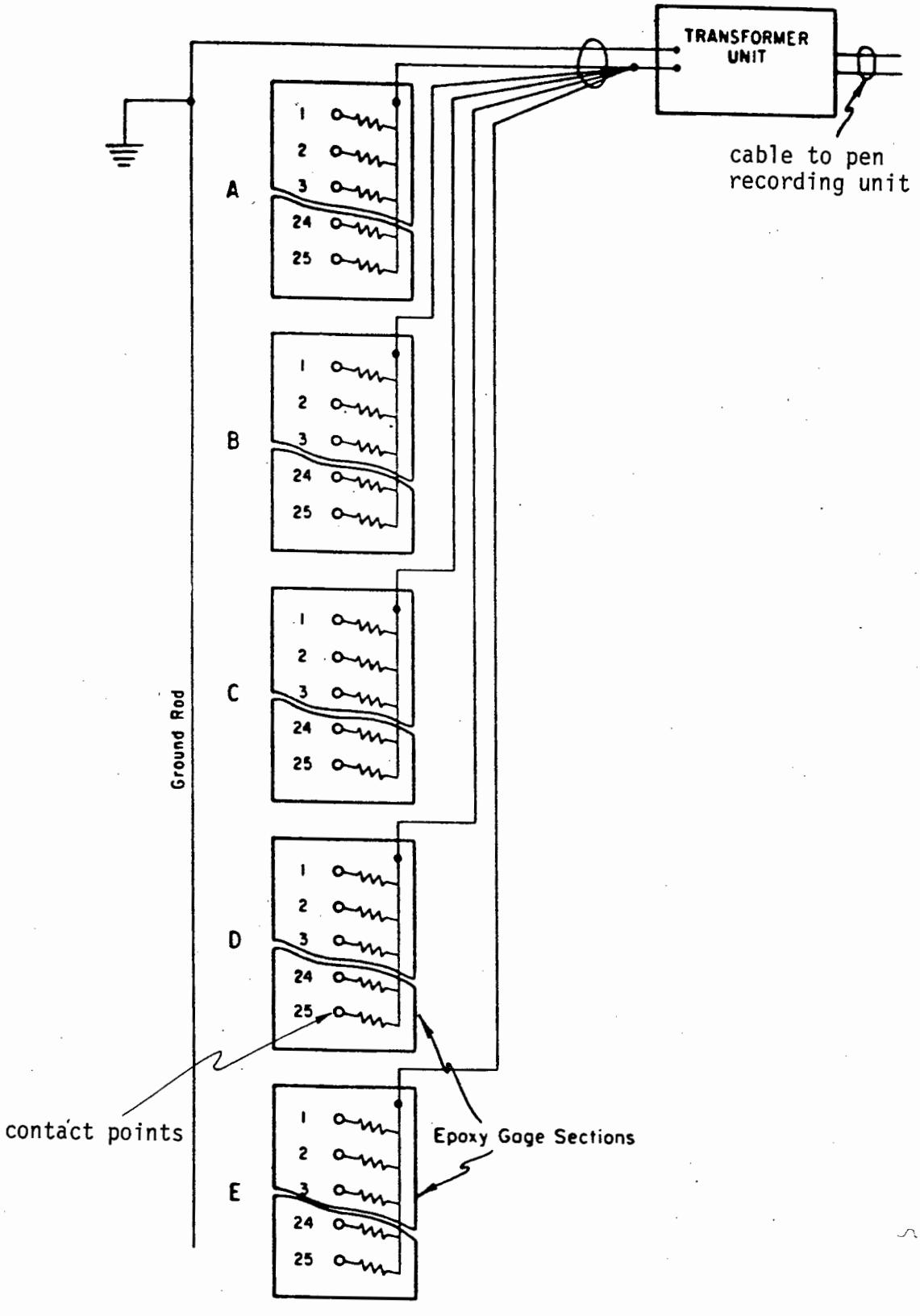

Figure 1.6 : Circuit diagram of parallel-type step-resistance wave gauge

after Williams (1969)

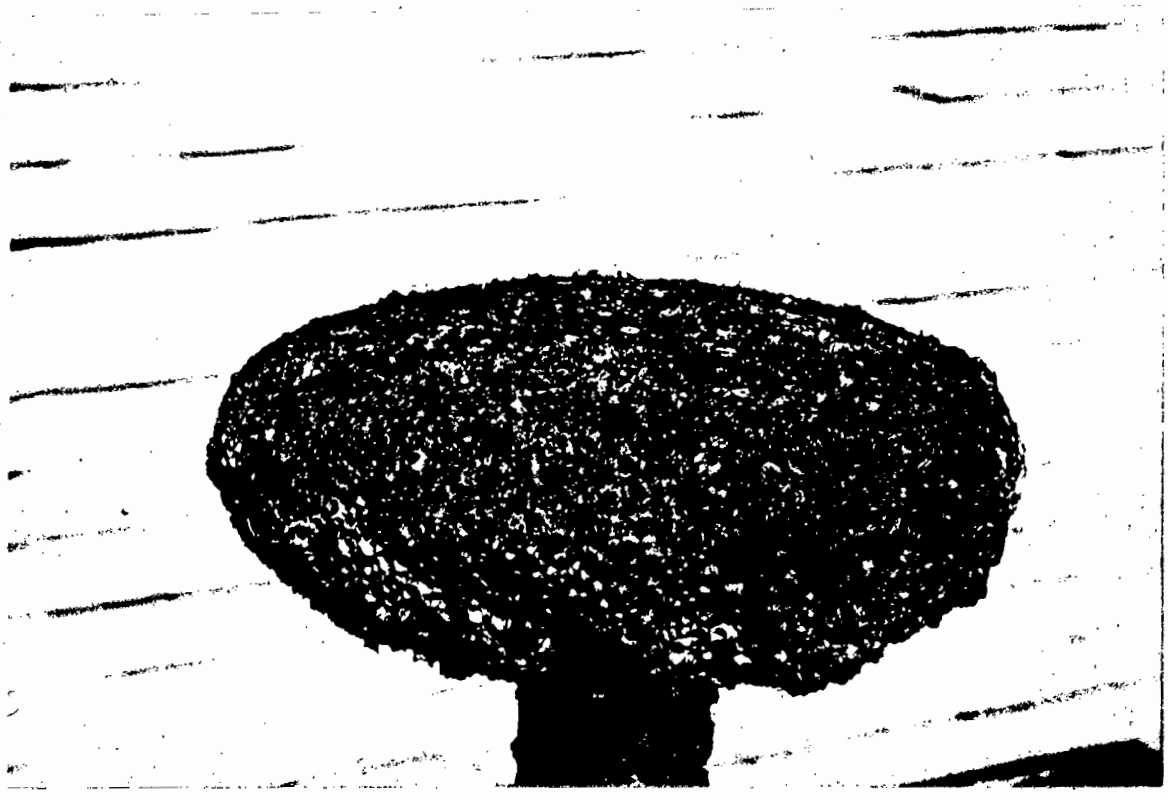

Figure 1.7 : Growth on Marine Instrumentation
(an electromagnetic current meter)

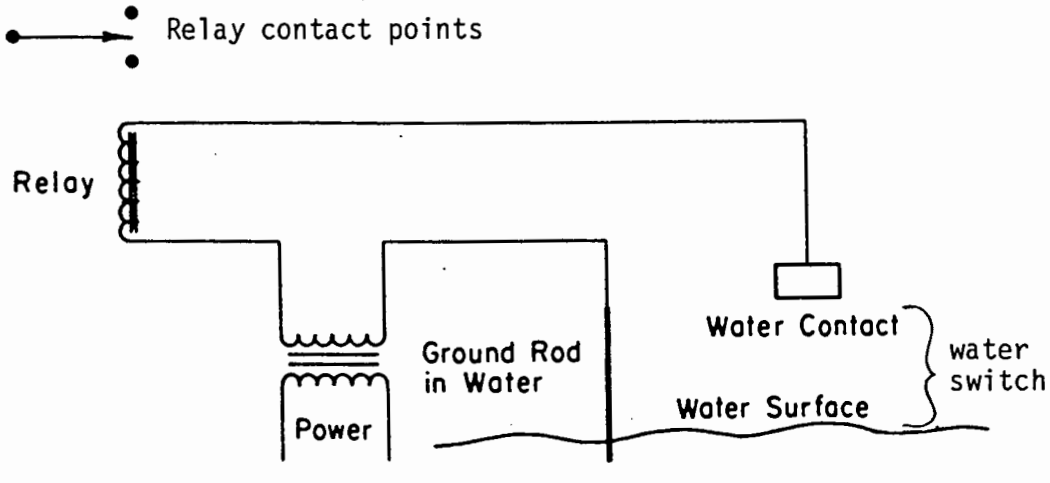

Figure 1.8 : Simplified diagram of relay-type, step-resistance gauge.

after Williams (1969)

leakage e.g. if the contact points are mounted on thin wires, the cross-section of a water film on the wires will be very small and therefore more resistant to current leakage (Verhagen, 1957, p 227).

Current leakage through films of water is aggravated by the growth of marine life on the gauge (e.g. Fig. 1.7), as this growth tends to retain moisture. Since the growth is more prominent on the lower side of the gauge, excessive wet marine growth causes exclusion of the troughs of waves in the wave record (since the bottom of the gauge is constantly wet, the gauge does not record the troughs of waves). Thus wave gauges must be periodically cleaned, and painted with anti-fouling paint.

The salinity of sea water can affect gauge accuracy. For example, in the case of the parallel-type step-resistance gauge, the sea water serves as a current path between the resistors and the ground rod; low salinity water has a high resistance, which will erroneously be included in the circuit. Therefore the gauge should not be located in regions where salinity may drop, e.g. near the mouth of an estuary.

Corrosion of the contact points occurs; therefore they must be replaced and maintained, since corroded points cause an increased resistance, which causes errors. In addition, the use of an alternating current avoids polarization, which causes corrosive electrochemical action.

(d) The relay-type step-resistance gauge:

From the above it can be seen that the occurrence of a film of water, variations in salinity, and corrosion can cause erroneous variations in resistance. This can be reduced by the use of relays (which, in this case, are electromagnetically operated switches, activated at a precise voltage). The principle of gauge operation is that water completes a circuit consisting of a power supply, a relay and a switch in series (the switch is the water itself), as illustrated in Fig. 1.8. A circuit similar to that of Fig. 1.8 exists for each water contact point spaced along the vertical length of the gauge. As the water level fluctuates, the contact points of the relay switch cause

either inclusion or exclusion of precise resistances in an adjacent recording circuit; thus the resistance recorded is proportional to the water surface elevation. Since these resistances are precise (i.e. uncontaminated by leakage, corrosion, and variations in salinity), and because the relay is activated at a precise voltage, erroneous variations in resistance are reduced.

Relay operated gauges can be designed to accomodate large changes in salinity. For example, the C.E.R.C. relay type gauge (Williams, 1969, p 45) achieves this by the use of a pilot lamp; this protects the relay from an overload (i.e. excessive electric power) in high salinity water, and lowers resistance, to ensure that it still operates, in less conductive low salinity water.

Since relays operate mechanically, they have a limited lifespan, due to the high switching rate. Therefore relays should be made easily accessible, to facilitate replacement.

(e) The stepped voltage wave gauge:

A further development of the above-mentioned gauge is the use of integrated circuit elements, instead of relays. These integrated circuit elements are switched from a high voltage state to a low voltage state, depending on whether or not there is a connection of water with the staff contact points. The voltages thus switched into the circuit are summed electronically, to represent water surface elevation (Bowler, 1974, p 579-584).

This gauge is cheaper and less complex than the relay type of gauge, and has lower current requirements. It is extremely reliable and is not adversely affected even by fairly heavy marine growths. However, it is expensive to manufacture due to a multiplicity of connections.

(f) The accuracy and performance of step-resistance gauges:

Several wave gauges measure changing electrical properties, corresponding to the fluctuating water level, in a continuous fashion (discussed below); therefore the total error in measurement incurred is the sum of all errors due to the presence of a water film, corrosion, etc. Step-resistance gauges have the advantage that by

using relays or integrated circuit elements these errors can be reduced. However, the maximum resolution capability of step-resistance gauges is limited by the spacing of electrical contact points on the staff; this is of the order of 50 mm.

1.2.2.2 Resistance wire staff gauges

Most resistance wire staff gages comprise an insulated cylinder, wound with a helix of uninsulated resistance wire. This wire must be resistant to corrosion; nichrome wire is often used. Electrical connections are made to the top of this wire and to the seawater (i.e. to ground). As the level of the sea varies with wave action, it short-circuits an amount of resistance wire proportional to the water surface elevation. Thus the resistance is linearly proportional to the water surface elevation (provided that the resistance of the wire is high compared to that of the sea water). Therefore, with a constant current, the output voltage (which is recorded) will be proportional to the submergence of the staff, i.e wave height.

A second type of resistance wire gauge has a double metal wire (stainless steel can be used) fixed vertically in the sea. The resistance between the wires varies linearly with water surface elevation. If a constant current is supplied to the gauge, the measured output voltage will be proportional to length of wire exposed, i.e. proportional to wave height. (Farmer and Ketchum, 1960, pp 77-99)

It must be noted that the accuracy of the gauges is affected by corrosion and marine growth; periodic maintenance is therefore important. Large salinity variations also affect accuracy.

1.2.2.3 Capacitance-type wave staffs

This type of gauge operates as follows:

An insulated wire is sealed at its lower end which is immersed in the sea. The insulator of the wire serves as the dielectric (i.e. the insulating material sandwiched between two conductors) of a variable capacitor; the sea water and the central conductor wire serve as the two conductors of the capacitor. Change in water surface elevation are sensed as changes in capacitance, which results in a proportional, measurable voltage.

Unfortunately, marine growth on the insulator (i.e. on the dielectric) changes the capacitance and causes errors.

1.2.2.4 Inductance-type wave staffs

The property of inductance is used in the operation of a wave staff as follows:

(1) A coil, with an alternating current applied to it, is vertically immersed in the sea. As sea water rises through the coil, the inductive impedance to the alternating current is increased, and vice versa (impedance in an alternating current is comparable to resistance in a direct current). Thus the recorded a.c. is proportional to water surface elevation.

(2) Another idea which can possibly be employed in a wave gauge is to apply a constant alternating current to the primary coil of a transformer with its coils vertically penetrating the sea surface. This induces a current in the secondary coil. As sea water rises through the coils, the induced current will increase, and vice versa. This current, representing water surface elevation, can be recorded.

Fortunately, the inductance type of wave gauge is not adversley affected by marine growth. However, changing salinity will result in large errors which are difficult to compensate for.

1.2.2.5 Transmission line gauges

These gauges make use of electromagnetic waves. In an example, two vertical stainless steel wire ropes focus electromagnetic waves, which reflect off the water surface. The frequency can be adjusted so that there is no phase shift (i.e. no phase difference) between the incident and reflected electromagnetic waves. In this way frequency is proportional to the distance from the transmitter/receiver to the water surface i.e. proportional to wave height (Ribe and Russin, 1974, p 402-403).

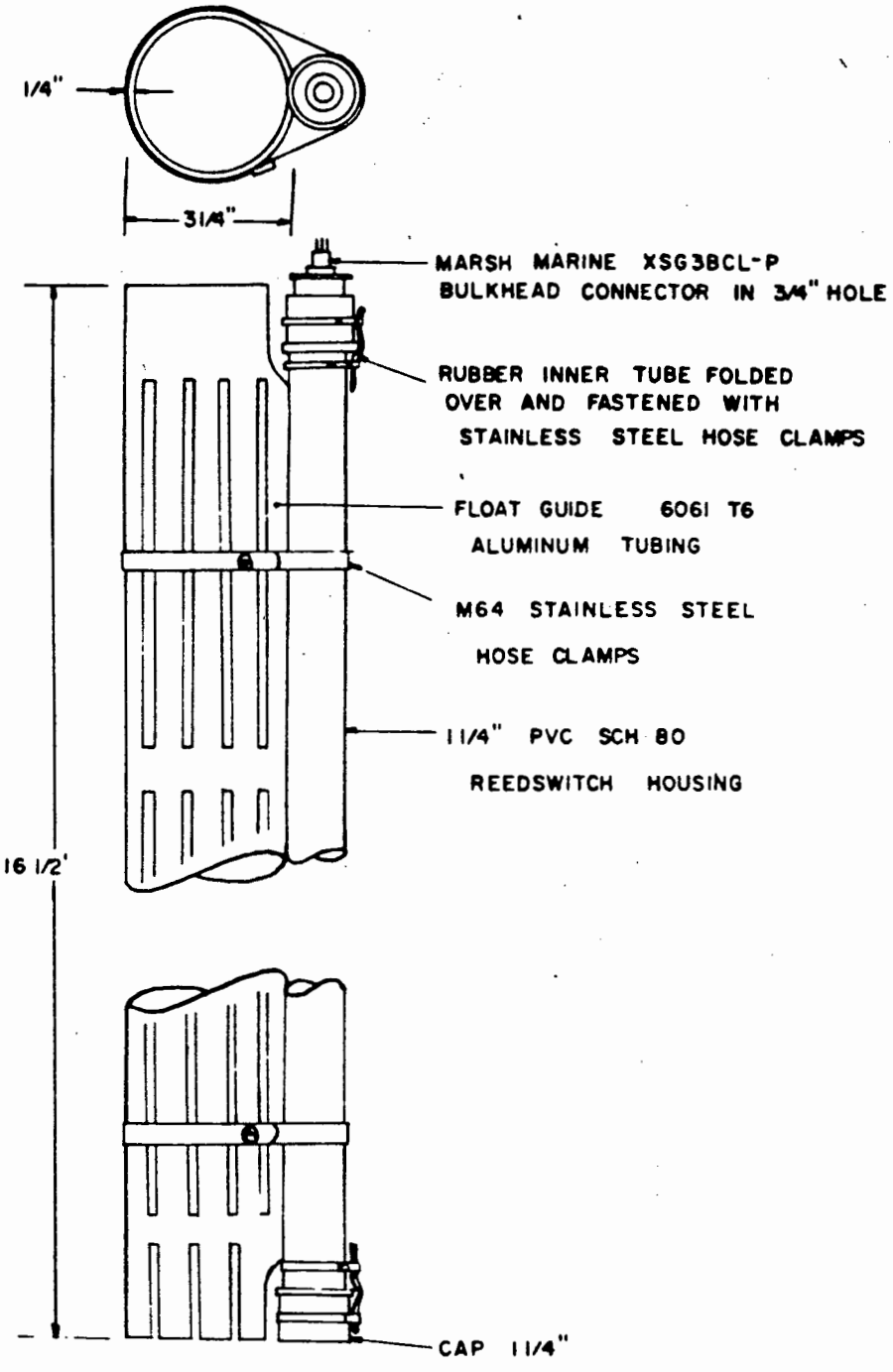

Figure 1.9 : Reed switch gauge.

Kronengold et al (1965)

1.2.2.6 Reed switch type gauges

The operation of this gauge is simple: a series of magnetic reed switches are activated by a magnetic float which follows the rise and fall due to waves (a reed switch is a switch which has contacts mounted on ferromagnetic reeds sealed in a glass tube, designed for activation by an external magnetic field).

Kronengold et al (1965, pp 273-280) describe a gauge in which the float contains a bar magnet. It is guided by a slotted aluminium tube (Fig. 1.9). The reed switches are situated adjacent to the float path, but isolated from the sea water. They are connected to a network of resistors supplied by a fixed voltage source. Since the reed switches include or exclude resistors from the circuit, the output is a voltage proportional to the float position.

As there is no electrical contact with the water, problems such as current leakage, and resistance changes due to corrosion are eliminated. However, marine growth accumulates in the float tube; therefore periodic cleaning is necessary.

1.2.2.7 Comparisons between wave staffs

Various comparisons between wave gauges have been conducted, for example:

(i) Ploeg (1972, p 137) compares the measurements of a transmission line wave gauge with a step-resistance gauge with "nearly always identical results."

(ii) Gerhard et al (1955, p 241) find a "one to one correlation between wave records" from a step-resistance gauge and a continuous wire gauge.

(iii) Ribe and Russin (1974,p403) compare two spirally wound resistance gauges and a transmission line gauge, with the result that "comparison appeared excellent."

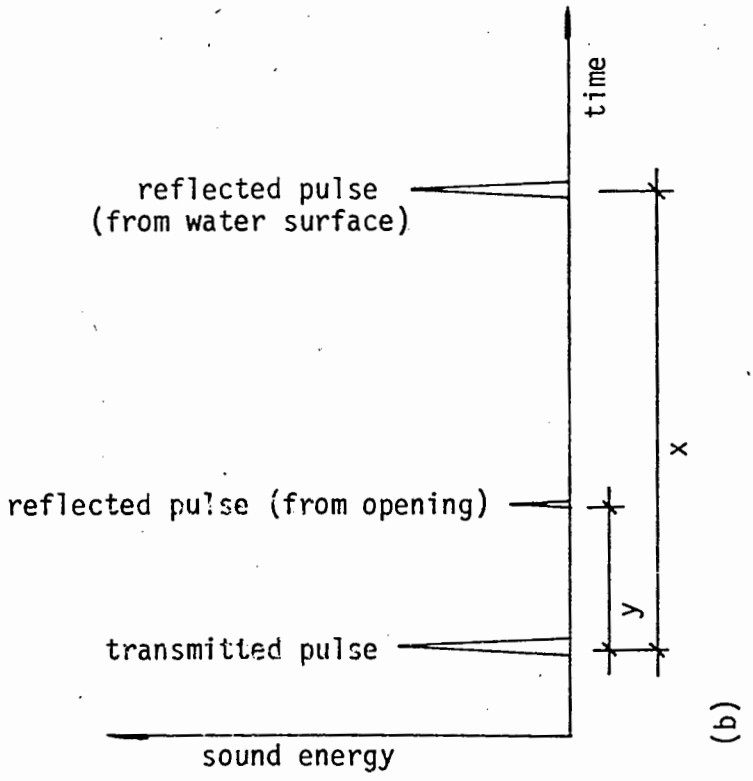

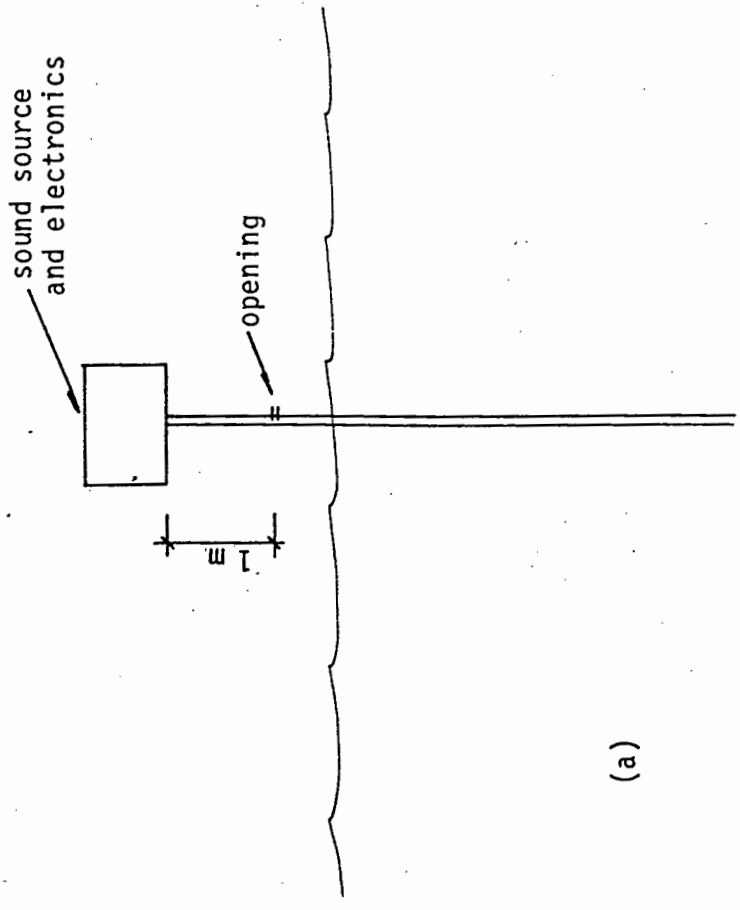

Figure 1.10 : C.S.I.R. Acoustic wave gauge.

1.2.3 An acoustic wave gauge

The C.S.I.R. (Council for Scientific and Industrial Research, Stellenbosch, South Africa) make use of a wave gauge which functions as follows: (Davies,1989) .

A pulse of sound is transmitted down a tube situated vertically in the water surface. The tube has a small opening at 1 metre from the sound source (Fig 1.10a). This causes reflection of some of the sound energy. The remaining sound energy reflects off the water surface. The transmitted and reflected pulses of sound energy are detected. A typical plot of this energy versus time appears in Fig 1.10b; the distance, d, from the sound source to the water surface is found from the simple relationship:

$$d = x/y \qquad (1.1)$$

where: x = the measured time for the transmitted sound pulse to reflect off the sea surface and return to the sound source.

y = the measured time for the transmitted pulse to reflect off the opening and return to the sound source.

By using this relationship, the instrument is self-calibrating; this is necessary since the speed of sound varies with moisture and temperature. The gauge transmits 4 pulses of sound per second, and in this way a digital record of water surface elevation is obtained electronically.

The gauge is extremely accurate and can even be used to detect very minor changes in sea level. Marine growth accumulating in the tube can easily be cleaned by pulling a cork disc through it.

1.3 WAVE MEASUREMENT WITH SUBSURFACE INSTRUMENTS

This class of wave instruments consists mainly of pressure-operated gauges. In addition, acoustic gauges are sometimes used. These types of gauges are usually fixed at the ocean floor, therefore they are useful at sites where shipping is hazardous to other types of gauges.

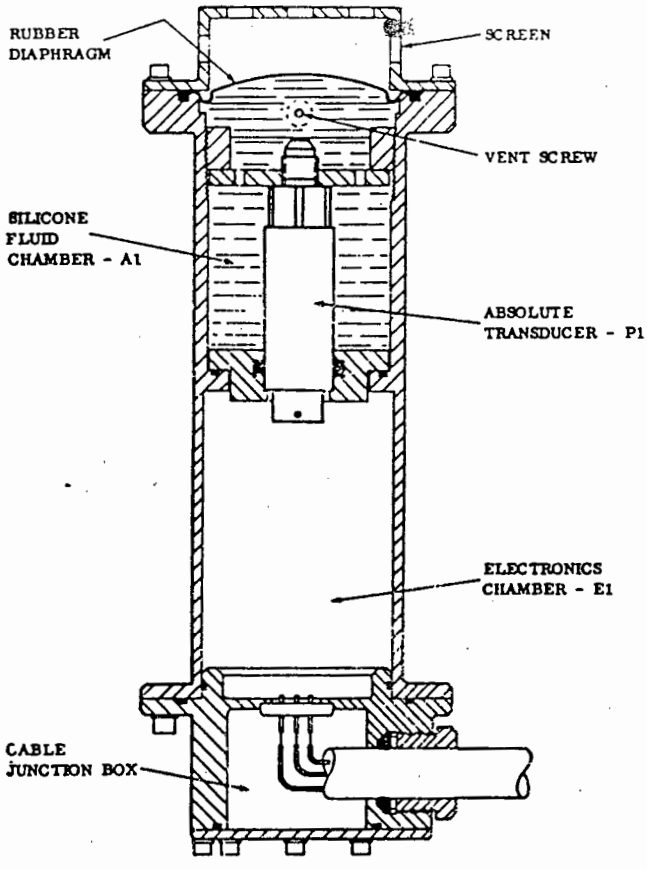

Figure 1.11 : Section of an absolute pressure gauge.

Bowler (1974)

(a) COMPLETE ASSEMBLY

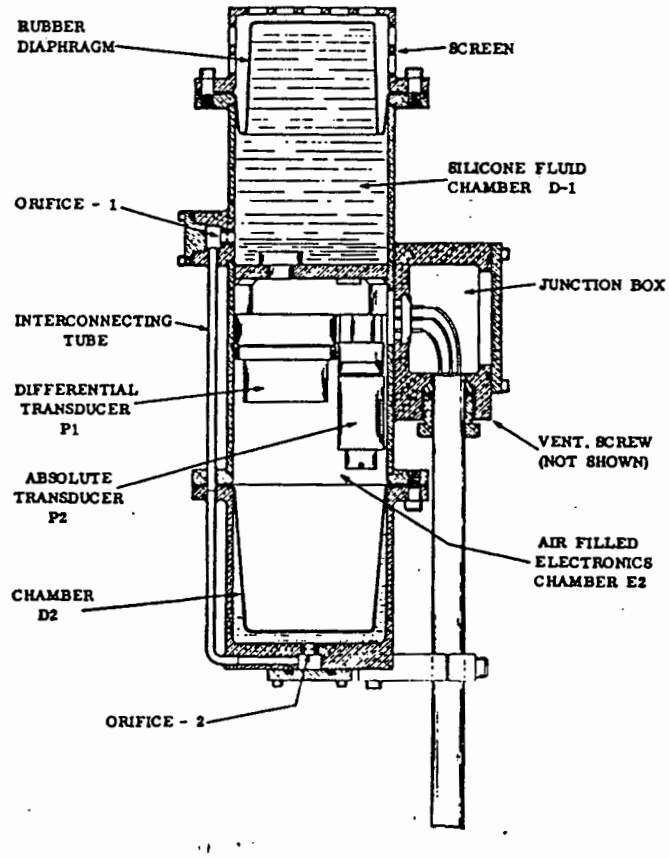

Figure 1.12 : Differential pressure gauge

after Bowler (1974)

Passing waves cause pressure fluctuations at subsurface pressure gauges, due to corresponding depth variations. These pressure fluctuations are detected and recorded at the gauge, or transmitted to a shore station (usually through undersea cables). The result is a record of pressure versus time, i.e. the pressure record. The various types of pressure gauge and their principles of operation are discussed below. Unfortunately, the pressure fluctuations due to the passage of waves are attenuated below the surface, due to hydrodynamic effects. Therefore, theoretical analysis of the surface wave record, from the pressure record, is necessary. This is also discussed below.

1.3.1 Types of pressure gauge and their principles of operation

Pressure gauges are either absolute or differential. Absolute pressure gauges measure the absolute, or total pressure surrounding them. This pressure is a sum of two parts:

(1) Quasi-static pressure, which is due to the water depth from the mean water level at which they are fixed; this depth varies due to tides and storm surges only (the variation is several metres in some locations).

(2) Dynamic pressure, which is due to the varying water surface elevation as waves pass overhead.

Differential pressure gauges measure only the dynamic pressure (i.e. part (2) above). Dynamic pressure constitutes a smaller range of pressures than the absolute pressure; therefore differential gauges are more sensitive than absolute pressure gauges. In comparisons of wave gauges both Ploeg (1972, p 137) and Bowler (1974, p 576) show that the differential type gauge is superior to the absolute type. Furthermore, differential pressure gauges are often designed to measure the quasi-static pressure separately, as this is needed in the calculation of the wave record from a pressure record.

The absolute pressure gauge: Fig. 1.11 illustrates an absolute type of pressure gauge. In this particular gauge, silicone oil (A1) is contained by a rubber diaphragm, which is protected by a perforated screen. External

water pressure on the diaphragm is transferred, through the silicone oil, to a transducer (P1), which converts absolute pressure to a proportional voltage. This voltage is converted to a proportional frequency and transmitted to a shore station for recording.

The differential pressure gauge is illustrated in Fig. 1.12 . Surrounding water is in contact with the rubber diaphragm, behind a perforated screen. (Fig. 1.12, top). The silicone fluid chamber D1 assumes the absolute pressure of the water. Chamber D-1 and D2 are connected by an interconnecting tube. Since orifice 1 and orifice 2 are restricted, short term pressure fluctuations (i.e. the dynamic pressure due to waves) do not affect pressure in chamber D2. Long term pressure variations (e.g. due to tides) however, do allow time for oil seepage into chamber D2. Thus chamber D2 assumes the quasi-static pressure. This pressure is transferred via another rubber diaphragm (Fig. 2, bottom) to an air filled chamber E2. The difference between the absolute and quasi-static pressure (i.e. the dynamic pressure) is sensed by the differential pressure transducer P1, which is exposed to both chambers, D1 and E2. In addition the quasi-static pressure alone is sensed by transducer P2, which is exposed to chamber E2 only. As in the case of the absolute pressure gauge, these transducers convert pressure into a recordable voltage.

In both the absolute and the differential types of gauge, pressures are converted by transducers to a proportional recordable form, such as an electrical voltage or frequency. Some examples of the operation of various transducers are:

(1) Pressure changes move a bellows and a connected cantilever beam. This beam movement varies the voltage of a potentiometer (Folsom, 1949, pp 693-694).

(2) Pressure changes move a bellows attached to the core of a linear differential transformer, which produces a d.c. voltage (Williams, 1969, p63).

(3) The Bourdon tube is a helical, hollow, flattened metal tube, filled with a fluid, such as silicone oil. The seawater pressure is transferred, through a rubber diaphragm, to the fluid. The fluid

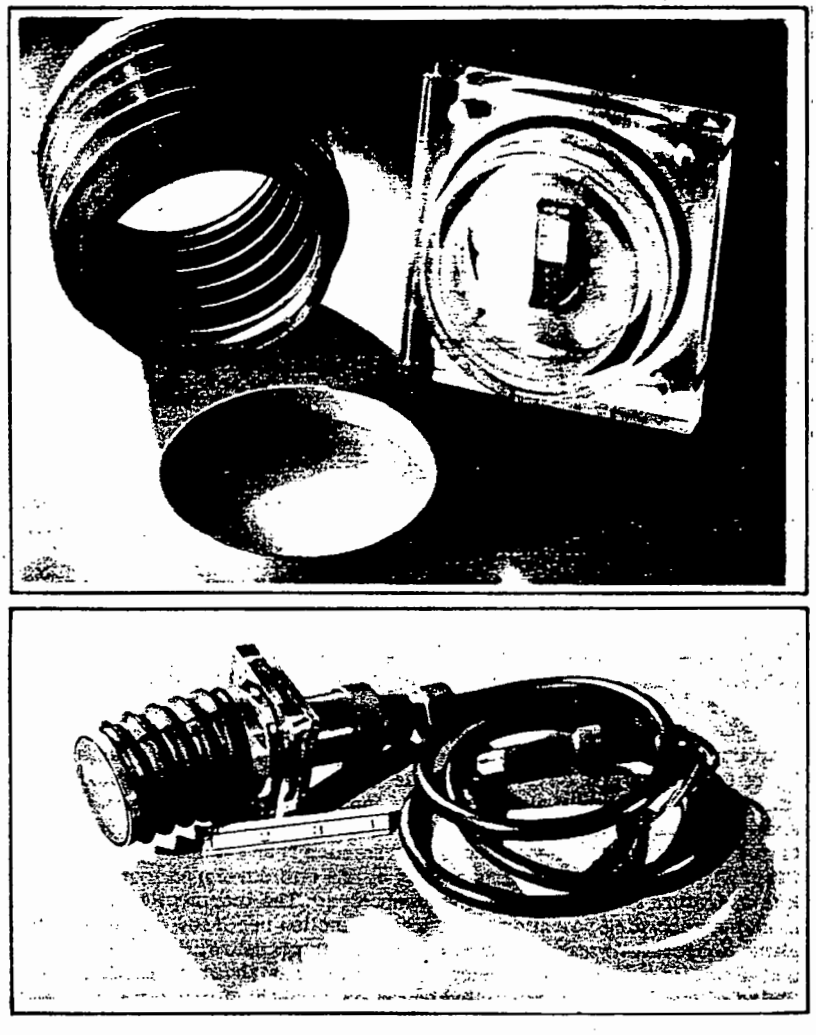

Figure 1.13 : Views of the Mark V (thermopile) shore wave recorder showing the thermopile and bellows (above) and the assembled unit (below).

Folsom (1949)

increases the pressure inside the Bourdon tube, thereby tending to straighten it, and causing a mechanical deflection, which can be recorded. Bass and Byrnes (1974,p190-199) use an optical lever system, composed of photocells and an electromagnet, to obtain greater sensitivity and less hysteresis.

(4) A wire in a evacuated cylinder is electronically oscillated at its natural frequency. The wire is attached to a diaphragm which yields under pressure. Thus increasing pressure slackens the wire and decreases the frequency of oscillation, and vice versa. The result is a recordable frequency which is proportional to pressure (Larsen and Fenton, 1974, p 198).

(5) A thermopile is a circuit with junctions between different metals. If these junctions are at different temperatures, a current is generated, through the thermo-electric effect. The thermopile has junctions attached to a copper block exposed to the sea, and junctions situated inside a gas filled bellows. Water pressure changes cause volume changes in the bellows. These volume changes on the bellows cause temperature changes in the gas, which induces current in the thermopile (because the junctions will then have different temperatures). This induced current is therefore proportional to pressure, and is recorded. Fig 1.13 illustrates a thermopile gauge, which is actually expendable. (Folsom, 1949)

(6) Movement of a plate by water pressure causes mechanical stress on a quartz disk. Thus, by the piezo-electric effect a voltage is induced which is proportional to the pressure (the piezo-electric effect is defined as "the generation of electric polarization in certain dielectric crystals as a result of the application of mechanical stress").

(7) A flexible rubber air bag is connected to a pressure recording device on shore (less than 100 m away) A mechanically operated pen records pressure fluctuations on the rubber bag (Draper, 1967, p 215).

In addition to the above examples, the movement of a bellows may be detected by means of strain gauges, changes is electrical inductance, and changes in electrical capacitance.

1.3.2 Calculation of the surface wave record

Having obtained a subsurface pressure record from the above-mentioned instruments, it must be corrected to a surface wave record. The following relationship from linear wave theory is used to correct a pressure pulse, Δp (due to a wave), at a depth z to a surface pressure pulse Δp_o:

$$K = \frac{\Delta P}{\Delta p_o} = \frac{\cosh\left[\frac{2\pi(d-z)}{L}\right]}{\cosh\left[\frac{2\pi d}{L}\right]} \qquad (1.2)$$

where K = the subsurface pressure response factor
L = the wavelenth of the wave
d = the water depth

The surface pressure pulse is the pressure, at mean water level, due to a wave of amplitude H/2 , i.e.

$$\Delta p_o = w.H/2 \qquad (1.3)$$

where w = the specific weight of sea water.

Thus, the continuous surface wave record may be obtained from a continuous pressure record taken at depth z. If the pressure record is taken at the ocean floor (i.e. where z = d) then equation 1.2 becomes:

$$K = \frac{1}{\cosh\left[\frac{2\pi d}{L}\right]} \qquad (1.4)$$

The wavelength in the above (according to linear wave theory) is related to wave period, T, as follows:

$$L = 2\pi \left[g\, T^2 \tanh\left(\frac{2\pi d}{L}\right)\right] \qquad (1.5)$$

where g = 9.81 m/s^2, the acceleration due to gravity

In the above the depth, d, is obtained by calculating the average pressure head in a record from an absolute type pressure gauge, or from a separate measurement of the quasi-static pressure head, as occurs in some differential gauges.

Since wave periods are superimposed and confused in a time domain wave record (as shown in Sec. 2.2.1), the pressure response factor is best applied in the frequency domain. A digital time domain pressure record may be converted to the frequency domain using the Fast Fourier Transform (FFT) (dealt with in chapter 2). After applying the pressure response factor, the inverse FFT will yield the wave record. Larson and Fenton (1974,p199-201), and Esteva and Harris(1970,pp101-116) describe this process.

Using equations 1.2 to 1.5 it can be shown that surface pressure fluctuations are increasingly attenuated with depth and with frequency (or wavelength). Therefore high frequency waves may be well attenuated or even excluded from the wave record (this occurs when $L < 2d$). Fortunately these high frequency waves are not important for engineering, since they have very little energy. In addition, wave records without high frequency components (i.e. without high frequency waves) are easier to analyse manually (e.g. by Draper's method, Sec. 2.1.2). However, because of attenuation, high frequency pressure pulses require a large value of K to convert subsurface pressures to surface pressure values. Caution must be taken not to convert high frequency noise at the same time. Such noise can originate from the power system or the pressure transducer of the gauge, etc. (Lee and Wang, 1984, p 273). To avoid this type of error: "some investigators have assumed the shape of the pressure power spectrum at high frequencies" (Kim and Simons, 1974, p41). In other words, with the amplitudes of lower frequency waves known, they assume the amplitudes of high frequency waves likely to occur.

In general, the theory described above to obtain wave records (equations 1.2 to 1.5) has been found to be inaccurate. For example, Seiwell (1947, p 722-724) compares compensated pressure records to records taken at the surface; here K is found to be a factor of 1.35 too small. Gerhardt et al (1955, pp 239-243) and Folsom (1949, pp 691-693) show similar results; this type of result is summed up by Esteva and Harris (1970, p101): "several recent

comparisons of records from surface profile gauges with compensated records from pressure gauges have shown systematic differences. In general, the differences have been attributed to inadequacy of the compensation formula." More optimistically, Lee and Wang (1984, p285) find that the response factor, K, is reliable for intermediate depths. However, they find that in shallower water, the effect of wave nonlinearity and currents affect K; they therefore present modifications to the analysis.

1.3.3 Problems encountered

Pressure gauges are generally connected to a shore station by undersea cables. These cables deteriorate, particularly in areas of erosion, such as in the surf zone. In addition, ships anchors and cables, and fishing nets cause damage. If a current or voltage signal, representing measured pressures, is transmitted to shore, a damaged cable may cause false readings, which could go undetected. Therefore it is preferable to transmit a frequency signal representing measured pressures, since such signals are correct even if weakened, and failures occuring in the cable are immediately obvious. An alternative to the use of undersea cables is a pressure gauge which can be dropped at the area of interest together with a battery pack. The pressure signal from the gauge is then transmitted from a radio enclosed in a buoy attached to the gauge. Recording at the gauge is also possible.

Currents at a depth can also be problematic. Some gauges are anchored underwater, their buoyancy suspending them at the required depth. A horizontal current may force them to move sideways and downward due to tension on the anchor line. This downward movement can cause erroneous pressure measurement, especially if the current fluctuates. The situation can be improved by increasing the buoyancy of the pressure gauge.

Surface currents affect pressure recording of waves in two respects:

(i) by changing the wavelength. (from equations 1.2 to 1.5 it can be seen that a change in wavelength, L, affects the pressure response) ;

(ii) a dynamic effect leading to a change in dynamic pressure - this directly affects recorded pressures.

Figure 1.14 : INES Wave Recorder

Zwamborn et al (1972)

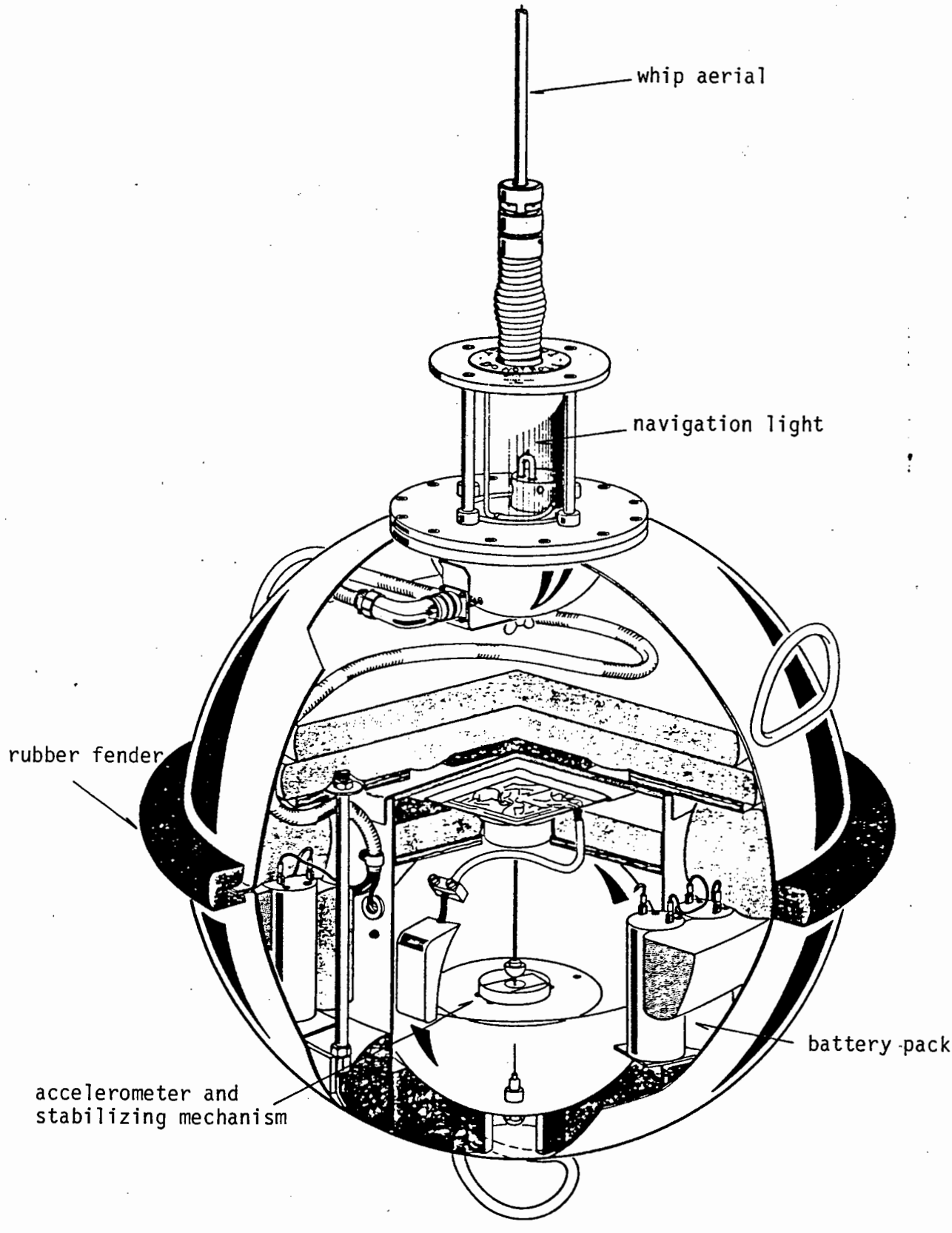

Figure 1.15 : A Datawell Waverider buoy.

Datawell (1976)

Lee and Wang (1984, p 282) describe how these surface current effects can be compensated, provided current measurements are obtained.

Marine growth, although less active at depth, can cause fouling of pressure gauges. Therefore periodic maintenance will be necessary. Fouling can be retarded by the use of antifouling paint and Peacock (1974, p175) mentions the use of a filter for marine growth.

1.3.4 Acoustic wave gauges

These instruments also operate below the sea surface. They transmit acoustic pulses which reflect off the surface, and are received. The time interval between transmission and reception is measured; this interval indicates the water surface elevation. An example is the INES (INverted Echo Sounder) developed by the C.S.I.R., illustrated in Fig. 1.14.

Unfortunately, during storms at the measuring site, the boundary layer between air and water is often ill-defined, due to bubbles from blown-off wave tops; as a result, sound pulses will be scattered rather than reflected, and important storm wave records are not recorded.

1.4 WAVE MEASUREMENT WITH FLOATING SURFACE INSTRUMENTS

A wave record can be obtained by recording the movement of a buoy due to waves on the ocean surface. This can be achieved, for example, by measuring and recording the tension history of an elastic member to which the buoy is tethered (InterOcean). Another method is the measurement of buoy accelerations to obtain buoy movements; the displacements of the buoy are calculated by integrating the measured accelerations twice. This principle is employed in the ship-borne wave recorder and in the Waverider buoy (manufactured by Datawell, Haarlem, The Netherlands). The Waverider buoy is probably the most commonly used wave measuring instrument (illustrated in Fig. 1.15). Its extensive use by organisations such as the C.S.I.R. and C.E.R.C. is a reflection of its reliability and accuracy.

Waves can also be measured from a buoy which is restricted from response to wave action; these buoys are normally longitudinal and are called spar buoys. Wave records can be obtained from one or more instruments fixed to the spar buoy, such as staff gauges and/or pressure gauges.

1.4.1 Accelerometer Buoys

As mentioned above, double integration of measured acceleration of a wave buoy due to wave motion yields its displacement; a record of this displacement is the wave record. Acceleration is measured by an accelerometer mounted in the buoy. Examples of the operation of accelerometers are:

(1) A mass is fixed to the free end of a horizontal flexible arm. Accelerations of the mass cause a proportional bending of the arm which can be detected with strain gauges.

(2) A mass, suspended in an oil filled casing, is connected to the grounded plate of a capacitor; the other plate is fixed. Accelerations of the mass move the grounded plate, causing the capacitance to vary; this in turn varies the frequency of an oscillator; the resulting signal is recorded. (Boiten, 1960, pp 115-117)

(3) A minute, micromachined silicon mass is suspended by multiple beams to an outside frame, as illustrated in fig 1.16. Piezoresistors located in the beams change their resistance (which is measurable) as the motion of the suspended mass varies the strain in the beams. This type of accelerometer was innovated by the C.S.I.R. (Davies, 1989).

1.4.1.1 Processing and transmission of the acceleration signal

The acceleration signal obtained from the accelerometer may be transmitted directly to a shore station, and integrated thereafter. In general however, the acceleration signal is integrated in the buoy. In addition, useful parameters (e.g. the significant wave height and the zero-upcrossing period, described in Sec. 2.1) can be calculated *in situ* (Blair, 1974, pp 254-271); (Adamo et al, 1978).

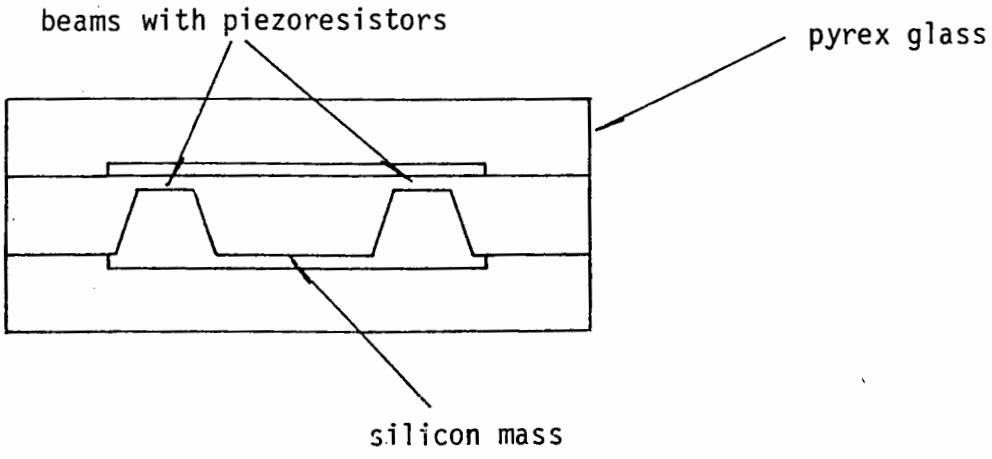

Figure 1.16 : Micromachined silicon accelerometer.

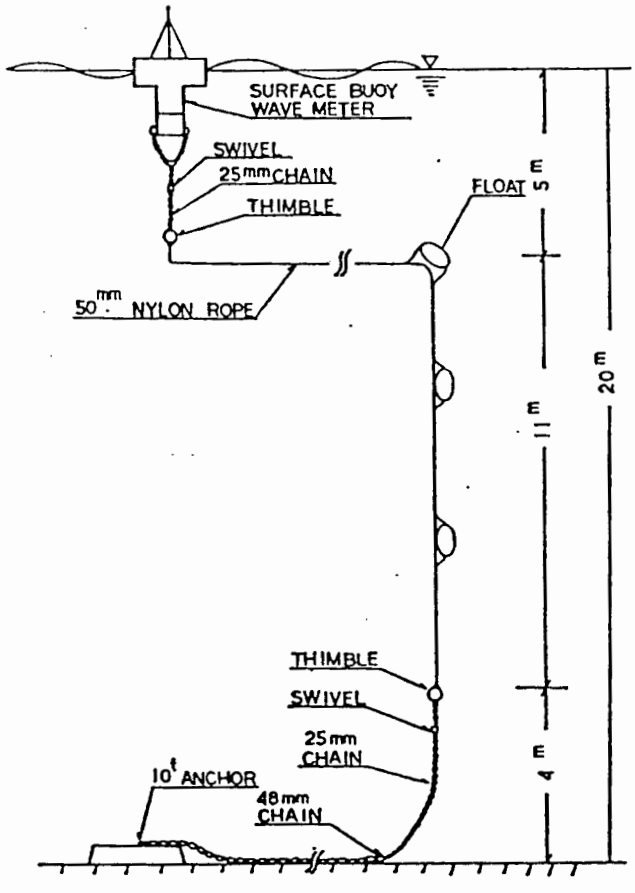

Figure 1.17 : Accelerometer buoy mooring

Hashimoto and Yamaguchi (1980)

The wave information can be telemetered by radio to a shore station. Transmission usually occurs at set times; alternatively, continuous recording can be triggered off by a radio signal from the shore station.

The range of transmission is generally dependent on conditions; for example, the Waverider buoy can transmit a dependable signal over 50 km if waves are below 10 m in height, but waves above 10 m deflect the signal (e.g. 25 m waves lower the range to 30 km). However, unlimited range is possible, with the use of a satellite communications link (Adamo et al, 1978).

Signals received at shore stations can be transmitted to a central station by telephone line (this occurs at the C.S.I.R.). In this way a faulty system can be immediately detected; however the transmission is sometimes affected by ship radio interference, which is difficult to detect in a record (Coetzee, 1988). This can be avoided by recording the signal in the buoy, but retrieval of the recording is tedious, and a fault in the system may go undetected for long periods.

1.4.1.2 Common problems encountered

(a) High frequency noise:
The accelerometer may tend to detect all movements, including high frequency vibrations which are of no interest (i.e. high frequency noise); these can be excluded by damping. Damping may be electromagnetic (Marks and Tuckerman, 1960, p 104) or by using a viscous fluid (Boiten, 1960, pp 115-117). The undesirable high frequency noise can also be removed by electronic or numerical filtering (Sec. 2.2.3.3)

(b) Tilting of the buoy:
The acceleration recorded may be erroneous due to the tilting of a buoy as waves pass. This can be counteracted as follows:

(i) By using an appropriate buoy hull shape, e.g. a spherical buoy is less susceptible to tilting than other shapes.

(ii) By mooring considerations, e.g. a heavy mooring line attached directly beneath a buoy will tend to keep it upright.

(iii) By maintaining the accelerometer in a vertical position; this may be achieved by mounting it on a gyroscope, or by having it floating on a fluid.

(iv) The tilt history of the buoy can be measured with tilt sensors; from this record, corrections for tilt can be calculated.

(v) A stabilizing leg attached to the bottom of the buoy will tend to keep it upright (Bowler, 1974, p 566).

(vi) An accelerometer may be suspended from a surface buoy, at a depth where wave influences are negligible. Since any lateral and tilting motions of the float are "essentially eliminated", only vertical accelerations are measured (Reynolds and Hoffman, 1974, p642).

(c) Mooring:

Accelerometer buoys are usually moored at the site of interest, although some are free floating e.g. the expendable SPLASHNIK buoy (Marks and Tuckerman, 1960, pp 100-113). Unfortunately, strong winds and surface currents can cause tension on moorings which can affect buoy behaviour and the resulting wave record. In addition, severe sea conditions may induce large dynamic stresses to mooring lines, resulting in losses. This situation is improved by using subsurface floats (illustrated in Fig 1.17) and rubber mooring chord. Nevertheless, the C.S.I.R. has lost Waverider buoys with unknown causes; it is suspected that some of the losses are due to tampering (Coetzee, 1988).

(d) Collision with ships:

Buoys are susceptible to collision with ships. Precautions must be taken:

(i) Mooring buoys are avoided where ship traffic is heavy.

(ii) Buoys generally have navigation lights.

(iii) Buoys are designed to withstand collision, e.g. the Waverider buoy has a rubber fender, and a thick shell which stays watertight even if largely deformed by a collision.

1.4.1.3 Obtaining the wave record.

Accelerometer buoys have a different response at different frequencies (particularly at the natural frequency of the buoy, at which resonance occurs). Therefore the amplitudes in a record of the buoy's displacements

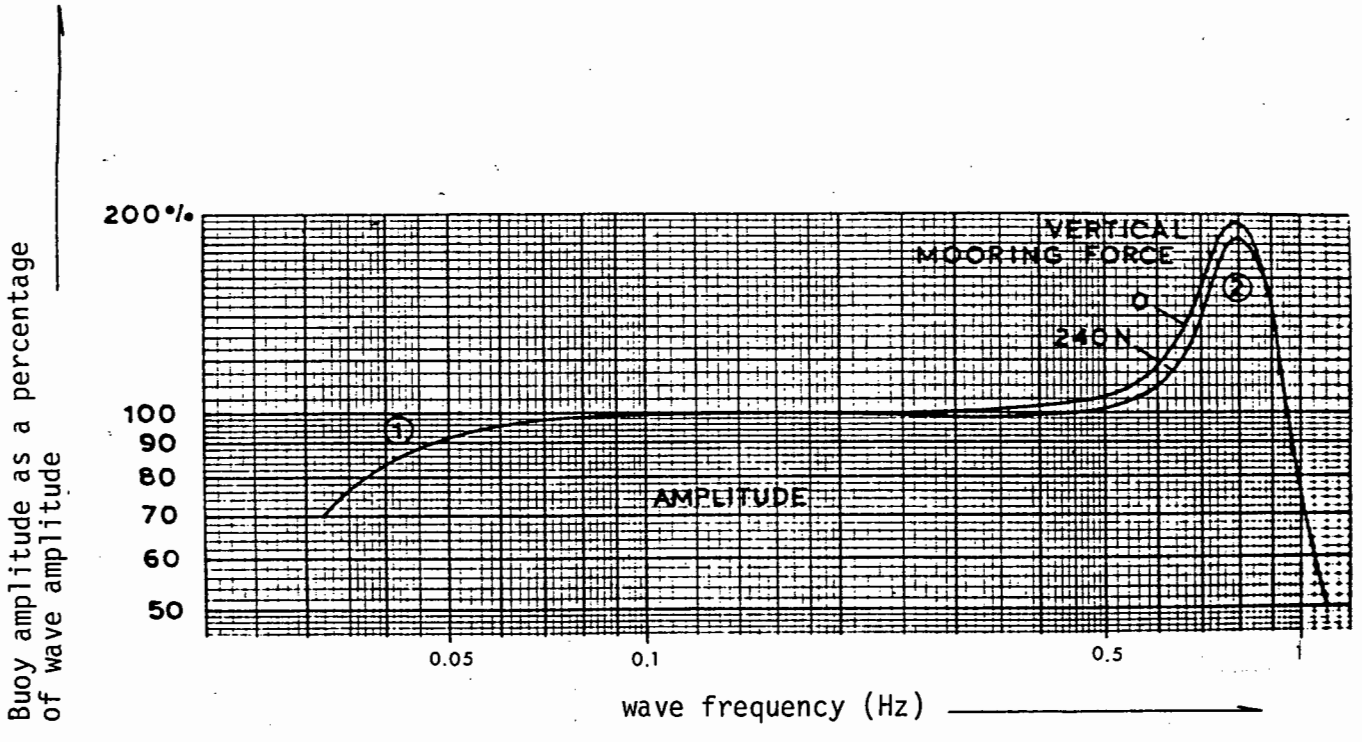

Figure 1.18 : Transfer function for a Waverider buoy.

Datawell (1976)

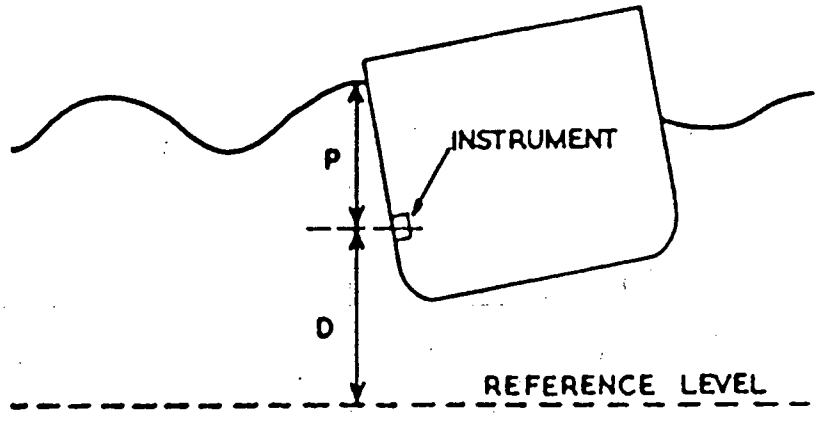

Figure 1.19 : Principle of the SBWR

Tucker (1956)

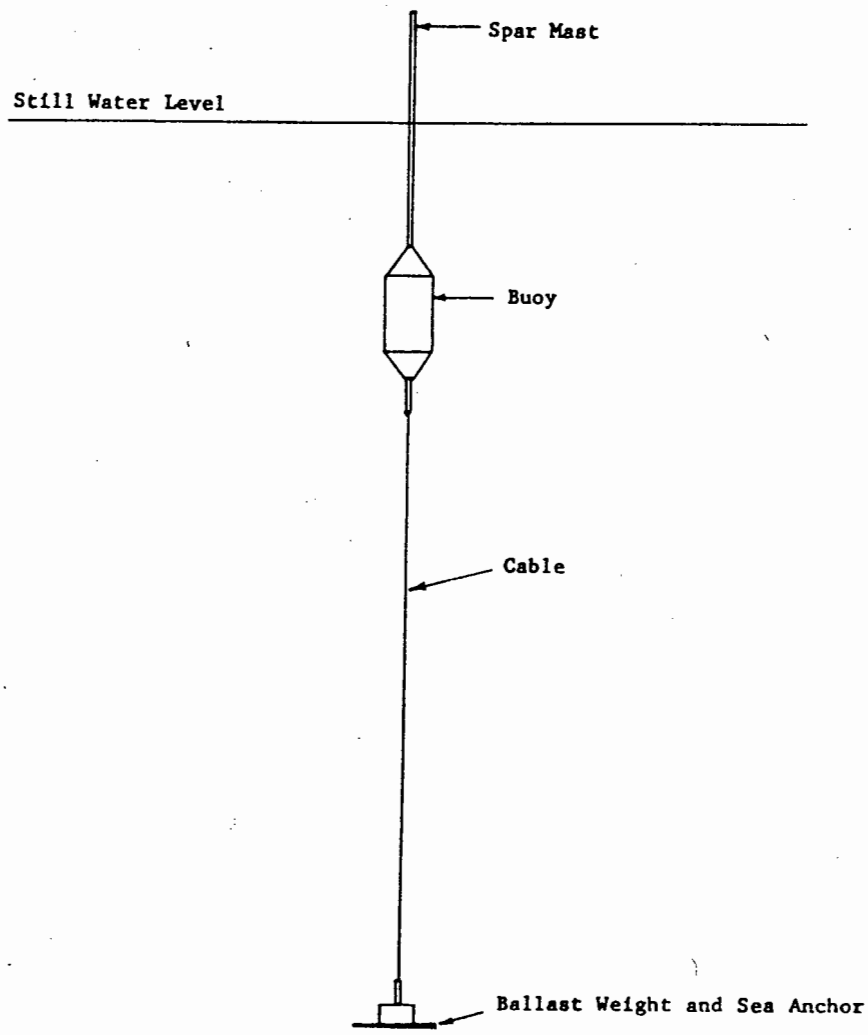

Figure 1.20 : Spar buoy.

Black (1964)

(from doubly integrated acceleration) will not always represent actual wave amplitudes. Thus corrections must be made from an empirically determined transfer function (such as Fig. 1.18). This is best achieved by transforming the record of displacements of the buoy to the frequency domain (as shown in Sec.1.2.2), then applying the transfer function correction. If required, the wave record can then be obtained by transforming the corrected record back to the time domain.

1.4.2 The ship-borne wave recorder (S.B.W.R.)

The S.B.W.R. combines the use of accelerometers and pressure sensors. Tucker (1956, pp 112-118) describes this wave recorder in detail; the accelerometers and pressure sensors used are similar to those discussed above (in Sec. 1.4.1. and Sec. 1.3.1). Referring to Fig. 1.19:

The water height, P, above the instrument is measured with a pressure sensor. The vertical displacement of the instrument from an imaginary reference level, D, is found by double integration of the measured acceleration. The sum of these heights, P+D, is the height of the water surface above the reference level. A continuous measurement of this value (P+D) yields the wave record.

Short waves approaching the ship on the opposite side to the instrument may be partially reflected, and therefore not fully measured. Alternatively short waves approaching from the same side as the instrument, may be increased in height by reflection. Therefore, a S.B.W.R. is fixed on each side of the ship, and the average of their two outputs is taken.

Unfortunately the S.B.W.R. does not respond to short waves, because the pressure sensors are at some depth (usually approximately 3 m) below the surface. In addition:"there are several uncertainties in the response of the instrument to wavelengths comparable or shorter than the length of the ship" (Tucker, 1956, pp 112-118). Therefore, the instruments main limitation is its "inability to measure waves with periods of less than about 4 seconds."

1.4.3 Spar buoys

Another approach to wave measurement is the use of a buoy which is designed to remain stationary in the sea. This is achieved by designing the buoy so that its natural frequencies occur outside the range of frequencies likely to be encountered at the measurement site. This is generally achieved with a longitudinal spar buoy e.g. Fig 1.20. Most of the buoy's volume is placed below the water surface, where wave action is less effective, and restoring moments are provided, to minimize pitching motions. In addition, a large sea anchor (Fig 1.20) reduces heaving motions.

Wave measuring instruments such as wavestaffs and pressure gauges can be attached to such a buoy. Finkelstein (1964,p40) uses an annular accelerometer float which rides up and down the mast of the buoy to measure waves. Spar buoys can be anchored, free-floating, or tethered to a vessel.

1.5 THE MEASUREMENT OF WAVE DIRECTION

Ocean waves of various heights and frequencies travel in different directions. Directions of dominant trains of waves can easily be measured with instruments such as the Clinometer and the D.O.S.O. gauge, as described below. Alternatively, the distribution of directions of waves can be obtained from the 2-dimensional directional wave energy spectrum, which shows the occurrence of wave energy in the component frequencies and directions of waves (Fig. 1.3). The analysis of this spectrum requires measurements of the variations in at least three hydrodynamic properties, for example:

(i) water surface elevation with slopes of the water surface (in two orthogonal directions) ;
(ii) water surface elevation together with two horizontal current velocities in orthogonal directions ;
(iii) water surface elevation at three points in the ocean.

Many of these measurements can be made with instruments discussed above (in Secs. 1.2, 1.3, and 1.4), as well as some more specialised instruments, as described below. In addition wave direction measurements can be made by photography and radar; this is described later (Sec. 1.6.).

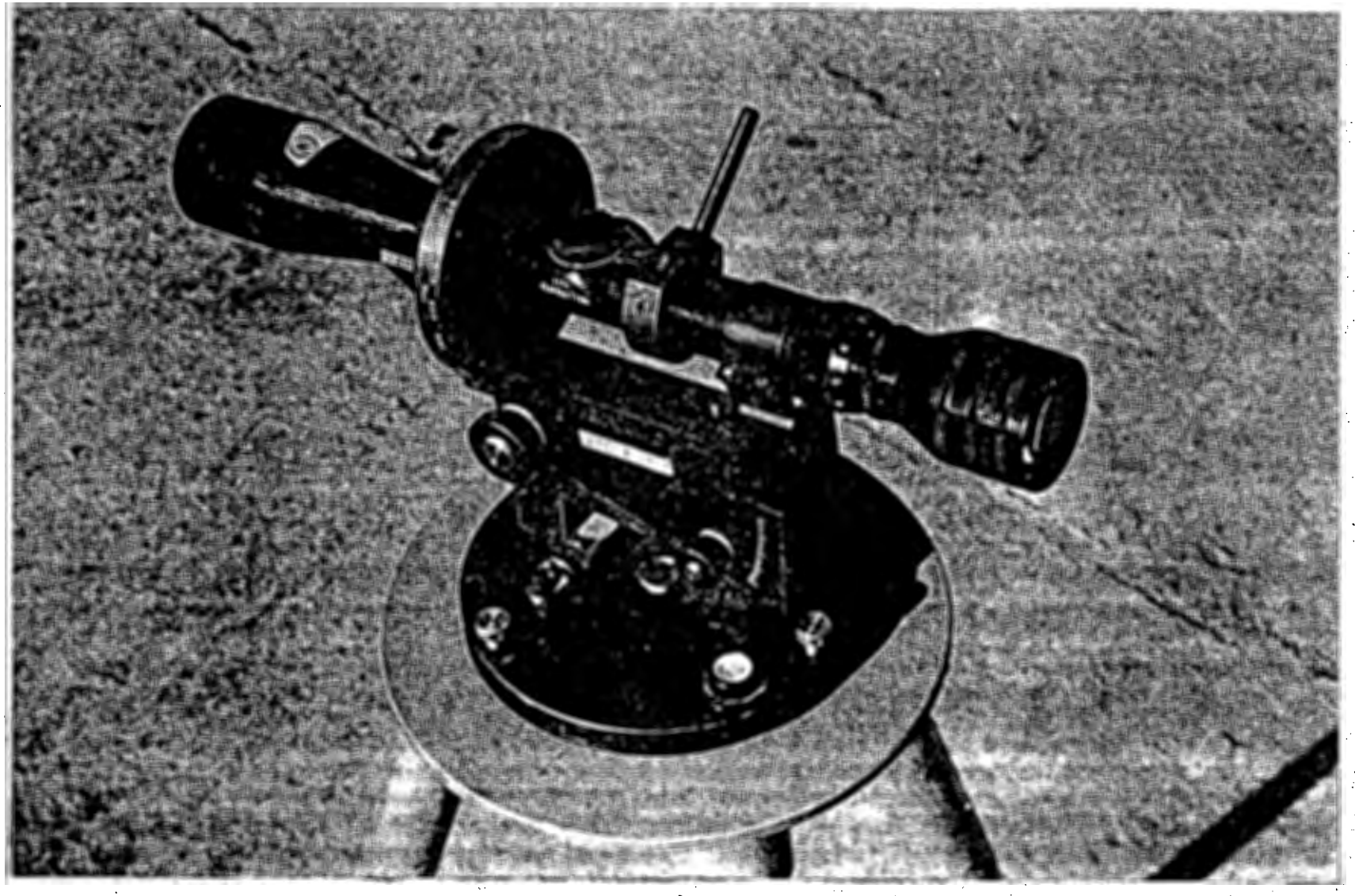

Figure 1.21 : The Wave Clinometer

Zwamborn et al (1972)

1.5.1 The clinometer

Fig. 1.21 illustrates the clinometer, a specially adapted telescope developed by the C.S.I.R. It is mounted on a stand, so that its axis can be inclined at either 3, 5, or 7½ degrees to the horizontal. To measure wave direction, a horizontal cross-hair in the telescope is aligned with prominent wave crests by turning the instrument about its vertical axis; the horizontal angle is then read off from a graduated disc mounted on the telescope, to yield the wave direction from the geometry of the system. Wave height and period can also be estimated by observing the movements of a floating buoy between vertical graduations in the telescope (Zwamborn et al, 1972, p 82).

The accuracy of wave direction measurements is greater when the telescope is inclined at 5 or 7½ degrees, therefore the instrument should preferably be sited at a high vantage point.

Unfortunately the instrument has some disadvantages:

(i) measurements requires an operator ;
(ii) fog can hinder measurement ;
(iii) short, steep waves which are generated locally may hide more significant long swells, from distant storms. This problem is alleviated in shallower water where shoaling increases the amplitude of long swells.

These shortcomings can be overcome by the use of other wave measuring instruments, such as the D.O.S.O. gauge, developed by the C.S.I.R.

1.5.2 The D.O.S.O. gauge

Fig. 1.22 illustrates the D.O.S.O. gauge; D.O.S.O. stands for "Direction Of Swell Orthogonals". Refering to the figure, the gauge operates as follows: The forwards and backwards components of wave orbital motion cause the nylon brush to tilt the pendulum, which is freely mounted in the neoprene diaphragm, until contact is made with the annular resistance coil. Since

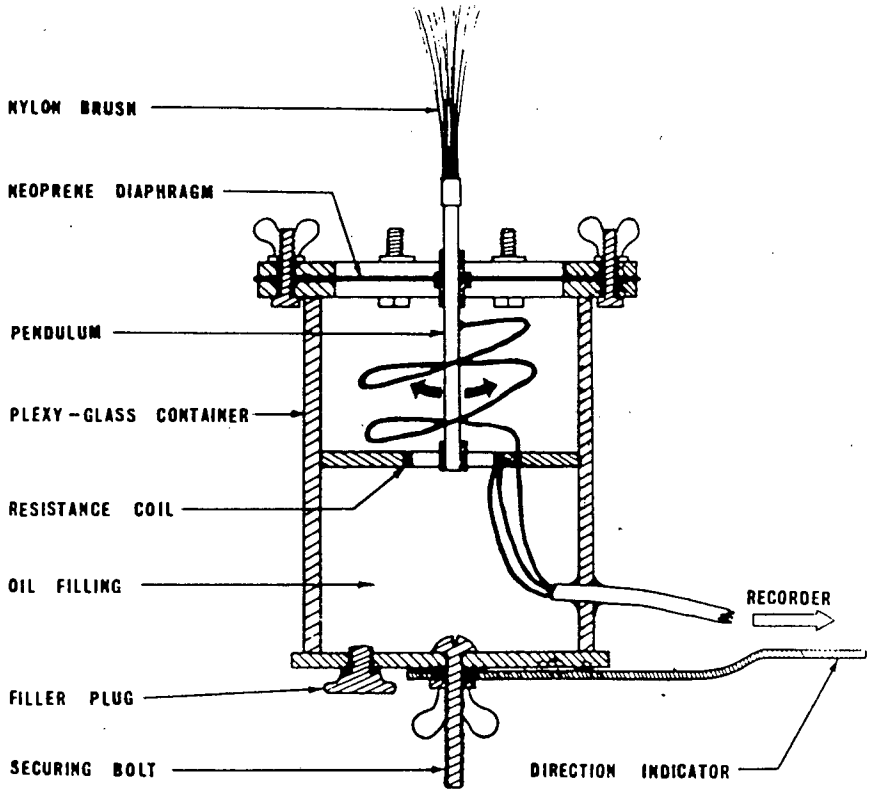

Figure 1.22 : Section through a D.O.S.O. gauge.

Retief and Vonk (1974)

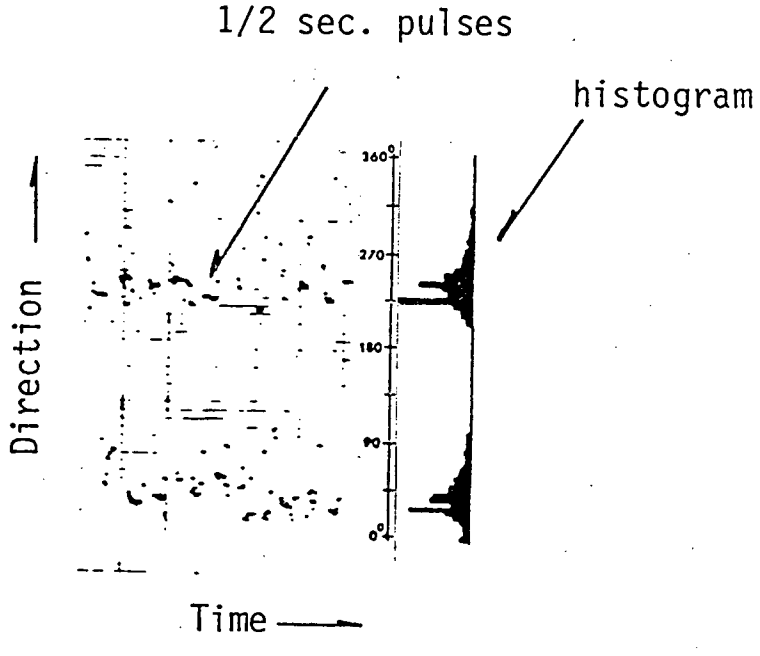

Figure 1.23 : Data presentation

after Retief and Vonk (1974)

this coil has linear characteristics, voltages recorded at pendulum contact are proportional to wave orbital motion direction, which corresponds to wave direction. (Retief and Vonk, 1974, pp 212-224).

Half second pulses of the voltage, corresponding to the direction, are recorded, as shown in Fig. 1.23 (digital recording on magnetic tape is also possible, by a self contained recorder which can be left unattended for one month). These pulses are then summed, to yield two histograms representing the forwards and backwards components of wave orbital motion; the larger histogram represents the stronger forwards motion. The histogram shows the directions in which waves are travelling; peaks are representative of dominant trains of waves, e.g. in the histogram of Fig. 1.23, the two peaks in the histogram represent two dominant trains of wave (one at approximately 225 degrees and another at approximately 243 degrees)

The D.O.S.O. gauge is clamped to a tripod on the sea bed, at a depth where orbital motion is detectable. Its sensitivity can be adjusted to eliminate background water movements, such as longshore currents, and to react to stronger orbital motions only; this is achieved by varying the lever-arm length of the nylon brush. In spite of this, however, strong rip currents can affect readings. Nevertheless, the gauge provides a "simple and reliable means of measuring the direction of waves approaching a coastline" (Retief and Vonk, 1974, p 221).

1.5.3 Wave run-up on a pile

The profile of water run-up on a pile, as a wave passes, is symmetrical. Electronic gauges on the circumference of the pile can detect the wave run-up profile; the direction of this profile corresponds to the wave direction. James and Hallermeier (1976, pp 379-391) conducted laboratory tests on a gauge using the above principle; it is found to be accurate, but requires further development for practical use in the ocean.

1.5.4 The tilting spar

An air-filled spar is connected to a sea bottom anchor assembly, at about 10 m depth, by a universal joint. Accelerometers are mounted orthogonally at

the top of the spar. These detect movements of the spar due to horizontal currents caused by the orbital motion of waves. Wave direction corresponding to these orbital current directions, can therefore be determined.

Horizontal motions detected by accelerometers are digitized and telemetered to a shore station. Wave direction is then analysed, by means of the Fast Fourier Transform, described in 1.2.2. The result is a distribution of wave direction versus wave frequency. Directions obtained thus have been compared to directions obtained from other instruments (e.g. a pressure gauge array, introduced below) to yield "generally good agreement" (Lowe et al, 1974, p 236).

1.5.5 Arrays of measuring instruments

As mentioned above, the directional wave energy spectrum can be analysed from measurements of water surface elevation at three (or more) points in the ocean. This is achieved with an array of wave measuring instruments. An array is a group of at least three instruments, spaced several metres apart (in theory, the resolution of directional spectra increases with the number of wave instruments; however this does not occur in practice, because of errors in measured data). Arrays generally comprise wave buoys, wave staffs or pressure gauges.

Directional wave energy spectra can alternatively be calculated from various other combinations of measurents, taken by instruments such as the pitch-and-roll buoy, and a differential pressure gauge, described below.

1.5.6 The pitch-and-roll buoy

This instrument measures water surface elevations from vertical accelerations in the same way as accelerometer wave buoys, described in 1.4.1. However, unlike the above-mentioned accelerometer buoys, these buoys are designed to follow varying wave slopes; this allows the angle of tilt of the buoy, as waves pass, to be recorded in two orthogonal directions. These two records, together with the water surface elevation record, are used to analyse the directional wave spectrum. Hashimoto and Yamaguchi (1980, pp 101-119) describe the pitch-and-roll buoy. The C.S.I.R. are at present

conducting field tests on a triangular arrangement of three connected buoys, designed thus to follow wave slopes well. The same principle of operation applies to this device.

1.5.7 The differential pressure gauge for wave direction

The fluctuating slope of the sea surface can be obtained by recording the pressure slope (i.e. the difference in pressures between two points underwater). This can be measured by a differential pressure transducer which has openings exposed to the water at two points A and B; the difference in pressure between the two points causes movement of a mechanical diaphragm, which generates a proportional electrical voltage.

Bodge and Dean (1984, pp 755-769) describe a gauge which measures differential pressures in 2 orthogonal directions, as well as the absolute pressure. These three measurements are used to calculate the directional spectrum. The gauge is found to be far more sensitive than an array of pressure gauges, for directional measurements.

1.5.8 Miscellaneous direction gauges

Various other gauges have been developed to measure hydrodynamic properties for the calculation of directional wave energy spectra, for example:

- The Cloverleaf buoy is an extension of the pitch-and-roll buoy; it measures water surface curvatures in addition to slopes, resulting in a higher resolution directional spectrum (Mitsuyasu et al, 1975, pp 750-759). However, its use has been "confined to occasional research projects" (Tucker, 1989, p173)

- Ayela et al (1985, pp 709) describe a direction sensor which records accelerations with three orthogonally mounted accelerometers.

- Izumiya et al (1988, pp 207-216) and Buchan et al (1984, pp 287-303) describe measurement for directional spectra using

wave gauges together with current meters which measure wave orbital motions.(Triaxial current meters (Sec. 3.2.1.2) can also be used.)

1.6 WAVE MEASUREMENT FROM ABOVE THE SURFACE

Waves can be measured from a remote location, such as from an aircraft or satellite, or at closer range, such as from the bows of a ship. Measurements with the use photography, radar, laser, and ultrasound are dealt with in this section.

1.6.1 Aerial photography

Single aerial photographs, and stereophotograph pairs may be analysed to obtain useful wave information.

1.6.1.1 Single aerial photographs

These photographs usually reveal prominent, long-crested trains of waves; their directions and lengths can be measured. In order to obtain quality photographs for manual analysis, certain criteria must be followed:

(i) The sea state must be suitable for a meaningful image, i.e. waves of desirable length and height must be present. Local wind chop is helpful, as it adds texture to the surface.

(ii) The optimum scale must be selected; this is accommodated by altitude. Generally the appearance of wave crest organisation increases with altitude.

(iii) Lighting and exposure are critical in producing photographs of a usable quality. High sun angles are best, for wave-crest enhancement in all directions (McClenan and Lee Harris, 1975, pp 12-27).

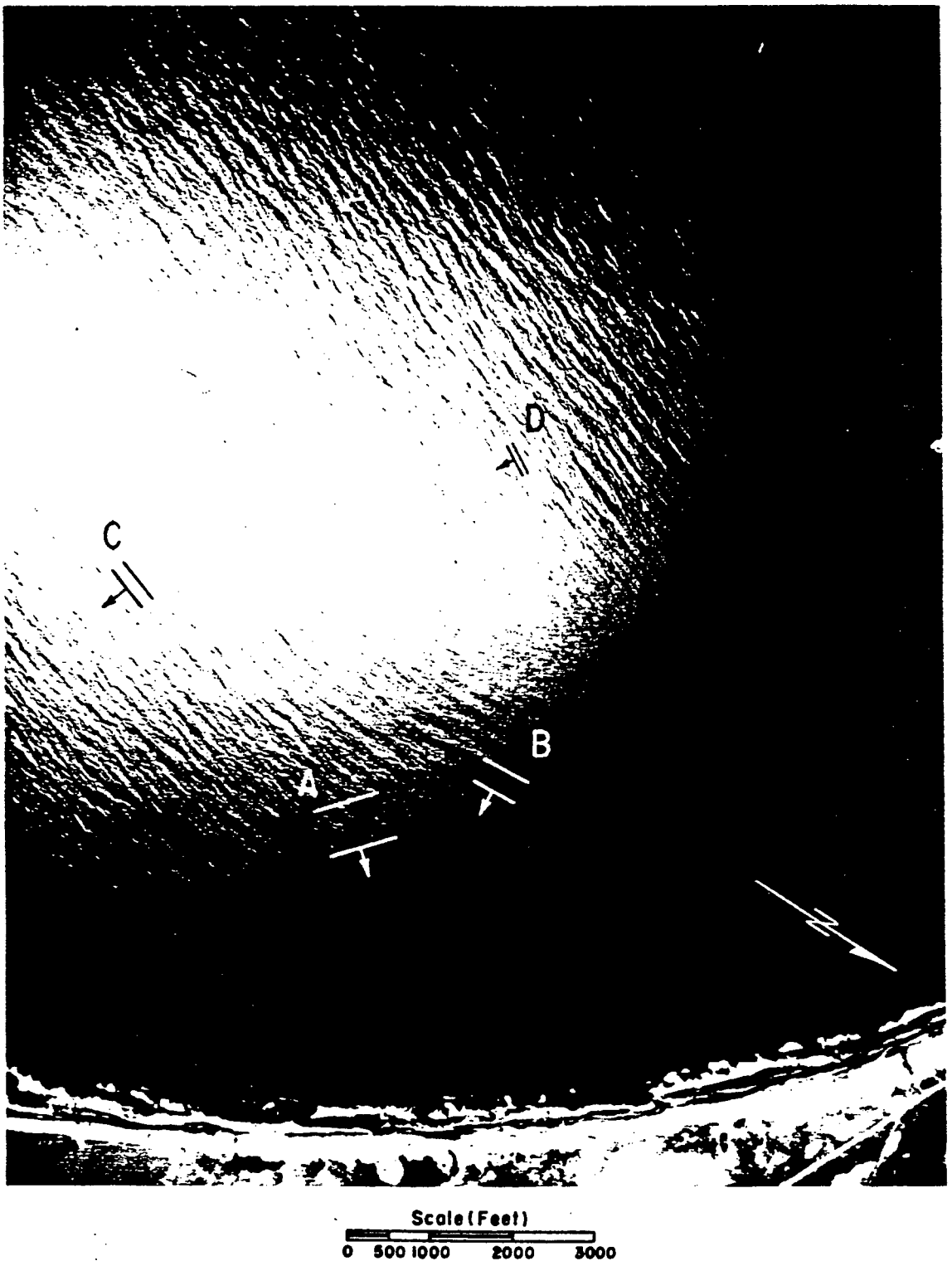

Figure 1.24 : Obtaining wave lengths and wave directions from an aerial photograph.

after McClenan and Lee Harris (1975)

Fig. 1.24 illustrates the manual extraction of prominent wavelengths and wave directions from an aerial photograph. This information can be used to enhance one-dimensional spectra with directional information (McClenan and Lee Harris, 1975).

Another approach is to process aerial photographs optically to yield a two-dimensional spectrum of optical density (i.e. brightness), with the use of an arrangement of lenses and a laser beam (this is called the holographic method). The resulting two-dimensional image spectrum (called a hologram) is found to be similar to the directional wave energy spectrum (The reason for this similarity is that the lenses have the same transfer function as a Fourier integral; Sec. 2.2.2 deals with the use of Fourier integrals to obtain wave spectra). According to Ichiye and Sugimori (1974, pp 139-151), a directional spectrum could possibly be produced from a hologram together with a wave record. Research is continuing on this topic.

1.6.1.2 Stereophotography

The human brain can combine two slightly different images received by the eyes into one three-dimensional impression. With two photographs taken of an object from two positions, a three-dimensional image can be artificially observed (this is called artificial stereoscopy). To obtain accurate measurements in these photographs, a complicated apparatus, incorporating a stereoscopic viewing device, is required; measurements in all three dimensions are then possible.

The two stereophotographs must be taken from two aircraft. Holthuijsen et al (1974, p 159) make use of two helicopters. It is important that the cameras are synchronised - this is achieved using a radio signal. Details of this radio system and the selection of appropriate cameras are discussed by Holthuijsen et al (1974, p 160).

To obtain correct spatial co-ordinates from stereophotos, a level of reference and a scale is required. An arbitrary level of reference can be chosen. The scale of a photo can be obtained:

(i) By including a known length in a photograph e.g. a ship of known length.

(ii) By registering the altitude of the aircraft.

(iii) By recording the distance between the cameras. Holthuijsen et al (1974, p 158) achieves this with a third camera; this is used to photograph one of the helicopters from the other; the distance between them can be obtained geometrically, from the known dimensions of the photographed helicopter.

Stereophotographs are analysed manually with the use of specialized apparatus. The result is a "contour map" of the ocean surface. From this, using spectral analysis, the directional wave energy spectrum can be obtained.

Stereophotography covers a large representative area of the ocean surface, and it is a very accurate method. However, it has some disadvantages:

(i) It is time consuming.

(ii) It is expensive, due to aircraft usage.

(iii) Photography is limited to daylight hours and good weather.

Another form of remote measurement, which is unaffected by these factors, is radar.

1.6.2 Wave measurements with radar

Radar electromagnetic waves transmitted onto the sea surface are reflected in a fashion dependent on surface wave forms. The reflected electromagnetic waves, called backscatter, are detected by a radar receiver. This received signal contains useful information about the ocean surface.

One of the only limitations of radar is that reflection of radar waves from heavy rain and snow can make measurements impossible; this effect is

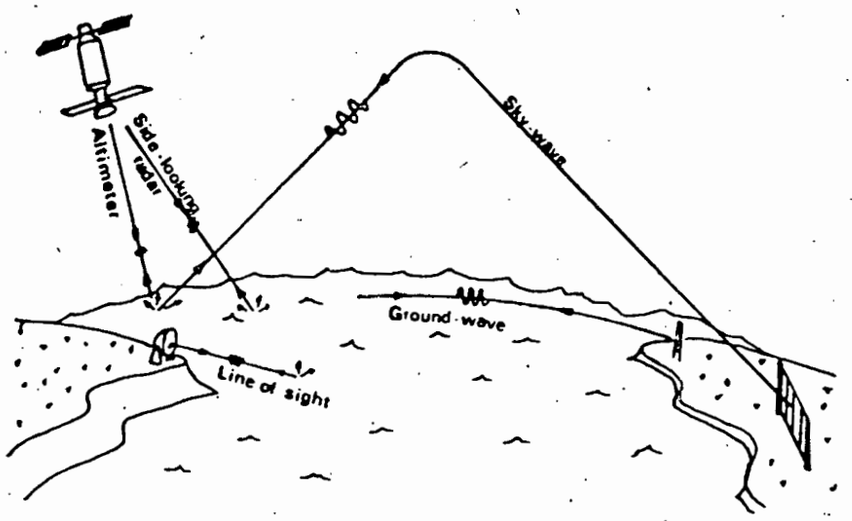

Figure 1.25 : Radar techniques

Cracknell (1981)

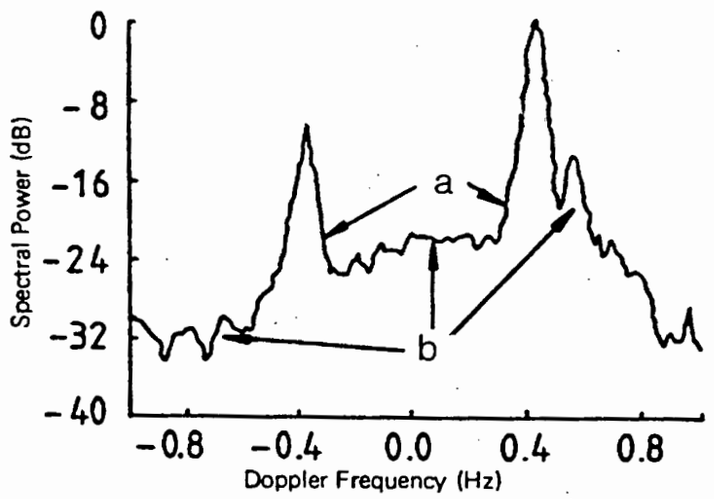

Figure 1.26 : The Doppler Spectrum, showing
(a) first order peaks ;
(b) the second order spectrum.

after Cracknell (1981)

Since θ is generally close to 0°:

$$L \approx \frac{\lambda}{2}$$

i.e. ocean waves with half of the wavelength of the radar waves cause Bragg scattering. In addition, this phenomenon only occurs for waves moving directly toward and directly away from the radar (each of the two directions causes a Bragg line in the Doppler spectrum).

The high spectral power of the first order peaks is basically due to constructive interference of backscattered radio waves which are in phase. (Mattie and Lee Harris, 1978, pp 175-176). By varying the frequency of the radar, the direction and wavelength of specific trains of waves in the ocean can be interpreted from these peaks; Cracknell (1989, p 315) and Teague et al (1977, p 13) discuss this.

Second order backscatter power ((b) in Fig. 1.26) surrounds the first order peak. It arises from "second order wave dynamics" and "double scatter of radio waves" (Heron, 1985, p 397). This second order spectrum is more useful, since the root mean square wave height (accurate within 10 %), the one dimensional wave energy spectrum, and the directional distribution of waves can be obtained from it (the significant wave height can be calculated from the root mean square wave height; Sec. 2.1.2.1.).

H.F. ground-wave radar operates from a coastal station, as illustrated in Fig. 1.25. Since H.F. dekametric waves bend around the earth's surface (due to refraction), ranges of up to 400 km are practical.

Alternatively,sky-wave H.F. radar waves can be reflected off the ionosphere to the site of interest. Ranges of the order of 3000 km are possible, and ocean areas for detection can be selected at random. Unfortunately the technique is affected by ionosphere conditions; Anderson (1986, p 158) states: "it is generally accepted that for a substantial fraction of the time, measurements based on the second order spectrum will not yield accurate results." Maresca and Carlson" (1978, p 195) confirm that "ionospheric contamination" of radar signals is "the largest error source" for measurements based on second order spectra. Techniques are used to

minimize the effects of unsuitable ionospheric conditions, e.g. Earl and Ward (1986, p 164-173) and Maresca and Carlson (1978, p193) describe the determination of an optimum radar frequency, according to ionospheric conditions which are detected with specialized equipment.

Although skywave radar is not effective in measuring individual waves, wave parameters, such as the significant wave height, can be interpreted; comparisons of these were made with parameters obtained from wave measurements taken at wave buoys, oil platforms and from aircraft; Maresca (1976,p286) concludes: "H.F. Skywave radar can provide operational surface data that are as accurate as the more recognized *in situ* measurements."

1.6.2.2 Microwave radar

Microwave radar waves have wavelengths of the order of a few centimetres. Unlike H.F. radar, these waves propagate in a straight line. Thus the sea surface to be measured must be in the line of sight of the radar. The waves are transmitted onto the ocean surface and are backscattered, mainly due to Bragg scattering (as described above in 1.6.2.1). Since their wavelength is short, they are Bragg scattered by short waves i.e. capillary waves and short gravity waves. The long gravity waves of interest are detected through the modulation (i.e. the changing of wave properties) of radar waves, when backscattered. This modulation is due to at least three processes: (Mattie and Lee Harris, 1978, p 176)

(i) The convergence zone on the front face of long ocean waves increases the height and decreases the length of short capillary waves (from which the radar waves are backscattered), as shown in Fig. 1.27. This is discussed by Reece and Shemdin (1974, pp 82-92), by Reece (1978, pp 203-214), and by Wright (1978, p 87-107).

(ii) Radar backscatter power is a function of the grazing angles (θ_2 and θ_2 in Fig 1.28) incident on long gravity waves.

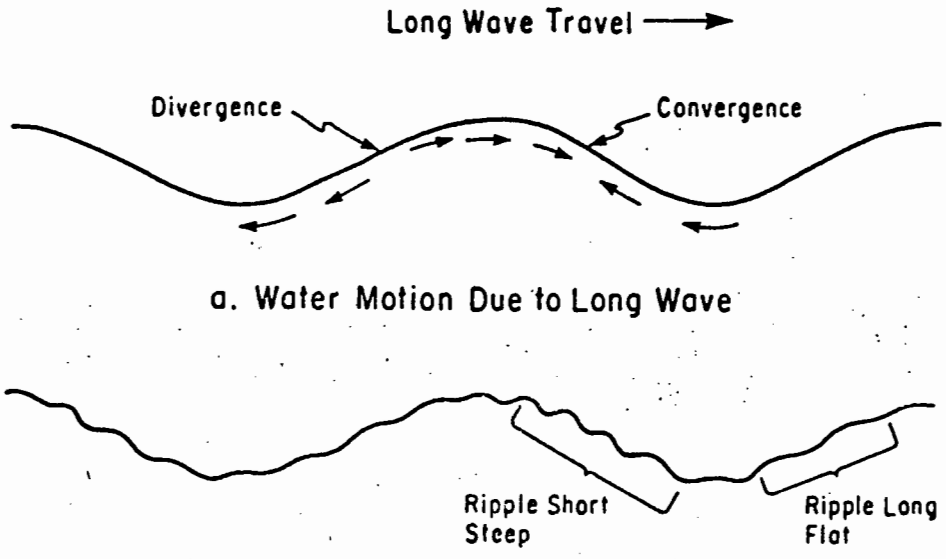

Figure 1.27 : Modulation of short waves by long waves.

after Mattie and Lee Harris (1978)

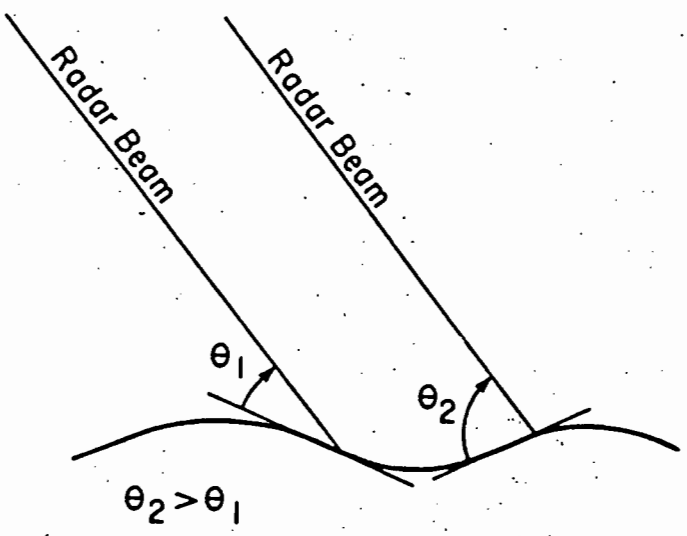

Figure 1.28 : The effect of a long gravity wave on grazing angles.

after Mattie and Lee Harris (1978)

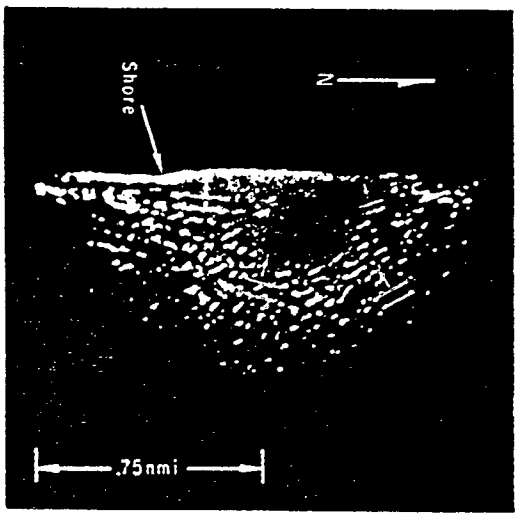

Figure 1.29 : The radar image.

Mattie and Lee Harris (1978)

(iii) When the grazing angle is low, the crest of a wave may "shelter" the following trough from incident radar waves, causing a contrast of backscatter from different parts of long gravity waves.

Since backscatter occurs mainly from short waves which are generated by local wind, long waves may not be detected in the absence of local wind, or in the presence of oil slicks (Mattie and Lee Harris, 1978, p174). For example, the C.E.R.C. groundbased radar requires a minimum wind speed of 2.5 m/s to obtain a meaningful image.

Microwave radar can be used to obtain two-dimensional images of the ocean, similar to aerial photographs. The advantage over aerial photography is that it functions overnight and during storms. Fig. 1.29 shows that wavelengths and wave directions of wave trains can be manually extracted from a radar image (in the figure, wavelength is represented by parallel lines; and direction by a third line). However, wave height cannot be measured directly.

As with aerial photography (Sec.1.6.1.1), it is possible to obtain a two-dimensional spectrum of brightness. It has been found (Shemdin et al, 1978, pp 193-202) that these spectra have surprising similarities to spectra from pitch-and-roll buoy measurements. However, "much more theoretical and experimental work is still needed to relate, in an absolute manner, the directional spectrum of a radar image to that of the surface waves" (Elachi, 1978, p 169)

Various types of microwave radar are discussed below:

(a) Shorebased radar:

Fig. 1.29 is an example of an image obtained from a shorebased radar. Shorebased radar may be fixed, or mobile e.g. C.E.R.C. have a microwave radar mounted on a trailer, which provides two-dimensional radar images, as mentioned above (Sec. 1.6.2.2). This radar was compared with four *in situ* wave gauges, including an array of 4 pressure gauges (Grosskopf et al, 1983, p 254-271). The radar compared well with the other instruments, however it "did not always

successfully identify multidirectional wave components at different frequencies". In other words, some wave trains were not detected.

(b) Side-looking airborne radar (S.L.A.R.):

S.L.A.R. is generally used from aircraft to obtain an image of the sea surface (it detects waves by means of the amplitude modulation of microwaves as they are backscattered). In an experiment, spectra derived from a S.L.A.R. were compared to wave energy spectra (Sec. 2.2) measured by a Datawell Waverider buoy. The result was that "although measuring techniques are completely different, the shapes of the curves (i.e. the spectra) are strikingly similar."

(c) Synthetic aperture radar (S.A.R.):

S.A.R. is a more advanced form of microwave radar than S.L.A.R., for wave measurement. It can be operated from an aircraft or satellite travelling in a straight line. Microwave pulses are transmitted and received in such a manner as to be equivalent to a single antenna as long as the flight path (hence a long aperture, or antenna, is effectively "synthesised")

From the S.A.R., an image similar to an aerial photograph is obtained. From this image, wavelength and wave direction can be obtained easily and reliably. Wave height cannot be measured directly, and may only be estimated from empirical relations.

A problem with airborne (or satellite mounted) radar is that it does not take an instantaneous "snapshot" of the ocean. Therefore, if a scene is processed as if the ocean were stationary, the image will be distorted, since waves move during the time taken to image them. This complication is affected by the direction of flight; the best radar image is obtained when the direction of wave propagation is perpendicular to the aircraft flight line (Shuchman et al, 1983, p 90-96).

In order to obtain an indication of the performance of S.A.R., Shemdin et al (1978, p 201) compare S.A.R. data with that of a pitch- and-roll buoy. Agreement in the dominant wave direction "within a few degrees" was found. In addition, a comparison of spectra derived from the radar

image with spectra from a pitch-and-roll buoy was "surprisingly good, considering little is known about imaging mechanisms from the S.A.R.". Moreover, Mattie et al (1981, p 87-93) compare wave data from S.A.R. to that from aerial photographs, land based radar, and an array of pressure sensors, with the result that "intercomparison of data from these 4 systems shows good agreement among the imaging systems" (i.e. among the remote sensing systems).

(d) The radar altimeter:

A radar altimeter transmits microwave pulses to the sea surface. The shape of the reflected pulse is altered according to the heights of waves. A graph of the backscatter power versus time for the reflected pulse can be recorded and matched with a theoretical graph, derived from Gaussian wave distributions corresponding to a particular significant wave height. Thus, the significant wave height can be estimated (Walsh et al, 1978, pp 253-276). From "tests done so far" the Seasat-1 radar altimeter has an accuracy of within 10 % of the significant wave height, or 0,5 m, whichever is greater. (Townsend, 1980, p 80-92)

(e) Shipborne radar:

This radar may be used while a ship is in motion, to obtain a wave record. A radar transmitter on the bows of the ship transmits electromagnetic microwaves vertically down onto the ocean surface below it. The waves are reflected back by the fluctuating sea surface; there is a Doppler shift in frequency due to the movement of the surface. This Doppler shift is detected and represents the water surface velocity in the vertical direction; integration of this velocity yields displacement of the water surface.

In order to account for ship motions, an accelerometer is also installed just behind the bow. The acceleration measured is integrated twice to obtain the ship's displacement from a reference level, which is then combined with the radar record to obtain the actual wave record.

Yasuda et al (1985, pp 138-143) describe this type of gauge. Kaplan and Ross (1968, pp 501-505) describe the comparison between a radar of

the above type with a similar acoustic sensor. The result is that "the outputs of the sonic and radar sensors are in excellent agreement with each other".

1.6.3 Laser

A wave record can be obtained using a laser beam, transmitted by an aircraft, which reflects off the sea surface. The instantaneous aircraft elevation above the sea surface is determined by comparing the phases of the transmitted and reflected signals. Thus, the wave record can be interpreted from the elevation record of an aircraft flying at constant altitude.

This laser type of instrument is extremely accurate; at a height of 60 m, and an aircraft velocity of 240 km/hr, ripples of 2,5 cm height can be recorded (Olsen and Adams, 1974, pp 2185-2187). However, because of aircraft expenses, the technique is not suitable for routine wave measurement.

1.6.4 An ultransonic instrument

An ultransonic altimeter can be attached to the bow of a ship; its height above the ocean surface is determined by electronically by measuring the delay between transmitted and reflected ultrasonic pulses. As occurs with the shipborne radar (Sec 1.6.2.2), an accelerometer detects ship displacements; this record is combined with the ultrasonic record to yield the wave record (Kaplan and Ross, 1968, pp 501-507).

1.7 CONCLUSION

It is clear that there are many well-developed techniques for wave measurement. The following conclusions are pertinent:

(i) Wave staffs are useful where an attachment structure is available; provided that they are regularly maintained, they provide results sufficiently accurate for engineering purposes.

(ii) Pressure gauges are useful where shipping traffic is heavy; however accuracy is lost in the analysis of the surface wave record.

(iii) The most successful and extensively used instrument for wave measurement, at a single point, is the Waverider buoy.

(iv) Effective means of measuring the direction of prominent wave trains have been devised, particularly with the D.O.S.O. gauge.

(v) The most promising technique for wave measurement is the use of HF radar. It has the advantage over conventional point measurement techniques since large areas of the ocean can be covered at one time; directional information can also be obtained.

BIBLIOGRAPHY : CHAPTER 1

Adamo, L.C., Steele, K.E. and Burdette, E.L. 1978 "A GOES-reporting Waverider Buoy", Proceedings Oceans '78, Vol. 1, pp 31-36.

Anderson, S.J. 1986 "Remote Sensing with the Jindalee Skywave Radar", I.E.E.E. Journal of Oceanic Eng., Vol.OE-11, No.2, pp.158-163.

Ayela, G., Ezraty, R., Hue, J.P., Coudeville, J.M. 1985 "Spear-F, a Wave Height Spectrum Buoy via ARGOS and the New IFREMER static Wave Directional Sensor", Ocean Engineering and the Environment, Vol.2, pp.707-712.

Bass, J.C. and Byrnes, R.M. 1974 "Precision Electro-optical Wave and Tide Gauge", Proc. of the International Symposium on Ocean Wave Measurement and Analysis, Vol.2, pp.190-199.

Biglow, J.W. 1965 "Low Cost Wave Recording System", Marine Sciences Instrumentation, Vol 4, pp 94-98.

Black, D.L. 1964 "A Stabilized Buoy for Oceanographic and Meteorological Instrumentation", Buoy Technology, March 1964, pp.458-472.

Blair, P.M. 1974 "Buoy for Recording Ocean Wave Height and Period", Proc. of the International Symposium on Ocean Wave Measurement and Analysis, Vol.1, pp.254-271.

Bodge, K.R. and Dean, R.G. 1984 "Wave Measurement with Differential Pressure Gauges", Proc. of the 19th Coastal Eng. Conf, Vol.1, pp.755-769.

Boiten, E.H. 1960 "Wave Height Measuring Equipment", Proc. of the 7th Coastal Eng. Conf., Vol.1, pp.114-125.

Bowler, E.H. 1974 "A Description of Three Wave Measuring Instruments", Proc. of the International Symposium on Ocean Wave Measurement and Analysis, pp.562-584.

Buchan, S.J., Steedman, R.K., Stroud, S.A., and Provis, D.G. 1984 "A Shallow Water Directional Wave Recorder", Proc. of the 19th Coastal Eng. Conf., Vol.1, pp.287-303.

Cartwright, D.E.	1961	"The Use of Directional Spectra in Studying the Output of a Wave Recorder on a Moving Ship", Ocean Wave Spectra, May 1961, p.211.
Coetzee, L.	1988	Personal Interview, C.S.I.R., November 1988.
Cracknell	1981	Remote Sensing in Meteorology, Oceanography, and Hydrology, pp.312-356.
Datawell bv.	1976	Data Sheet for Waverider f1, Zomerluststraat 4, Haarlem, The Netherlands.
Davies, J.	1989	Personal Interview, C.S.I.R., May 1989.
Draper, L.	1970	"Remote Sea-wave Measurement - a Survey", Underwater Science and Technology Journal, 2, pp 81-86.
Earl, G.F. and Ward, B.O.	1986	"Frequency Management Support for Remote Sea State Sensing using the Jindalee Skywave Radar", I.E.E.E. Journal of Oceanic Engineering, Vol. OE-11, No.2, pp.164-173.
Elachi, C.	1978	"Radar Imaging of the Ocean Surface", Boundary Layer Meteorology, Vol.13,p.169.
Esteva, D. and Lee Harris, D.	1970	"Comparison of Pressure and Staff Wave Gauge Records", Proc. of the 12th Coastal Eng. Conf., pp.101-116.
Farmer, H.F. and Ketchum, D.D.	1960	"An Instrumentation System for Wave Measurement, Recording and Analysis", Proc. of the 7th Conf. in Coastal Eng., pp.77-99.
Finkelstein, J.L.	1964	"A Stabilized Wavemeter for the Measurement of Open Ocean Waves", Buoy Technology, pp 39-46.
Folsom, R.G.	1949	"Measurement of Ocean Waves", Trans. of the American Geophys. Union, Vol.30, No.5, pp.691-699.
Gerhardt, J.R., Jehn, K.H. and Katz. I.	1955	"A Comparison of Step-, Pressure-, and Continuous Wire Gauge Wave Recordings in the Golden Gate Channel", Trans. of the American Geophys. Union, Vol.30, No.5, pp.691-699.

Grosskopf, W.G., Aubrey, D.G., Mattie, M.G. and Mathiesen — 1983 — "Field Intercomparison of Nearshore Directional Wave Sensors", I.E.E.E. Journal of Oceanic Engineering, Vol.OE-8, No.4.

Hashimoto, H. and Yamaguchi, O. — 1980 — "Development of a Surface Buoy Wave Meter", Coastal Engineering in Japan, Vol.23, pp.101-119.

Heron, M.L. — 1985 — "Line Broadening on H.F. Ocean Surface Radar Backscatter Spectra" I.E.E.E. Journal of Oceanic Engineering, Vol.OE-10, No.4, p.397.

Holthuijsen, L.H., Tienstra, M. and van der Vliet, G.J. — 1974 — "Stereophotography of the Sea Surface, an Experiment", Proc. of the International Symposium on Ocean Wave Measurement and Analysis, Vol.1, pp. 153-169.

Ichiye, T. and Sugimori, Y. — 1974 — "Holographic Method of Wave Spectrum Measurement", Proc. of the International Measurement and Analysis, Vol.1, pp.139-152.

Inter Ocean Systems Inc. — Wavebuoy data sheet.

Izumiya, T., Isobe, M., Shimuzu, T., Hosogai, T. and Aoki, T. — 1988 — "Field Measurement of Directional Spectra with Combined Systems of Wave Gauges and Current Meters", Coastal Engineering in Japan, Vol.31, No.2, pp.207-217.

James, W.R. and Hallermeier, R.J. — 1976 — "Nearshore Wave Direction Gage", Journal of the Waterways, Harbors and Coastal Engineering Division, A.S.C.E., Vol.102, No.WW4, pp. 379-391.

Kaplan, P. and Ross, D. — 1968 — "Comparative Performance of Wave Measuring Systems mounted on Ships in Motion at Sea", Marine Sciences Instrumentation, Vol.4, pp.501-505.

Kim, Y.Y. and Simons, L.H. — 1974 — "Sea State Measurements from Pressure Records", Proc. of the International Symposium on Ocean Wave Measurement and Analysis, Vol.1, pp.40-53.

Kronengold, M., Loewenstein, J.M. and Berman, G.A. — 1965 — "Sensors for the Observation of Wave Height and Wind Direction", Marine Sciences Instrumentation, Vol. 3, pp.273-288.

Larsen, L.H. and Fenton, D.	1974	"Observations of Waves in the North Pacific", Proc. of the International Symposium on Ocean Wave Measurement and Analysis, Vol.1, pp. 197-213.
Lee, D. and Wang, H.	1984	"Measurement of Surface Waves from Subsurface Gauge", Proc. of the 19th Coastal Eng. Conf., Vol.1, pp. 271-286.
Lowe, R.L. Inman, D.L. and Winant, C.D.	1974	"Current Measurements using a Tilting Spar", Proc. of the 14th Coastal Eng. Conf., Vol.1, pp.225-239.
Maresca, W.J. and Carlson, C.T.	1978	"HF Skywave Radar Measurement of Hurricane Winds and Waves", Proc. of the 16th Coastal Eng. Conf., Vol.1, pp.190-207.
Marks, W. and Tuckerman, R.G.	1960	"Splashnik - the Taylor Model Basin Disposable Wave Buoy", Proc. of the 16th Coastal Eng. Conf., Vol.1, pp.190-207.
Mattie, M.G. and Lee Harris, D.	1978	"The Use of Imaging Radar in Studying Ocean Waves", Proc. of the 7th Coastal Eng. Conf., Vol.1, pp. 100 -113.
Mattie, M.G., Hsiao, S.V. and Evans, D.D.	1981	"Wave Direction Measured by Four Different Systems", I.E.E.E. Journal of Oceanic Engineering, Vol.OE-6, No.3, pp.87-93.
McClenan, C.M. and Lee Harris, D.	1975	"The Use of Aerial Photography in the Study of Wave Characteristics in the Coastal Zone", Technical Memorandum No.48, C.E.R.C., U.S. Army Corps of Engineers.
Mitsuyasu, H.,Tasai, F., Suhara, T.,Mizuno, S.Ohkusu, M., Honda, T. and Rikiishi, K.	1975	"Observations of the Directional Spectrum of Ocean Waves Using a Cloverlear Buoy", Journal of Physical Oceanography, Vol.5, pp.750-759.
Olsen, W.S. and Adams, R.M.	1974	"A Laser Profilometer", Journal of Geophys. Res., Vol.75, Mar-Apr 1974,, pp.2185-2187.
Peacock. H.G.	1974	"C.E.R.C. Field Wave Gauging Program", Proc. of the International Symposium on Ocean Wave Measurement and Analysis, Vol.1, pp.170-185.
Pilon, J.J.	1974	"Wave Gauges in Coastal Areas", Proc. of the International Symposium on Ocean Wave Measurement and Analysis, Vol.1, p.600.

Ploeg, J.	1972	"Some Results of a Directional Wave Recording Station", Proc. of the 13th Coastal Eng. Conf., Vol.1, pp.131-143.
Reece, A.M.	1978	"Modulation of Short Waves by Long Waves", Boundary Layer Meteorology,Vol.13, pp.203-214.
Reece, A.M and Shemdin, O.H.	1974	"Modulation of Capillary Waves by Long Waves", Proc. of the International Symposium on Ocean Wave Measurement and Analysis, Vol.2, pp.82-92.
Retief, G. de F., and Vonk, A.P.M.	1974	"A Low-cost Inshore Wave Direction Indicator", Proc. of the 14th Coastal Eng. Conf., Vol.1, pp.212-224.
Reynolds, J.R. and Hoffman, J.F.	1974	"Least Cost Gauge Buoy for Measurement and Analysis of Ocean Waves", Proc. of the International Symposium on Ocean Wave Measurement and Analysis, Vol.1, pp.639-648.
Ribe, R.L. and Russin, E.M.	1974	"Ocean Wave Measuring Instrumentation", Proc. of the International Symposium on Ocean Wave Measurement and Analysis, Vol.1, pp.396-416,
Schuchman, R.A., Maffet, A.L. and Klooster, A.	1983	"Static and Dynamic Modelling of a S.A.R. Imaged Scene", I.E.E.E. Journal of Oceanic Engineering, Vol. OE-8, pp.90-96.
Seiwell, H.R.	1947	"Investigation of Underwater Pressure Records and Simultaneous Sea Surface Patterns", Trans. of the American Geophys. Union, Vol.28, No.5, pp.722-724.
Shemdin, O.H., Brown, W.E., Staudhammer, F.G., Schuchman, R., Rawson, R., Zelenka, J., Ross, D.B., McLeish, W., Berles, R.A.	1978	"Comparison of In Situ and Remotely Sensed Ocean Waves off Marineland, Florida", Boundary Layer Meteorology, Vol.13, pp.193-202.
Stilwell, D.	1969	"Directional Energy Spectra of the Sea from Photographs", Journal of Geophys. Res., Vol.74, Mar-Apr 1969, pp.1974-1986.
Stilwell, D. and Pilon, R.O.		"Directional Spectra of Surface Waves from Photographs", Journal of Geophys. Res., Vol.79, March, .

Takahashi, T. and Soejima, T.	1974	"Coastal Wave Observation and Information for Engineering Use in Japan", Proc. of the International Symposium on Ocean Wave Measurement and Analysis, Vol.2, pp.62-81.
Teague, C.C., Tyler, G.L. and Stewart, R.H.	1977	"Studies of the Sea Using H.F. Radio Scatter", I.E.E.E. Journal of Oceanic Engineering, Vol.OE-2, No.1. pp.12-19.
Townsend, W.F.	1980	"An Initial Assessment of the Performance Achieved by the Seasat-1 Radar Altimeter", I.E.E.E. Journal of Oceanic Engineering, Vol. OE-5, No.2, pp.80-92.
Tucker, M.J.	1956	"A Shipborne Wave Recorder" Proc. of the First Conf. on Coastal Engineering Instruments, Berkeley California, Oct. 31-Nov 2, 1955, pp 122-118.
Tucker, M.J.	1989	"Interpreting Directional Data from Large Pitch-Roll-Heave Buoys", Ocean Engineering, Vol. 16, No. 2, pp 173-192.
Verhagen, C.M.	1957	"Improvements in the Electric Step Gauge for Measuring Wave Heights", Proc. of the 6th Coastal Eng. Conf., p.225.
Walsh, E.J. Uliana, E.A. and Yaplee, B.S.	1978	"Ocean Wave Heights Measured by a High Resolution Pulse-limited Radar Altimeter", Boundary Layer Meteorology, Vol.13, pp.263-276.
Williams, L.C.	1969	"C.E.R.C. Wave Gauges", Technical Memorandum no.30, C.E.R.C., U.S. Army Corps of Engineers.
Wright, J.M.	1978	"Detection of Ocean Waves by Microwave Radar; the Modulation of Short Gravity and Capillary Waves", Boundary Layer Meteorology, Vol.13, pp.87-107.
Yasuda, A., Kuwashima, S. and Kanai, Y.	1985	"A Shipborne-type Wave-height Meter for Oceangoing Vessels, using Microwave Doppler Radar", I.E.E.E. Journal of Oceanic Engineering, Vol.OE-10, No.2, April 1985, pp.138-143.
Zwamborn, J.A., van Schaik. C. and Harper, A.	1970	"Ocean Wave Research in Southern Africa", Proc. of the 12th Conf. on Coastal Eng., Vol.1, pp.13-32.
Zwamborn, J.A.,	1972	"Coastal Engineering Measurements",

Russel, K.S. and Nicholson, J. — CSIR Report ME 1148, Stellenbosch.

CHAPTER 2: THE ANALYSIS OF WAVE RECORDS

Once a wave record has been measured (as discussed in Chapter 1), it may be analysed to obtain useful parameters. There are two types of analysis:

(i) Statistical methods.
(ii) Spectral analysis.

In this chapter, statistical methods, involving simple, manual analysis, are intially discussed. This is followed by spectral analysis, which is more complex, and requires the use of microcomputers. Thereafter, the presentation of analysed parameters, in forms useful to the coastal engineer, is dealt with. Finally, some applications of analysed wave parameters in coastal engineering are outlined.

2.1 STATISTICAL METHODS OF WAVE DATA ANALYSIS

This involves simple manual treatment of wave data. The methods apply to analogue wave records, such as strip chart records, which are roughly 20 minutes long (e.g. Fig. 2.2). Since this type of recording is still in use at present, these methods are relevant, even though spectral analysis is more efficient.

Firstly, the wave height and wave period must be defined. As shown in Fig. 2.1, vertical lines are drawn at the point where the wave record crosses the zero line (i.e. mean record line), from above to below. An interval between these lines defines a single value of the zero-crossing period, T_z (an average of all of these periods in the record is usually obtained). The wave height, H_z, is defined as the distance from the lowest to the highest point of the wave trace during the interval, as shown.

If all the wave heights obtained in this way are ranked in height, the average height of the one-third highest waves is the <u>significant wave height</u> ($H_{1/3}$ or H_s). It will be shown later (Sec. 2.3), that this parameter is very useful in coastal engineering. This technique of obtaining the significant

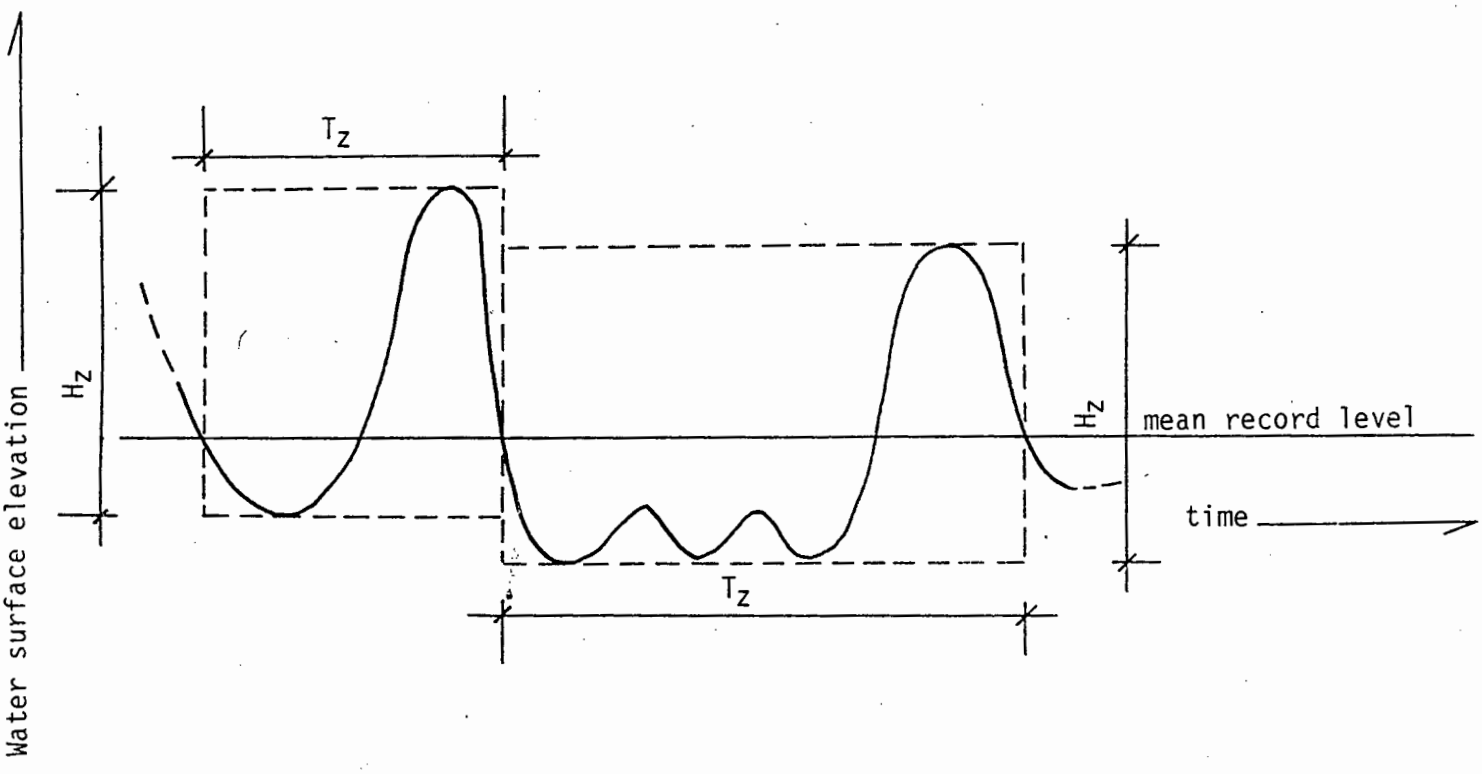

Figure 2.1 : Definition of wave height, H_z and period, T_z

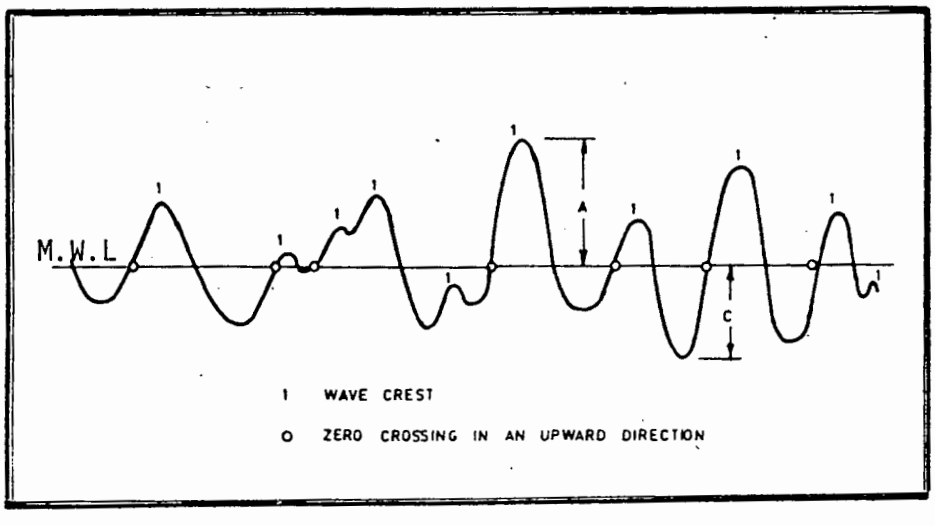

Figure 2.2 : An illustration of the simple measurement of a wave record (only short length of record shown).

after Dattatri & Nayak (1976)

wave height, and the zero-crossing period is extremely tedious; therefore, easier statistical methods have been devised, such as the C.E.R.C. method, and the Draper method.

2.1.1 The C.E.R.C. method

This method assumes that the statistical array of wave heights from a record conform to the Rayleigh distribution. From this distribution, the significant wave height may be shown to be the (0,135 N)th highest wave, where N is the number of waves in the record. Thus, the significant wave height can be found by simply ranking the larger waves in descending order and counting down to the (0,135 N)th wave. (The significant wave height found in this fashion is called H_{CERC}). In this process, the number of waves, N , can be estimated easily by dividing the total deviation of the record by the average wave period, T_{CERC} (or T_c). T_{CERC} is found by taking the average period of a few of the best formed waves in the record.

The Shore Protection Manual (C.E.R.C, 1977) elaborates on this technique, providing graphs and examples. In addition, it is shown that the average of the highest wave of any percentage occurrence in the record can be found (e.g. $H_{2\,!}$, the average of the highest 10% of waves in the record, or H_{2} , the average of the highest 1% waves in the record).

2.1.2 The Draper method

The C.E.R.C method is susceptible to subjective interpretation. A far more objective method is described by Draper (1966, pp 1-11); this is a modification of Tuckers method (Tucker, 1961, p 231).

2.1.2.1 Practical Aspects

Fig. 2.2 illustrates a typical wave record, in which the mean water level (M.W.L.) may be drawn in by eye. Draper (1966) recommends that a 10 to 15 minute wave record is analysed. This involves extracting the following parameters from the wave record:

(i) the distance of the highest crest (A in Fig. 2.2) from the mean water level ;

(ii) the distance of the lowest trough (C in Fig. 2.2) from the mean water level ;

(iii) the number of crests, N_c (see Fig. 2.2) ;

(iv) the number of times, N_z, that the record crosses the mean water level moving in the upward direction (see Fig. 2.2).

From these parameters, a number of useful values can be calculated; including wave periods, the spectral width parameter, and wave heights.

(a) Wave periods

The most useful period obtainable from the Draper method is the zero-upcrossing period, T_z . According to Tucker (1963); "for most engineering purposes, T_z is the most significant wave period, since it tends to be the period of the largest waves in the record. It is also the one which appears more often in the statistical formulae." It is calculated simply :

$$T_z = \frac{\text{Record duration (seconds)}}{N_z} \qquad (2.1)$$

The crest period, T_c , can also be useful :

$$T_c = \frac{\text{Record duration (seconds)}}{N_c} \qquad (2.2)$$

Unfortunately, T_z is not accurate in all cases (Manchar et al, 1976, pp 273-277), particularly when the wave spectrum is bimodal. Period parameters obtained from spectral analysis (Sec. 2.2) are generally more reliable.

(b) The spectral width parameter, ϵ

This value indicates the width of the range of frequencies covered by the wave components in the sea, thereby indicating the occurrence of a regular swell or of waves of random height and direction. It is calculated as follows :

$$\epsilon^2 = 1 - (T_c \backslash T_z)^2 \qquad (2.3)$$

It can be useful in physical modelling, where the ϵ measured in the model can be compared to the prototype value of ϵ to check similarity.

(c) Wave height

The Draper method, as with the C.E.R.C. method, is based on the assumption that wave heights follow the Rayleigh distribution. With this assumption, the root mean square wave height (H_{rms}) can be calculated from the parameters A, C and N_z (Draper, 1966). Thereafter, $H_{1/3}$, the significant wave height, and H_{max}, the most probable value of the highest wave in some specified time interval, can be calculated from H_{rms}.

2.1.2.2 The reliability of the Draper method

According to Tucker (1963, p 314), the measurement of parameters A and C is not reliable, because wave recording instruments tend to yield spurious outputs. In addition, the theory on which the method is based was derived for (a) a narrow spectrum and (b) for the case where there is no correlation between successive waves in a sample (Tucker, 1963, p 314): this is obviously not always the case, since (a) waves may have a wide spectrum (i.e. waves may have a wide range of frequencies), and (b) waves generally travel in groups. Nevertheless, according to Draper (1963), relationships between wave parameters obtained experimentally are sufficiently close to theoretical relationships, for practical engineering purposes. Furthermore, Dattatri and Nayak (1976) found Tucker's method (on which the Draper method is directly based) to be applicable to waves off the West Coast of India; where the error in the computations, in a comparison with more refined, detailed calculations, was found to be less than 15%.

With the development of computers and digital wave recorders, spectral analysis is generally used in preference to the statistical treatment discussed here, since it yields a more complete description of the sea state. In addition, the significant wave height, the zero-upcrossing period, and other useful parameters can be obtained.

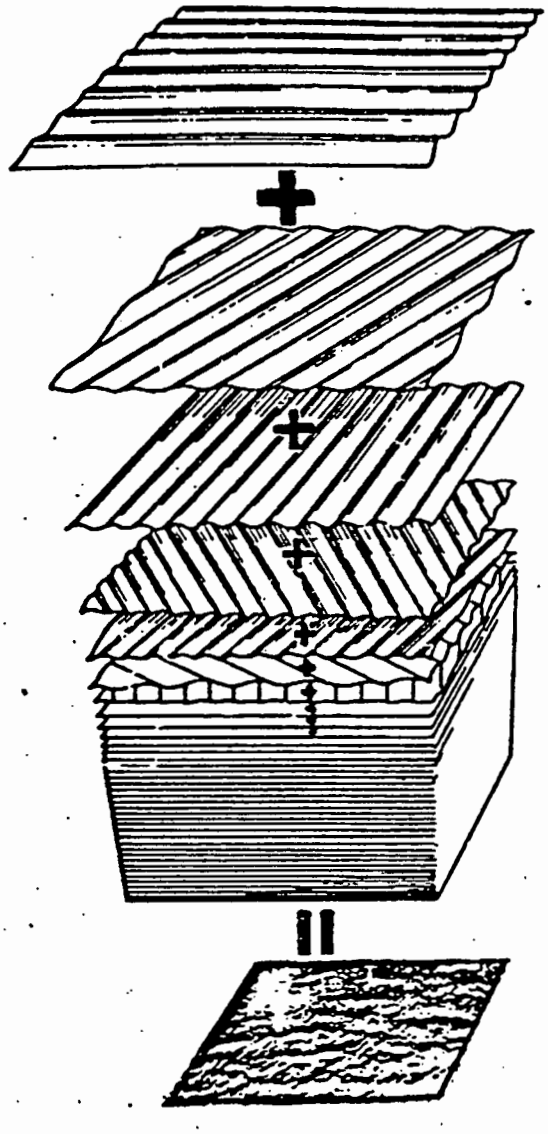

Figure 2.3 : The Sea Surface as the sum of sine waves.

after Bascom (1959)

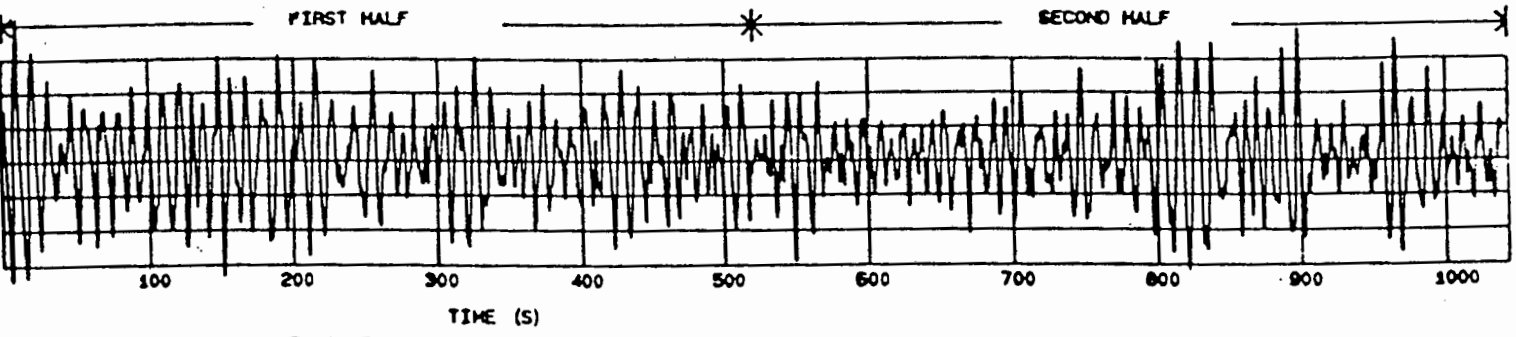

WAVE RECORD

Figure 2.4 : Wave record - recorded at Slangkop on 24-04-1988 with a Waverider buoy.

Environmental Data Processing, C.S.I.R.

s = energy density in m^2 contained in frequency band Δf

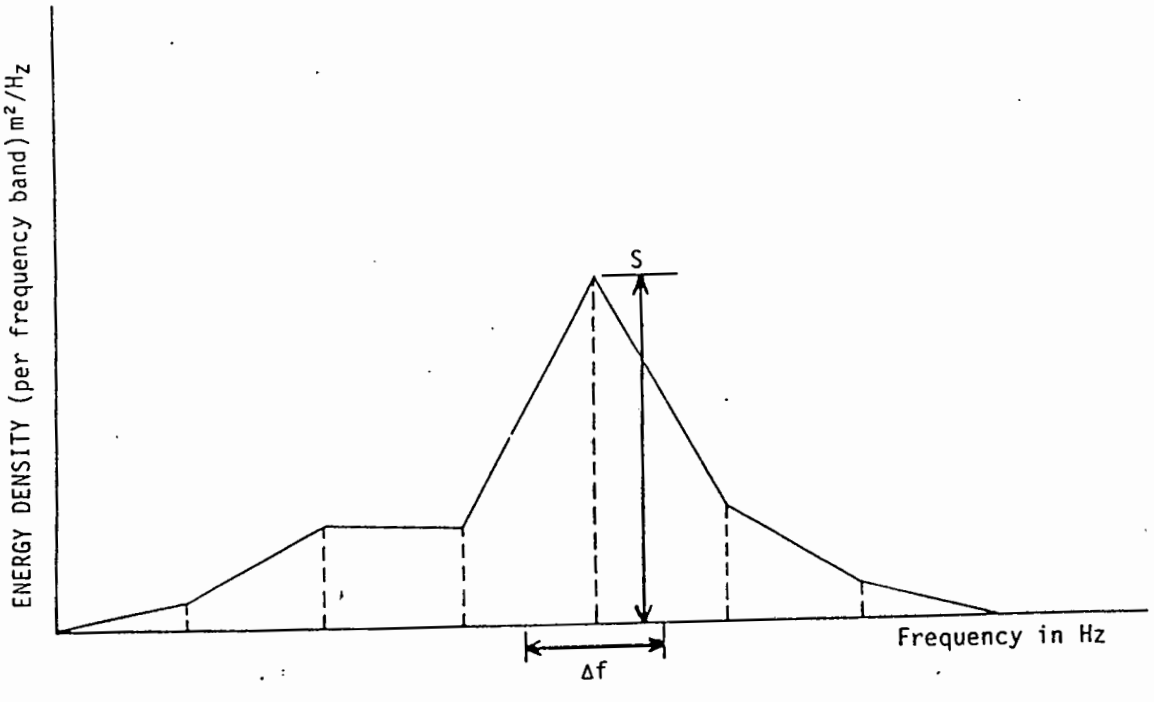

Figure 2.5 : The Wave Energy Spectrum (simplified).

2.2 SPECTRAL ANALYSIS OF WAVE DATA

2.2.1 Introduction

The motion of the sea can be considered as being the sum of an infinite number of sinusoidal wave trains of different heights, directions, periods, and phases; this is illustrated in Fig. 2.3. As shown in Chapter 1, wave recording instruments at a point can record the motion of the sea surface, to yield a record of sea surface elevation versus time (Fig. 2,4). From this wave record it is possible, by using Fourier analysis, to extract information concerning which component sinusoidal waves (or frequency components) make up the record. The final result is a graph relating the frequencies to the associated energies of these frequency components. Because of discretisation in calculations, and the use of a finite time wave record, frequencies are divided into bands and the energy contained in each band, i.e. energy density, is yielded (Fig. 2.5). This graph is described as the wave energy spectrum.

Wave energy spectra are useful to coastal engineers in the following instances :

(a) The design of harbour layouts. For example, Campbell et al (1979, p4) refer to the use of spectra in the layout design of Cape Town harbour.

(b) Designing for the oscillatory or pulsating forces of waves on elastic structures, such as oil rigs.

(c) Physical modelling, to reproduce irregular wave conditions.

(d) Design of coastal structures (useful parameters such as the significant wave height, H_{mo} , and the peak period, T_p , can be calculated from the spectrum).

(e) Determining safe depths of channels with respect to the motion of ships. For example, very large ships are brought into motion when the energy quantity in the frequency interval 0,035 to 0,1 Hz exceeds a certain value. (Broeders and van Loenen, 1974, p546).

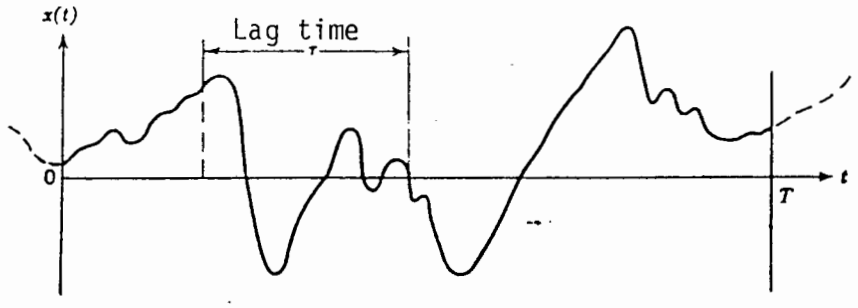

Figure 2.6 : A hypothetical wave record.

after Bendat and Piersol (1971)

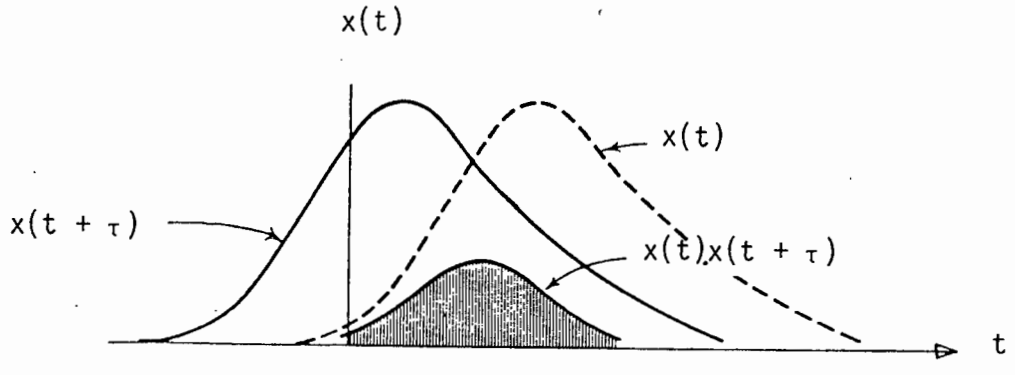

Figure 2.7 : The autocorrelation function represented by an area (shown shaded).

after Bracewell (1978)

(f) Early warning systems for storm waves, if the typical shapes of spectra preceding storms are known (useful for construction requiring calm conditions (Lawson and Youll, 1980, p.412)).

(g) The design of submarine pipelines (Alexander et al, 1984, 2726-2736).

There are 3 methods of calculating the wave energy spectrum:

(i) By the Fourier transform of the autocorrelation function ;
(ii) by using the Fast Fourier Transform (FFT) ;
(iii) the method of Maximum Entropy.

(i) and (ii), the more commonly used methods, are discussed in this thesis, where many aspects are common to both.

The wave energy spectrum can be calculated from a digitised wave record using computer programs, which have been adapted for use on microcomputers, found in appendix 1 and 2. The quality of such spectra depends on the users choice of various parameters. This requires an understanding of certain concepts; thus, this section deals firstly with background theory to spectral analysis. Thereafter, the preprocessing of wave data, an essential ingredient for a meaningful wave spectrum, is discussed. Following this, the concepts of leakage, confidence, and resolution, are explained, and the means of controlling them are discussed. Finally, some alternative approaches to spectral analysis are outlined.

In this chapter, use is made of computer programs to illustrate the effects of various parameters on wave spectra. In addition, frequent reference is made to the techniques used by the C.S.I.R. in South Africa.

2.2.2 Background theory

2.2.2.1 Wave Energy Spectra via autocorrelation

(a) The Autocorrelation Function

A record, of length T, of the water surface elevation taken at a point (i.e. an ocean wave record) may have the appearance of Fig. 2.6. The

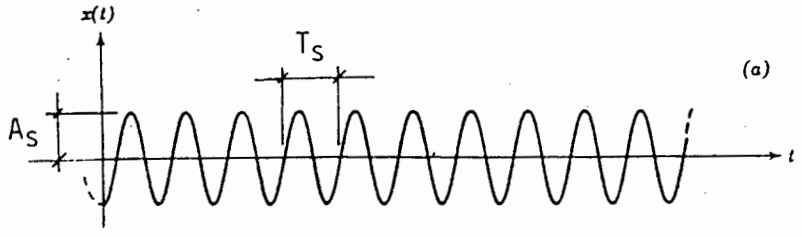

Figure 2.8(a) : A continuous sine wave.

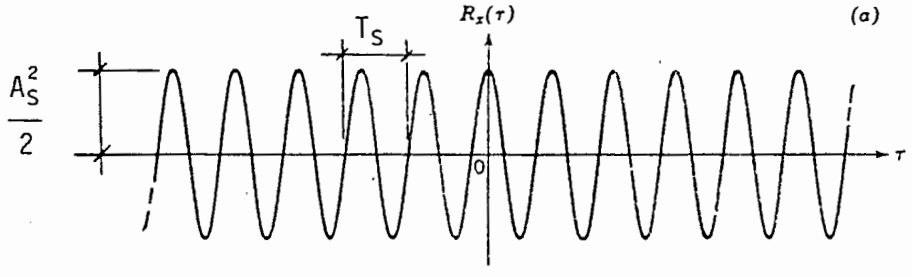

Figure 2.8(b) : Autocorrelation of the continuous sine wave.

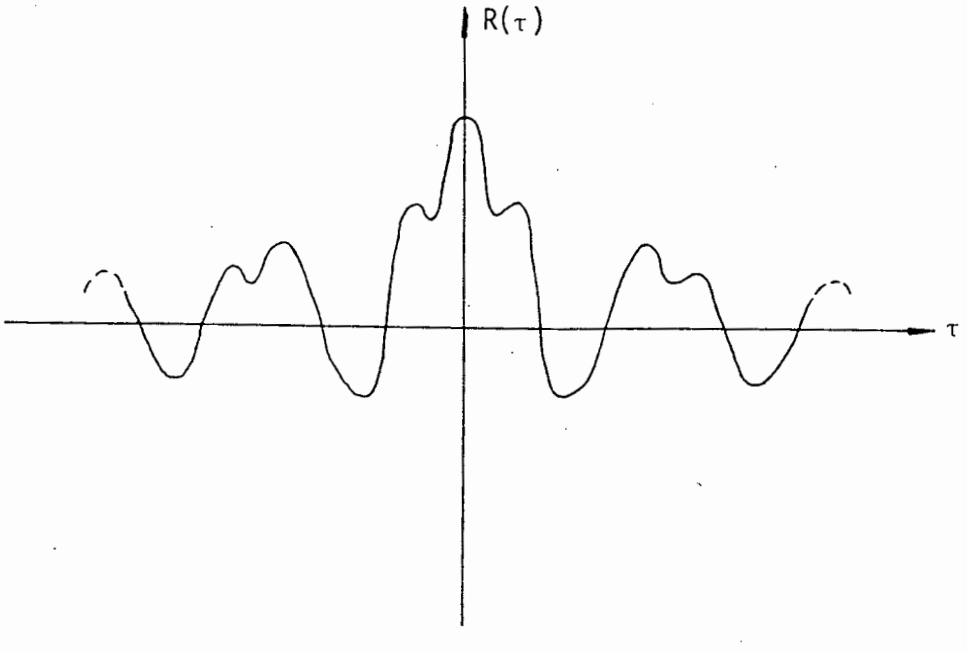

Figure 2.9 : Hypothetical autocorrelation of the wave record of Figure 2.6.

autocorrelation of this describes the dependence of data values at one time, x(t), on values of data at another time x(t + τ). τ is known as the lag time. According to Bendat and Piersol (1971, pp 18-20), this autocorrelation function is defined as

$$R(\tau) = \lim_{T\to\infty} 1/T \int_0^T x(t)\, x(t+\tau)\, dt \qquad (2.4)$$

This function is always a real valued, even function. Fig. 2.7 illustrates the idea of autocorrelation as the area under a curve.

Fig 2.8(b) illustrates the autocorrelation of the continuous sine wave of Fig. 2.8(a), which has amplitude A_s and frequency f_s (where $f_s = 1/T_s$). This autocorrelation function of Fig. 2.3(b) has the equation:

$$R(\tau) = A_s^2/2 \cos 2\pi f_s \tau \qquad (2.5)$$

The hypothetical ocean wave record of Fig. 2.6 can be viewed as being made up of an infinite number of superimposed sine waves of various frequencies (f_1 , f_2 , f_3 , ...) amplitudes (A_1 , A_2 , A_3 , ...) and phases (θ_1 , θ_2 , θ_3 , ...). It follows with the use of equation 2.5, that the autocorrelation of this function may be pictured as an infinite number, n , of superimposed cosine functions of amplitudes ($A_1^2/2$, $A_2^2/2$, $A_3^2/2$, ...) and frequencies (f_1 , f_2 , f_3 , ...). This may have the appearance of Fig. 2.9 . (Phase information is lost during autocorrelation). It will later be shown that such a function may be used to calculate the energy spectrum.

For practical use, a discrete, finite estimate of the autocorrelation function of equation (2.4), for a discretely sampled wave record with sampled values x_n where n = 1, 2, 3, ...N, is:

$$R(rh) = 1/(N-r) \sum_{n=1}^{N-r} x_n\, x_{n+r} \qquad r = 0, 1, 2, \ldots, m \qquad (2.6)$$

where h = the constant sampling interval

r = the lag number, where lag τ = rh

m = the maximum lag number, where the maximum lag τ(max) = mh

N = the number of sampled points in the wave record.

This estimate is used in computer calculations of energy spectra, as shown later, in section (c) below. It will also be shown, in later sections, how the above parameters are selected.

(b) The Fourier Transform

The Fourier Transform F(f) of a function x(t) is defined as

$$F(f) = \int_{-\infty}^{+\infty} x(t).e^{-j2\pi ft}\, dt \quad . \qquad (2.7)$$

The Euler identity is used here, i.e.

$$e^{-jx} = \cos(x) - j.\sin(x) \qquad (2.8)$$

where $j = \sqrt{-1}$, the symbol of complex notation.
This implies that F(f) will have a real and imaginary part. In particular, even and odd parts of function x(t) are represented by real cosines and imaginary sines respectively.

Equation (2.7) is derived from a Fourier series, as shown in Ramirez (1985, 28-29) and Champeney (1973, p.218), where an inverse relation is also derived. It transforms the function x(t) from the time domain to the frequency domain. In particular, this Fourier transform will extract the amplitude, A_o , (in the frequency domain) of a single infinite sine wave, at its particular frequency ($f_o = 1/T_o$). The concept of a sine wave described in both the time and frequency domains (or planes) is illustrated in Fig. 2.10 . Furthermore, the Fourier transform will, ideally, extract this information for each component sine wave in a wave record. It is interesting to note that phase information, although less relevant to spectral analysis, can also be obtained.

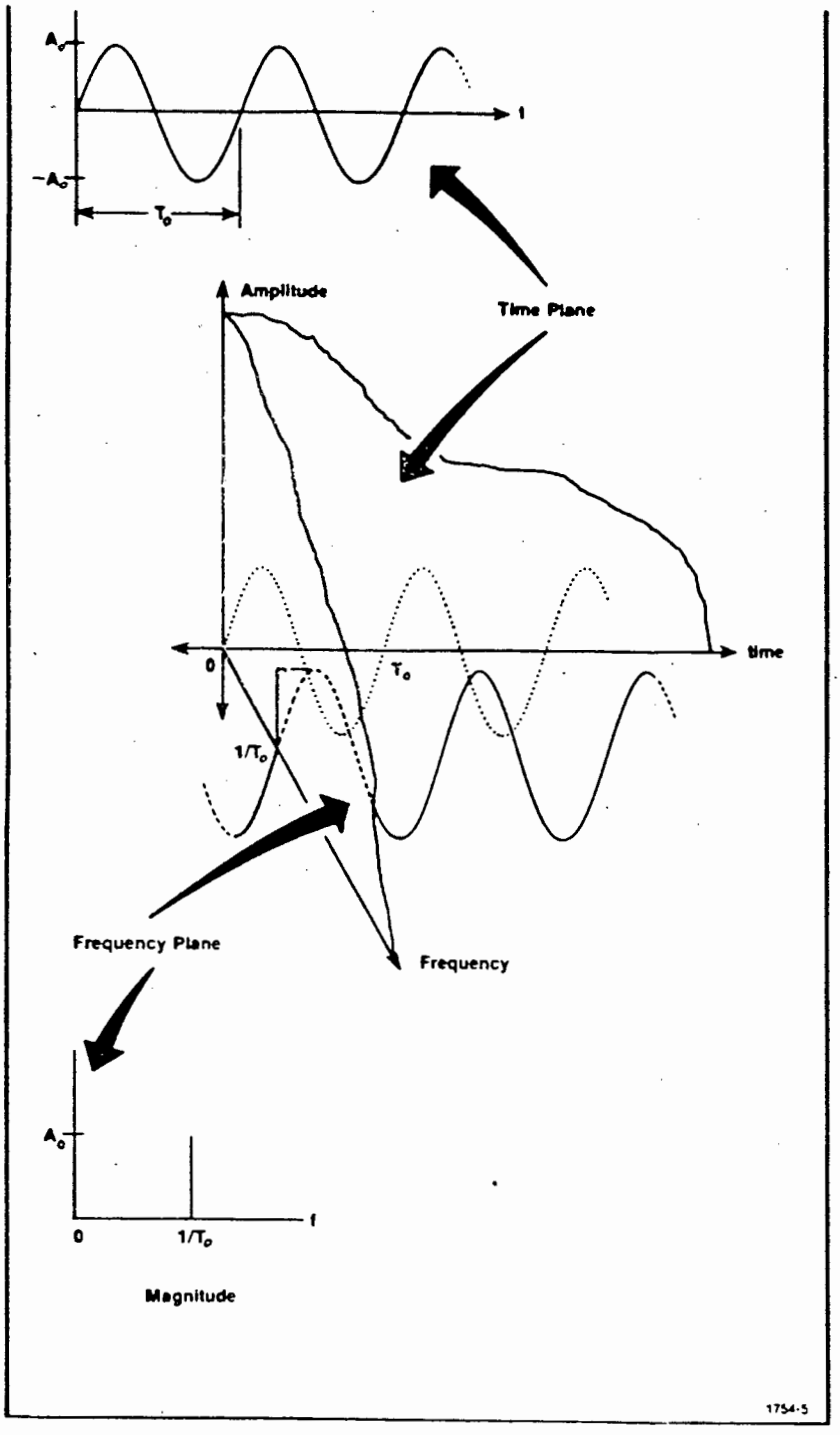

Figure 2.10 : A Sine Wave described in both the Time and Frequency Planes.

after Ramirez (1985)

(c) The Energy Spectrum

This may be viewed as follows: if the autocorrelation of an infinite sine wave (Fig. 2.8(b)) is transformed by Fourier transform, its amplitude will be extracted at its particular frequency. Fig. 2.11 illustrates a plot of this information. This spike is actually the energy spectrum for a sine wave of amplitude A_s. (It is evident here that this energy is proportional to wave height squared, as in linear Airy wave theory). Furthermore, if the autocorrelation of a wave record (Fig. 2.9) is also transformed, the resulting plot will have an infinite number of these spikes, with heights of $\frac{1}{2}A_1^2$, $\frac{1}{2}A_2^2$, $\frac{1}{2}A_3^2$, ..., at frequencies of f_1 , f_2 , f_3 , ... Each spike represents a component sine wave of the autocorrelation record. This plot is actually the energy spectrum for the wave record of Fig. 2.6 .

It must be noted that the type of energy spectrum described above is not practically possible because wave records are of a finite length, and because the wave data is usually discrete. Nevertheless the above discussion reveals that the energy spectrum is the Fourier transform of the autocorrelation function ; thus substituting $R(\tau)$ for $x(t)$ in equation (2.7) ;

$$S(f) = \int_{-\infty}^{+\infty} R(\tau).e^{-j2\pi d\tau}\, d\tau \qquad (2.9)$$

S(f) is the symmetrical 'two-sided' (i.e. positive and negative) energy spectrum, as discussed in Bendat and Piersol (1971, p77). Since negative frequencies are meaningless in wave analysis, the one sided spectrum is defined: (Fig. 2.12 illustrates the concept of a two-sided and one-sided energy spectrum).

$$G(f) = 2\,S(f) \qquad 0 < f < +\infty$$
$$\text{otherwise zero} \qquad (2.10)$$

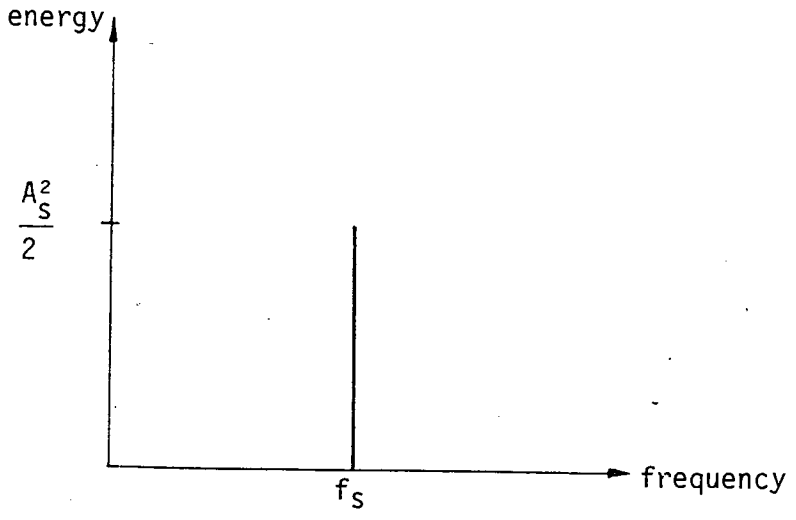

Figure 2.11 : The energy spectrum of the single infinite sine wave of Figure 2.8(a).

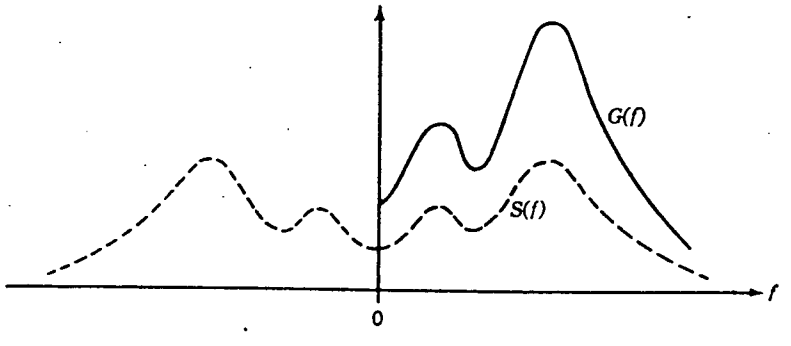

Figure 2.12 : One-sided and two-sided spectral density functions.

after Bendat and Piersol (1971)

Therefore :

$$G(f) = 2 \int_{-\infty}^{+\infty} R(\tau).e^{-j2\pi f\tau}\, d\tau \qquad (2.11)$$

where $0 < f < +\infty$,

and since $R(\tau)$ is real and even, as explained in Appendix 3,

$$G(f) = 2 \int_{-\infty}^{+\infty} R(\tau).\cos(2\pi f\tau)\, d\tau \qquad (2.12)$$

This is clarified in Appendix 3.

A discrete estimate of equation (2.12), using the trapezoidal rule for integration, is (Bendat and Piersol, 1971, 315-317):

$$G_k = 2h\left[(R(0) + 2\sum_{r=1}^{m-1} R(rh)\cos(\pi rk/m) + (-1)^k R(mh)\right] \qquad (2.13)$$

where k = 0,1,2,....,m. This is the harmonic number.

G_k = the raw (unsmoothed) estimate of the energy spectrum G(f) at harmonic k, corresponding to frequency $f = k.f_c/m$. This is also termed the energy density.

$R(rh)$ = the estimate of the autocorrelation function at lag number r (equation 2.6)

r = the lag number

h = the constant time interval between digitised samples of the wave record

m = the maximum lag number

f_c = 1/(2h) is the Nyquist frequency - discussed below in section 2.2.3.1 .

This equation forms the basis of a computer program to calculate wave energy spectra, found in appendix 1. Choice of the above-mentioned parameters is later discussed.

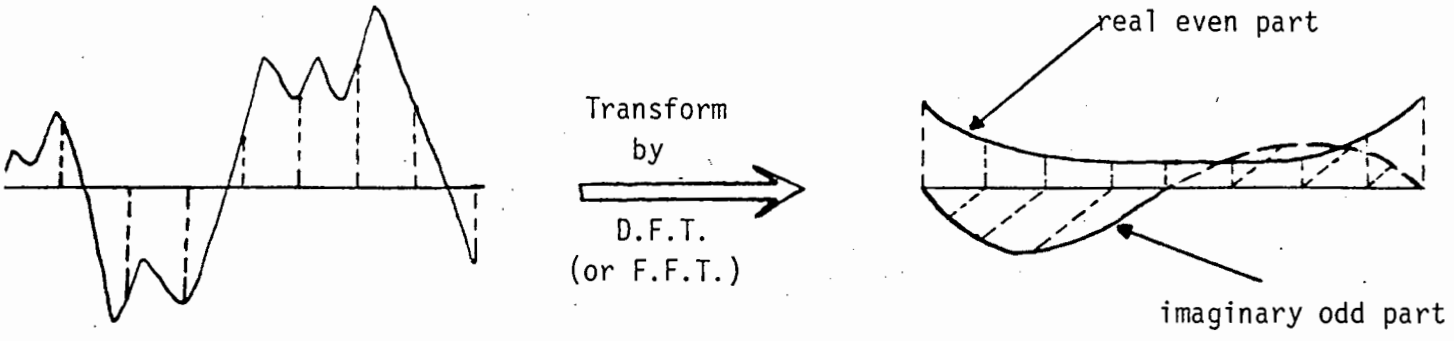

N equally spaced values (in time) x(n) sampled from the wave record

N equally spaced values X(k) (each has real and imaginary part) in the frequency domain.

Figure 2.13 : Graphical Representation of the D.F.T.

after Ramirez (1985)

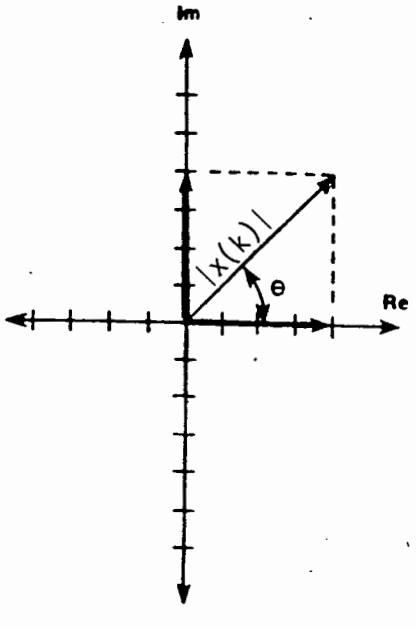

Figure 2.14 : An Argand diagram showing the interpretation of magnitude, $|x(k)|$ and phase, θ

after Ramirez (1985)

2.2.2.2 Wave Energy Spectra via the FFT

In the above section, the autocorrelation estimate was transformed to the frequency domain. Alternatively, the digitised wave record itself can be transformed, and simple manipulation of this will yield the wave energy spectrum. The transformation is achieved by means of the Discrete Fourier Transform (DFT).

(a) The discrete Fourier transform

Section 2.2.2.1(b) discussed the Fourier transform, which yields the amplitude (and phase), at the relevant frequencies of the component sine waves, from a wave record. The discrete Fourier transform is an approximation to this. In particular, N equally spaced samples of a wave record can be transformed to N samples in the frequency domain, by means of the DFT. Fig. 2.13 illustrates this concept. The DFT has the form :

$$X(k) = \sum_{n=o}^{N-1} x(n)e^{-j2\pi kn/N} \qquad (2.14)$$

where N = number of samples being considered

n = the time sample index. It has values 0,1,2,....,N-1

k = the index for the computed set of discrete frequency components. It has values 0,1,2,....,N-1 .

x(n) = the discrete set of water surface elevations samples from the wave record (see Fig. 2.13).

X(k) = the set of Fourier coefficients obtained by the DFT, each coefficient having a real and an imaginary part (see fig. 2.13).

j = the symbol of complex notation, indicating the imaginary part of a complex quantity ($j = \sqrt{-1}$)

(as indicated in Ramirez (1985, p.68), h, the sampling interval, is scaled to 1. in this equation).

(b) Interpretation of Fourier coefficients

The complex Fourier coefficients X(k) represent magnitude and phase of the frequency components of the wave record at particular frequencies. Fig. 2.14 illustrates how magnitude, $|X(k)|$, is obtained using the simple relationship:

$$|X(k)| = \sqrt{Re^2 + Im^2} \qquad (2.15)$$

where Re = the real part of the Fourier coefficient, X(k)
Im = the imaginary part of the Fourier coefficient, X(k).

In addition, Fig. 2.14 illustrates how phase, θ , is obtained.

(c) The Fast Fourier Transform

The Fast Fourier Transform (FFT) is an elegant, time efficient method for computing the DFT. It is complicated and is therefore perhaps best considered to be a "black box" which does the job well. Nevertheless, Bergland (1968) gives a very understandable derivation of the FFT. Higgins (1974) and Cochran (1967) also deal with the FFT.

It is appropriate to consider how much more efficient the FFT is, compared to the DFT. To transform N samples of the wave record to the frequency domain (as in Fig. 2.13), the DFT will require N x N complex number multiply-and-add operations, while the FFT will require only N.LogN such operations. Fig. 2.15 shows that the computer time saving should be significant for a transform of many points (i.e. large N). Bergland (1969, p.43), Higgins (1974), and Cochran (1967) deal with this.

Possibly the only disadvantage of the FFT is that it requires that the number of samples, N, must be a power of 2 . For example, the C.S.I.R. use the FFT to transfer $2^{10} = 1024$ samples.

FFT computer routines are available in package form, such as floppy disc for use on microcomputers (e.g. The Turbo Pascal Numerical Methods Toolbox (Borgland, 1986)) and in the form of FORTRAN program listings (Higgins, 1974, p.773); Ramirez. 1985, p.169).

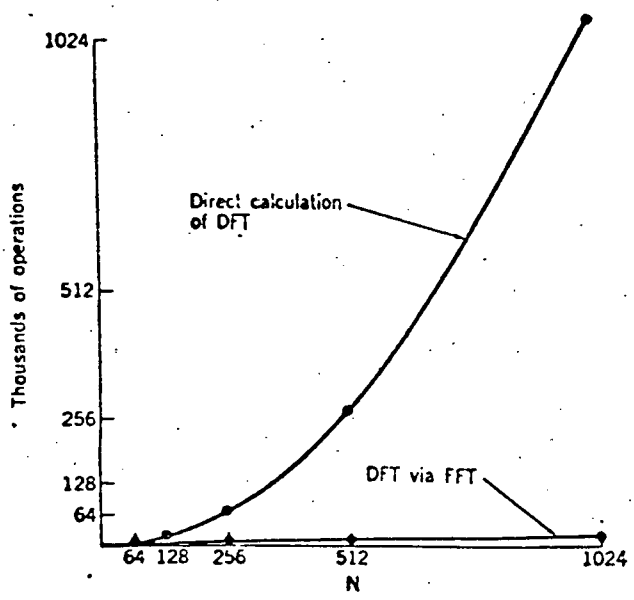

Figure 2.15 : The number of operations for calculating the D.F.T. directly, or with the F.F.T.

Bergland (1969)

(d) The Energy Spectrum

Bendat and Piersol (1971, pp. 82-84) show the derivation of an alternative expression for G(f) (the one-sided energy spectrum of equation (2.12)) :

$$G(f) = 2 \lim_{T\to\infty} \frac{1}{T} E \{|X(f,T)|^2\} \qquad (2.16)$$

where E = expected value of { }

$|X(f,T)|$ = the magnitude, at frequency f , of the complex value X(f,T)(calculated in the same fashion as $|X(k)|$ in equation (2.15)

$$X(f,T) = \int_0^T x(t)\, e^{-j2\pi ft}\, dt \quad . \qquad (2.17)$$

They then show that the DFT of equation (2.14) is a discrete version of equation (2.17), (Bendat and Piersol, 1971, p.301). Thus, a formula for G_k, the estimate of the energy spectrum G(f), emerges from equation (2.16), in terms of the Fourier coefficients of the DFT, X(k) (Bendat and Piersol, 1971, p.327):

$$G_k = 2h/N\ |X(k)|^2 \qquad (2.18)$$

where the magnitude, $|X(k)|$ is obtained from equation (2.15).

G_k is also called the energy density. The formula is used in a computer program (Appendix 2) to calculate the energy spectrum via the FFT.

Another observation from the above derivation is that the two approaches to calculating the wave energy spectrum (via FFT or autocorrelation) are very similar.

2.2.2.3 Parameters from the wave energy spectrum

(a) The Significant Wave Height, H_{mo}

The significant wave height is used extensively in the design of coastal structures. It can be estimated using statistical methods, where it is termed H_s or $H_{1/3}$. Alternatively, it can be calculated from the wave energy spectrum (Marks, 1963), where it is termed H_{mo} :

$$H_{mo} = 4\sqrt{m_o} \qquad (2.19)$$

where

$$m_o = \int_0^\infty G(f)\, df \qquad (2.20)$$

where $G(f)$ = the energy spectrum.

Equation (2.20) is simply interpreted as the area under the wave energy curve.

Equation (2.19) is valid if it is assumed that the Rayleigh distribution applies to the wave heights of the wave record. By assuming this, other wave height parameters, such as H_1 and H_{10} , can also be calculated (Goda, 1985). Wilson and Baird (1972, 116-118) show that significant wave heights calculated with equation 2.19 compare well with those calculated by the Draper method.

(b) The Peak Period, T_p

This is the period corresponding to the highest value of energy density in the spectrum. It can simply be read off from the spectrum. Since it is representative of the highest wave energy, it is commonly used for the design of coastal structures, at the C.S.I.R. (van Tonder, 1988).

When the wave energy spectrum has two prominent energy peaks (i.e. a bimodal spectrum), the peak period may not be representative of conditions, and the zero-upcrossing period, $T_{mo,2}$, may be used.

(c) The Zero-upcrossing period, $T_{m0,2}$

This period, which originated from statistical methods (where it has the symbol T_z), may also be calculated from the wave energy spectrum (Manohar et al, 1976, p.275).

$$T_{mo,2} = 2\pi \sqrt{\frac{m_o}{m_2}} \qquad (2.21)$$

where m_o is obtained from equation (2.20) ,
and

$$m_2 = \int_o^\omega f^2 \, G(f) \, df \quad . \qquad (2.22)$$

(d) The significant period, $T_{1/3}$

This is the period corresponding to the significant wave (of height $H_{1/3}$). It can be estimated as follows:

$$T_{1/3} = \frac{T_p}{1,05} \qquad (2.23)$$

2.2.3. Practical spectral analysis

The object of spectral analysis is to calculate a meaningful wave energy spectrum. This means :

(i) adjacent peaks of energy must be distinguishable - according to the users needs ;
(ii) no incorrect or irrelevant information should occur ;
(iii) there must be a reasonable level of confidence in the spectrum, according to the users needs ;
(iv) parameters such as the significant wave height, H_{mo} , and the period of peak energy density, T_p , can be obtained.

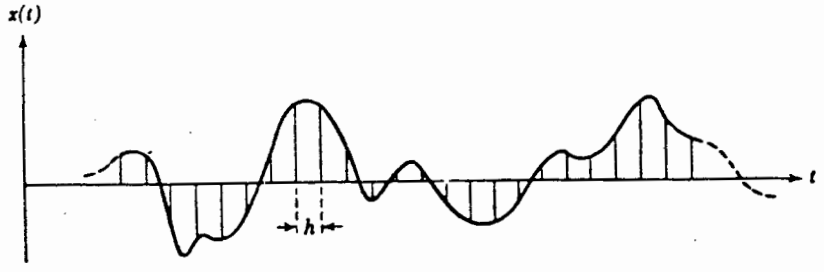

Figure 2.16 : Sampling at equal intervals.

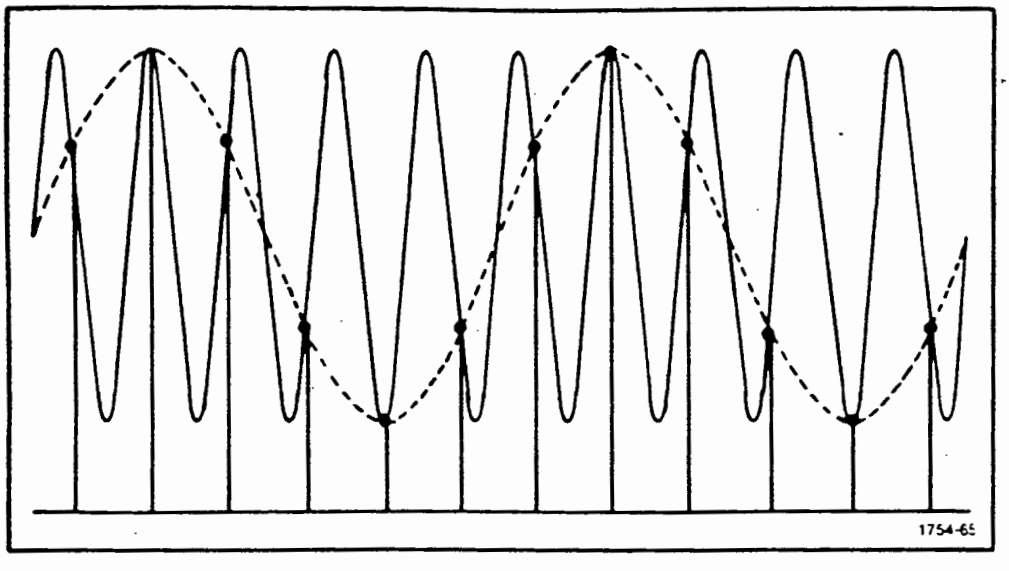

Figure 2.17 : Aliasing caused by a sampling interval too large.

Ramirez (1985)

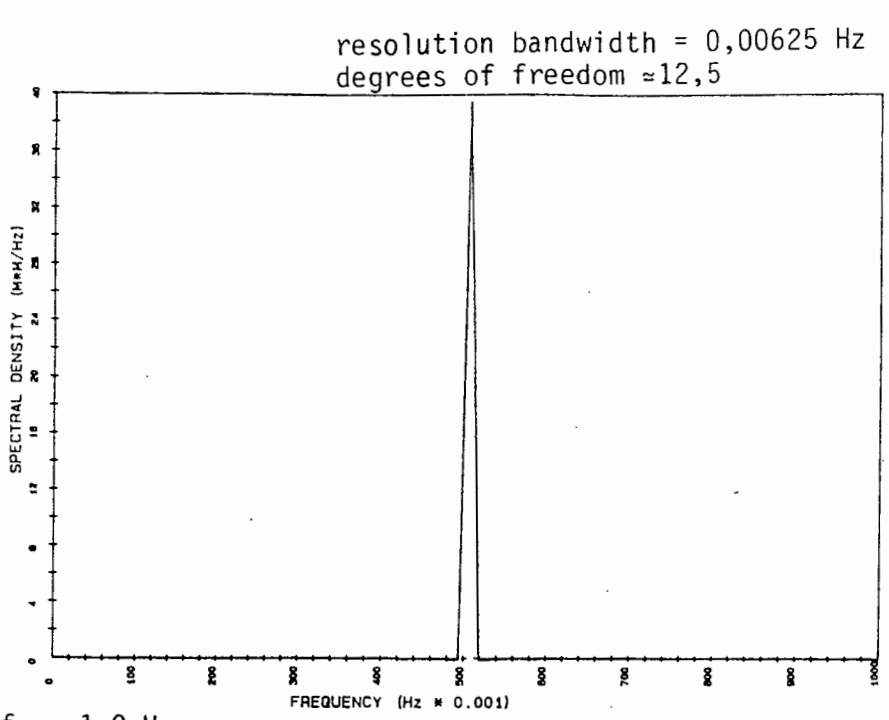

(a) f_c = 1,0 Hz

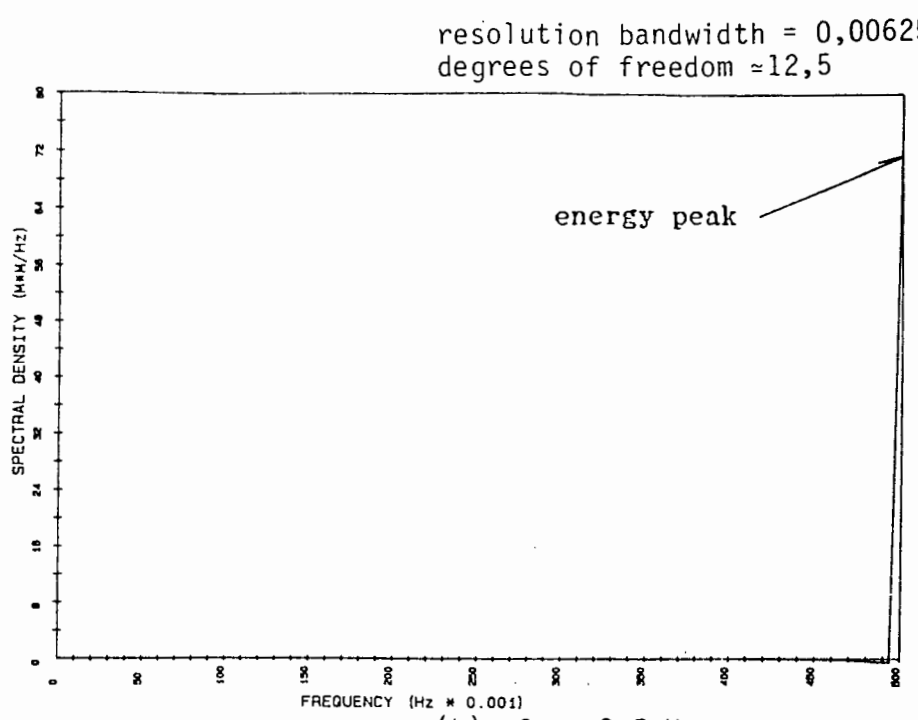

(b) f_c = 0,5 Hz

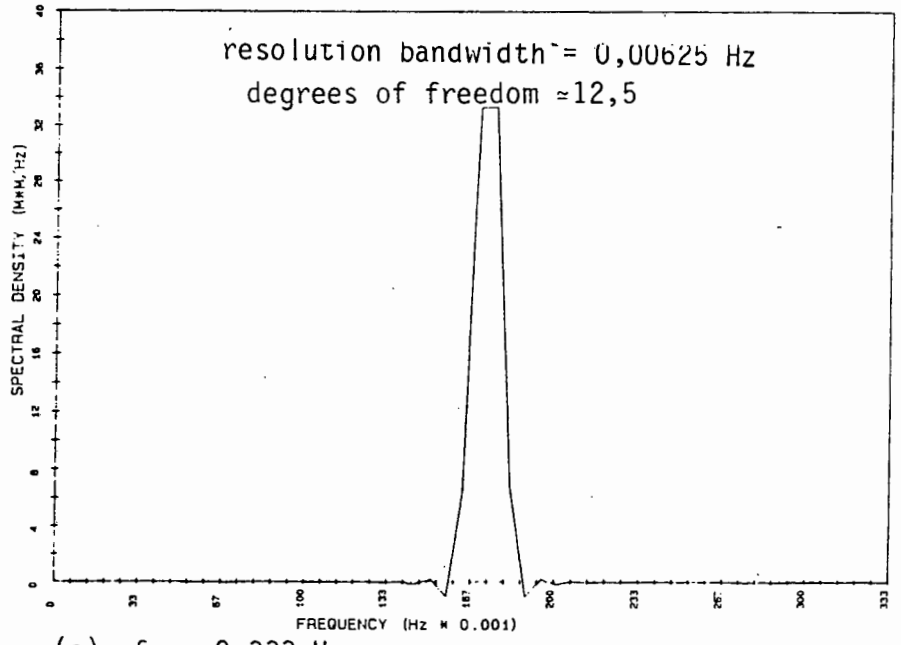

(c) f_c = 0,333 Hz

Figure 2.18 : Energy spectra for a sine wave of frequency 0,5 Hz, with various Nyquist frequencies, f_c .

In order to obtain such an energy spectrum :

(i) wave data must be correctly preprocessed ;
(ii) the correct choices of parameters, e.g. the number of digital data points, must be made.

With regard to preprocessing before spectral analysis, data must be sampled, qualified and possibly filtered. Sampling is the process of obtaining digital data representing the elevation of the water surface. Data qualification involves checking that a wave record is valid and reasonably free of errors. Another form of data processing at this stage is filtering. These topics are discussed below.

2.2.3.1 Sampling

Discrete data from wave records is required for spectral analysis. Such data can be sampled by a digitiser from an analogue wave record. More often though, discrete data is recorded directly by a wave recorder. Which ever way it occurs, data is usually sampled at equal intervals, h , as shown in Fig. 2.16.

Sampling with the interval h too small yields correlated and redundant data, and therefore an unnecessary increase in calculation time and cost. Alternatively, sampling with h too large leads to confusion between high and low frequency components. This concept is illustrated in Fig. 2.17, where a high frequency component is mistakenly identified as a low frequency component, due to an excessively large interval, h. This phenomenon is called aliasing.

Consideration has to be given to avoiding this problem. In sampling a wave record (Fig. 2.16), at least 2 samples per period of a frequency component (sinusoidal wave) are required, to define it. Thus, the highest frequency component that can be sampled is :

$$f_c = 1/2h \qquad (2.24)$$

where h = the sampling interval in seconds
f_c = the Nyquist or folding frequency, in hertz.

If frequencies higher than this occur, when the energy spectrum is calculated their energies will be "folded back" into the frequency range from 0 to f_c hertz. Clearly, this aliasing can cause an erroneous energy peak in the spectrum.

To illustrate aliasing, a sine wave with unit amplitude and a period of 2 seconds (i.e. a frequency of 0,5 Hz) was generated. Fig. 2.18 illustrates the energy spectra for the sine wave with:

(a) a Nyquist frequency of 1,0 Hz - above the sine wave frequency of 0,5 Hz.

(b) a Nyquist frequency of 0,5 Hz - equal to the sine wave frequency.

(c) a Nyquist frequency of 0,333 Hz - below the sine wave frequency.

It is clear that in Figs. 2.18(a) and (b), energy peaks occur at 0,5 Hz - as expected. In Fig. 2.18(c) however, an erroneous aliased energy peak occurs, indicating a Nyquist frequency too high for this case.

Finally, the aliasing of frequencies above f_c occurs in a specific fashion: for any frequency f in the range. $0 < f < f_c$, the higher frequencies which can be aliased with f are defined by :

$$(2f_c \pm f) \ , \quad (4f_c \pm f) \ , \ \ldots\ldots , \ (2nf_c \pm f) \quad .$$

TABLE 2.1 Examples of Sampling Intervals for Spectral Analysis.

Location	Organisation	Wave recorder	Interval, h (secs)
South African Coast	C.S.I.R.	Waverider buoy	0,5
North Sea	Royal Netherlands Meterological Institute	Waverider buoy	0.5
Japan	Disaster Prevention Research Institute	Capacitance-type wave gauge	0,5
Great Lakes	Great Lake Environment Research Laboratory	Various types	0,333
Japan	Port and Harbour Research Institute	Step-resistance staff gauge	0,5 or 1,0

Bendat and Piersol (1971, pp.229-230) and Ramirez (1985, pp.115-123) discuss this further.

What is the best sampling interval, h , to use? This depends on :

(a) the frequency response of the wave gauge used.
(b) On the wave climate of the area.
(c) On the type of wave of interest e.g. a large h would be used to sample long-period surf beat.

As an example, the C.S.I.R. use a sampling interval of h = 0,5 seconds. Thus the Nyquist frequency is :

$$f_c = 1 / 2h = 1 / (2 \times 0{,}5) = 1 \text{ Hz} \quad .$$

Here, aliasing of frequency components just above 1 Hz will still occur, but since waves of this frequency have very little energy, the resulting effects will be negligible. It is interesting to note that the Waverider buoy does not respond to frequencies above 1,4 Hz, therefore no aliasing can occur from these frequencies.

Wilson et al (1974, p.105) suggests, as a rule of thumb, an interval between 0,75 and 1,5 seconds. However, from an anlysis of 171 surface wave records and 15 linearly simulated wave profiles, Goda (1974, p.336), suggests a sampling interval of less than 1/20 of the period of peak spectral energy. (On the South African coast this period is often about 10 seconds (van Tonder, 1988)). As a further guide, Table 2.1 indicates some examples of sampling intervals used. It is interesting to note that on the Great Lakes, where wave periods are shorter, the interval is small.

2.2.3.2 Data qualification

Errors in wave records may be caused by :

(i) wave recording instrument malfunction ;
(ii) electronic faults - in data transmission or digitising.

An example of (i) occurs with the Waverider buoy: the accelerometer of the buoy is mounted on a stabilised platform. If the buoy spins more than 6 times in 2 minutes, the suspension system of this platform becomes entangled. Since the platform has a natural period of 40 seconds, the result is that the zero line (mean water surface elevation) of the wave record will shift with this period of 40 seconds. Such an instability of 40 second period has been detected in the past at C.S.I.R. (Coetzee, 1988).

An example of (ii) above occurs when the telemetered signal of the waverider buoy is affected by ship radio interference: this is difficult to detect (Coetzee, 1988).

Data which is free of these errors mentioned above, is likely to be stationary and normally distributed. Thus, to determine whether the data is good, these two qualities should be tested. Prior to this, any outliers should be detected and possibly corrected. Several other tests can also be performed on data. All of this constitutes data qualification; descriptions follow.

(a) Outliers

Outliers, i.e. sample values which deviate excessively from the mean, should be tested for, and either corrected, or the entire wave record rejected.

In order to test for these values, the mean and standard deviation are first calculated. Outliers are then detected by their excessive deviation from the mean in terms of standard deviations. For example, according to Houmb et al (1974, pp.32-33), values deviating more than 5 standard deviations from the mean are considered erratic. This method of using the standard deviation as a criterion for erratic values is also employed by the C.S.I.R. (Visser et al, 1980).

These erroneous values can be corrected by discarding them and interpolating. This is done by the C.S.I.R. (Visser et al, 1980) and by C.E.R.C. (Thompson, 1974, p.838). If the number of outliers exceeds a certain value, the wave record may be rejected. C.E.R.C. rejects a record if more than 2,5% of the data values are doubtful.

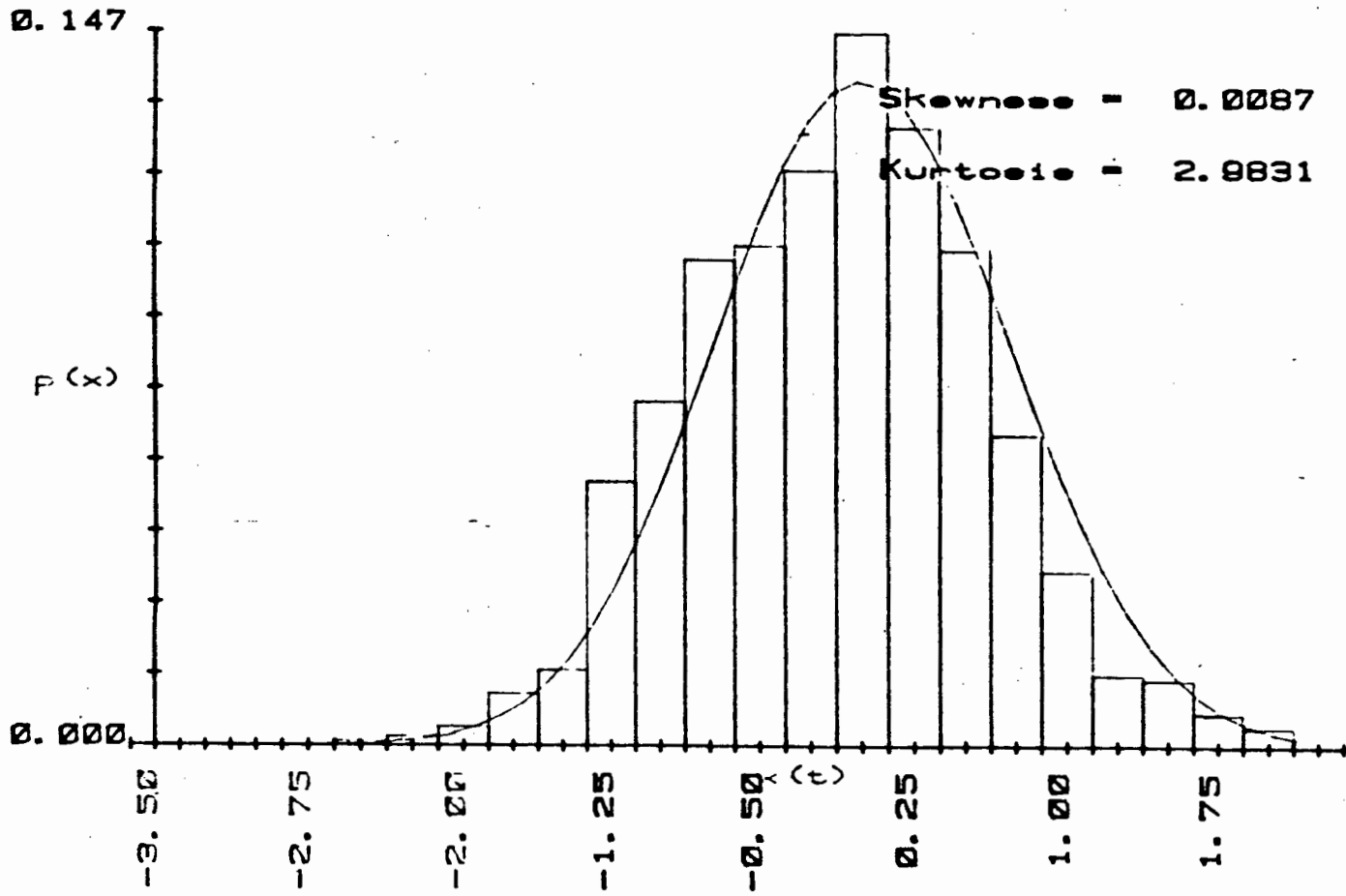

Figure 2.19 : The probability density function of the wave data compared to the theoretical normal distribution. In this case the calculated skewness and kurtosis are not significant and therefore a normal distribution can be assumed.

(b) Test for stationarity:

If the properties of the wave record do not change significantly with time, the process is considered to be stationary. Stationarity can be tested statistically by means of the Run test (Bendat and Piersol, 1971, p.235). The C.S.I.R. use another procedure; a wave record of 2048 data points is split in half. For each half, statistics such as the mean, standard deviation and significant wave height (discussed in section 2.2.2.3) are calculated and compared, using statistical tests such as t and f tests.

In the t test, use is made of the t - distribution to determine if there is a significant difference between the means of each half of data. (Walpole and Myers, 1978, p.204). In the f test, use is made of the f - distribution to test if there is significant equality of the variance of each half of data (Walpole and Myers, 1978, p.220). In both the t and f tests, the acceptible levels of significance are determined by "experienced observers" at the C.S.I.R., according to Rossouw et al, (1982, p.89).

(c) Test for Normality

To quote Marks (1963): "Examination of seakeeping records has established the (almost) Gaussian distribution as a basic property". In addition, according to Visser (1979, p.7), testing the normality of the probability density function (Bendant and Piersol, 1971, p.15) of the data is important for data qualification. It follows that a normal distribution will help to indicate whether a good (and typical) wave record has been recorded. In addition, the normal distribution of wave amplitudes is a prerequisite for the calculation of some useful statistics, such as the calculation of the significant wave height, H_{mo}, calculated from the wave energy spectrum.

In order to test for normality, the probability density function of the amplitudes of the wave record can be measured and compared to the theoretical normal distribution. This is done at the C.S.I.R. as illustrated in Fig. 2.19. Skewness and kurtosis, defined in Helstrom (1984, p.100), are measures of normality, and are also tested. Another test for normality is the Chi-square goodness-of-fit test (Bendant and Piersol, 1971, pp.119-122).

(d) Further tests

The C.S.I.R. employ detailed data qualification, which was refined by "experienced observers" (Rossouw et al, 1982, pp.89-90). This includes the tests discussed above, as well as :

1. Test for flatheads (i.e. consecutive values which are the same, to the nearest 10 mm).
2. Test for slope - to ensure that the slope of two consecutive data points is less than the theoretical maximum slope that the water surface can attain.
3. Test for a linear trend in the data, and this can be corrected, as shown in Bendat and Piersol (1971, pp.288-291).
4. Test for energy values at low frequency. Such values are beyond the frequency range of response of the waverider buoy. Thus, any such values occurring are likely to be wrong.

2.2.3.3 Filtering

This is the process of extracting components of desired frequencies only, from a wave record. A high pass filter will yield only high frequency components e.g. if the component of the tide existed on a wave record, it could be eliminated with a high pass filter. Alternatively a low pass filter will yield only low frequency components e.g. if only the tide, and no waves of high frequencies were required in the above example, a low pass filter would be ideal. These concepts are illustrated in Fig. 2.20. In addition, another type of filter is the band pass filter which yields components of frequencies in a desired band.

Filtering can be achieved physically by the recording instrument itself e.g. the waverider buoy does not respond to frequencies above 1,4 Hz and below 0,034 Hz, and therefore filters these frequencies out. Another example is pressure-sensor wave gauges, which do not respond to high frequencies and thereby filter them out. Alternatively, filtering can be achieved digitally, as discussed in Bendat and Piersol (1971, pp.291-299).

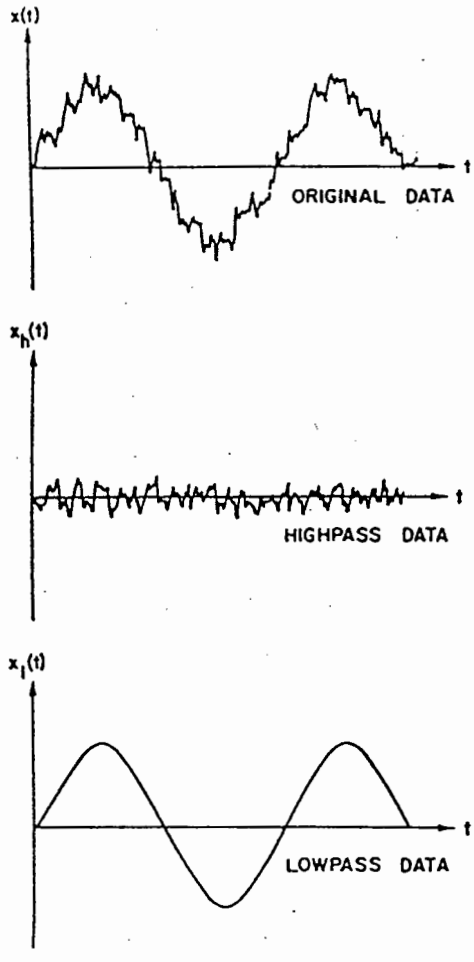

Figure 2.20 : Illustration of highpass and lowpass filtering.

Bendat and Piersol (1971)

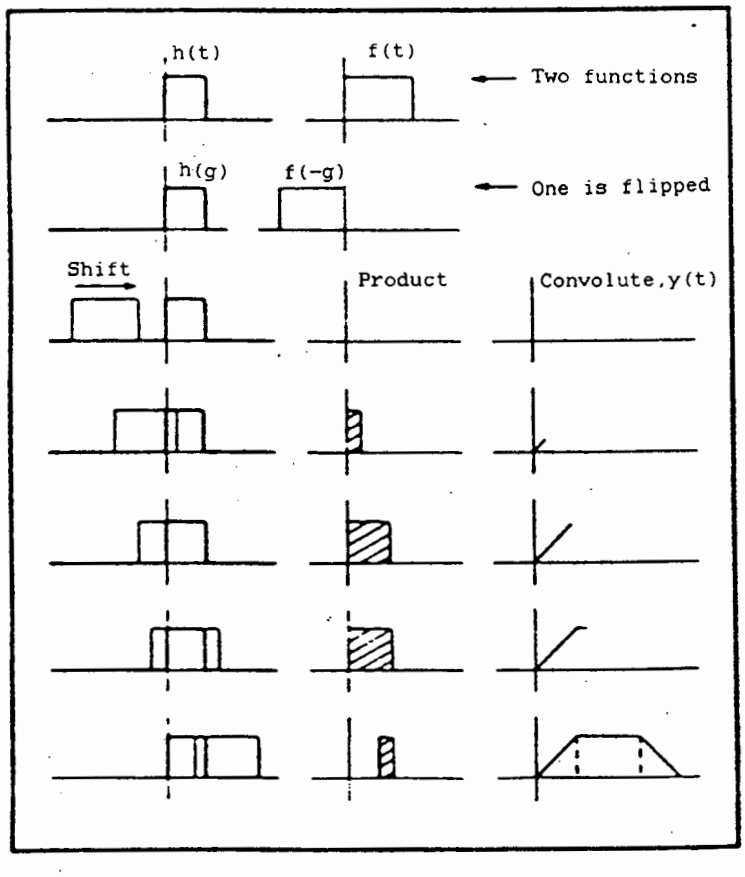

Figure 2.21 : Convolution performed graphically.

Ramirez (1985)

2.2.3.4 Spectral windows and spectral leakage

An understanding of these concepts is important when computing wave energy spectra. In this regard, convolution is another important concept.

(a) Convolution

The convolution of two functions, h(t) and f(t) will yield a function y(t) by means of the integral :

$$y(t) = \int_{-\infty}^{+\infty} h(g)\, f(t-g)\,dg \qquad (2.25)$$

where g is a dummy variable to facilitate the shifting of one function past the other during convolution.

The integral can be roughly interpreted as the rolling together of two functions to yield a new function having the major features of their constituents (Visser, 1979, p.11). Fig. 2.21 provides a graphical explanation of convolution, which is actually a process of shifting the two functions h(t) and f(t) past each other, multiplying them, and integrating this result.

Another pertinent concept is the following :

Multiplication in the time domain is equivalent to convolution in the frequency domain. In other words, (1) multiplying two functions h(t) and f(t) together to form g(t), and then transforming them to the frequency domain, will have the same effect as (2) first transforming them to the frequency domain, and then convolving them :

(1) may be described:

$$h(t) \times f(t) = g(t) \xrightarrow{\text{Fourier Transform yields}} G(f)$$

(2) may be described:

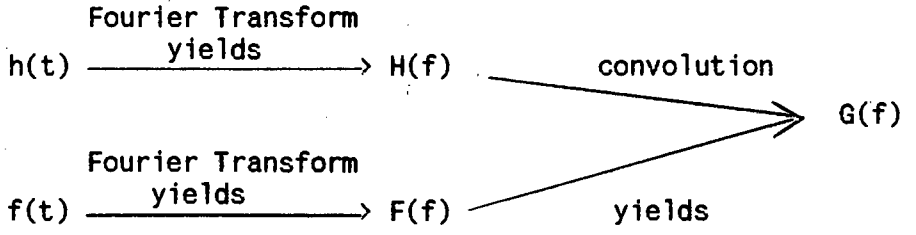

where H(f), F(f) and G(f) are Fourier transforms of h(t), f(t) and g(t) respectively.

These concepts are discussed in Jenkins and Watts (1968, p.44).

(b) Leakage

In order to obtain the wave energy spectrum, a function is transformed to the frequency domain. This function may be the autocorrelation function (as in section 2.2.2.1) or the wave record (as in section 2.2.2.2). Whichever function is transformed, it will be of finite length. This finite function is equivalent to the multiplication of an infinite function by a unit rectangular window function, as illustrated in Fig. 2.22. The Fourier transform of this rectangular window yields a function of the form:

$$\frac{\sin(x)}{x}$$

as illustrated in Fig. 2.23. This function is a spectral window.

As discussed in section (a) above, multiplication in the time domain is equivalent to convolution in the frequency domain. Thus, the Fourier transform of the finite function (of Fig. 2.22(c)), is equivalent to the transform of the continuous function (of Fig. 2.22(a)) convolved with the spectral window of Fig. 2.23. Because of the shape of the spectral window, with its large side lobes, during this convolution there is an undesirable shift of energy between frequencies. This energy shifting is a source of error called leakage.

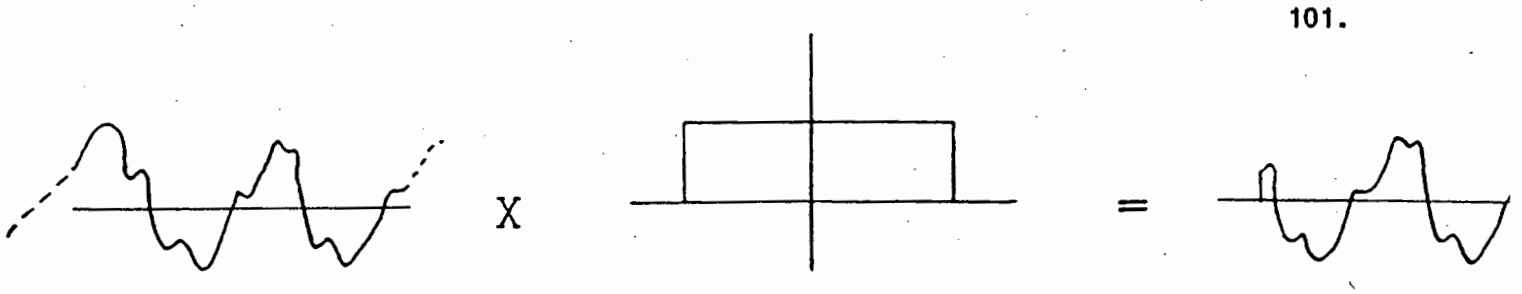

(a) The infinite function (b) The rectangular window function (c) The finite function

Figure 2.22 : The concept of a finite function as a windowed portion of an infinite function

Figure 2.23 : The window function of the form $\frac{\sin x}{x}$, which is the transform of the unit rectangular window function.

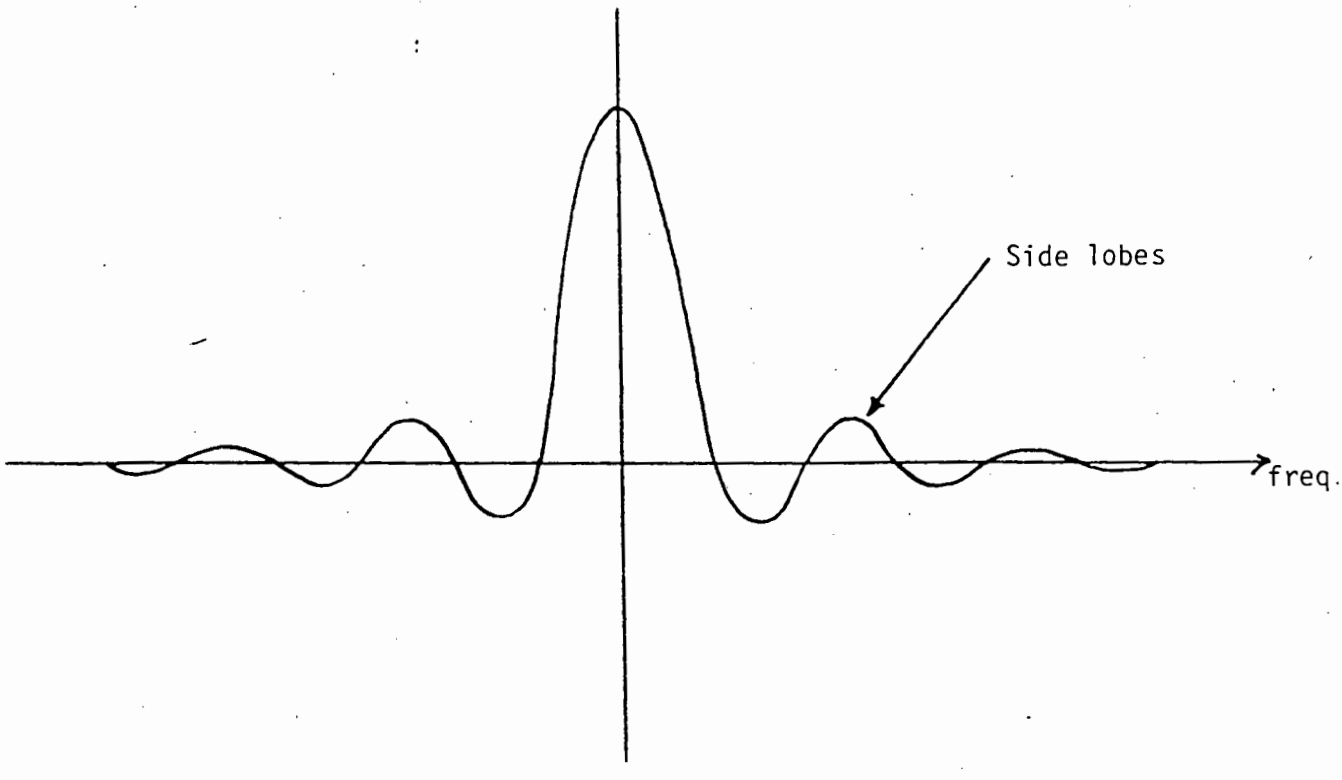

In order to suppress leakage, it is necessary to modify the shape of the rectangular window function, or to use another window function. There are several of these, which reduce leakage through their shape in the frequency domain, Harris (1978) discusses windows in detail. Examples of common windows are the Parzen, Tukey or Cosine Taper, Hamming, Hanning, Bartlet, Lanzos and Lanzos Squared windows. The choice of window is subjective - it depends on the users needs. Fortunately this choice is not critical, since windows are similar to each other in performance (de Carvalho, 1970).

In the case of spectral analysis via Autocorrelation, the window function is usually applied to the autocorrelation estimate - windows are referred to as *lag windows* in this case. Alternatively, since multiplication in the time domain is equivalent to convolution in the frequency domain, it is possible to convolve the transform of the window function (i.e. the spectral window) with the spectrum, in the frequency domain. For example, Bendat and Piersol (1971, pp.318-319) show how a time domain Hanning lag window reduces to simple weighting of the calculated energy values, G_k , in the frequency domain. Fig. 2.24(a) and (b) illustrate the wave energy spectrum calculated without and with this spectral window respectively. The digital wave data which was used appears in Appendix 4 (measured with a waverider buoy). It is evident that the leakage in Fig 2.24(a) is vastly reduced by the window in Fig. 2.24(b). Wilson et al (1974, p.90) state that this window, together with the Hamming window, is the most common used. Furthermore, in a study of some common window functions, Wilson et al (1974, p.96) recommend use of this Hanning spectral window, combined with the triangular lag window, as "capable of achieving the most reliable energy form."

In the case of spectral analysis via FFT, the window function is generally applied to the wave record. The Cosine Taper (or Tukey) data window, usually tapering 10% of the wave record at each end, is commonly used, e.g. by the C.S.I.R. (van Tonder, 1988) and C.E.R.C. (Thompson, 1974, p.838). It is also recommended by Bendat and Piersol (1971, p.323). Fig. 2.25(a) and (b) illustrate a wave energy spectrum calculated without and with this Cosine Taper window respectively: it is evident that there is very little difference between these two

Figure 2.24 : The wave energy spectrum calculated (a) without the Hanning spectral window and (b) with the Hanning spectral window

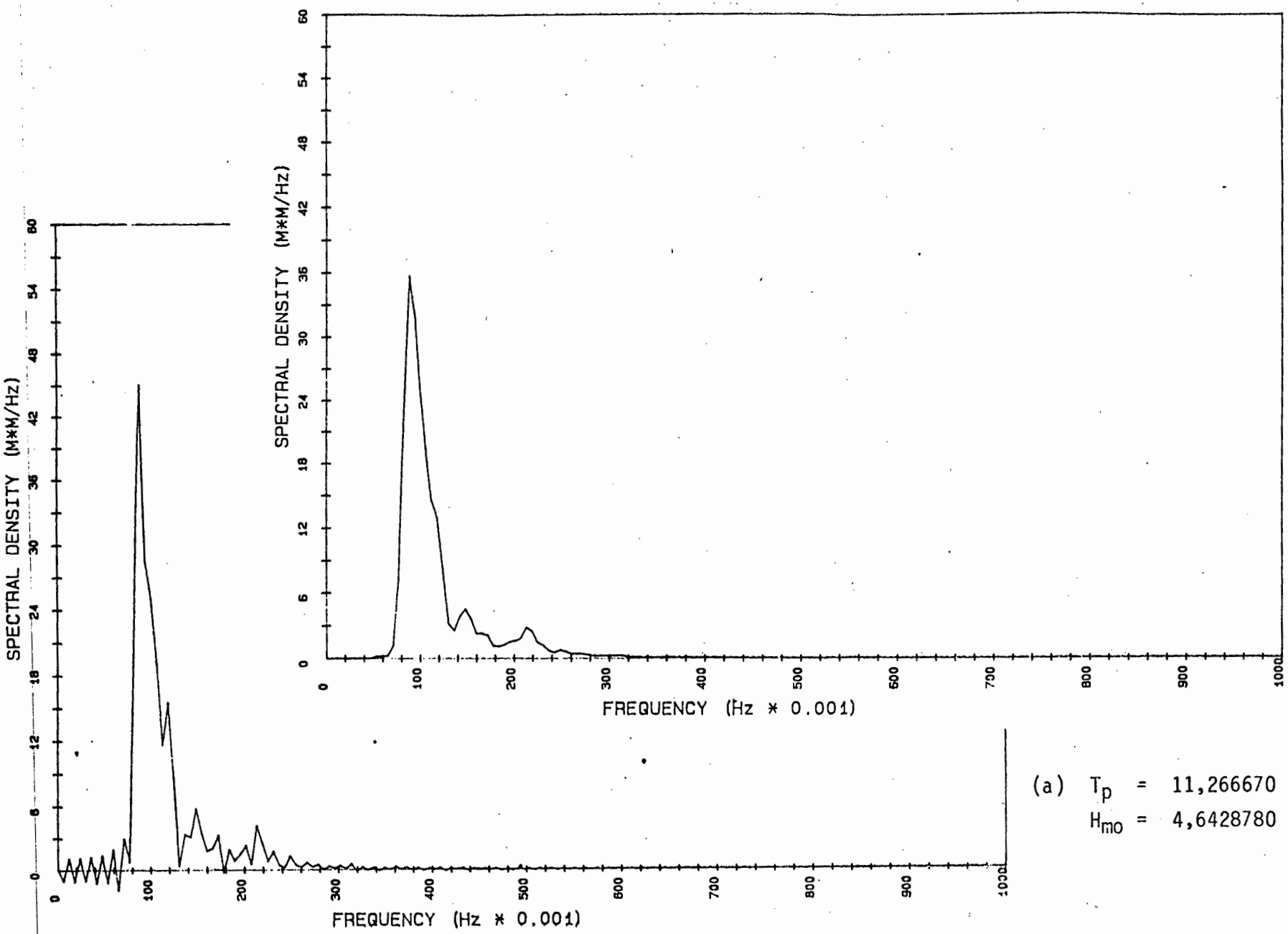

(b) T_p = 11,266670 se
H_{mo} = 4,6428780 m

(a) T_p = 11,266670 sec
H_{mo} = 4,6428780 m

Figure 2.25 : The wave energy spectrum calculated (a) without the cosine taper data window and (b) with the cosine taper data window

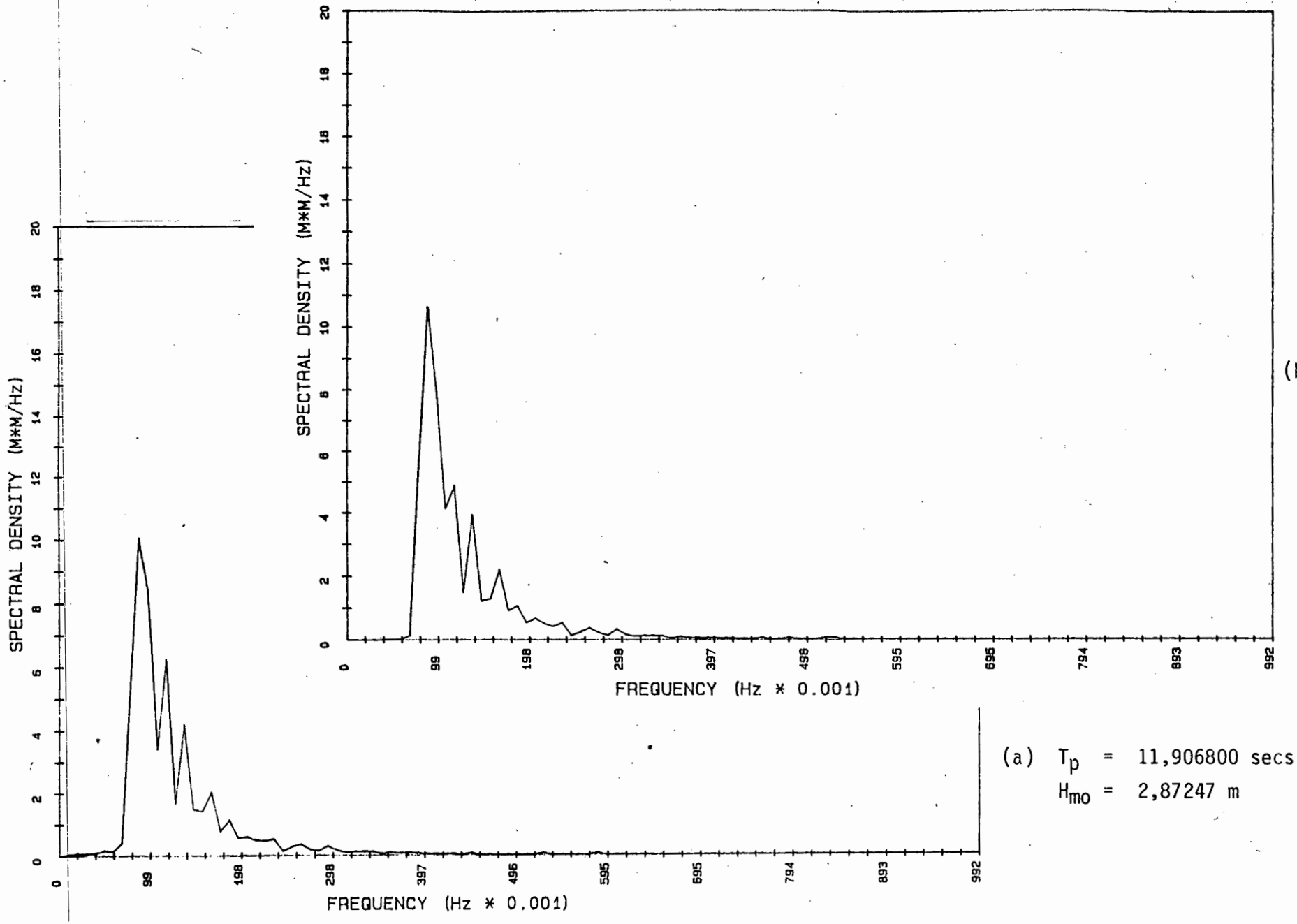

(b) T_p = 11,906800 sec
H_{mo} = 2,809231 m

(a) T_p = 11,906800 secs
H_{mo} = 2,87247 m

spectra. Furthermore, it is evident that the values of the peak periods for (a) and (b) are identical. In addition, their significant wave heights are also very similar. Thus, it appears that the use of this window function may be unnecessary at times, particularly when frequency smoothing is employed. (Discussed in section 2.2.3.5(b)). This view is shared by van Tonder (1988).

2.2.3.5 Confidence

Spectral energy determinations are estimates and are therefore subject to error. Thus, the nature of the errors in the estimates have been found to be distributed according to a chi-squared distribution having v degrees of freedom (Jenkins and Watts, 1968, p.243). This number, v, defines the confidence intervals for the spectral estimates G_k. This is covered in detail by Sand (1968, pp.8-9 and pp.32-35) and Jenkins and Watts (1968, pp.252-255).

Fig 2.26 illustrates the necessary practical information. An example will clarify: If a spectral estimate is chi-square distributed with 20 degrees of freedom then, from fig 2.26, there is an 80% probability that the spectral estimate will vary between 0.7 and 1.6 of its theoretical value. This defines the level of confidence for a spectrum.

The choice of the number of degrees of freedom that is acceptable is subjective. Wilson (1974, p105) maintains that v between 3 and 12 yields acceptable results (in spite of theoretically lower confidence). The C.S.I.R. use v = 20 (van Tonder, 1988).

(a) Confidence for spectra via autocorrelation

In this case the degrees of freedom, v, is related to the spectrum parameters by:

$$v = \frac{N - (m/4)}{(m/2)} \qquad (2.26)$$

$$\text{i.e.} \quad v \approx 2N/m \qquad \text{for } m << N \qquad (2.27)$$

where m = the maximum lag number (as in equation. 2.6)

N = the number of data values sampled from the wave record.

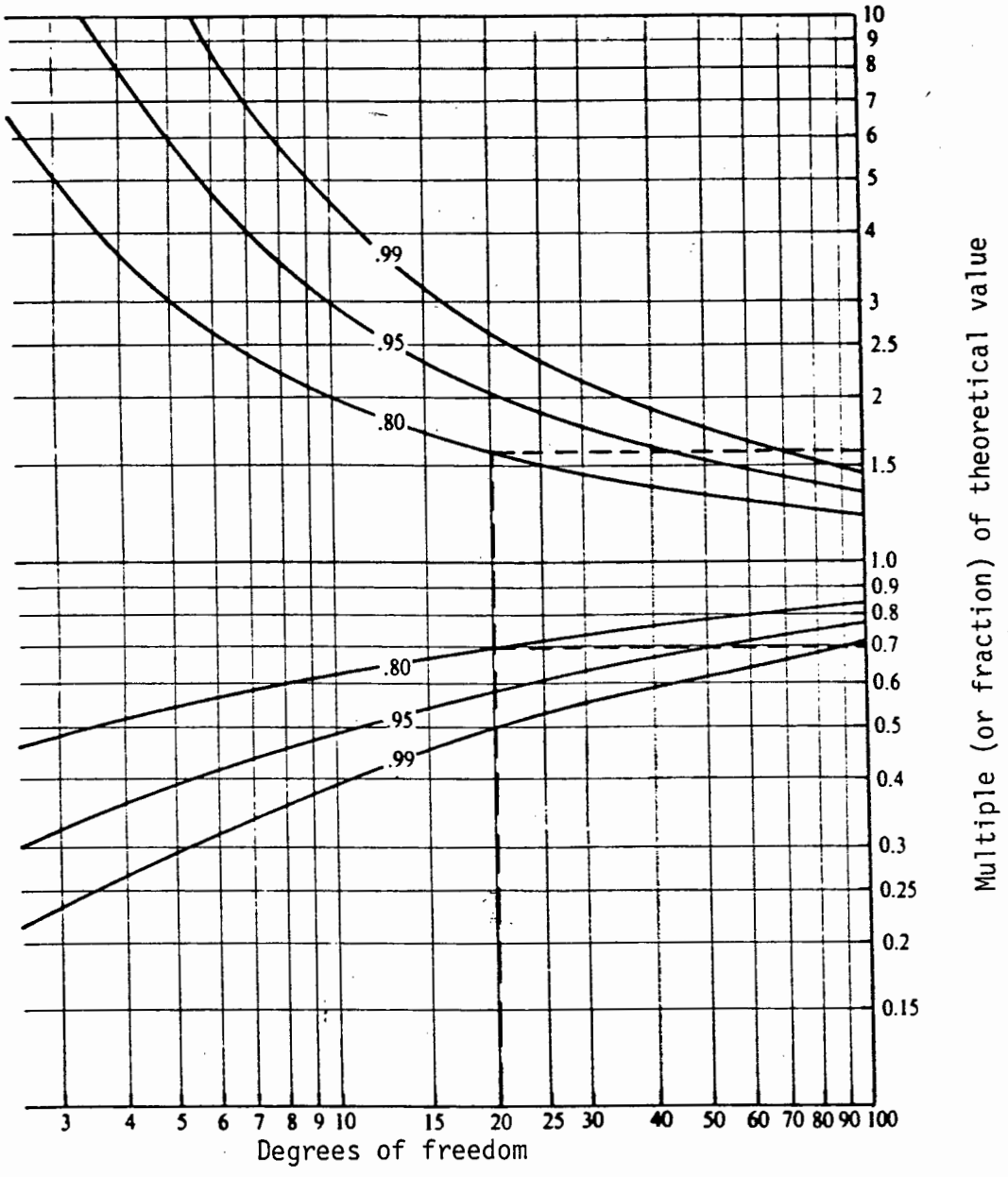

Figure 2.26 : The Chi-square distribution.
The parameters represent the probability of correctness.

Jenkins and Watts (1968)

The confidence for autocorrelation spectra is commonly controlled by the selection of parameters N and m. Alternatively, frequency averaging, discussed in section (b) below, could also be employed.

(b) Confidence for spectra via FFT

The wave energy spectral estimate found using the FFT methods outlined in section 2.2.2.2, have 2 degrees of freedom. Whereas the confidence in section (a) above can be improved by varying the lag number m, FFT spectral estimates are usually averaged in order to improve confidence. There are two types of averaging: frequency smoothing, and averaging whole spectra.

In the case of frequency smoothing, spectral estimates are smoothed over a number of adjacent frequency bands as follows:

$$\hat{G}_k = 1/L \; (G_k + G_{k+1} + \ldots\ldots + G_{k+L-1}) \qquad (2.28)$$

where

$\hat{G}_k$ = the smoothed spectral estimate corresponding to the central frequency of the adjacent frequency bands averaged.

L = the number of adjacent spectral estimates that are averaged

G_k = the unsmoothed energy density estimate - from equation 2.18

The result of equation 2.28 is that the spectral estimate $\hat{G}_k$ will have $v = 2 \times L$ degrees of freedom. (Bendat and Piersol, 1971, p328).

The effect of frequency smoothing is illustrated in Fig 2.27(a), (b) and (c). Spectral parameters apppear in Table 2.2; it is evident that in spite of changes in degrees of freedom and resolution, the significant wave height, H_{mo}, remains identical and the peak period remains similar. Since these parameters are not greatly affected by smoothing, the spectrum of Fig 2.27(c) is probably the most suitable, since it is the best defined.

TABLE 2.2 Spectral parameters for varying degrees of frequency smoothing

Figure	No. of adjacent bands averaged L	Degrees of freedom v	Effective bandwidth Δf (H_z)	Reduction	Peak period T_p (secs)	Significant wave height, H_{mo} (m)
2,27(a)	0	2	0,00195		10,240000	3,349876
2,27(b)	2	4	0,00391		10,343430	3,349875
2,27 (c)	4	8	0,00781		10,138610	3,349876

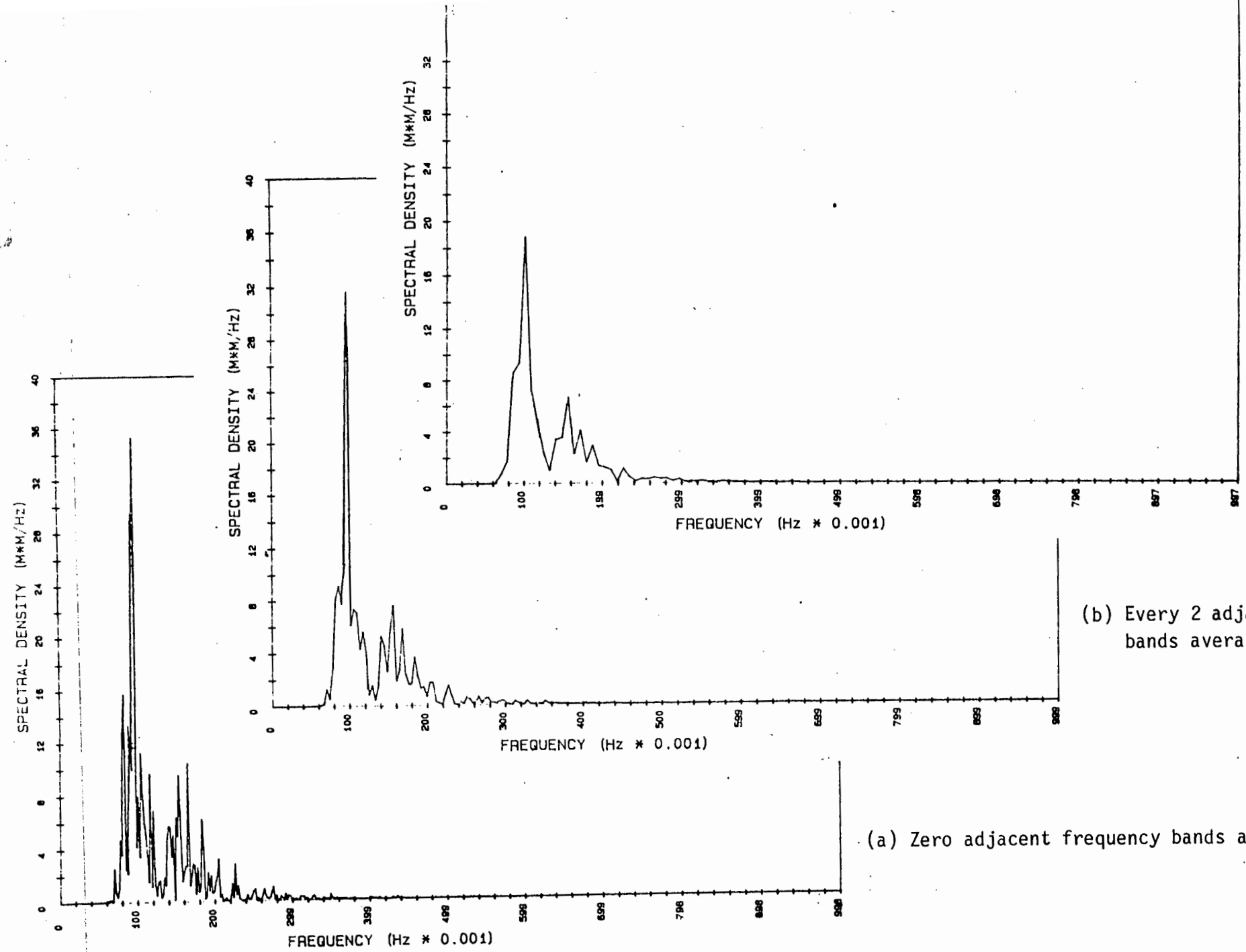

(c) Every 4 adjacent frequency bands averaged.

(b) Every 2 adjacent frequency bands averaged

(a) Zero adjacent frequency bands averaged.

Figure 2.27 : Wave energy spectra with varying degrees of frequency smoothing

The degrees of freedom can also be increased by averaging spectra e.g. the C.S.I.R. double the degrees of freedom to 20 by averaging 2 spectra of v = 10 (van Tonder, 1988). Liu et al (1974, p.66) average 16 spectra, of v = 2 each, to yield v = 32.

2.2.3.6 Frequency Resolution

Due to finite and discrete wave data and calculation methods, wave energy density occurs in frequency bands. The width of such frequency bands, called resolution bandwidth, dictates the frequency resolution of the spectrum; if these bands are too wide, narrow peaks in the energy spectrum could go undetected. Alternatively, if the bands are too narrow, excessive detail results.

(a) Resolution for spectra via Autocorrelation

Spectra of this type have a resolution bandwidth of:

$$\Delta f = 1 / 2hm \qquad (2.29)$$

This indicates the importance of the choice of h and m.

(b) Resolution for spectra via FFT

Spectra of this type have a resolution bandwidth of:

$$\Delta f = 1 / Nh \qquad (2.30)$$

However, frequency smoothing (discussed above) widens the bandwidth according to the number, L, of adjacent spectral estimates averaged. Thus, the effective bandwidth becomes:

$$\Delta f \text{ (effective)} = L / Nh \qquad (2.31)$$

For example, at the C.S.I.R.:

N = 1024

h = 0.5 sec

L = 5

Thus, the effective bandwidth is: $\Delta f = 5 / 1024 \times 0.5 = 0.00977$, which is adequate (van Tonder, 1988).

2.2.3.7 The effect of parameter choices

Computing wave energy spectra requires the choice of:

(1) the sampling interval, h. This was discussed in section 2.2.3.1
(2) the maximum lag number (for the autocorrelation type), m
(3) the number of data points, N.

(2) and (3) are discussed below:

(a) The choice of maximum lag number, m

It is evident that equations 2.27 and 2.29 present two conflicting features i.e. if the number of data points in the wave record, N, and the sampling interval, h, are fixed, then:

1. a large m will yield good frequency resolution, but poor confidence in the spectral estimates.

2. A small m will yield poor frequency resolution and good confidence in the spectral estimates.

Thus an appropriate value of m must be selected, according to the confidence and resolution required.

Fig 2.28(a), (b) and (c) illustrate the effect of increasing the maximum lag number, m. The approximate spectral parameters are presented in Table 2.3; it is evident that the significant wave heights are essentially the same, and that the peak periods are similar. In Fig 2.28(a), the detail in the spectrum appears excessive. Alternatively, Fig 2.28(c) has insufficient detail for locating spectral peaks. Thus, the spectrum of Fig. 2.28(b) is the most suitable.

TABLE 2.3 Spectral parameters for a varying maximum lag number

Figure	Max lag no, m	Degrees of freedom ν	Resolution bandwidth Δf (H_z)	Peak period T_p (secs)	Significant wave height, H_{mo}
2,28(a)	600	3,5	0,00167	10,344830	4,925810
2,28(b)	240	9,5	0,00417	10,000000	4,925817
2,28(c)	100	23,5	0,01000	10,000000	4,9225915

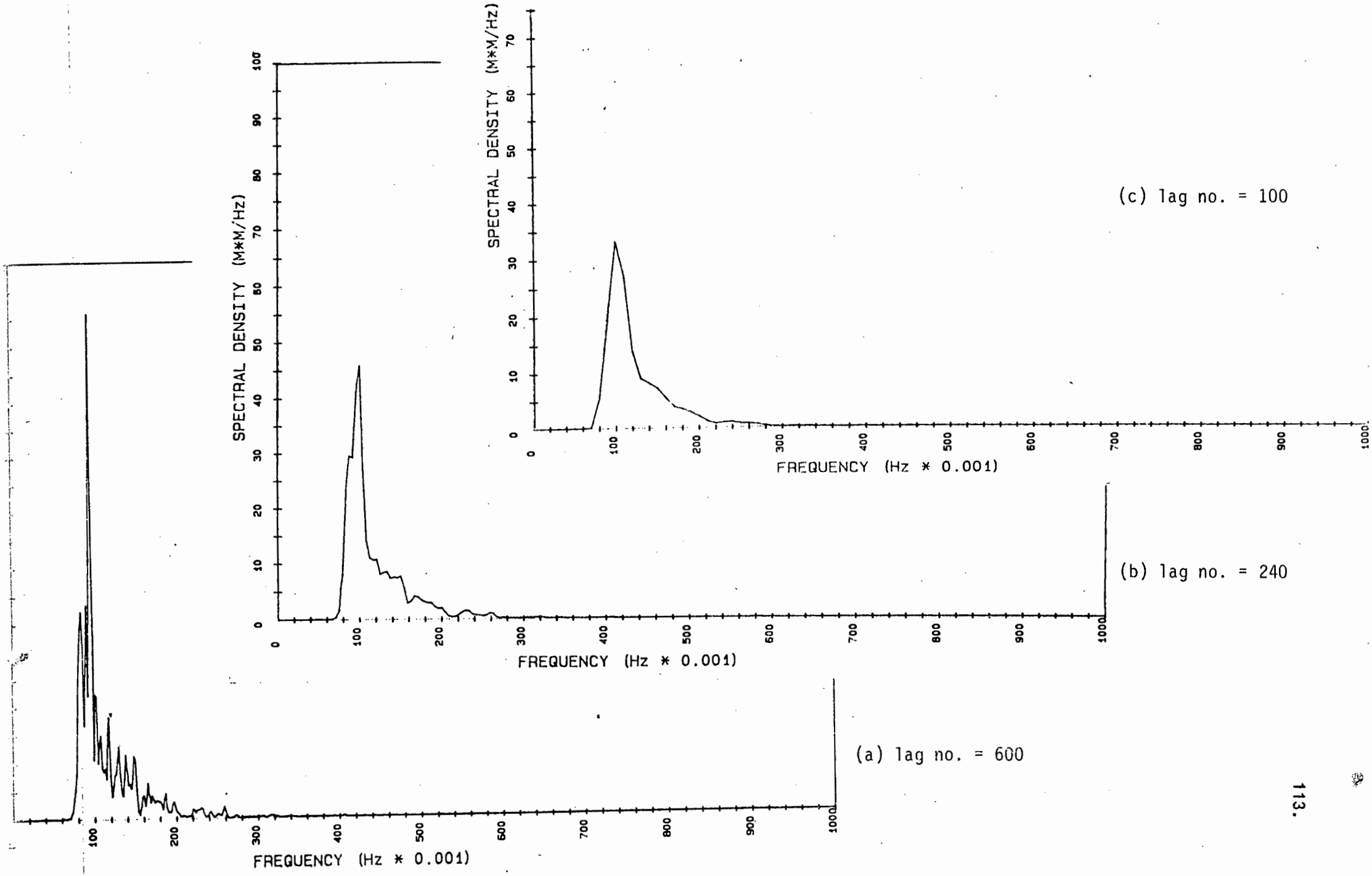

Figure 2.28 : Wave energy spectra calculated with varying lag

(b) The choice of record length (N)

The length of the wave record is defined:

$$T = Nxh \tag{2.32}$$

It was shown in section 2.2.3.1 that the choice of sampling interval, h, is determined by aliasing considerations. It follows, from equation (2.32) that the record length, T, is governed by the number of data points, N.

For the case of spectra via FFT, considering equation (2.30), it is evident that N affects the resolution bandwidth of the spectrum, i.e. a greater number data points leads to greater resolution. The confidence of spectral estimates, however, is not directly affected by N. (Tayfun et al, 1974,, p127). Indirectly though, an increased sampling rate will allow for greater frequency smoothing, for a particular resolution.

In the case of spectra via autocorrelation, from equation (2.26), it is evident that the N directly affects confidence of spectra i.e. a greater N leads to more degrees of freedom (greater confidence). Indirectly, a greater N will reduce leakage, and thereby improve resolution. (Harris, 1974, p118).

2.2.3.8 Comparison of Autocorrelation and FFT spectra

Fig. 2.29 illustrates spectra calculated by means of (a) autocorrelation and (b) FFT. It is evident that their shapes are similar. Any differences between their shapes are primarily due to:

1. different windowing and smoothing techniques (as discussed above) ;
2. different resolution bandwidth and confidence intervals.

TABLE 2.4 Spectral parameters for spectra via (a) auto (b) FFT

Figure	Type of analysis	Degrees of freedom	Resolution bandwidth	Peak period	Significant wave height
2,29(a)	Autocorrelation	11,6	0,00592	13,000	3,9485740
2,29(b)	F.F.T.	10	0,00977	13,474	3,9486730

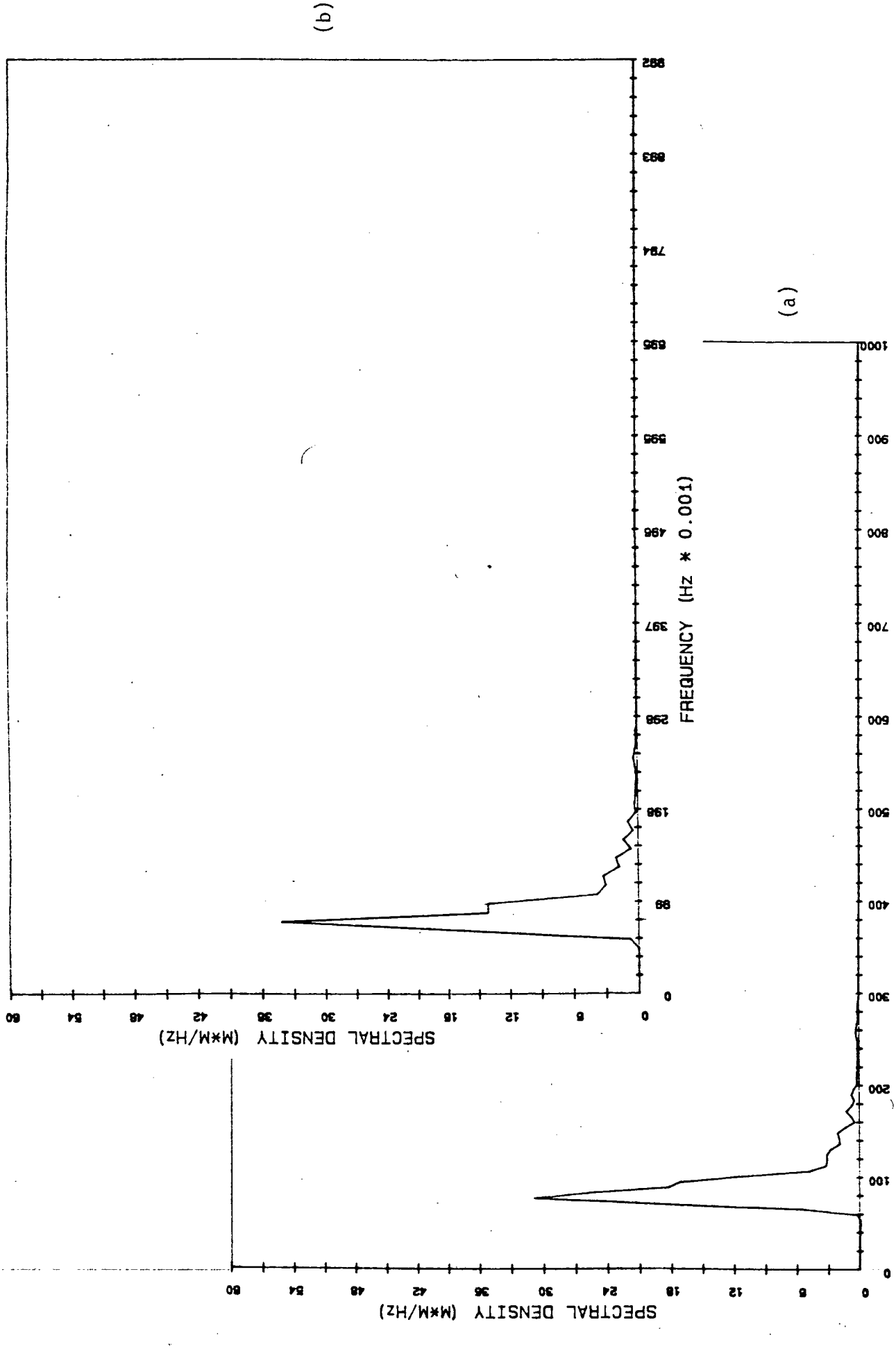

Figure 2.29 : Wave energy spectra calculated by means of (a) autocorrelation and (b) F.F.T.

Furthermore, it is evident from Table 2.4 that:

1. their significant wave heights, H_{mo}, are virtually identical ;
2. their peak periods differ marginally - this can be improved by increasing confidence and resolution.

2.2.3.9 The effects of shoaling on wave energy spectra

Significant changes in the wave energy spectrum occur as waves travel into shallower water (Hallermeier and James,1974,p698). In particular, wave energy transfer to a higher frequency region occurs (Tsuchiya and Yamaguchi, 1974, p 690). These changes are due to wave shoaling and refraction, according to linear wave theory, and also due to nonlinear effects. In order to deal with this:

(i) the whole wave spectrum can be adjusted to account for shoaling and refraction from deeper to shallower water.

(ii) The wave height of interest (usually the significant wave height) can be adjusted from deeper to shallower water. This approach is found to be satisfactory at the C.S.I.R. for most purposes (van Tonder, 1989).

2.2.4 Alternative approaches to spectral analysis

2.2.4.1 The method of maximum entropy for the analysis of spectra

This is a relatively new field, according to Alvarez and Loureiro (1986): "to the authors knowledge, no systematic applications for wind wave analysis have been reported." Descriptions of maximum entropy analysis of spectra are given by Alvarez and Loureiro (1986), for one-dimensional wave energy spectra, and by Briggs (1984, pp 485-499) for directional wave energy spectra. In both of these papers, the maximum entropy spectral analysis and the FFT spectral analysis are found to be comparable.

2.2.4.2 Theoretical spectra

If only limited wave data is available, the theoretical spectrum, although less accurate, may be useful. The usual input parameters required to obtain this spectrum include wave height and period. Additional parameters may help to obtain a more realistic spectrum shape. Examples of theoretical spectra are the Bretschneider, JONSWAP and Pierson-Moskowitz spectra. According to Liu (1984, pp 362-369) the JONSWAP spectrum is "perhaps the most widely used in wave modelling and engineering designs during the last decade."

2.2.4.3 Directional wave energy spectra

The above discussion is restricted to the one-dimensional wave energy spectrum. A more detailed description of wave conditions is the directional wave energy spectrum. As mentioned before (Sec. 1.1), this is a graphical plot which shows the occurrence of wave energy in the component frequencies and directions of ocean waves (illustrated in Fig 1.3). Directional spectra are used in:

(i) diffraction studies of waves (Goda, 1985) ;
(ii) refraction studies of waves (Goda, 1985) ;
(iii) the design of offshore towers and piles; for analysing vibration and the 3-dimensional analysis of structures with torsional loads ;
(iv) the prediction of the response of ships and floating drilling vessels.
(v) the design of wastewater outfalls ;
(iv) the analysis of coastal erosion and littoral sediment transport.

As mentioned in Chapter 1 (Sec. 1.5), the analysis of directional spectra generally requires at least three time series measurements. Alternatively, directional spectra can also be obtained from remotely sensed records e.g. stereophotography (Ichiye and Sugimori, 1974, p 184).

Lundgren and Davidson (1984) describe two principal methods of analysis; the correlation method, and the complete FFT method. Both of these methods have been elaborated, and further methods developed, such as the maximum entropy method, the maximum likelihood method and the Bayesian method. Naranya and Panicker (1974, pp 678-682) also discuss techniques of analysis.

Problems encountered in the computation of directional spectra are similar to those of one-dimensional spectra, such as leakage. In addition, the angular spread of energy is a problem. As a result, measurement and analysis techniques for directional spectra require further research and development.

Directional spectra and measurement is a popular research topic at present, since there is much room for improvement in this field.

2.3 PRESENTATION OF WAVE DATA

The data analysed spectrally or with statistical methods (such as the Draper method) can be presented on an annual and/or seasonal basis. Forms of presentation are:

(i) Scatter diagrams.
(ii) Graphs of the probability of exceedance of wave height.
(iii) Histograms of period.
(iv) Histograms of spectral width parameter.
(v) Persistence diagrams.
(vi) Lifetime wave diagrams.
(vii) Presentations of a group of wave energy spectra.

The construction of these plots, and their uses, is discussed below.

2.3.1 Scatter Diagrams

These diagrams are usually prepared on a seasonal basis. The likely ranges of wave heights, and of wave periods, are divided into 10 (or more) equal intervals each. Each analysed wave record yields a pair of values: wave height (usually the significant wave height) and a corresponding period

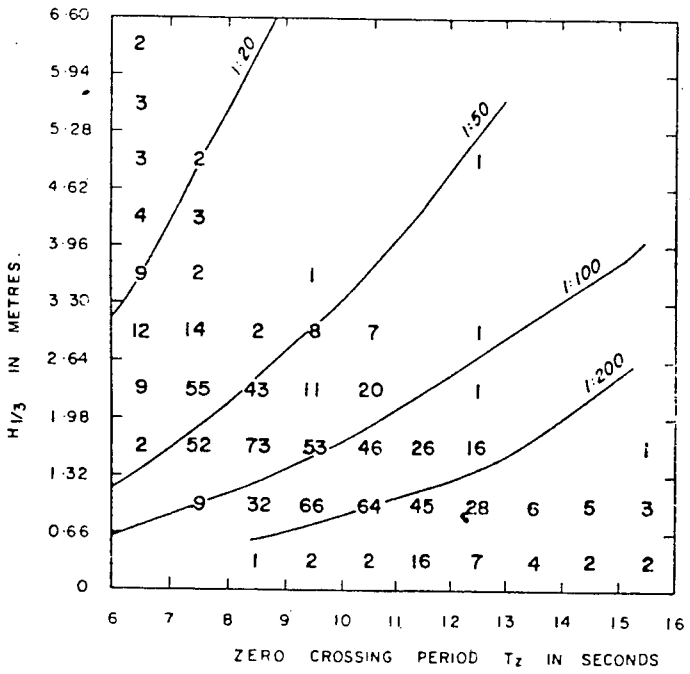

Figure 2.30 : Scatter Diagram, Sandy Bay.

(Deane, 1974)

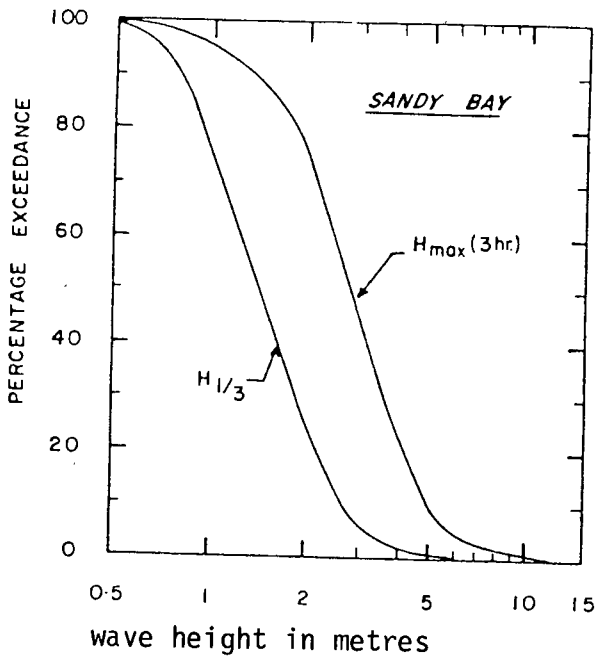

Figure 2.31 : Wave height exceedance graph, Sandy Bay, Eastern Caribbean (Deane, 1974)

(usually T_z or T_p). The number of occurrences of pairs in the same interval of height and period are totalled, and presented in the diagram e.g. Fig.2.30.

The diagram (Fig. 2.30) includes lines indicating wave steepness, H/L, where L, the wavelength, is calculated from the period by means of linear wave theory. Thus, the frequency of occurrence of waves of various steepnesses can be assessed. Wave steepness is a parameter required in wave reflection calculations, and in determining the height of breaking waves.

2.3.2 The wave height exceedence graph

These diagrams can be prepared for various wave height parameters, such as H_{10} ,H_s or H_{max} . The wave height range is divided into equal intervals. The number of occurrences of wave heights in each interval are totalled, for all the wave records in a season. (This data can easily be extracted from the scatter diagram). These totals are accumulated, starting at the greatest height, to yield the number of times a given value of wave height is exceeded. These summations can be expressed as a percentage of the total number of wave heights (each obtained from a wave record). For example, Fig. 2.31 illustrates an exceedence graph for $H_{1/3}$, and for H_{max} for every 3 hour period. (This is obtained from 15 minute wave records taken every 3 hours for a year, in the Eastern Carribean).

An exceedence graph of $H_{1/3}$ may be used, for example, to calculate useable construction time. An exceedence graph of H_{max} may be used to estimate the probable utilization of high speed craft such as hovercraft/hydrofoil, where one unusually large wave can impede progress. These graphs are also used in decisions on methods of construction, and on the best time of year for special operations, such as caisson placement.

2.3.3 The histogram of wave period

Periods, usually for a season, are separated into intervals, e.g. of one second. For each interval, the percentage occurrence of periods (in a season) can be expressed, to yield a histogram. Histograms may be drawn up for various periods, such as T_z and T_p . Fig. 2.32 is an example.

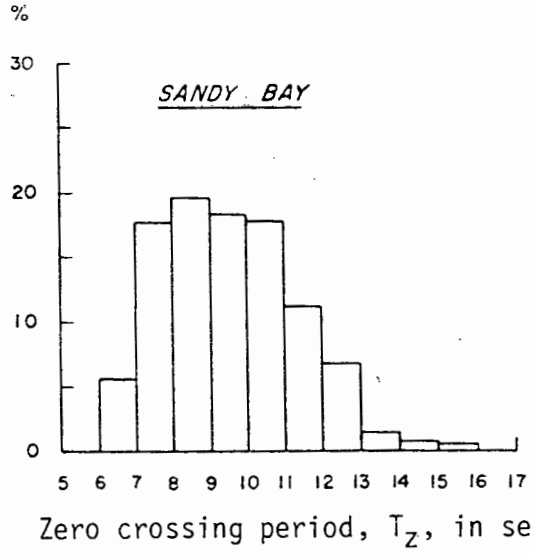

Figure 2.32 : Histogram of zero crossing periods for Sandy Bay, Eastern Caribbean. Deane (1974).

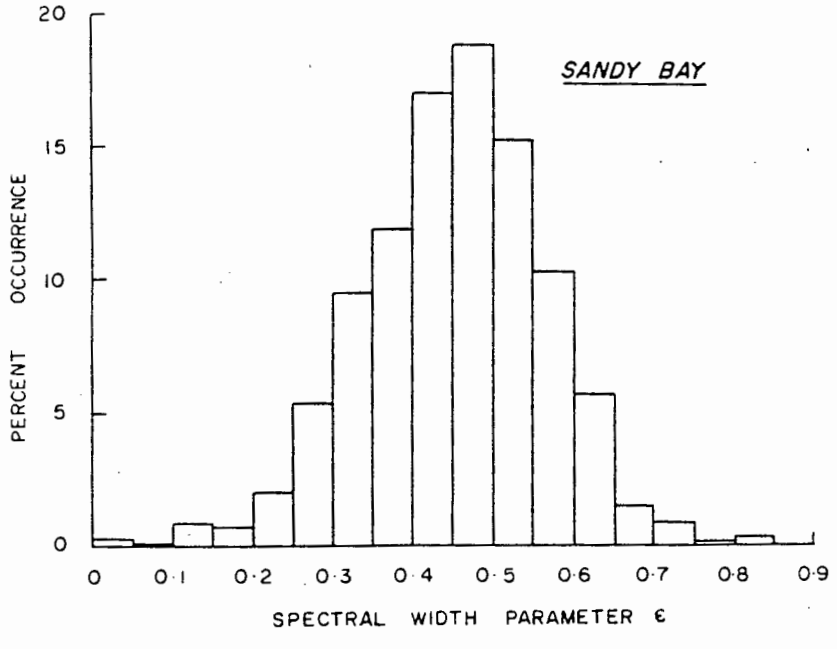

Figure 2.33 : Histogram of spectral width parameter, ε, for Sandy Bay, Eastern Caribbean. Deane (1974)

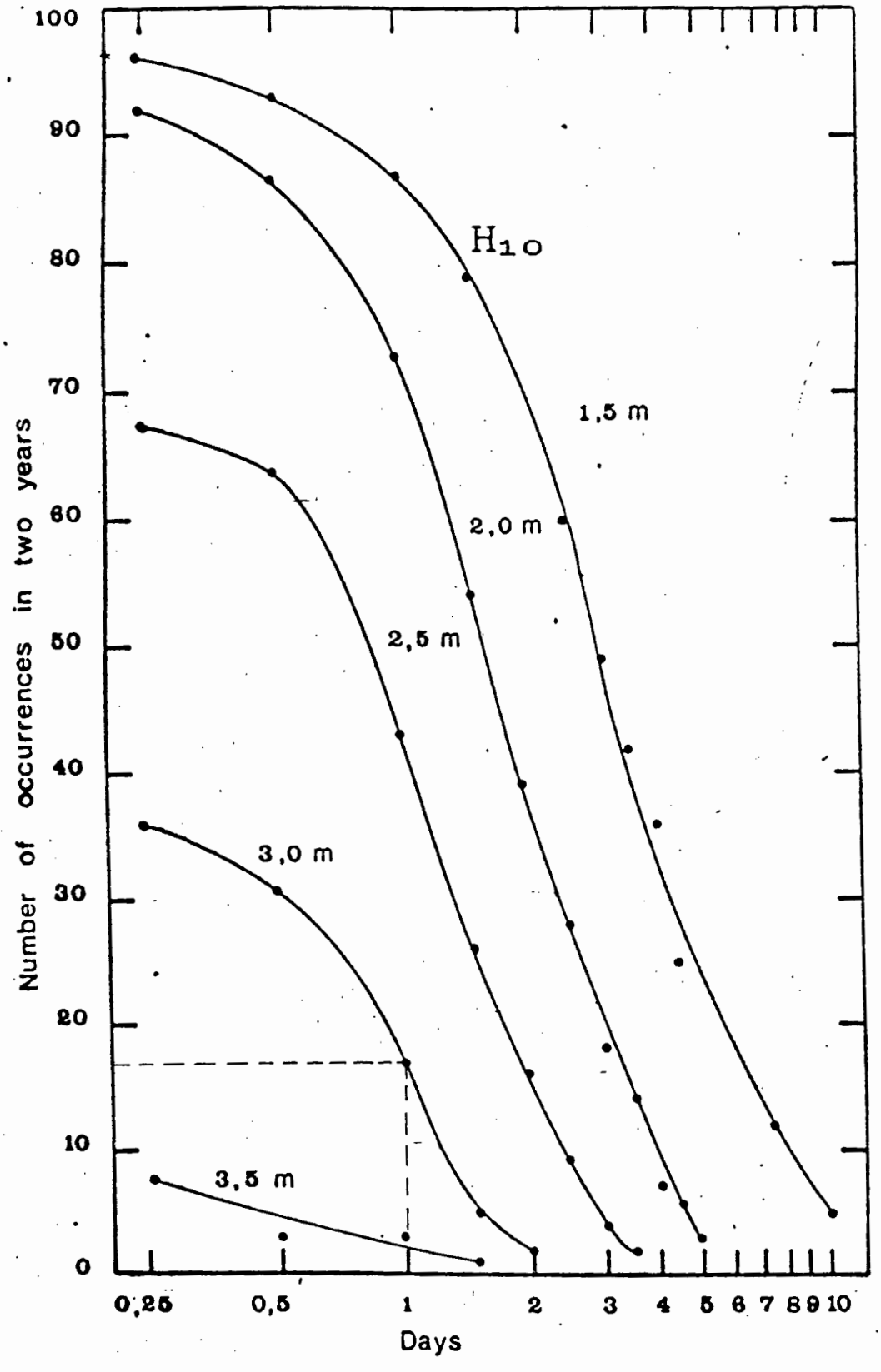

Figure 2.34 : Persistence of waves greater than or equal to a given height, H_{10}, for a two year period.

2.3.4 The histogram of spectral width parameter

Similarly to the above (Sec 2.3.3), the spectral width parameter is also expressed as a percentage occurrence in a time period, usually a year. Fig. 2.33 is an example. These diagrams give an indication of the type of conditions (regular swell or random sea) which occur.

2.3.5 Persistence diagrams

It is often important to know how long a particular condition will last e.g. for planning construction programs, or for planning operations from a moored vessel. To obtain the persistence diagram, a graph of wave height is plotted throughout the year from all the wave records; for each height level the duration of every occasion when conditions are at, or above that level is listed. The information may be presented as shown in Fig. 2.34. As an example to clarify, it is shown in Fig. 2.34 that a wave height (H_{10} in this case) of 3 m or more persists for 1 day, 17 times in two years.

These diagrams are sometimes referred to as *persistence of storms* diagrams. An alternative approach is to quantify the number and duration of calm periods, so that working time on operations such as pipe-laying, which can only proceed in prolonged calm conditions, can be estimated. The resulting diagram is known as the *persistence of calms* diagram.

2.3.6 Lifetime wave diagram

A prediction of the most severe conditions over a long period, such as 50 years, is often required for design purposes (Sec. 2.4.1.1). The highest wave in a long period is predicted as follows:

The proportion of time, say one year, for which a wave height e.g. H_5 or H_{max} is exceeded is calculated as in section 2.3.2 above. This information is plotted on graph paper with distorted scales representing the log-normal, Weibull, or Gumbel type 1 distribution (Khanna, 19742, pp 309-317). If the data tend to be on a straight line, then this line is extrapolated to cover higher return periods, such as 100 years (this is illustrated in Fig. 2.35). If the data lies on a curve, and there does not appear to be a constraint

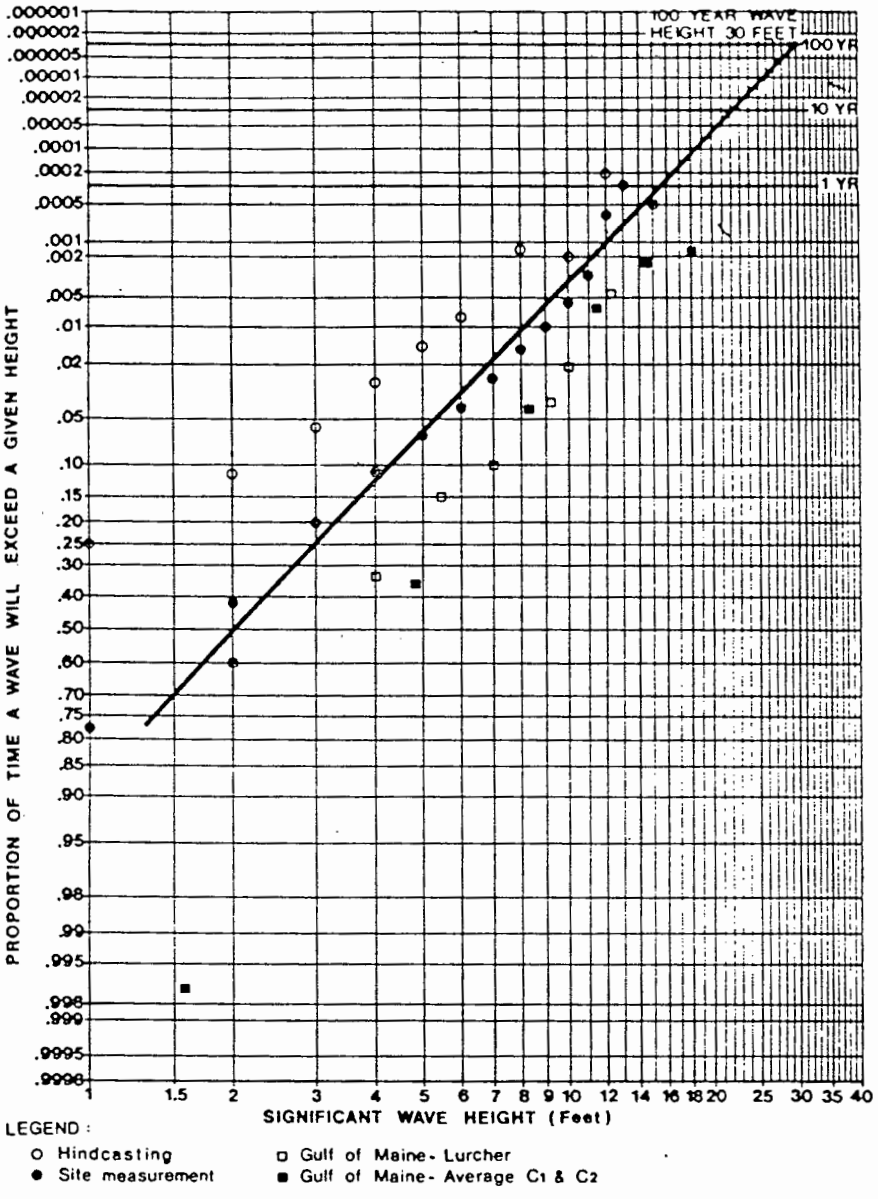

Figure 2.35 : Life-time Wave - Log normal plot.

Khanna et al (1974)

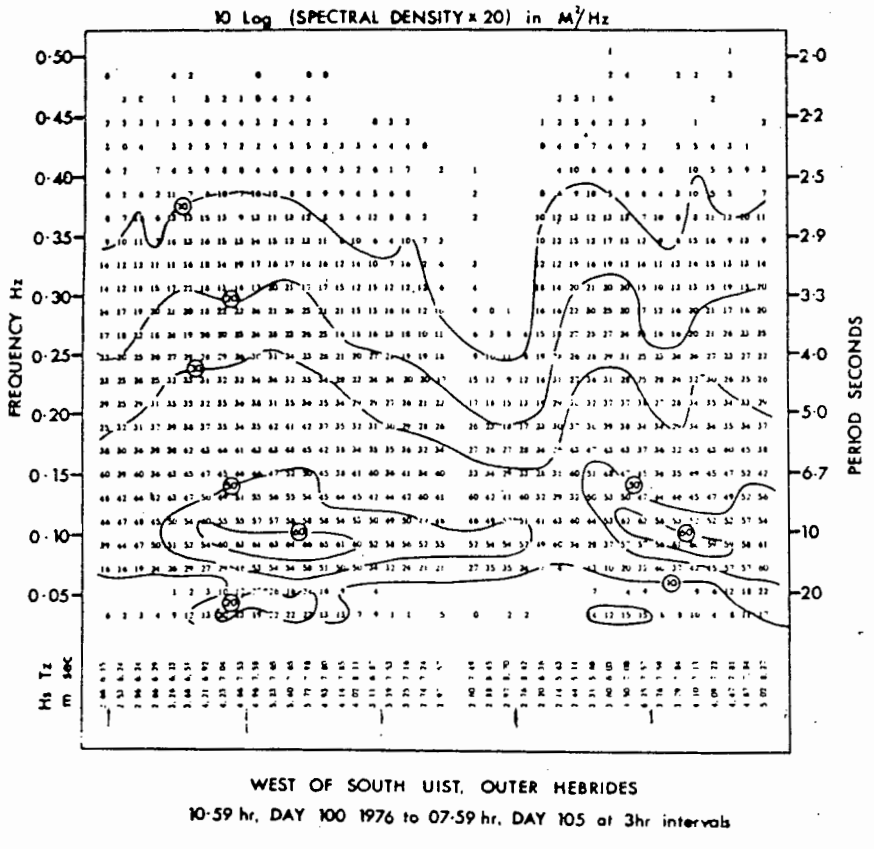

Figure 2.36 : Presentation of spectra for five consecutive days.
Draper (1976)

caused by water depth, fetch distance, wind speed, refraction, diffraction etc., then another distribution should be tried (Khanna, 1972, p 317). Examples of other distributions which can be used for this purpose, are the Fretchet,Pearson and exponential distributions.

2.3.7 The presentation of one-dimensional wave energy spectra

A method of presenting several wave energy spectra in one diagram is as follows:

Each spectrum is presented as a column of numbers, each number representing an energy density at its corresponding frequency. As shown in Fig 2.36, these spectra (in column form) are listed adjacent to each other in chronological order, from left to right. Contours of wave energy can then be drawn. From this diagram it is possible to identify the arrival of swell and the generation of waves (Draper, 1976, p 5).

2.4 THE APPLICATION OF ANALYSED WAVE DATA IN COASTAL ENGINEERING

Having discussed the analysis of wave data in detail, some mention should be made of the use of the analysed data, particularly since waves cause the largest hydraulic forces imposed on structures in the coastal zone. The application of analysed wave data in the design of coastal structures,in physical modelling, and in sediment studies is discussed.

2.4.1 Analysed wave data in the design of coastal structures

2.4.1.1 The design wave height

Various wave height parameters have been discussed above, e.g. H_1 , H_{10} , H_s H_{max} etc. For the design of a particular structure,the parameter to use for design must be selected. In addition, the most probable highest wave, of the selected parameter type, must be determined for a particular period of time e.g. 100 years.

The type of design wave height parameter selected depends on the mode of failure for which the structure is designed. In the case of structures designed on a total failure basis, such as offshore oil platforms and monolithic breakwaters, the probable maximum wave height, H_{max}, is often used for design. According to the Shore Protection Manual (C.E.R.C, 1977), in the case of *rigid* structures, such as cantilever sheetpile walls, one very high wave can cause a sudden failure; therefore, the design wave in this case would be selected close to H_1. *Semi-rigid* structures, such as steel sheetpile cell structures, can absorb considerable high wave action before failure; therefore the design wave would be selected between H_1 and H_{10} . *Flexible* structures, such as rubble mound structures, will fail by degrees in excessively high wave conditions; therefore the design wave height is normally H_s. However, this height could be selected higher (up to H_{10}), depending on

(i) the frequency of occurrence of damaging waves ;
(ii) the economics of construction, of protection given, and of the maintenance required, for the rubble mound structure.

Once the type of design wave parameter is selected, from the above considerations, its highest value likely to occur in a period of time, usually of the order of 50 to 100 years, must be found. This is achieved with a lifetime wave diagram, as discussed in section 2.3.6 . The resulting parameter is used in the design calculations.

The degree of knowledge of the structure, and of its type of failure, also affects the design wave height in an indirect fashion. For example, if physical modelling is used for a proposed structure, a large degree of knowledge about the structure is obtained, and therefore a smaller factor of safety (and effectively a smaller wave height) can be used.

Breaking waves:
If the water depth on the seaward side of a structure is shallow, then it may be subjected to broken and breaking waves. The Shore Protection Manual (C.E.R.C.,1977) deals with the calculation of the depth of wave breaking and, if breaking occurs, the design breaker height, H_b. This is restricted to monochromatic waves only (i.e. sinusoidal waves of a single period and amplitude). Goda (1985) presents a reliable design analysis technique for

random breaking waves. This is developed from a computational model of random wave breaking, checked against laboratory data. The result of the analysis is the design H_s and/or the design H_{max}, corresponding to either a breaking or a nonbreaking condition.

For the above analyses the input parameters are the design wave height parameters mentioned above, adjusted primarily for refraction (and also for diffraction and friction if necessary).

Wave period is an important parameter in design. It affects wave steepness, which is relevant to wave reflection and wave breaking. The C.S.I.R. make frequent use of T_p ,since it is the period at which the highest wave energy occurs. If wave energy spectra are bi-modal, however, T_p will not represent the period of highest wave energy unambiguously; T_z may be appropriate in this case (van Tonder,1989).

2.4.2 The application of analysed wave data in physical modelling

If only a monochromatic wave generator is available, the significant wave height is often used to represent an irregular wave. However, this is the least adequate form of representing the sea surface; errors may be large. For the design of offshore structures, such as oil drilling rigs, and monolithic structures, H_{max} is used in the model.

Irregular wave generators can be used to represent the sea surface. Wave energy spectra are used in this reproduction of irregular waves; the process (used at the C.S.I.R.) to reproduce waves measured at Richards Bay in a model, is as follows.

From waverider buoy wave records, taken for 20 minutes every 6 hours, wave energy spectra are calculated. The significant wave height, H_{mo}, corresponding to a particular storm condition, is defined; only spectra having H_{mo} above this defined H_{mo} are considered. These spectra are normalised i.e. the energy densities are divided by the peak energy density and the corresponding frequencies are divided by the frequency of peak energy density. The resulting spectra are averaged, to yield a general spectral shape (this shape often compares well with certain theoretical spectra, such as the Pierson - Moskovitz spectrum). Thereafter, from a scatter diagram, or from

histograms, various representative combinations of H_{mo} and T_p are selected. The general spectral shape is then multiplied by these selected combinations of H_{mo} and T_p, to obtain spectra for use in the physical model. Direction information is also available from measurements taken at the site, mainly with a clinometer.

The wave generator at the C.S.I.R. can operate with up to 64 spectral components, each defined by an amplitude, A, a frequency, f, a direction, θ, and a phase angle, ϕ. The amplitude A is obtained from the wave energy spectrum, for each frequency band, from the formula:

$$G_k = \tfrac{1}{2} A^2/\Delta f$$

where G = the energy density
Δf = the frequency bandwidth
A = the amplitude of the component

The frequency f is the frequency corresponding to the centre of each frequency band. The phase angle, ϕ, is input randomly. The wave angle, θ, is determined from direction measurements taken at the site (with a clinometer). This is sufficient information to simulate actual wave conditions.

Range action

Physical wave models can also be used to determine the effects of range action in harbours. Range action occurs if harbour boundaries are such that the frequency of an incident wave corresponds to one of the natural modes of oscillation (i.e. resonant frequencies) of the water body, causing amplification of waves at that frequency. At the CSIR, the procedure is as follows.

Firstly, a numerical model is used to detect range action for a particular harbour configuration. The input of the model is a white noise spectrum i.e. a spectrum having components at every frequency. The output of the model is a spectrum with distinct peaks at the resonant frequencies of that harbour layout. Such mathematical models were used in the development of Cape Town harbour (Campbell, 1979, pp 7-12). Thereafter the physical model will be tested with regular (monochromatic) waves at these resonant frequencies (van Tonder, 1989). The harbour configuration will be adjusted accordingly.

Long period waves (caused by the grouping of waves) which cause resonance, can be detected as a peak in the low frequency region of the energy spectrum e.g. In Saldanha Bay moored ships tended to move excessively; it was discovered that the natural period of ship moorings corresponded to the period of long period waves, which were evident in the wave energy spectrum (van Wyk, 1989).

2.4.3 The application of analysed wave parameters in sediment studies

The nett movement of sediment is caused largely by longshore currents which are caused by waves approaching the shore at an angle. Wave parameters used in this type of analysis are the significant wave height, H_s , the peak period, T_p, and direction information.

It is difficult to obtain wave direction information of the accuracy required for this type of analysis. If only a single wave direction (such as from clinometer readings) is available, a theoretical directional spread, in the form of a cosine function, may be used in the analysis, to simulate the directional variation of actual sea waves. Preferably, direction information can be obtained from directional wave energy spectra (Schoonees, 1989).

2.5 CONCLUSION

The following significant points have emerged in this chapter:

(i) Limited information can be obtained from statistical methods of analysis.

(ii) Analysis of one dimensional wave energy spectra clearly yields a more detailed description of the sea state and some useful parameters for coastal engineering.

(iii) The quality of the wave energy spectrum is shown to be highly sensitive to the choice of input parameters; particularly the number of sampling points, the sampling interval, and the maximum lag number (for autocorrelation analysis).

(iv) There are several ways of presenting analysed wave data; these are very useful for coastal engineering applications.

BIBLIOGRAPHY : CHAPTER TWO

Alvarez, J.C. and Loureiro, A.M.	1986	"Maximum Entropy Spectral Estimation for Wind Waves", Proc. of the 20th Coastal Eng. Conf., Vol. 1, pp 3-16.
Bendat, J.S. and Piersol, A.G.	1971	Random Data : Analysis and Measurement Procedures. New York, Wiley-Interscience.
Bergland, G.D.	1969	"A Guided Tour of the Fast Fourier Transform", I.E.E.E. Spectrum, July 1969.
Bracewell, R.N.	1978	The Fourier Transform and its Applications. New York, McGraw-Hill.
Broeders, W.P.A. and van Loenen	1974	"Wave Conditions and Coastal Structures", Proc. of the International Symposium on Ocean Wave Measurement and Analysis, Vol.1, pp.543-561.
Briggs, M.J.	1984	"Calculation of Directional Wave Spectra by the Maximum Entropy Method of Spectral Analysis", Proc. of the 19th Coastal Eng. Conf., Vol. 1, pp 484-499.
Campbell, N.P., Russel, K.S. and Toms, G.	1979	"The Development of Table Bay Harbour", PIANC, Vol. 11, No. 33, pp 316.
Cartwright	1961	"The Use of Directional Spectra in Studying the Output of a Wave Recorder on a Moving Ship", Ocean Wave Spectra, May 1961, p.211.
Champeney, D.C.	1973	Fourier Transforms and their Physical Applications. London and New York, Academic Press.
Coastal Engineering Research Centre,	1977	Shoe Protection Manual. Washington, D.C., U.S. Government Printing. U.S. Army Office.
Cochran, W.T. et al	1967	"What is the Fast Fourier Transform?" I.E.E.E. Transactions on Audio and Electroacoustics, Vol. AV-15, No.2, June 1967, pp.45-55.
Coetzee, L.	1988	Personal interview, C.S.I.R., November 1988.

Datawell, B.V.	1976	Manual for Waverider f1; Zomerluststraat 4, Haarlem, TheNetherlands.
Dattatri, J. and Nayak, I.V.	1976	"Ocean Wave Record Analysis by Tucker's Method - an evaluation". Proc. of the 15th Coastal Eng. Conf., Vol.1, pp.289-300.
Deane, C.	1974	"Wave Climate in the Eastern Caribbean" Proc of the International Symposium on Ocean Wave Measurement and Analysis, 1.
de Carvalho, M.M., Ramos, F.S., Moraes, C de Campos	1970	"Spectral Computations on Pressure Wave Gauge Records", Proc. of the 12th Coastal Eng. Conf., Vol.1, pp.65-83
Draper, L.	1963	"Derivation of a 'Design Wave' from Instrumental Records of Sea Waves", Proc. Institution of Civil Engineers, Vol.26, pp.305-316.
Draper, L.	1966	"The Analysis and Presentation of Wave Data - a Plea for Uniformity", Proc. of the 10th Coastal Eng. Conf., Vol.26, pp.305-316
Draper, L.	1976	"Revisions in Wave Data Presentation", Proc. of the 15th Coastal Eng.Conf., Vol.1, pp.3-9.
Goda, Y.	1974	Estimation of Wave Statistics from Spectral Information", Proc of the International Symposium on Ocean Wave Measurement and Analysis, Vol.1,pp.320-337.
Goda, Y.	1985	Random Seas and Design of Maritime Structures, University of Tokyo Press, Japan.
Harris, F.J.	1978	"On the Use of Windows for Harmonic Analysis with the Discrete Fourier Transform", Proceedings of the I.E.E.E., Vol. 66, No.1, January 1978.
Helstrom, C.W.	1984	Probability and Stochastic Processes for Engineers. New York, Macmillan Publishing Company.
Higgins, R.J.	1974	"Fast Fourier Transform : an introduction with some minicomputerexperiments", American Journal ofPhysics, Vol.44, No.8, August 1974 pp.766-773.

Hoffman, D. 1974 "Analysis of Wave Records and Application to Design", Proc. of the International Symposium on Ocean Wave Measurement and Analysis, Vol.1, pp.235-253.

Houmb, O.G. Pederson, B. and Steinbakke, P. 1974 "Norwegian Wave Climate Study", Proc. of the International Symposium on Ocean Wave Measurement and Analysis, Vol.1, pp.25-39.

Jenkins, G.M. and Watts, D.G. 1968 Spectral Analysis and its applications. San Francisco, U.S.A., Holden-Day Inc.

Khanna, J. and Andru, P. 1974 "Lifetime Wave Height Curve for Saint John Deep Canada", Proc. of the International Symposium on Ocean Wave Measurement and Analysis, Vol.1, pp.301-319.

Lawson, N.V. and Youlll, P.H. 1980 "Realtime Wave Analysis, Newcastle, Australia", Proc. of the 17th Coastal Eng.Conf., Vol.1, pp.412-420.

Lee Harris, D. 1970 "The Analysis of Wave Records", Proc. of the 12th Coastal Eng. Conf., Vol.1, pp.85-100.

Liu, P.C. 1984 "On a Design Wave Spectrum", Proc. of the 19th Coastal Eng. Conf., Vol.1, pp.362-369.

Liu, P.C. and Robbins, R.J. 1974 "Wave Data Analysis at GLERL", Proc. of the International Symposium on Ocean Wave Measurement and Analysis", Vol.1, pp.64-73.

Lundgren, H. and Davidson, E. 1984 "Description of Natural Sea States", Proc. of the 19th Coastal Eng. Conf. Vol. 1, pp 501-511.

Manohar, M., Mobarek, I.E. and El Sharaky, N.A. 1976 "Characteristic Wave Period", Proc of 15th Coastal Eng. Conf., Vol.1, pp.273-288.

Marks, W. 1963 The Application of Spectral Analysis and Statistics to Seakeeping. New York, The Society of Naval Architects and Marine Engineers. Reprinted 1968.

Mitsuyasu, H. and Mizuno, S. 1976 "Directional Spectra of Ocean Surface Waves", Proc. of the 15th Coastal Eng. Conf., Vol.1, pp.329-348.

Panicker, N.N. and Borgman, L.E.	1970	"Directional Spectra from Wave-gauge Arrays", Proc. of the 12th Coastal Eng. Conf., Vol.1, pp.117-136.
Panicker, N.N. and Borgman, L.E.	1974	"Enhancement of Directional Wave Spectrum Estimates", Proc. of the 14th Coastal Eng. Conf., Vol.1, pp.258-279.
Ramirez, R.W.	1985	The FFT, Fundamentals and Concepts. Englewood Cliffs, New Jersey,Tektronix Inc.
Rossouw, J, Coetzee, L.W., and Visser, C.J.	1982	"A South African Wave Climate Study", Proc. of the 18th Coastal Eng. Conf., Vol. 1, p 87.
Shillington, F.A.		Surface Waves near Cape Town 1 : Measurement and Statistics, Dept. of Oceanography, UCT.
Thompson, E.F.	1974	"Results from the CERC WaveMeasurement Program". Proc of the International Symposium on Ocean Wave Measurement and Analysis, Vol.1, pp.836-855.
Tucker, M.J.	1961	"Simple Measurement of Wave Records", Dock and Harbour Authority, Vol.42,p.231.
Tucker, M.J.	1963	"Analysis of Records of Sea Waves", Proc. Instn. Civ. Engnrs, Vol 26, pp.305-316.
Van Tonder, A.	1988	Personal interview, C.S.I.R., November 1988.
Visser, C.J.	1979	A Practical Approach to Understanding Wave Data Evaluation and SpectralAnalysis. ECOR Coastal Engineering Course, Stellenbosch, 1979.
Walpole, R.E. and Myers, R.H.	1978	Probability and Statistics for Engineers and Scientists. New York, Macmillan Publishing Co.
Wilson, J.R. and Baird, W.F.	1972	"A Discussion of Some Measured Wave Data", Proc. of the 13th Coastal Eng. Conf., Vol.1, pp.113-130.
Wilson, B.W., Chakrabarti, S.K. and Snider, R.H.	1974	"Spectrum Analysis of Ocean Wave Records", Proc of the International Symposium on Ocean Wave Measurement and Analysis, Vol.1, pp.87-106.

CHAPTER 3: CURRENT MEASUREMENT

3.1 INTRODUCTION

Data on current velocities, and on current circulation patterns is required for many applications, for example:

i) For the design of structures such as offshore drilling platforms.

(ii) For the determination of harbour breakwater configurations to allow safe access for vessels.

(iii) For planning operations which are sensitive to currents, such as laying undersea cables and placing caissons.

(iv) To predict sediment movements (dealt with in chapter 4).

(v) To predict the movements of pollutants, particularly for the design of outfalls and the selection of waste disposal sites.

(vi) To calculate the directional wave energy spectrum, from wave orbital current measurements. These spectra have many uses (described in Sec. 1.2.4.1)

(vii) To serve as warning systems; current measurements can be observed as they occur (i.e. 'real time' measurement). If excessive currents are observed, construction or operations (e.g. drilling) can be delayed to avoid disaster.

In general, the velocity of horizontal currents is measured. These currents comprise short-period, fluctuating currents produced by wave action, and quasi-steady, ambient currents caused by long-term phenomena (such as tides, winds, density gradients and mass transport). The primary objective of current measurement is to determine the ambient, quasi-steady current velocity only, since the short-period currents can be calculated from wave records, using linear wave theory (and other theories). The ambient current

velocity can be interpreted from measured current records, by filtering out the short-period fluctuating currents. An alternative form of current measurement is needed, however, to calculate the directional wave energy spectrum (Sec. 1.5); this is calculated from a record of the short-period wave-produced currents, including vertical currents.

There are traditionally two main categories of sea current measurement technique, classified by the frame of reference used:

(i) Eulerian techniques, whereby currents are measured relative to the earth (typically with moored current meters).

(ii) Lagrangian techniques, whereby currents are measured from the trajectories of water particles (typically using free-drifting buoys).

Another technique is current profiling, i.e. determining the distribution of current velocity versus depth. Furthermore, currents can be measured by remote sensing; particularly H.F. radar, which yields average currents over large areas of the sea.

This chapter deals with current measurement techniques. Emphasis is placed on the principle of operation of instruments, the technique of obtaining measurements, and the interpretation of measurements. In addition, comments are made on the performance and accuracy of techniques, as well as any significant advantages, disadvantages and common problems encountered.

3.2 EULERIAN CURRENT MEASUREMENT

This type of measurement is most useful for determining current velocities at the site of interest, e.g. a proposed harbour site. In general, moored Eulerian current meters are used.

3.2.1 Eulerian current meters

Some Eulerian current meters operate by mechanical means e.g. by rotating propellers; others operate by detecting changes in physical properties (e.g.

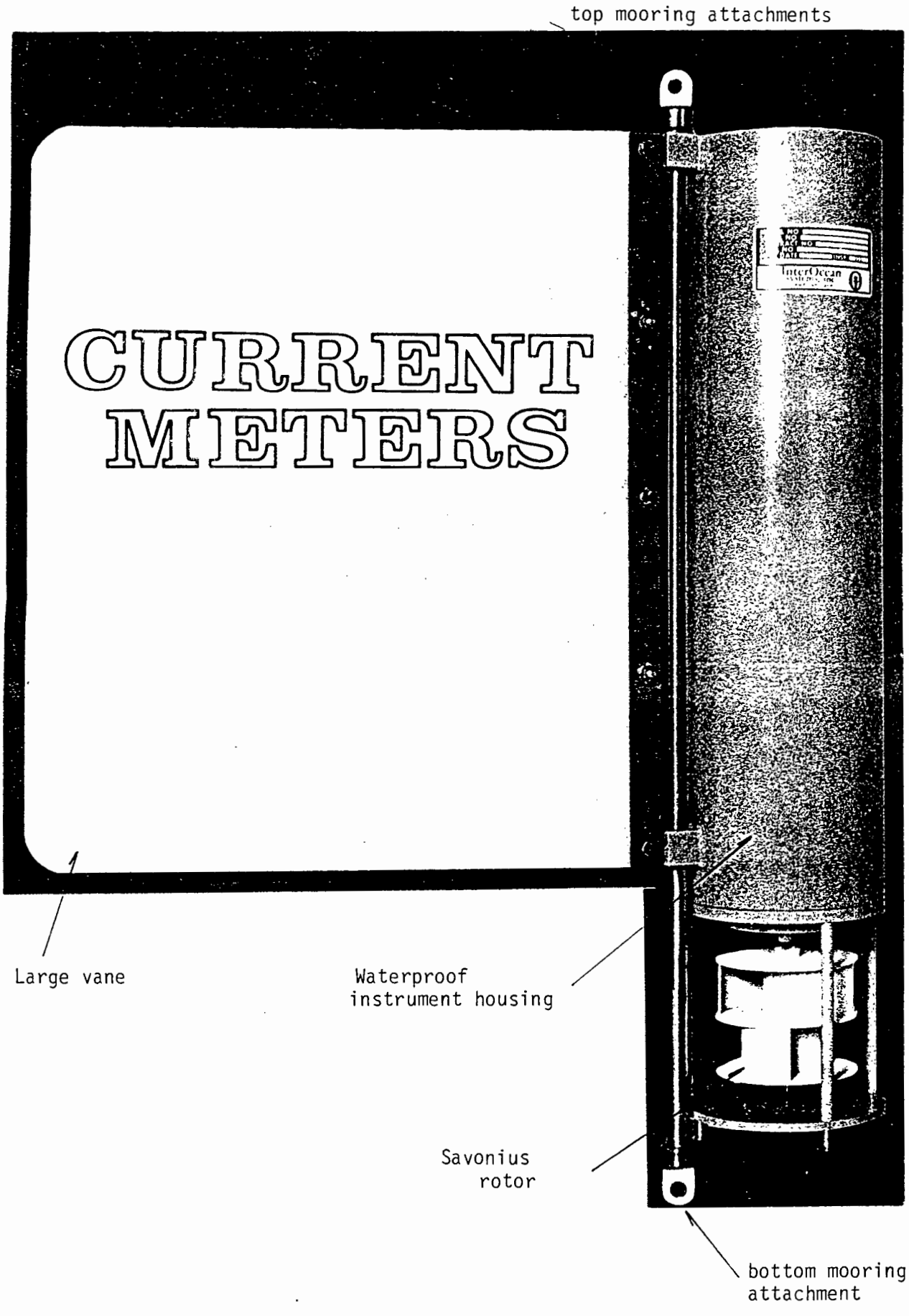

Figure 3.1 : A Rotor-vane current meter.

induced electric current) corresponding to the water flow. The direction and the speed of the current may be measured separately; alternatively, components of current velocity measured in two directions may be combined, to obtain the resultant current vector. Various types of Eulerian current meters are discussed below.

3.2.1.1 Rotor-vane current meters

The motion of water can drive a rotor. The Savonius rotor (Fig. 3.1), which turns about a vertical axis, is commonly used. This rotor has minimal friction, since it turns on bearings, and its weight is adjusted to be neutrally buoyant. The vanes of the rotor are arranged so that the direction of rotation is the same, regardless of the current direction; the rate of rotation is proportional to the current speed. The rotations are summed mechanically or electronically, over a period. The meter is calibrated so that the number of rotations represents a "length" of water which has passed the rotor. This length, divided by the time period, yields the mean current speed for that period.

Direction is determined with the use of a vane (Fig. 3.1), and a compass mounted within a waterproof casing. With a large vane, the entire meter is orientated in the current direction, which is then electronically recorded from the compass. The Aanderaa RCM4 current meter, used by the C.S.I.R., operates in this way.

Unfortunately this type of meter is totally unsuitable for current measurement near the ocean surface, since it does not have adequate response to reversing flows due to wave action, leading to large velocity errors (Woodward, 1985, pp 755-762). It is therefore used at greater depths which are free of wave action.

A small pivoted vane, as employed on the vector averaging current meter (VACM), is more suitable for use near the surface, since it is more sensitive to fluctuations in current direction (The C.S.I.R. construct their own VACM). However, even though the VACM measures currents near the sea surface far more accurately than the Aanderaa RCM4, it is still not suitable for current measurement in strong wave motion (Botes,1988).

3.2.1.2 Propeller current meters:

Components of current can be recorded in two horizontal, orthogonal directions. The vector-measuring current meter (VMCM), illustrated in Fig.3.2, operates in this way: two pairs of axially connected propellers are orthogonally mounted; four electronic pulses are recorded for each propeller rotation, and the corresponding direction of rotation (forward or reverse) is also recorded. The sum of rotations over a period yields the mean current velocity component for that direction; the resultant current velocity for that period can be calculated from these components. The VMCM is designed to measure currents near the surface (Winant et al, 1978, p 130).

Another system has impellers mounted in three orthogonal directions. As in the above, pulses corresponding to impeller rotations are recorded, with pulse length indicating the direction of rotation (Dextraze, 1968, p 671). The current velocity components in three orthogonal directions are recorded; the directional wave energy spectrum can be calculated from this data (Sec. 1.5.).

3.2.1.3 Electromagnetic current meters

As discovered by Faraday in 1831, if a conductor is moved through a magnetic field, an electric potential is induced. Electro-magnetic current meters make use of this principle; the water itself serves as the conductor, and the magnetic field is generated by a solenoid. The water flowing through this field induces an electric potential, perpendicular to the water current. Provided that no electrical power is drawn, this electric potential is independent of the water conductivity (which is related to salinity). With two pairs of sensing electrodes, two components of this electric potential can be detected. These components are converted, by means of a calibration curve, to two components of the current velocity, from which the resultant current velocity can be calculated (Huntley and Bowen, 1974, p 540).

This type of current meter is ideal for the measurement of rapidly oscillating near-surface current measurements, since it has no moving parts and a fast response time (Forristall and Hamilton, 1978, p 208). Furthermore, if the meter constructed is rugged and compact, surf zone measurements are feasible.

Boundary layer flow fluctuations cause difficulties in the calibration of this type of meter (McCullough, 1985, p 46-A-2). This is affected by the shape of the sensing head, which contains the solenoid and the sensing electrodes The InterOcean S4 meter alleviates the problem with a unique shape (i.e. a ribbed sphere) (Cushing, 1976, p 25-C-2).

Instead of using a solenoid to produce a magnetic field, the geomagnetic field (i.e. the earths magnetic field) can be used. As shown in Fig. 3.3, a relatively constant vertical component of the geomagnetic field permeates every point on the earths surface. Water flowing through this magnetic field produces an electrical potential which can be measured with sensitive sensing electrodes (Gonsalves and Brainard, 1981, pp 233-237); through a calibration, current velocity can be obtained from this measured potential.

Fluctuations of the earths magnetic field can occur, although this is generally not a problem. However, electrical and magnectic fields, from ships nearby, can cause errors (Sanford, 1982, p 104).

3.2.1.4 Acoustic flow meters

A sound of a particular frequency is transmitted from a sound source, and is reflected off moving particles (such as plankton) in a current. By the Doppler effect, the frequency of the reflected sound will change from that which is transmitted, due to the motion of the water particles relative to the sound source. This change in frequency, which is sensed by a transducer and recorded, is proportional to the velocity component of the moving water particles, in the direction of the transducer. Two orthogonal velocity components can be determined in this fashion, from which the resultant current velocity can be calculated. This type of instrument, which is made by Neil Brown Instrument Systems, has a rapid response, a high sensitivity and requires only small amounts of power (McCullough, 1977, p 46-A-2).

Another acoustic instrument has a transducer which is oriented in the direction of the current, by means of a vane; the current speed is then measured directly, and current direction is obtained from a compass (Kronengold and Vlasak, 1965, pp 237-250; Squier, 1965, pp 585-593). This type of meter is capable of measuring currents of "both small and large magnitude with great accuracy" (Squier, 1968, p 591).

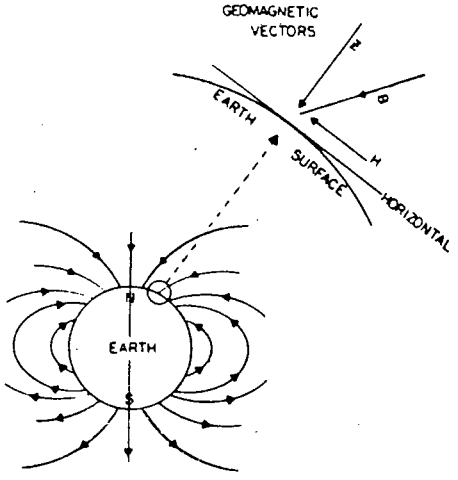

Figure 3.3 : The Geomagnetic Field.

Gonsalves and Brainard (1981)

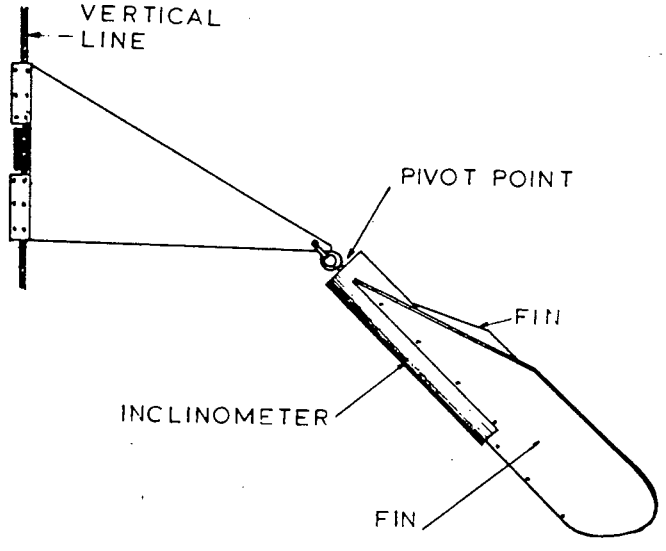

Figure 3.4 : High-sensitivity inclinometer current meter attached to a vertical line.

Daubin et al (1977)

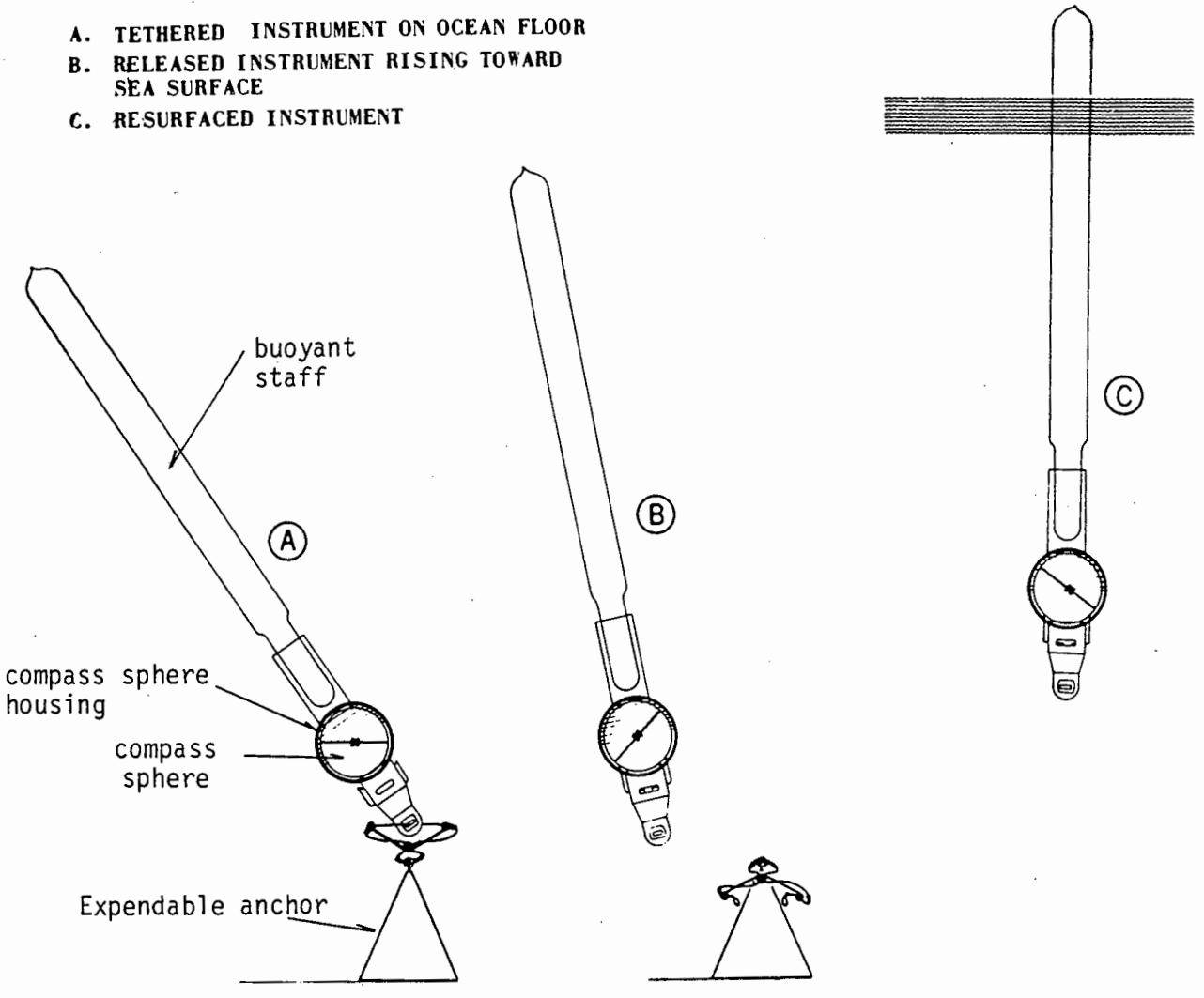

Figure 3.5 : The "buoyant staff" instrument.

Niskin (1965)

3.2.1.5 Current meters operated by fluid drag

A water current causes a drag force on a body situated in its path. This drag force may cause the body to deflect; the direction and degree of deflection may represent the current direction and velocity respectively. Various current meters exploit this principle, to measure currents.

(a) The inclinometer current meter:

Fig. 3.4 illustrates an inclinometer current meter; it is about 1 m long, including its fins, and it is negatively buoyant at the depth it is used in seawater. Water drag on the instrument causes it to face the current direction, and to tilt. The angle of tilt is related, through a calibration, to the current velocity, and is measured with an inclinometer i.e. a tilt sensor. Direction is measured by means of a compass. (Daubin et al, 1977, p POSTER-K-2). The instrument can be adjusted to measure a particular range of currents by changing the size of the fins. It is best suited for deep ocean low-velocity current measurement.

(b) A "buoyant staff" current meter:

This instrument obtains a single, instantaneous measurement of current strength and direction after dropping it onto the sea bed, as follows:

The base of a buoyant staff is attached to an anchor (which is expendable) in such a way that it can tilt in any direction in response to a current, as illustrated in Fig. 3.5(a). A graduated magnetic-compass sphere orients itself in its graduated housing (Fig. 3.5.(a)) so that it is level, and it faces north. A mechanical disc dissolves in the sea water and thereby causes a mechanical spring action which:

(i) clamps the magnetic-compass sphere in position, thereby recording the current speed (related to the sphere tilt angle, through a calibration), and the current direction (from the sphere orientation) ;

(ii) releases the buoyant instrument, which then floats to the surface, as illustrated in Figs. 3.5(b) and 3.5(c).

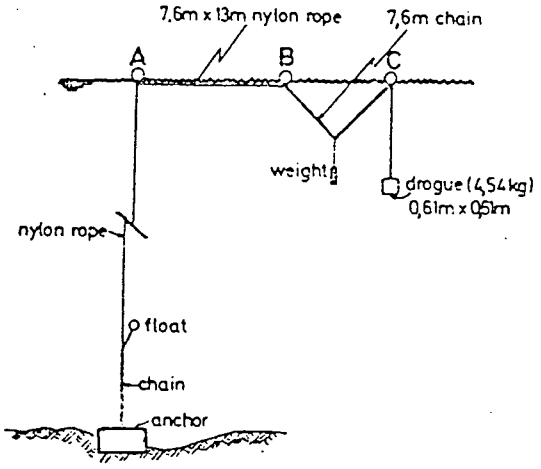

Figure 3.6 : The moored current buoy system.

Figure 3.7 : Interpretation of the moored current buoy system.

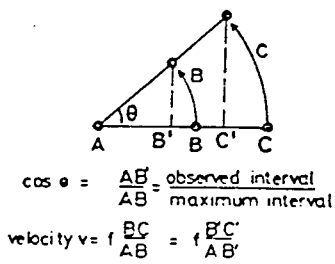

$$\cos\theta = \frac{AB'}{AB} = \frac{\text{observed interval}}{\text{maximum interval}}$$

$$\text{velocity } v = f\frac{BC}{AB} = f\frac{B'C'}{AB'}$$

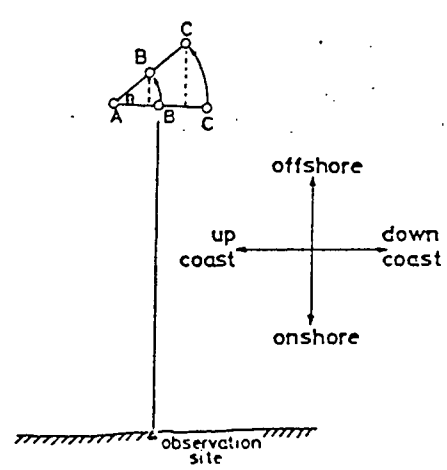

The device can be easily deployed and retrieved by a single person, from a small craft (Niskin, 1965, pp 123-131). Since it only obtains a single instantaneous measurement, it is only suitable for recording steady currents.

(c) A moored buoy current measuring system

This device, devised at the C.S.I.R., uses 3 buoys, as illustrated in Fig 3.6; buoy B is connected to buoy A by a nylon rope; buoy C is in turn connected to buoy B by a chain, with a weight attached halfway along its length. A drogue, in the form of a perforated buoy, is suspended with a rod from buoy C, at the depth at which the current is to be measured (usually about 3 m).

Fig. 3.7 shows that when the line of buoys is perpendicular to the observers line of sight, then the distance from buoy A to buoy B will be a maximum, and is a known distance. If the buoys lie at an angle, then the determination of the distance AB' will yield the angle, θ , from the relationship (Zwamborn et al, 1972, pp 79-82):

$$\cos\theta = \frac{AB'}{AB} \qquad (3.1)$$

As the current velocity increases, the observed distance between buoys B and C increases, due to the drag on the drogue. Correspondingly, the ratio of observed distances between buoys, B'C'/AB', will increase. For a particular current velocity, this ratio of distances, B'C'/AB', remains constant for any direction. The relationship between current velocity, V, and the distance ratio is as follows (Zwamborn et al, 1972, p80):

$$V = f\left(\frac{\text{observed distance } B'C'}{\text{observed distance } AB'}\right) = f\left(\frac{\text{distance } BC}{\text{distance } AB}\right) \qquad (3.2)$$

where f = "a function of"

From the calibration of the system, in the field and in the laboratory, the relationship between the distance ratio and velocity is obtained (i.e. the function, f, described in equation 3.2)

In order to obtain the distance ratio, B'C'/AB', the distances between the buoys can be determined:

(i) by means of a telescope/binoculars fitted with a graticule;
(ii) by means of a theodolite;
(iii) from photographs; self-recording is possible with the use of a camera with a motor-drive, and a timer (Botes, 1989).

Zwamborn et al (1972, p 81) show that the accuracy of both velocity and direction measurements vary with the angle θ . In addition, the accuracy is dependent on the technique of measuring the distance between buoys, and on the distance from the observation point to the system (at Mossel Bay, adequate current measurements are taken at about 3 km out to sea by photography with a telephoto-lens camera). Other factors affecting the accuracy and reliability of the system are:

(i) the problem of determining, from the appearance of the buoys, whether the current is moving onshore or offshore ;
(ii) the possibility of the anchor dragging ;
(iii) the possibility of the chain becoming entangled.

Although this system does not compare, in accuracy, to other current meters, such as rotor-vane types, it is nevertheless inexpensive, simple and effective for obtaining a direct visual observation of the current, and it can easily be deployed using a ski-boat.

3.2.1.6 Hot film current sensors

A constant electric current is supplied to a thin film of platinum. When placed in a sea current, a loss of heat in the film occurs, corresponding to the velocity of a water current component flowing past it; this heat loss causes a corresponding change in electrical resistance of the film. Thus, the resistance is related to the velocity of the water current component. In order to determine the resultant current velocity, four platinum films are situated around a cylinder of quartz; the resultant current velocity is interpreted, through a calibration, from the resistances measured in the four films.

The instrument is practical for measuring current speed and direction to within 2% accuracy; this is "compatible with ocean facility design and construction requirements" (Edgerton, 1976, p 25-A-3). However, the instrument accuracy is seriously affected by marine growth.

3.2.1.7 The laser Doppler velocimeter.

With this instrument, the velocity of water flow is determined from the Doppler shift in the frequency of laser light scattered from particles in the water (Lee et al, 1974, pp 558-565). The instrument requires a considerable amount of power, making it difficult to operate for long periods at sea; since it is capable of small scale microstructure current measurements, it is more suited to laboratory applications (McCullough, 1977, p 46-A-2). Nevertheless a laser Doppler velocimeter has been developed to measure currents at the sea bed (Agrawal and Terry, 1982, p 145-148).

3.2.1.8 Data recording

Current velocity measurements may either be recorded in situ, or telemetered to a shore station for recording. Data can be recorded by mechanical means e.g. by analogue strip-chart recorders, whereby currents are continuously recorded by a mechanically operated pen. Photographic recording is another possibility, e.g. Lovenvirth (1964, p 464) uses a system of fibre-optics and a camera, to record measurements from a rotor-vane instrument on film. However, since the processing of data on film and on strip-charts is extremely tedious, data is usually recorded in a digital form, on magnetic tape. This form of data is easily processed by computer. It must be noted, though, that even though it is commonly used, magnetic tape of recording is actually not totally reliable; data can be lost though mechanical and human error. This is overcome by the use of solid state recording (i.e. recording in a computer-type memory). The most important advantage of this is the elimination of mechanical moving parts, which improves reliability and reduces the maintenance required (Cheng and Wang, 1985, p 752-762).

3.2.1.9 Problems encountered in Eulerian current measurement

A common problem is the fouling of current meters with marine growth (Fig. 1.7). Different sensors are affected in varying degrees, e.g. Electro-

magnetic sensors are relatively unaffected by fouling; the hot film current sensor, however, is extremely sensitive to marine growth; the Savonius rotor is "relatively insensitive to marine fouling" but large amounts of growth will lead to the underestimation of current velocities (Magnell, 1982, p 34). Fouling of direction vanes causes slow and erratic direction response, with a tendency to cause speed overestimation when oscillating wave motion is dominant. This problem is partially remedied by using anti-fouling paint, and by periodic cleaning.

Other common problems encontered are:

(i) Battery failure; one instrument company reports a 10 % failure rate of current meters (over 18 months) for this reason (Howard and McFarlane, 1978, p 180).

(ii) Damage to current meters; if instruments are bulky, awkward to handle, and have vulnerable parts, damage occurs easily during deployment, which is often difficult at sea (Howard and McFarlane, 1978, p 180).

(iii) Electronics failure; this can cause a stoppage in recording or indecipherable or erratic recordings. Errors in recordings can be detected by means of data quality program checks.

(iv) Corrosion; attention must be paid to corrodable parts of current meters, such as bearings, and sensing electrodes.

(v) Loss of current meters; there is a high risk of loss, because of the rough environment in which meters are often deployed (Botes, 1977).

3.2.2 The technique of Eulerian current measurement

In order to determine the current environment at a site (e.g. for an engineering design), a current measurement program must be initiated. This involves the selection of appropriate current meters, their deployment at the appropriate location for an appropriate time span, and their subsequent retrieval.

3.2.2.1 The selection of current meters

The most appropriate type of current meter for a particular measurement program depends on various factors:

(i) The depth at which current measurements are required; if measurements of surface currents, which fluctuate rapidly, are required (e.g. for estimating movements of a buoyant effluent), a current meter with a rapid response will be needed e.g. an electromagnetic current meter. For deeper subsurface measurement, a large rotor-vane current meter, for example, will suffice.

(ii) The current velocity to be measured; for example, for the design of outfalls, the measurement of low velocity currents is important, since they cause the accumulation of excessive quantities of effluents; therefore current meters with a high response to weak currents will be necessary. Alternatively, for the design of structures, the measurement of strong currents is important, since they cause the maximum loading; in this case, current meters capable of recording high velocities will be necessary.

(iii) The cost of current meters (roughly R15 000-R40 000), and of the engineering projects for which measurements are required; for example, engineering projects involving huge sums of money will warrant expenditure on expensive, and therefore superior current meters. Howard and McFarlane (1978, p 179) discuss this topic further.

(iv) The required accuracy of measurement; for example, if only a rough estimate of longshore currents is needed, a less precise inexpensive instrument, such as the moored buoy system, will suffice.

If several current meters are needed, it is practical and economical to obtain several of the same make. This facilitates easier servicing with common spare parts, and a thorough knowledge of the particular make of meter.

3.2.2.2 The time period of a measurement program

The time period of a measurement program depends on the nature of currents to be measured; if the currents are dominantly tidal, a minimum record length of 30 days maybe adequate; however, for other currents, recording for a year may be necessary (Howard and McFarlane, 1978, p 178)

3.2.2.3 The location and mooring of current meters

The location at which measurements are required is dependent on the application e.g. for a marine pipeline, several measurements along the proposed route will be needed (McKeehan, 1978, p 192); for an oil rig design, construction, and operation, measurements at all depths will be needed.

Since structures are generally absent at measurement locations, current meters are generally attached to moorings. There are several possible combinations of anchors, floats and mooring line. An example is the popular and practical U-type mooring, which is employed by the C.S.I.R. (Fig. 3.8). Alternatively, if a structure, such as an oil rig, is present at the site of measurement, current meters may be fixed to a taut wire rope stretched between the steel members of the structure, provided that the structure does not significantly affect the water flow.

3.2.2.4 The deployment and retrieval of current meters

The bulk and weight of the moorings lines and anchors generally necessitates the deployment of current meters by ship. Various instruments however, can be deployed by aircraft. For example, the hot film current sensor (described in Sec. 3.2.1.5) is sufficiently light to allow deployment from the air (together with the subsurface mooring) with a parachute. Furthermore, this sensor can be retrieved by an aircraft, as follows:

(i) The aircraft deploys an acoustic-release command module into the sea.

(ii) This module emits an acoustic signal.

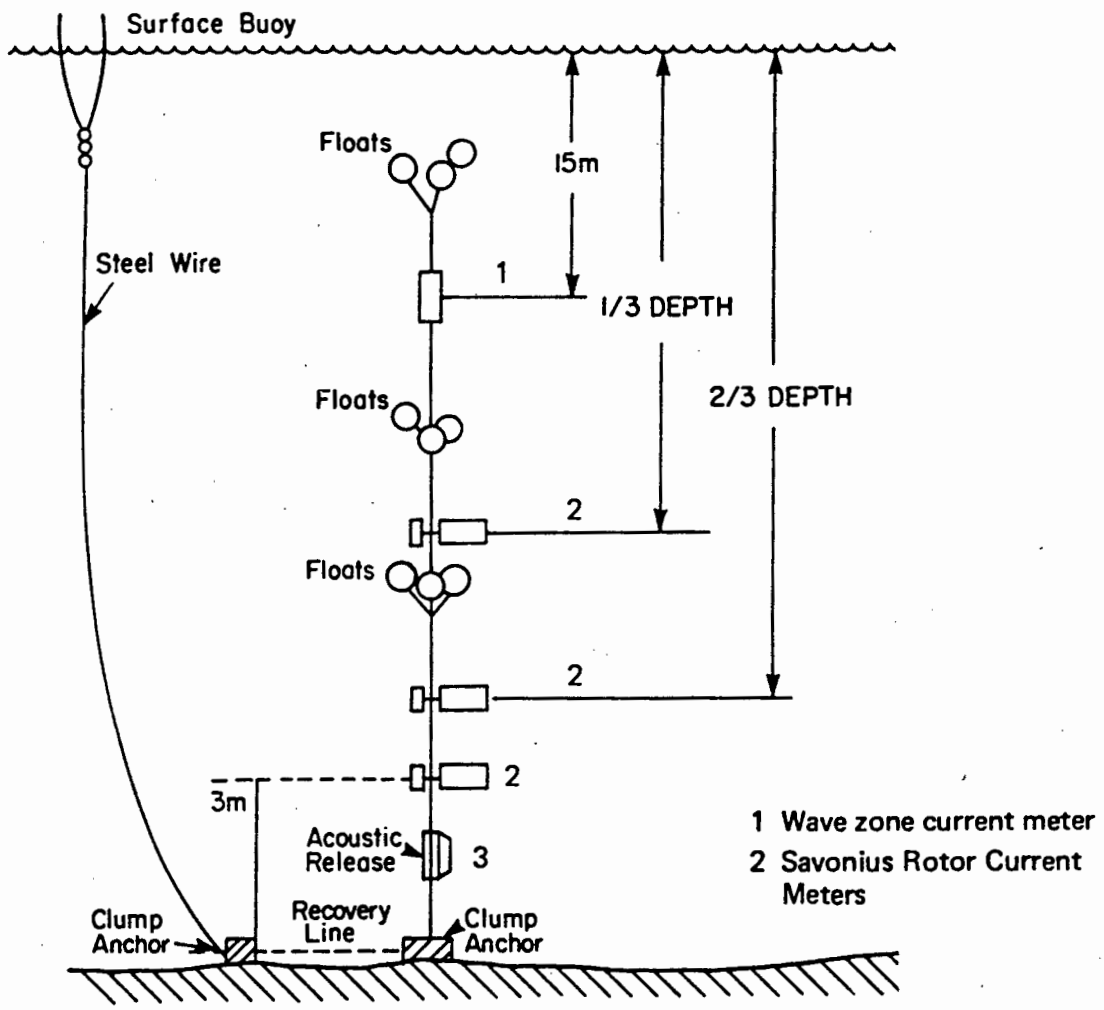

Figure 3.8 : The U-type mooring.

Stacey and Spring (1978)

(iii) The signal activates an acoustic release in the mooring (this is a link in the mooring which is cut loose by a specificd acoustic signal)

(iv) The hot film current sensor and its recorder float to the surface.

(v) Using a winched line and a grapnel, the instrument is retrieved by the aircraft.

Use of an aircraft is advantageous since it is quicker, more economical, and less weather-dependent than a ship (Lancaster, 1985, p 27).

Current meters are generally retrieved by ships. The U-type mooring (Fig. 3.8) is extremely useful, since it allows three options of retrieval, thereby avoiding potential loss of current meters:

(i) Acoustic release activation; current meters and floats are then recovered at the surface; this is the preferred option. The remainder of the mooring is separately retrieved.

(ii) If the acoustic release fails, the entire string can be retrieved, starting with the marker buoy.

(iii) Failing this, the third option is to drag for the recovery line, however there is "a good chance of instrument damage or mooring loss" (Stacey and Spring, 1978, p 175).

3.2.3 The interpretation and analysis of Eulerian current measurements

3.2.3.1 Sampling and averaging

As mentioned previously (Sec. 3.1), only velocity measurements of ambient, quasi-steady currents are of interest; undesirable short-period fluctuating current measurements are generally excluded by averaging data. This may be achieved in situ, or on shore at a later stage. The type of averaging employed depends on the the manner in which current velocities are detected, or sampled :

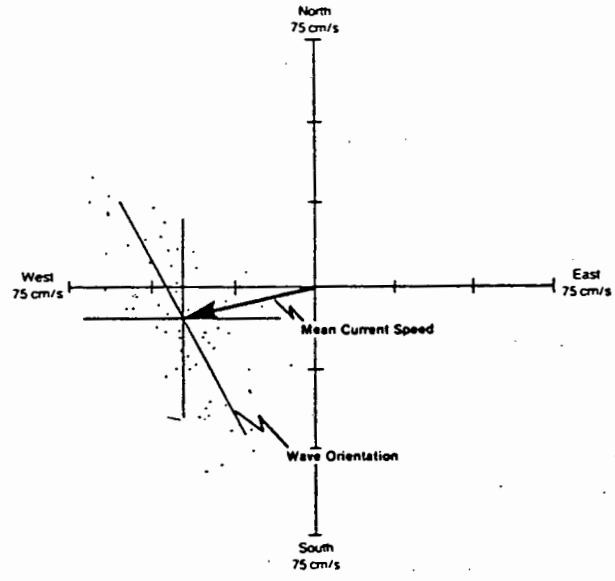

Figure 3.9 : Sixty consecutive 1-second velocity samples illustrate typical 1-hour burst-mode data obtained with an NBIS instrument at the 3-m level. Scatter points represent the heads of instantaneous vectors at 2000 GMT on April 11, 1979,

Frey (1982)

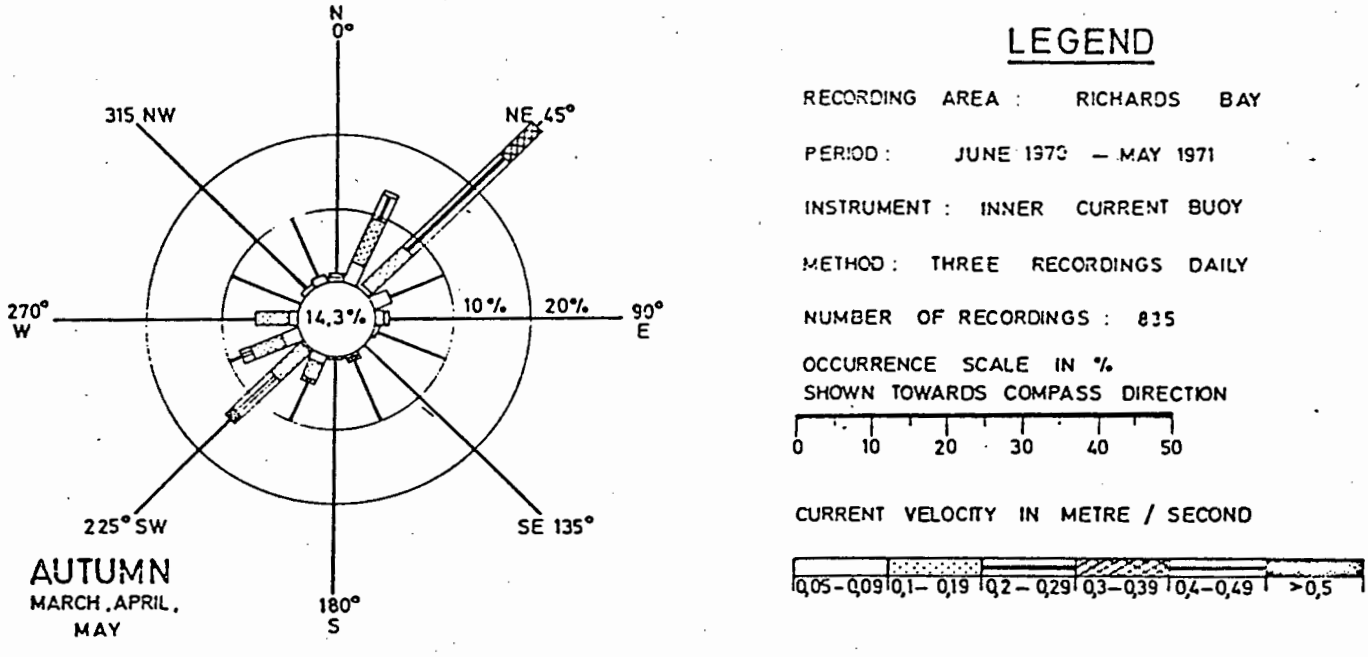

Figure 3.10 : A current rose.

(a) continuous sampling:

This refers to the continous detection of currents over a time interval; for example, by the continous rotation of the Savonius Rotor. The average speed, in this case, is determined (through a calibration) from the number of rotations recorded in the time interval, as discussed in Sec. 3.2.1.1..

(b) burst sampling:

This refers to the instantaneous detection of current velocity components, per time interval. In general, two orthogonal current velocity components are detected, from which the current velocity is obtained, for every second. The average of these current velocity vectors for a period yields the quasi-steady, ambient current, as illustrated in Fig. 3.9. In the figure, the wave-induced currents, and their exclusion by averaging, is evident.

3.2.3.2 Data analysis for presentation

In order to facilitate easy interpretation, data measured over a long period can be presented in useful forms, such as the current rose. The current rose is constructed by dividing the current speed and direction into categories; the number of occurrences of currents in each category is then totalled, for the period of measurement (eg. one year). The data is presented graphically, as illustrated in Fig. 3.10. This type of presentation is useful for decisions on the timing of phases of offshore construction, or the timing of operations such as drilling.

3.2.3.3 Current parameters

The maximum current velocity likely to occur in a time period may be required, for example, for the design of oil platforms and pipelines. Since this velocity is not likely to be recorded in the limited time period of the measurement program, theoretical models are used. Short term current measurements can be used to calibrate mathematical models, which in turn are used to hindcast currents for extreme events (e.g. extreme tides, severe storms, etc.). The hindcast currents are then statistically extrapolated in order to obtain an estimate of the maximum currents for a specific time period (such as 100 years) (Stacey and Spring, 1978, p 170).

Another useful parameter is the average of currents for long periods; this parameter is useful during oil exploration, for determining the movements of effluents, and for estimating the general circulation for cooling water intakes and discharges (Stacey and Spring, 1978, p170).

3.2.4 Measurement accuracy

The following factors affect measurement accuracy:

3.2.4.1 Cosine response

As mentioned above, apart from measurements for directional wave energy spectra, only horizontal currents are of interest. "Cosine response" describes a current meter's ability to reject vertical components of flow while measuring horizontal flow, assuming that the current meter is moored perfectly horizontally. In other words, it is the ability of a current meter to measure only the component $V.\cos\theta$ of a flow velocity, V, flowing at an angle, θ, to the horizontal plane (McCullough, 1978, p 14). The cosine response of current meters "has been addressed by manufacturers" (McKeehan, 1978, p 196). In particular, propellers can be designed to have "excellent cosine response" (McCullough, 1977, p 46-A-2) e.g. the Vector measuring current meter.

3.2.4.2 Tilting

Current meters are generally attached to a mooring line, which may tilt, resulting in an erroneous response to currents. To counteract this, sensors can be used measure a record of the tilt; the record can subsequently be used to correct current measurements. Another solution is to mount the current meter on a gimbal, which maintains it in the horizontal. Furthermore, in order to accurately determine direction, compasses are kept horizontal, for example, with a gyroscope.

3.2.4.3 Mooring lines:

The action of mooring lines can influence current measurements, especially near-surface measurements where wave orbital motions are prominent (McCullough, 1985, p 46-A-3; Kushmir,1987,382). At greater depths, wave

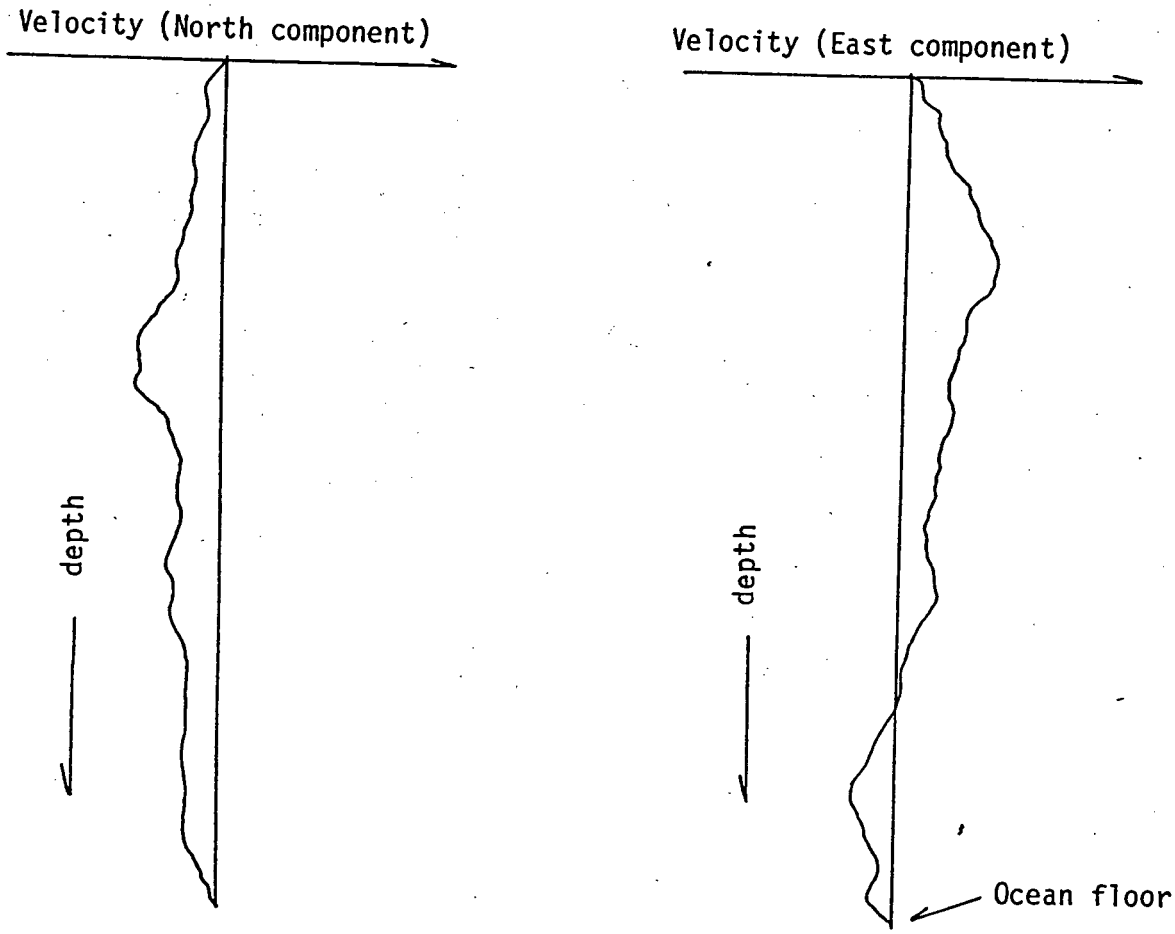

Figure 3.11 Current Velocity Profiles in two orthogonal component directions.

action is damped out (see Sec. 1.3.2), therefore deep moorings are less problematic. However, mooring dynamic response to internal waves "is probably a more frequent problem than we now realise in continental shelf areas" (Scarlet, 1978, p 166).

3.2.4.4 Laboratory calibration

Current meters are generally calibrated in the laboratory under steady state flow conditions (Halpern, 1977, p 46-D-1); these calibrations will probably be approximate in fluctuating, unpredictable near-surface flows occurring in the ocean. Thus measurement accuracy can be affected by relying too heavily on laboratory calibrations. However, with careful planning, sufficient accuracy can be obtained for engineering purposes, for which accuracy requirements are generally $\pm$ 5 % for speed and $\pm$ 5° for direction. For determining wave energy spectra, however, an accuracy of $\pm$ 2 % is desirable (Stacey and Spring, 1978, p 171)

3.3 PROFILING

For engineering purposes, particularly for oil platform design, construction and operation, current data at all depths are of interest. This data can be measured by means of profiling instruments, to obtain a current profile, i.e. a graph of depth versus either the current velocity, or the current velocity components, in two orthogonal directions (Fig. 3.11). Many current profilers operate in a similar fashion to Eulerian current meters. They are generally self-recording, or they telemeter data to a station. Some examples of profilers are described briefly below:

3.3.1 The cyclesonde profiler:

Eulerian-type current meters may be lowered on a winch, or by another mechanism, to measure the current profile. An example of such an instrument is the cyclesonde, which records currents in the same fashion as the rotor-vane current meter. By means of buoyancy changes (in a similar fashion to the submarine), it ascends and descends a taut wire mooring, in order to measure the current profile, as illustrated in Fig. 3.12. By means of an attached transmitter buoy, data is telemetered to a shore station.

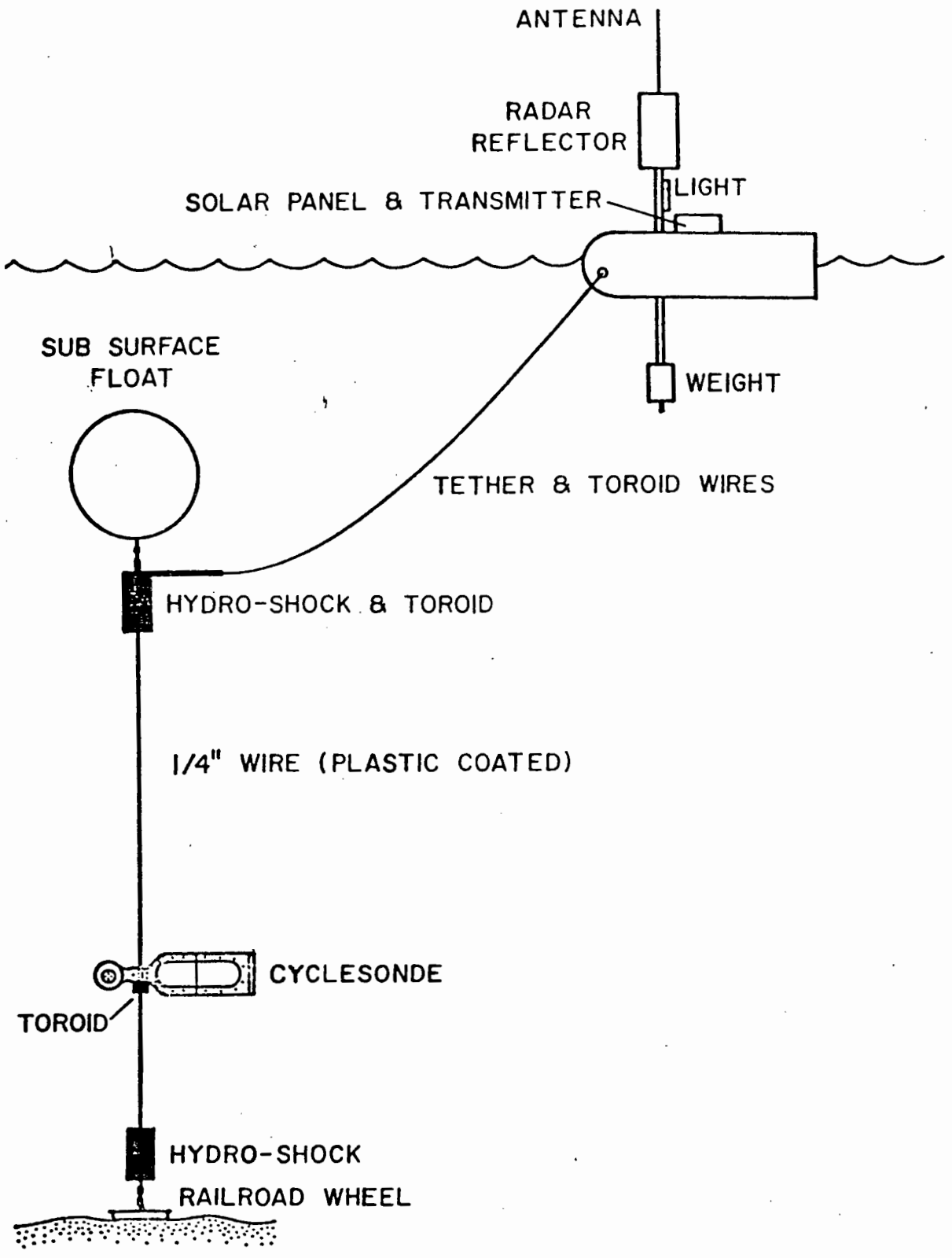

Figure 3.12 : Taut wire subsurface mooring used to deploy the Cyclesondes on continental shelves (0-300 metres). The Cyclesonde may profile from ∿1 metre above the bottom to within 15 metres below the sea surface.

van Leer and Leaman (1978)

3.3.2 Acoustic techniques of profiling

By acoustically tracking a sinking instrument, using sonar, a current velocity profile can be obtained, from the measured trajectory of the instrument (Cole, 1981, pp 257-267).

Another technique uses the acoustic Doppler effect; a number of acoustic transducers are mounted in various orientations at the sea bed. Current velocity components normal to each transducer are determined from the measured Doppler frequency shift between sound pulses transmitted, and reflected off particles in the water (as previously described in Sec 3.2.1.4). The location of these current velocity components, at various points along the sound path, is also determined, by electronically determining the return times of reflected sound energy (with 'time gating'). The current velocity components from the transducers are combined, to determine the current velocity at various depths; thus the current velocity profile is measured (Appel et al, 1985, p 723).

Current profiles can be measured from ships with acoustic Doppler techniques. However, there are many sources of error, due to ship motions and errors in navigational fixes. (Regier, 1982, p 117)

3.3.3 The electromagnetic profiler

An expendable instrument described by Lancaster (1985, pp 24-28) measures horizontal currents by means of the electromagnetic technique (using the geomagnetic field) described in Sec 3.2.2. Since the instrument descends at a known velocity, and since the time of the start of descent is known, the corresponding depth can be determined; together with the current measurements, the current velocity profile results. The instrument is connected to a buoy with a thin electric wire; the buoy transmits the profile information to a ship.

3.3.4 The absolute velocity profiler

The electromagnetic free-falling profiler, mentioned above, measures horizontal current velocities relative to itself. However, it may be carried laterally by currents, so that it does not detect the absolute, true current

velocity profile (relative to the earth). By means of an acoustic Doppler transducer, the velocity of the instrument relative to the ocean floor can be detected; this measurement is used to correct the relative velocity profile, to obtain the absolute profile, relative to the earth (Sanford et al, 1978, p 137-151).

3.4 LAGRANGIAN CURRENT MEASUREMENT

This is the measurement of the trajectories of water particles; this is achieved by the tracking (measuring the path) of drifting objects (called drifters). Lagrangian measurement is particularly effective for determining patterns of water flow; this is needed for determining movements of pollutants, for the selection of waste disposal sites, and for the design of outfalls (the CSIR use Lagrangian techniques primarily for this purpose). Lagrangian measurement is also used to measure the velocity of currents in the surf zone, which affect sediment transport.

3.4.1 Drifters

There are many different types of free-drifting objects, or drifters, which can be used for Lagrangian current measurement. For example, to record surface currents, cards which float in the top layer of the water can be used; for surf zone measurements, simple drifters, e.g. tennis balls exuding dye, can be used; dye alone is also used to determine water flows.

The most common type of drifter is the drifter buoy; this consists of a floating surface buoy, from which a drogue is suspended, at the depth at which currents are to be measured (Fig. 3.13). Surface buoys are especially equipped for tracking, e.g. they may have brightly coloured flags for visual tracking, or a reflector for tracking by radar. Drifter buoys are often made of cheap materials, to render them expendable (i.e. the cost of retrieval of the float exceeds the cost of replacing it).

3.4.1.1 Drogues

There are several forms of drogues. They are designed to have a high drag coefficient, in order to move at a velocity close to the current velocity.

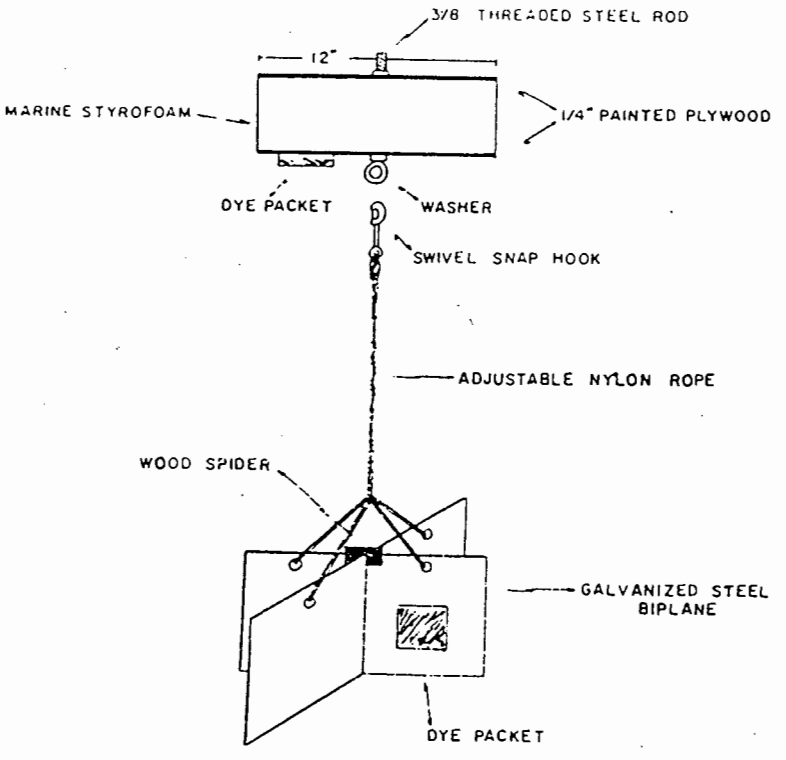

Figure 3.13 : A simple drifter buoy.

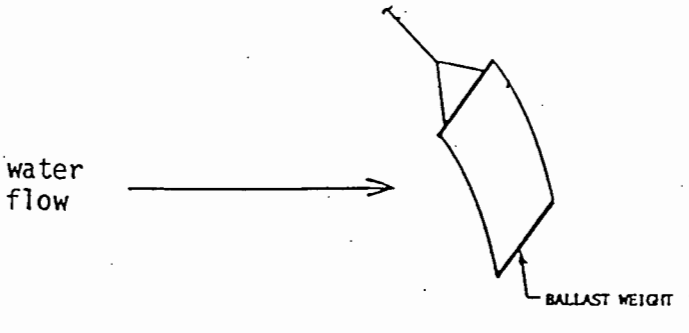

Figure 3.14 : The window shade drogue.

One example is in the form of a parachute - however this drogue is ineffective, since at a low relative velocity, between the water current and the drogue, it tends to hang in a closed-up state (Dornhelm, 1985, p46-C-2), thereby reducing the drag. Another common form of drogue shape is the crossed vane type, illustrated in Fig. 3.13. The window shade drogue (Fig 3.14) is effective, since it aligns itself perpendicular to the prevailing flow, due to its hydrodynamic characteristics (Vachon, 1977, p 46-B-2). In addition, it has a high drag coefficient, it is simple, and it is inexpensive.

3.4.2 Lagrangian techniques

3.4.2.1 Drift cards

A very simple, yet effective technique is the use of drift cards; since these cards drift in the top layer of the water, their movements represent surface currents. The procedure is to deposit a number of brightly coloured cards at a point of interest (such as the proposed location of a sewage outfall); these drift cards are later retrieved at certain positions of interest (e.g. environmental sensitive areas such as swimming beaches or nature reserves). The retrieval of a substantial fraction of the drift cards at a position indicates a definite water movement to that location.

3.4.2.2 Drifter buoys

(a) Deployment:
Drifters are generally deployed from aircraft or ships. For nearshore measurements they may be deployed by hand. Alternatively, a launcher, which operates on compressed air, similar to a mortar launcher, can be used (Zeigler and Tasha, 1968. p 436).

(b) Tracking:
The tracking of drifter buoys is usually achieved by obtaining position-fixing measurements at regular intervals. There are several different techniques:

(i) Visual techniques:

If drifter buoys are visible, their position can be periodically fixed using a sextant from a vessel (the position of the vessel is, in turn, fixed by conventional navigation means). Alternatively, the position of the drifter can be fixed from the shore, by the technique of intersection, with 2 or 3 theodolites.

Detection of drifters is facilitated by the use of bright or fluorescent paints, flares or smoke, flashing lights, or dye exuding from packs attached to the buoys (Walden and Webb, 1964, p 318).

(ii) Photography:

The position of drifter buoys can be determined by photogrammetry techniques. In this case, fixed markers, on the shore or on the buoys, are required as reference points, to calibrate the scale and direction of drifter buoy movement (Klemas et al, 1975, p 753). For nearshore current measure-ments, the position of drifter buoys can be obtained, at intervals, by photography with a camera suspended from a balloon. (Horikawa and Sasaki, 1972, p 114).

(iii) Radar:

Drifter buoys can be tracked using radar, if they are provided with radar reflectors. Radar is fortunately unaffected by lack of daylight. However, it is limited in rough sea conditions (drifter buoys are hard to detect amongst 'sea clutter'), and in heavy rain (radar waves are reflected by rain).

(iv) Radio techniques:

The position of a drifter can be determined with HF radio techniques. The CSIR use the Tellurometer system (of Plessey, South Africa); this is one of the most accurate systems available. Two arrangements of equipment are possible for measurement:

- A transmitter on the drifter/s, and three transmitters on shore.
- Three transmitters on shore, drifter/s with reflectors, and a receiver on a ship.

The former is susceptible to wind, because the drifter is bulky, due to the transmitter and aerial on it. The latter is far less susceptible to wind, however it is expensive, due to the cost of the ship (Botes, 1989).

(v) Subsurface acoustic technique:

A float can be designed to be neutrally buoyant at a particular depth, by using the appropriate combination of mass, volume and compressibility. The float has a transducer which transmits sound pulses. Two hydrophones, arranged as far apart as possible on a ship, receive the sound signals. The signals can then be interpreted to determine the position of the float, and to estimate its depth (Swallow, 1955, pp 74-81).

(vi) Satellite tracking:

Drifter buoys, transmitting radio waves at preselected frequencies, can be tracked by a satellite location system, called the Argos system (Garret, 1978, pp 155-159). This is achieved with Doppler frequency measurement techniques. Since location accuracy is roughly 5 km, and only 4 observations can be taken per day, this system is only suitable for monitoring large-scale current movements offshore.

3.4.2.3 Dye techniques

Dye can be used to obtain qualitative measurements of currents, for determining the movements of effluents. For example, dye was injected into a stormwater outlet in False Bay, South Africa. Aerial photographs are taken at intervals to obtain an indication of the rate and direction of dye dispersion. Fig 3.15 illustrates an aerial photograph; Fig. 3.16 illustrates the dispersion information obtained from such photographs.

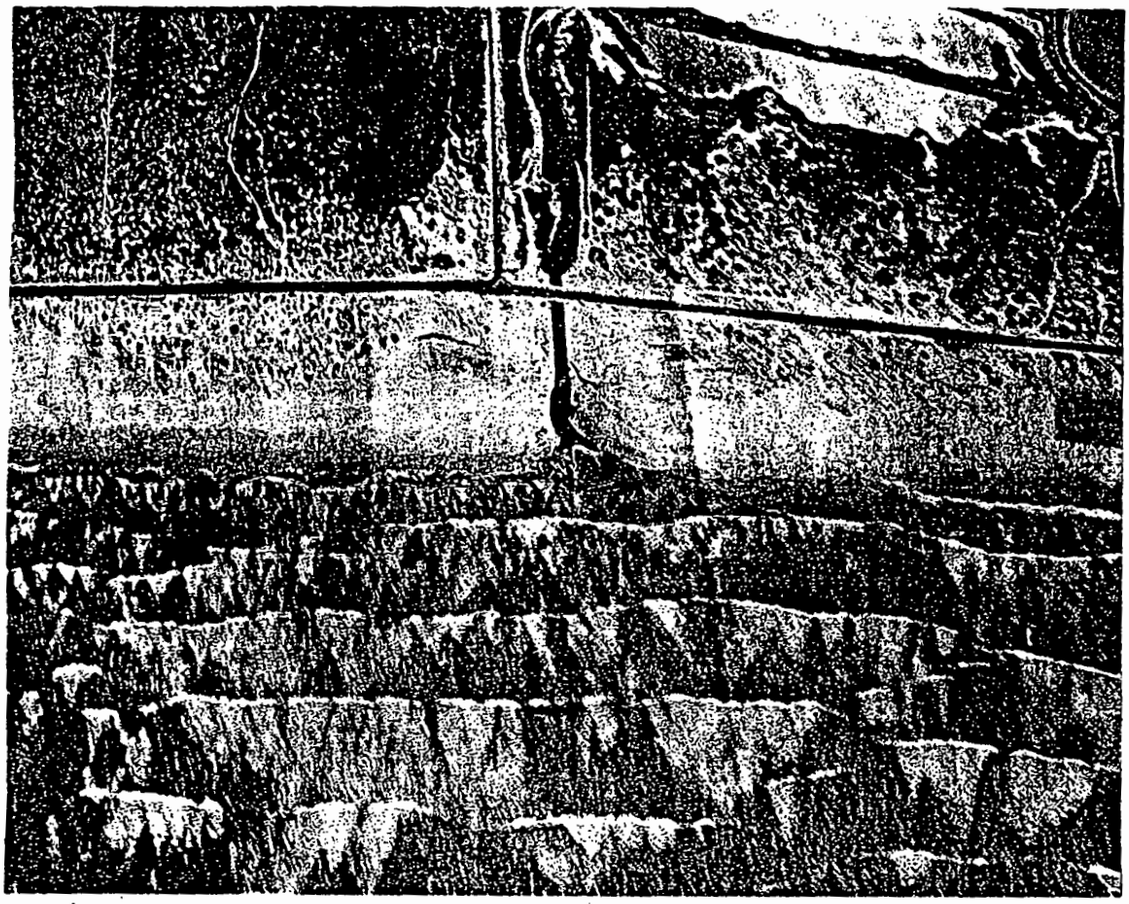

Figure 3.15 : An aerial photograph of dye dispersion.

Horler (1989)

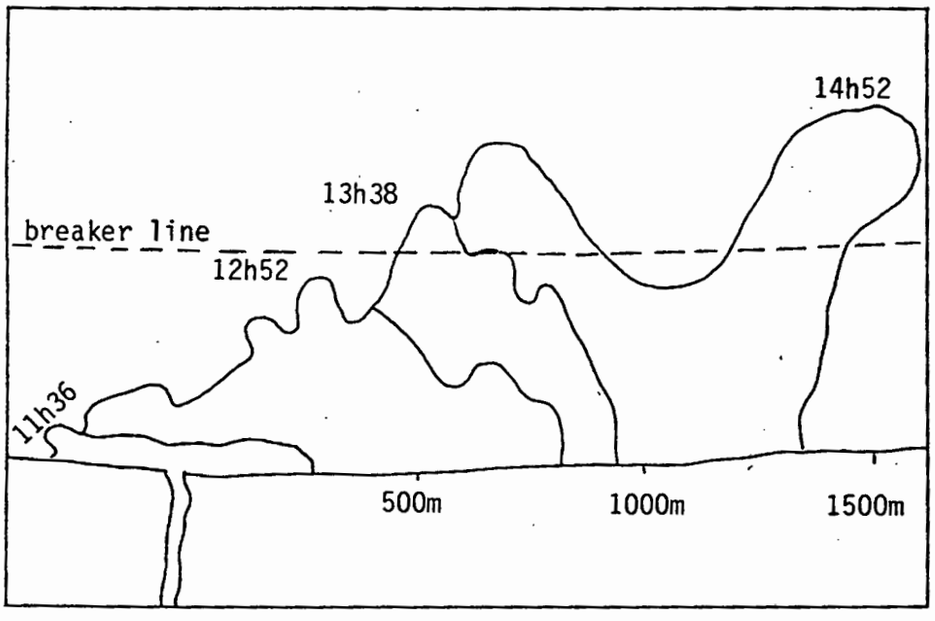

Figure 3.16 : The growth of a dye patch photographed on September 1, 1987, in Flase Bay.

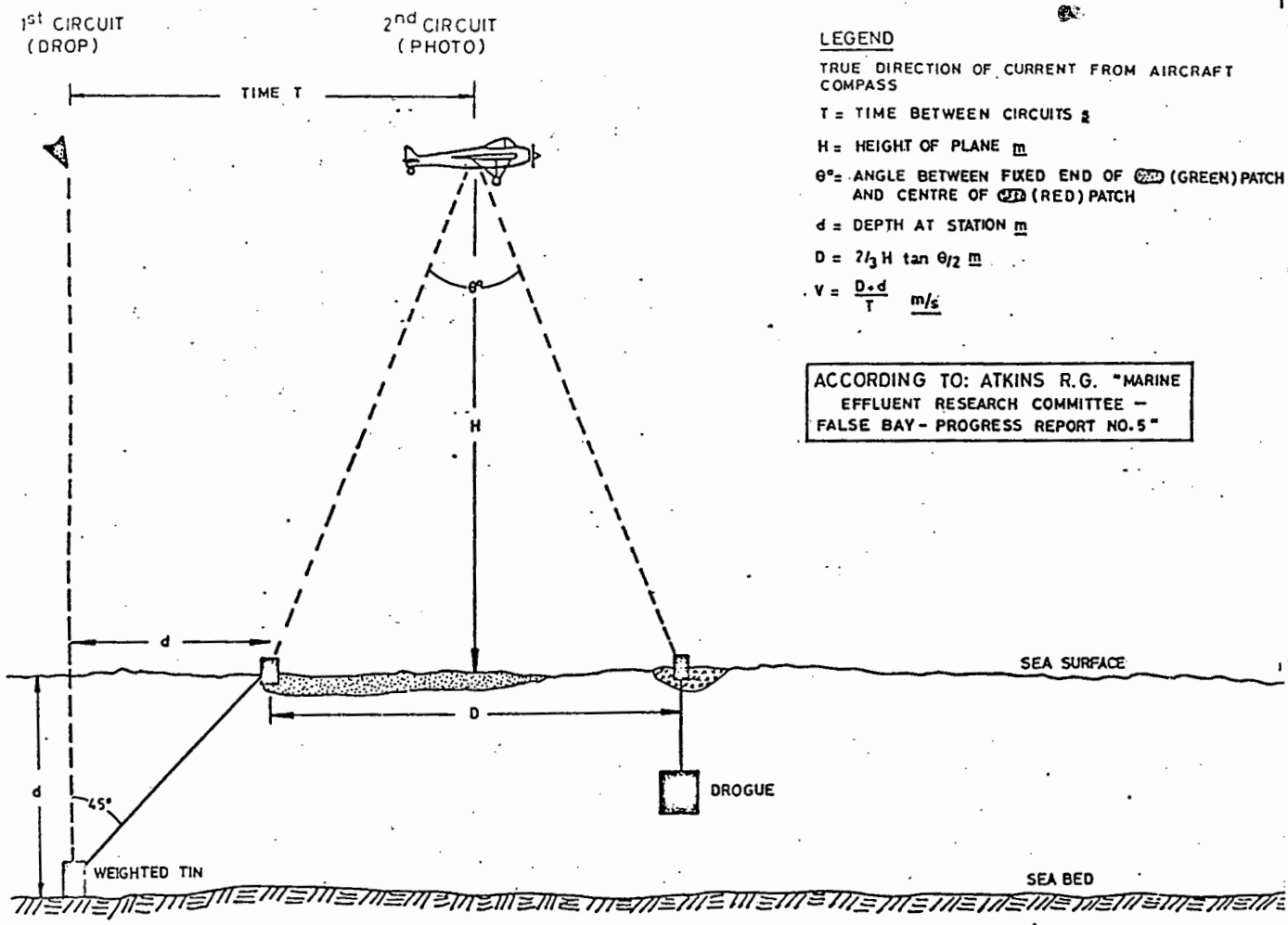

Figure 3.18 : The dye 'bomb' principle.

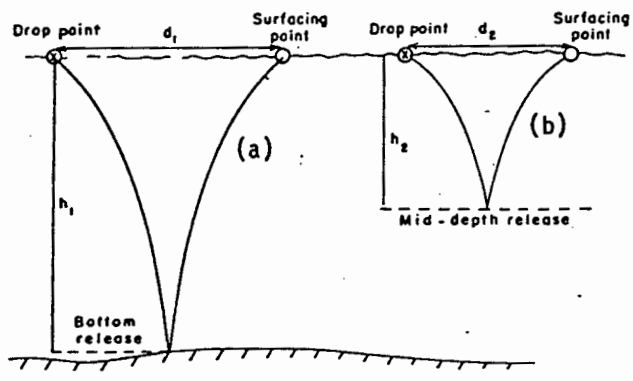

Figure 3.19 : The principle of the drop-sonde.

Neumann (1968)

A more quantitative measurement can be obtained with the dye 'bomb'. This 'bomb' consists of a weighted cannister containg two bags, each containing a float and a particular color of dye. One of these bags is attached to the cannister by a long nylon chord; the other has a cloth drogue attached, so that it serves as a drifter (Fig 3.17). The 'bomb'is dropped from an aircraft. On entering the water the 'drifter' bag is released and moves with the current. The other bag is held stationary by the weighted tin, which acts as an anchor (see Fig. 3.18); the deposition point is thereby marked. With photogrammetry techniques, the distance between this deposition point and the drifting bag, D, can be obtained after a time interval, T; as shown in Fig. 3.18, this information can be used to determine the current velocity.

3.4.2.4 The drop-sonde

The drop-sonde is used to measure the average velocity of a vertical column of water, in a simple fashion. The instrument is dropped into the sea at a known position; it descends at a constant known rate. At a pre-determined depth (h_2 in Fig. 3.19b) a weight is released by means of a pressure activated mechanism. Alternatively the weight can be released on impact with the ocean floor (Fig.3.19a). The release of a weight causes the drop-sonde to ascend, at a constant rate. On surfacing, the time, and displacement (d_1 or d_2 in Fig. 3.19) are recorded. Thus, the average velocity of the water column, of depth h_1 or h_2, is simply calculated from d_1/t or d_2/t respectively.

3.4.2.5 Simple surf zone technigue

Simplified measurements of longshore current velocities can be obtained by timing the movements of fluorescent dye floats (such as tennis balls filled with dye) in the nearshore zone. These floats can be deployed by hand (Zwamborn et al, 1972, p 77).

3.4.3 Accuracy

Ideally the trajectory of a drifter buoy float should precisely represent the trajectory of the water particles in a current. However, this is not exactly the case, because of the following errors:

(i) The drogue, suspended at at depth, requires some ballasting to prevent it from moving away from the required depth. The surface buoy has to be buoyant in order to support this ballast. However, the submerged volume of this surface buoy is subject to drag forces of surface currents, as well as the dynamics of waves (Vachon, 1977, p 46-B-1).

(ii) Wind drag on the surface buoy tends to alter its course.

(iii) The drag on the subsurface drogue will be such that the velocity of the current is greater than that of the buoy. Vachon (1977, pp 46-B-1 to 46-B-7) investigates the performance of various drogue shapes.

3.4.4 Analysis

Corrections may be applied for the above-mentioned errors, depending on the accuracy required for a particular application. For example, the C.S.I.R. apply a correction for wind with velocity over 10 knots, in some cases; this correction is theoretically calculated from wind drag.

The result of tracking drifters is a series of position fixes. The line joining these points reveals the trajectory of a drifter, which represents the trajectory of water particles in a current. Current velocities are determined by simply dividing the distance between two position fixes by the time interval between them.

3.5 REMOTE CURRENT MEASUREMENT

Several remote current measurement techniques were discussed in Sec. 3.3 above, since they are Lagrangian in nature. In addition to these, qualitative measurement by satellite, and HF radar techniques can be used.

3.5.1 Satellite measurements

Satellite information can be used in a qualitative way; current circulation patterns can be inferred from satellite imagery, from:

(i) the movements of suspended sediment, evident in satellite images obtained from infrared scatterometry (a microwave sensing technique) ;

(ii) the movements of fronts occurring at the boundary between waters of different properties. These fronts are detectable with infrared scatterometry. In addition, the boundaries of the major current systems can be detected with satellite Synthetic Aperture Radar (SAR is discussed in Sec. 1.6.2.2(c)) ;

(iii) the movements of oilslicks and waste materials. These can also be useful for environmental planning ;

(iv) slopes in the ocean corresponding to large density differences which drive large scale currents, such as the Gulf Stream; these can be detected with the satellite radar altimeter, which detects elevation accurately from the reflection of microwave pulses.

The limitations of this type of satellite information are:

(i) Current velocities cannot be obtained.

(ii) The detection of currents is limited to the upper few metres of the ocean.

3.5.2 Current measurement with H.F. Radar

With H.F. radar, the average surface current for an area of a few hundred square metres can be measured; this is generally achieved with a radar system called CODAR (Coastal Ocean Dynamics Application Radar). Another more recently developed system, based on CODAR, is OSCR (Ocean Surface Current Radar) (Prandle and Howarth,1986,p1).

3.5.2.1 Principle of operation

As described previously (Sec. 1.6.2.1), HF radio waves are Bragg scattered by ocean waves with half of the radar wavelength, $\lambda\backslash 2$ (Fig. 3.20). The result of this scatter is that two Bragg lines appear in the Doppler spectrum; one for the advancing ocean waves and one for the receding ocean waves (Fig. 3.21a). The Doppler frequencies, $+f_d$ and $-f_d$, at which the two

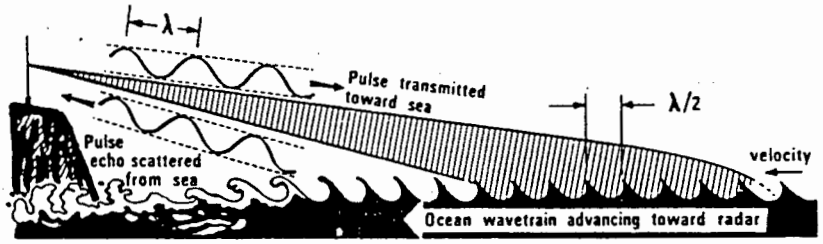

Figure 3.20 : Bragg scattering of radio waves by ocean waves.

Barrick et al (1978)

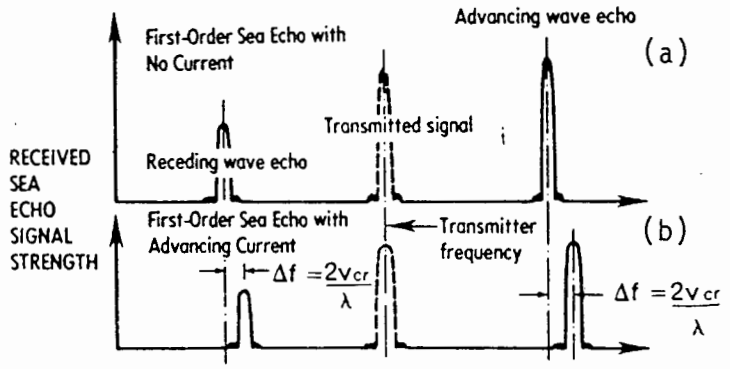

Figure 3.21 : The principle of radar current measurement.

Barrick et al (1978)

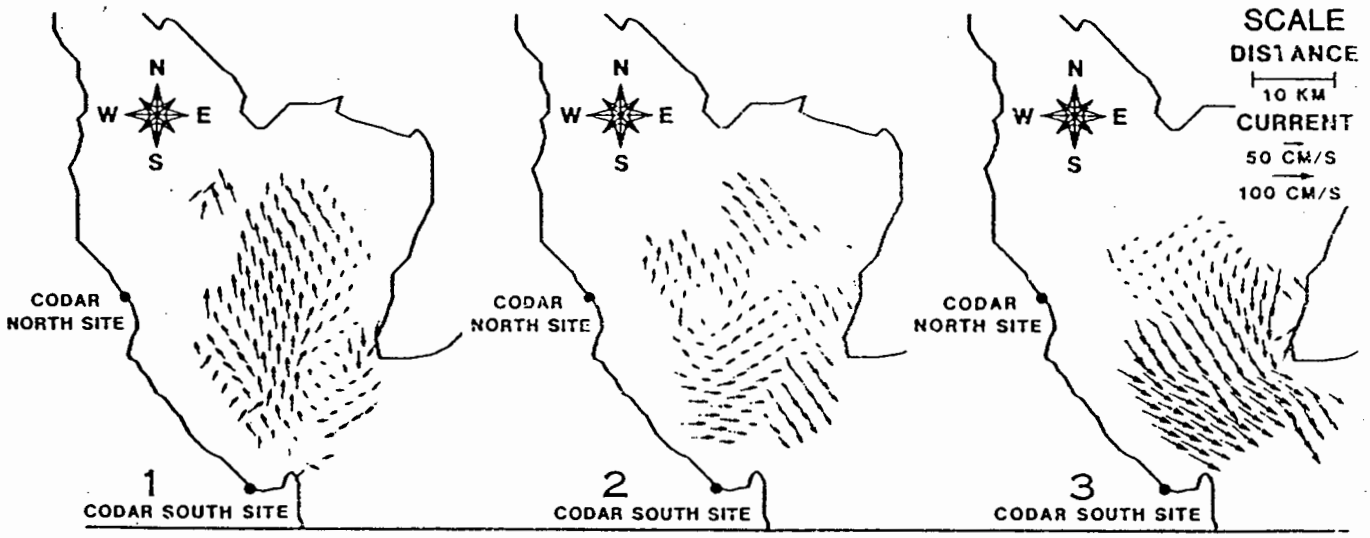

gure 3.22 : CODAR maps of Delaware Bay circulation at (1) 1226 hours EST, (2) 1352 hours, and (3) 1522 hours. Only vectors with uncertainties s than 10 centimeters/second were plotted.

Barrick et al (1985)

Bragg lines occur, are dependent on the phase velocity, or celerity, C, of the ocean waves of wavelength λ\2, as described by the relationship:

$$f_d = \frac{2c}{\lambda} \tag{3.3}$$

From linear wave theory:

$$C = \sqrt{\frac{gL}{2\pi}} \tag{3.4}$$

for waves in deep water, i.e. the wavelength is less than twice the water depth.

Therefore:

$$f_d = \frac{2\sqrt{\frac{gL}{2\pi}}}{\lambda} = \sqrt{\frac{g}{\pi\lambda}} \tag{3.5}$$

Thus, from equation 3.5, the Doppler frequencies, $+f_d$ and $-f_d$, can be predicted, from the radar wavelength (Barrick et al, 1978, p 60). Any deviation, Δf, from the predicted values is due to a deviation in velocity from the phase velocity of the ocean waves. This deviation in velocity is due to a component of current travelling towards (or away from) the radar, which transports the ocean waves. Thus, the velocity of the component of current can be determined from the measured Doppler frequency deviation, Δf, with the following relationship (derived similarly to equation. 3.3; (Robertson, 1989))

$$\Delta f = \frac{2\,V_{cr}}{\lambda} \tag{3.6}$$

where Δf = the difference between the predicted and measured values of the Doppler frequency of the Bragg lines (Fig 3.21b).

V_{cr} = the velocity of the component of current travelling directly towards (or directly away from) the radar.

The distance of the measured current component from the radar station is determined by measuring (using electronic time gating) the time delay between the radar echo and the radar transmission. The bearing of the current component is derived using a direction finding antenna array (Frisch and Weber, 1982, p 274). Thus, using the radar technique described, the position (bearing and range) and velocity of several current components, in a direction radial to the radar, can be obtained. For the CODAR system, each current component represents the average current over an area of about 1,5 km^2.

3.5.2.2 Analysis

Maps of currents: In general, two coastal radar stations are used, separated by about 30 km. Each station yields current velocity components radial to it, at positions on a grid, common to both stations. Thus, at each grid position, the actual current velocity is calculated from the two current velocity components. A graphical presentation of this is a current map, as illustrated in Fig. 3.22.

A disadvantage of this technique is that on (or near) a straight line joining the two radar stations, the current components cannot be combined to yield the actual current vector, since they lie on the same line.

In some cases, e.g. on an oil rig, only one radar station is possible. The current velocities can then be calculated from adjacent radial current components; mathematical models are used in this analysis (Barrick et al, 1985, p 45). The disadvantage of the technique involving one radar only, is that the spatial resolution of the velocity measurements is considerably reduced.

Trajectories:
Mean surface current velocities can be found by averaging velocities from several maps. Short-term tidal currents can be found by subtracting these mean current velocities from single current velocities. From this information, the likely trajectories of water particles, commencing at any time and position, can be computed. With the use of numerical models, wind effects can be included in these calculations. The calculated trajectories are used to predict the movements of pollutants (Frisch and Weber,1982, p 279).

3.5.2.3 Accuracy

A theoretical analysis of errors inherent in the CODAR system predicts 1 mm/s probable error in current estimates. However, in addition to this, there are larger sources of error:

(i) Second order hydrodynamic effects cause deviations from the approximation that currents simply transport ocean waves.

(ii) Electromagnetic refraction of radar waves near coastlines can distort the location (bearing and range) of current measurements (Georges and Woodward, 1981, p 228)

(iii) The largest error is due to fluctuations in amplitudes of radar echo, due to the randomness of the sea.

Errors (i) and (ii) can be minimised by careful antenna siting, and by applying corrections. Error (iii) is reduced by averaging the radar signal over time (roughly 20 minutes).

In an attempt to assess the accuracy of the HF radar technique, several comparisons have been made, for example:

(i) In a comparison between current components from CODAR with an acoustic Doppler measurement system: "Agreement is evident despite the different spatial scale sizes and depths of the two techniques" (Barrick et al, 1985, p 46).

(ii) Comparison has also been made with Lagrangian techniques: "The agreement is very reasonable, within the range of expected drifter variances" (Barrick et al, 1978, p 59).

iii) Furthermore in a comparison with the VACM: "We have shown that the current components of CODAR, and VACM near surface currents were well correlated" (Holbrook and Frisch, 1982, p 130).

3.6 CONCLUSION

The following significant conclusions emerge from this chapter:

(i) Eulerian current measurement at depth is reasonably trouble free; however the influence of wave action causes difficulties for surface measurement.

(ii) Lagrangian measurement is very effective, especially for outfall studies, but unattended automatic recording, for long periods, is not possible for a single location.

(iii) As with wave measurement, radar seems to be the most promising technique of surface current measurement; large areas can be covered and accuracy is adequate.

BIBLIOGRAPHY : CHAPTER 3

Agrawal, Y.C. and Terry, W.E. 1982 "Laser Doppler Velocimetry on the Sea Floor", Proc. of the I.E.E.E. Second Working Conf. on Current Measurement, January 1982, pp.145-150.

Barrick, D,E,, M.W. and Weber, B.L. 1978 "Ocean Surface Currents Mapped by Evans, Radar", Proc of a Working Conf. on Current Measurement, January 1978, pp.59-65.

Barrick, D.E., Lipa, B.J. and Crissman, R.D. 1985 "Mapping Surface Currents with CODAR", Sea Technology, October 1985, pp 43-45.

Botes, W.A.M. 1988 "Shallow Water Current Meters Comparative Study, False Bay - September 1987", C.S.I.R. Report T/Sea 8803.

Botes, W.A.M. 1989 Personal Interview, C.S.I.R., July 1989.

Cheng, R.T. and Wang, L. 1985 "Solid State Recording Current Meter Conversion", Ocean Engineering and the Environment, Vol.2, November 1985, pp.752-754.

Cushing, V. 1976 "Electromagnetic Water Current Meter", Oceans 76, pp.25C-1 to 25C-17.

Daubin, C.D., Scally, D.R. and Tusting, R.F. 1977 "Measurement of Deep-ocean Currents using Recording Inclinometers", Oceans '77 Conference Record, Vol.2, October 1977, pp. POSTER-K-1 to POSTER-K-6.

Dextraze, R.E. 1968 "A Three Axis Ducted Impeller Current Meter", Marine Sciences Instrumentation, Vol. 4, pp.671-674.

Dornhelm, R.B. 1977 "Current Measurements Offshore Humboldt Bay, California, for Proposed Ocean Outfall", Oceans '77 Conference Record, Vol.2, October 1977, pp.46C-1 to 46C-7.

Edgerton, G.A. 1976 "Current Measurement System for Ocean Engineering", Oceans '76, pp.25A-1 to 25A-7.

Frey. H.R.	1982	"Circulatory Survey Data Quality Assurance", Proc. of the I.E.E.E. 2nd Working Conference on Current Measurement, January 1982, p.36.
Frisch, A.S. and Weber. B.L.	1982	"Applications of Dual-Doppler HF Radar Measurements of Ocean Surface Currents", Remote Sensing of Environment, Vol.12, pp.273-282.
Forristall, G.Z. and Hamilton, R.C.	1978	"Current Measurements in Support of Fixed Platform Design and Construction", Proc of a Working Conference on Current Measurement, Jan 1978, pp.199-222.
Garret, J.	1978	"Drifting Buoys for Ocean Data Collection", Oceans '78, September 1978, pp.155-159.
Georges, T.M. and	1981	"Measuring Ocean Currents with HF Radar", Oceans '81 Conference Record, Vol.1, September 1981, pp.228-232.
Gonsalves, W.D. and Brainard, E.C.	1981	"Geomagnetic Electrokinetograph (G.E.K.): A Technological Advancement in Long Term, Continuous Monitoring of Fluid Flow Velocity", Oceans '81 : Conference Record, Vol.1, pp.233-238.
Halpern, D.	1977	"Review of Intercomparisons of Moored Current Measurements", Oceans '77 Conference Record, Vol.2, October 1977, pp.46D-1 to 46D-6.
Holbrook, J.R. and Frisch, A.S.	1982	"A Comparison of Near-Surface CODAR amd VACM Measurements in the Strait of Juan de Fuca, August", Proc of the I.E.E.E. Second Working Conf. on Current Measurement, January 1982, pp.125-130.
Horler, V.	1989	"Pollution Trapped by the Waves", Weekend Argus, August 12, 1989, p.22.
Horikawa, K. and Sasaki, T.	1972	"Field Observations of Nearshore Current System", Coastal Engineering in Japan, Vol.115, pp.1134-125.
Howard, M.K. and MacFarlane, C.F.	1978	"Current Measurement Instrumentation Sensors for Industrial Applications: Requirements, Problems and Proposed Solutions for the Next Generation of Instruments", Proc. of the International Symposium on Ocean Wave Measurement and Analysis, January 1978, pp.177-182.

Huntley, D.A. and Bowen, A.J.	1974	"Field Measurements of Nearshore Velocities", Proc. of the 14th Coastal Eng. Conf. Vol. 1, pp 538-557.
Klemas, V., Davis, G. and Wang, H.	1975	"A Cost Effective Satelite-Aircraft-Drogue Approach for Studying Estuarine Circulation and Shelf Waste Dispersion", Ocean 75 Conference Record, pp 751-760.
Kronengold, M. and Vlasak, W.	1965	"A Doppler Current Meter", Marine Sciences Instrumentation, Vol.3, pp.237-250.
Kushnir, V.M.	1987	"Determination of Systematic Error of Current Velocity Measurements Caused by Noise Factors", Oceanology, Vol.27, No.3, p.382.
Lancaster	1985	"Current Profiling in Near Real Time", Sea Technology, Vol. 26, No. 2, pp 24-29.
Lee, A. Greated, C.A. and Durrani, T.S.	1974	"Velocities under Periodic and Random Waves", Proc. of the 14th Coastal Eng. Conf., Vol.1, pp.558-565.
Lovenvirth, D.L.	1964	"A Computer System for Reading Richardson Current Meter Film", Buoy Technology, March 1964, pp.463-470.
Magnell, B.A.	1982	"An Intercomparison of Current Measurements from a Raytheon Special Moored System and a VACM on Georges Bank", Proc of the I.E.E.E. Second Working Conference on Current Measurement, January 1982, pp.59-78.
McCullough, J.R.	1977	"Problems in Measuring Currents near the Ocean Surface", Oceans '77 Conference Record, Vol.2, October 1977, pp.46A-1 to 46A-7.
McCullough, J.R.	1978	"Near-surface Ocean Current Sensors: Problems and Performance", Proc. of the International Symposium on Ocean Wave Measurement and Analysis, January 1978, pp.9-33.
McKeehan, D.S.	1978	"Water Current Measurements for Marine Pipeline Design", Proc. of the International Symposium on Ocean Wave Measurement and Analysis, January 1978, pp.191-197.

Neumann, G.	1968	Ocean Currents, New York, Elsevier Publishing Co., p.32.
Niskin, S.J.	1965	"A Low Cost Expendable Bathythermograph", Marine Sciences Instrumentation, Vol.3, pp.123-132.
Prandle, D. and Howarth, J.	1986	"The Use of HF Radar Measurements of Surface Currents for Coastal Engineers", International Conference on Measuring Techniques, April 1986, pp.1-14.
Sanford, T.B., Drever, R.G. and Dunlap, J.H.	1978	"Deep Ocean Velocity Profiles from Electromagnetic and Acoustic Doppler Measurements", Proc. of the International Symposium on Ocean Wave Measurement and Analysis, January 1978, pp.137-151.
Scarlet, R.I.	1978	"The Incomplete Current Meter", Proc. of the International Symposium on Ocean Wave Measurement and Analysis, January 1978, pp.165-167.
Squier, E.D.	1968	"A Doppler Shift Flowmeter", Marine Sciences Instrumentation, Vol.4, pp.585-593.
Stacey, R.A. and Spring, W.	1978	"Ocean Current Measurements in Support of Hydrocarbon Exploration and Production", Proc. of the International Symposium on Ocean Wave Measurement and Analysis, January 1978, pp.169-176.
Swallow, J.C.	1955	"A Neutral Buoyancy Float for Measuring Deep Currents", Deep-sea Research, Vol.3, pp.74-81.
Vachon, W.A.	1977	"Current Measurement by Lagrangian Drifting Buoys - Problems and Potential", Oceans '77 Conference Record, Vol.2, October 1977, pp.46B-1 to 46B-7.
Van Leer, J.C. and Leaman, K.D.	1978	"Physical Oceanographic Research using using the Attended Profiling Current Meter (APCM) and the Cyclesonde", Proc. of a Working Conf. on Current Measurement, January 1978, pp.77-93.
Waldon, R.G. and Webb, D.	1964	"Methods of Locating and Tracking Buoys", Buoy Technology, March 1964, pp.317-324.

Winant, C.D., Davis, R.E. and Weller, R.	1978	"Shallow Current Measurements", Proc. of a Working Conference on Current Measurement, January 1978, pp.129-135.
Woodward, M.J.	1985	"An Evaluation of the Aanderaa RCM4 Current Meter in the Wave Zone", Ocean Engineering and the Environment, Vol.2, Nov.1985, pp.755-762.
Zeigler, J.M. and Tasha, H.J.	1968	"Measurement of Coastal Currents", Proc. of the 19th Coastal Eng. Conf., Vol.2, pp.436-445.
Zwamborn, J.A., Russel, K.S. and Nicholson, J.	1972	"Coastal Engineering Measurements", Proc. of the 13th Coastal Eng. Conf., Vol.1, pp.75-94.

CHAPTER 4 : SEDIMENT MEASUREMENTS

There are three categories of sediment measurement discussed in this chapter:

(i) Measurement to determine sediment movements, regardless of the mechanisms of transport. This is generally achieved with tracer techniques.

(ii) Measurements to improve the understanding of sediment transport mechanisms, and to develop theoretical relationships to predict sediment transport. These measurements are generally carried out at specific points in the sea, by sampling and indirect techniques.

(iii) Measurements to determine cross-sections of nearshore bathymetry, i.e. nearshore profiles; these reveal information about sediment transport.

4.1 SEDIMENT TRANSPORT MEASUREMENT WITH TRACERS

Natural or artificial sediment can be labelled, or tagged, in order to make it easily identifiable. This is achieved, for example, by coating it with paint, or by incorporating radioactive substances in it. This sediment is injected onto the sea bed at the site of interest. Samples are subsequently taken, at intervals, to determine the concentration of the labelled sediment at various locations. Alternatively, tracer concentration may be determined in situ. The concentration data can be analysed to reveal information about sediment transport.

Although the accurate determination of long-term sediment transport is not possible from a tracer study, qualitative data on sediment movement, useful for engineering purposes, can be obtained. In particular, information can be obtained about (i) the direction of sediment movement; (ii) sediment dispersion; (iii) sources of sediment shoals; (iv) the relative velocity and

movement of sediment in various areas of the littoral zone; (iv) means of natural bypassing of sediment, past structures and channels; (v) the efficiency of sediment-retaining structures .

4.1.1 Sediment transport measurement with fluorescent tracers

4.1.1.1 Introduction

In this technique, sand grains are coated with fluorescent dye or brightly coloured paint; they are then injected onto the sea bottom at the site of interest. After a period, samples of the sediment in surrounding locations are taken, and the concentration of tracer grains in each sample is determined. Analysis of these results yields information about the rate and direction of sediment transport.

Since coating very small grains with dye or paint is impractical, and their detection in a sample is difficult, this technique is restricted to larger sediment sizes (i.e. sand and shingle). Because of this restriction to larger sediments, and because sampling from the sea bed (or the beach) occurs, this technique primarily concerns the bedload sediment (Thornton and Morris, 1977, p 656). (Bedload sediment is that which is transported by rolling along the sea bottom).

Fluorescent tracers are often used in sediment studies on beaches, to estimate the longshore transport direction and rate, although they are also sometimes used at greater depths. The period of these studies is typically from hours to a few days, depending on the expected rate of sediment movement.

Unfortunately the fluorescent tracer techniques have some disadvantages:

(i) Compared to radioactive tracer techniques, less information is obtained for the same cost.

(ii) They are very time-consuming and labour-intensive.

(iii) Unlike radioactive tracers, fluorescent tracers are difficult to detect; therefore there must be sufficient tracer to allow a likelihood of finding it in a given sample.

TABLE 4.1 QUANTITITES FOR FLUORESCENT TRACER SAND

	Coarse Sand Sieve $^{16}/_{40}$	Fine Sand Sieve $^{40}/_{100}$
Paint	2,5 litres	2,5 litres
Thinners	2,08 litres	1,85 litres
Sand	70 kg	45 kg

In spite of these disadvantages, compared to radioactive tracer techniques, fluorescent tracer techniques require less sophisticated equipment to label and detect sediment grains, and they do not require licensing and safety precautions. Another advantage over radioactive tracers is the potential use of different colours. This allows (i) the possibility of successive experiments in the same area, without confusion; (ii) the tracing of different size fractions of sediments, which are coloured differently; (iii) different coloured tracer can be injected at various locations, to determine origins of sediment accumulations.

4.1.1.2 Technique

(a) The manufacture of fluorescent tracer sands

The tracer sand should be similar to the sand at the measurement site in size, shape, and density. This is usually achieved by taking representative samples of sand from the site. Alternatively, a similar sand can be sieved and weighed (this may be done after coating it), to attain a particle size distribution similar to the in situ sand.

Various materials can be used to coat sand grains. At the University of Cape Town (U.C.T.), commercial fluorescent paint and thinners have been used; these were readily available, and required no expensive equipment in the manufacturing process. Fluorescent paint and an organic solvent can also be used together with a binding medium of resin (Knoth and Nummedal, 1977, p 386). Alternatively, Rhodamine-B dye with resin can be used (Readshaw, 1979, p 146). Once coated, the particle size distribution of the sand will be altered slightly,

although "any change in hydraulic properties" from the coating "is felt to be of a secondary engineering consideration" (Readshaw, 1979, p 140).

The procedure developed at U.C.T., to manufacture tracer sand, is as follows: A volume of the selected sand is placed in an oven (at 100 degrees Celsius) to dry; then it is placed in a rotary concrete mixing pan. Fluorescent paint mixed with thinners is added; the quantities used are given in table 4.1, for coarse and for fine sand. When thoroughly mixed, the sand is left on trays to dry. After drying, the sand is put through a mesh to break up agglomerated sand (i.e. clusters of sand grains).

(b) Injection of tracer sand at the measurement site

The position of injection depends on the objectives of the study. For example, in beach studies to determine longshore drift characteristics, tracer sands are usually injected at several points, or sometimes in lines, along a transect of the surf zone; at low tide this can be achieved on the beach. Alternatively, in some applications, e.g. a study of sediment movement beneath an oil rig, a single injection point may suffice (Bratteland and Bruun, 1974, p 979).

Tracer sand is usually introduced by spreading a thin layer on the natural sand bed. This discourages loss of the tracer immediately, by burial. It is important to ensure that the tracer sand is properly wetted, otherwise air bubbles will cause it to float on the sea surface initially, producing erroneous results. Thus, to ensure wetness, a surfactant (eg. dishwashing liquid) is mixed with the sand.

Injection at depth can be carried out by divers carrying bags of tracer sand. Alternatively tracer sand may be lowered, from a vessel or helicopter, in soluble bags, which dissolve to release their contents.

(c) Sampling and processing:

(i) Location and time of sampling

The sand is sampled in the region of expected sediment movement. For surf zone studies,this region is often made

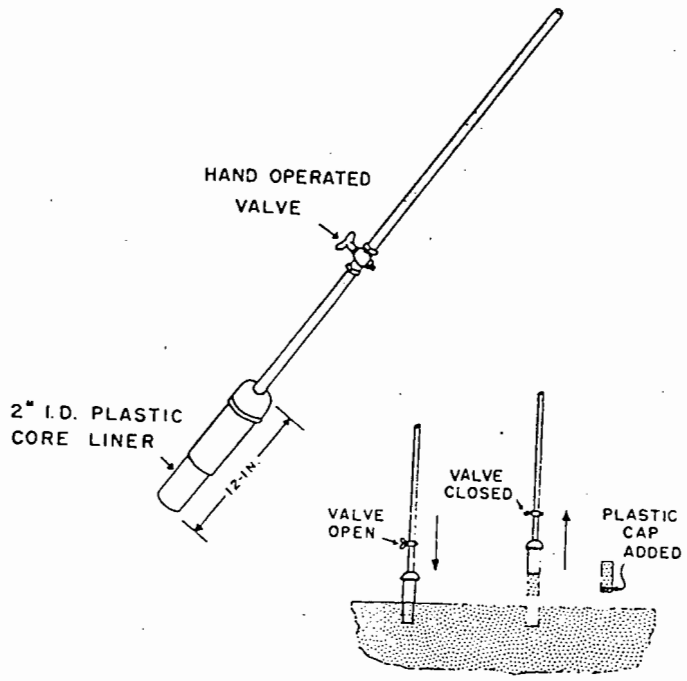

Device used to obtain sand cores within study area.

Figure 4.1 : Device used to obtain sand cores within study area.

Boon (1969)

obvious by patterns of erosion and accretion along the coast, particularly at structures extending into the surf zone. The furthest seaward extent of sampling is usually approximately at the breaker line at low water, since it is up to this point that most nearshore sediment transport occurs.

In the surf zone, samples are often taken simultaneously (if possible in practice) at positions on a grid; this is termed spatial sampling. The positions on the grid may be determined by conventional land surveying techniques. The grid must be sufficiently large, to ensure that significant concentrations of the tracer are sampled (Knoth and Nummedal (1977, p 386) use a 20 m x 10 m grid). Another approach is to take samples along a single transect of the surf zone, at intervals (e.g. 2 hours); this is called temporal sampling. In this case the total sampling period should be long enough to record concentrations, until virtually all the tracer sand has passed the transect due to longshore drift. These types of sampling form the basis of two analysis procedures (Sec. 4.1.1.3).

Beyond the surf zone, if the direction of sediment movement is unknown, samples may be taken on concentric circles around the injection point (Bratteland and Bruun, 1974, p980).

(iii) Methods of sampling

Samples may be taken by manually scooping up sand, or with corers (eg. Fig. 4.1; this device is driven into the sand with the valve open; the valve is then closed and the core is extracted, immediately sealing the bottom end with a plastic cap). In deep water, samples can be taken from a structure or a vessel with a mechanical grab sampler. Alternatively, divers can sample sediment with scoops, corers or a greased plate (to obtain a single layer of sand). However, the confidence level of fixing their position is low under these conditions.

(iv) Processing samples

The samples are washed, dried, and weighed. They are then spread evenly over a known area (e.g 100 cm^2), and the number

of tracer grains which fluoresce under ultraviolet light on the surface is counted.

(v) Concentration of tracer

The concentration of tracer particles in a sample is needed in analysis. In order to convert the number of tracer particles per area (say 100 cm^2) into concentration, a laboratory calibration is necessary:

Firstly, tracer and beach sand are mixed in known concentrations; for each concentration the number of tracers grains per 100 cm^2 surface area is counted; this is done repeatedly for each concentration in order to obtain a reliable average and to draw a calibration curve (Kadib, 1972, p 992) of counted particles versus concentration.

(vi) Depth of tracer

In addition to sample concentrations, the depth of burial of tracer, which reveals the depth of the mobile sand layer, is needed to analyse the flow rate of sediment (dealt with in the following Sec. 4.1.1.3). This depth can be sampled with corers (e.g. Fig. 4.1); if the walls of the corer are made of transparent perspex, the depth of tracer can be determined, under ultra-violet light, without disturbing the core sample.

The depth of the mobile sand layer can also be determined with the depth of disturbance rod; this consists of a round steel rod, which can be driven vertically into the sand (by a diver, if underwater). A loose-fitting washer is placed over the rod and allowed to fall to the bed. The position of the washer is measured from the top of the rod. Since this washer sinks to the base of the mobile layer after a time, subsequent measurements from the top of the rod yield the thickness of the mobile layer of sand (Greenwood et al,1979,p103).

A similar approach is to replace a vertical cylindrical column of beach sand with an identical column of tracer sand (of known

weight). After an interval, the remaining tracer sand can be removed and weighed to determine the depth of the column which was disturbed. (Kilner, 1988)

4.1.1.3 Analysis and Interpretation

(a) Sediment transport using concentration-weighted mean advection rate:
The flow rate of sediment, Q, can be estimated from the formula:

$$Q = V.B.d \qquad (4.1)$$

where V = advection rate of the sand.
B = the breadth of the mobile layer.
d = the depth of the mobile layer.

These quantities are described below:

The advection rate

The advection rate, V, is obtained from either spatial or temporal sampling. (Sec. 4.1.1.2(c)). In the case of spatial sampling, samples are taken on a grid, at various longshore distances y_i from the injection point, at time t; their concentrations, C_i, are determined. In the case of temporal sampling, samples are taken along a single transect, at a longshore distance y from the injection point, at times t_i; their concentrations, C_i, are determined. For both types of sampling, a concentration-weighted mean advection rate for sand in the longshore direction is given by (Inman et al, 1980, p 1225):

$$V = \frac{\sum_{i=1}^{n} \left[C \left(\frac{y}{t} \right) \right]_i}{\sum_{i=1}^{n} C_i} \qquad (4.2)$$

where n = the total number or samples

(depending on whether spatial or temporal sampling was done, either y or t will be fixed)

The breadth of the mobile sand layer

The breadth of the mobile layer of sand, B, is normally taken as the distance from the high water mark to the line of wave breaking at low tide. This is the region where most nearshore sediment occurs. The restriction to a fixed breadth of mobile sand is acceptible in "non-storm conditions", since "commonly no exchange of sediment occurs across the zone of primary breakers" (Knoth and Nummedal, 1977, p 392). This is supported by the results of dye tests conducted by the C.S.I.R., which show that effluents discharged in the surf zone get trapped there and "stay there 80 percent of the time" (Horler, 1989). Furthermore, although some longshore transport occurs seaward of the breaker zone, Thornton (1970, pp 291-308) found that longshore currents, which are responsible for sediment transport, decrease rapidly seaward of the breaker zone.

(a) The depth of the mobile sand layer

The depth of the mobile layer, d, is not well understood, and its determination from core samples is highly subjective (Inman et al, 1980, p 1225). For example, in some cases the depth of the mobile layer is taken to be the maximum depth at which tracer grains are found in a core sample; in other cases it is taken as the depth at which the tracer grain concentration becomes less than a certain quantity (e.g 1 grain/gram). In an attempt to standardise this depth estimate of the mobile layer, d_o, a formula is proposed by Inman et al (1980, p 1225):

$$d_o = 2 \frac{\int_{z=o}^{1} z.C(z)\, dz}{\int_{z=o}^{1} C(z)\, dz} \qquad (4.3)$$

where z = the depth in the bed

$C(z)$ = the tracer concentration at depth z

1 = a depth in the bed beyond which no tracer grains penetrate.

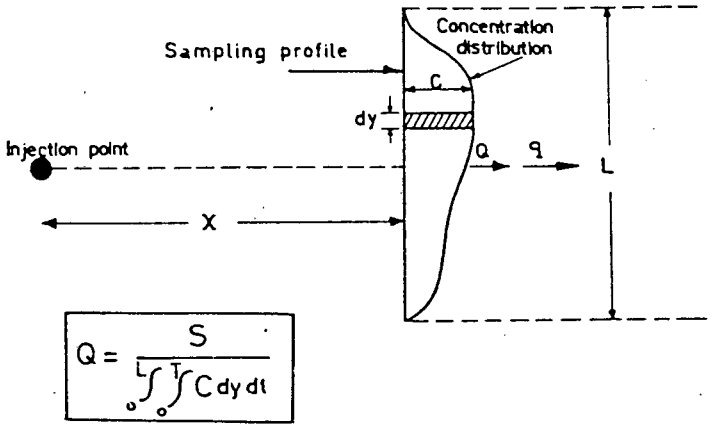

Figure 4.2 : Definition sketch for the dilution method.

Kadib (1972)

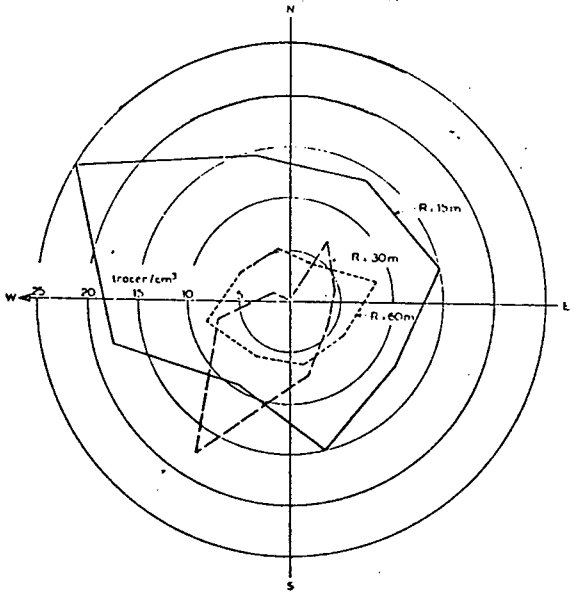

Figure 4.3 : Illustration of tracer concentration distribution for concentric circles of radius R.

Bratteland and Bruun (1974)

It has been found that the depth of the mobile layer is greatest in the swash zone, least in the central part of the surf zone, and increases again towards the point of wave breaking; this yields a bimodal distribution of the mobile layer depth. Thus, if inadequate samples (or measurements) are obtained, (particularly near the breakers in high surf conditions) then the depth of the mobile layer can be estimated in this region using a bimodal distribution (Inman et al, 1980, p1226).

(b) Sediment transport from the dilution method

Another approach to estimate the longshore sediment movement is the dilution method, which is based on the following principle:

If tracer sand is injected into a channel at a known steady rate, for a long time,and subsequently sampled at the channel bed at a section downstream, the samples will contain tracer material mixed with in situ material in the concentration C, where (Russell, 1960, p 419):

$$C = q/Q \qquad (4.4)$$

where q = the rate (mass per time) at which tracer is injected
Q = the rate at which sediment is transported past the injection point

Since Q is the quantity required:

$$Q = q/C \qquad (4.5)$$

If the boundaries of this movement in the surf zone are well defined, and if the littoral drift is in one direction only, then this equation will apply. From equation (4.5) Kadib (1972, p 987) derives the following :

$$Q = \frac{S}{\int_0^L \int_0^T C.dy.dt} \qquad (4.6)$$

where Q = the average rate of littoral drift per unit width at any distance x from the injection point.

S = the total amount of tracer which passes any sampling section during any period of time T.

T = the time between the first arrival of tracer to any sampling section, and its complete disappearance.

L = the length of any sampling line, across the surface, along which tracer is found.

Fig. 4.2 clarifies these parameters.

Equation 4.6 can be used to estimate littoral drift, provided the following conditions are satisfied:

(i) Littoral drift must have one major direction for most of the period of measurement.

(ii) Sampling positions, along transects of the surf zone, should not be far from the injection point.

(iii) Sampling should cover any seawards distance where tracer may be found (samples are usually as far out as the breaker line in non-storm conditions).

(iv) Sampling along a transect should continue from the moment tracer reaches the transect, until its complete disappearance.

In this technique, the depth to which samples are taken will directly affect the concentrations, C, which are obtained; this in turn will affect the calculated sediment transport rate, Q (equation 4.6). Therefore, it is important that samples are taken to the depth of the mobile layer, as discussed above (Sec. 4.1.1.3(a))

The dilution technique has been developed for the movement of material in two opposite directions (Russell, 1960, p 435). However, this method was found to be suitable only for shingle beaches, where there is a sharp dividing line between shingle on the upper beach and the sand lower down (shingle is beach material of smooth, well rounded pebbles that are roughly the same size). The method was found to be unsuitable on sand due to an unknown loss of tracer sand from the beach offshore.

(c) Shortcomings of analysis methods

(i) In general, due to limitations on funding, insufficient samples are obtained to obtain accurate estimates of sediment transport. More extensive sampling is needed because of variations in tracer concentration due to (a) patchy distribution of tracer on the beach (b) short term burial and re-excavation of tracer sands, and (c) beach topography which affects small scale water circulations (which transport sediment) (Inman et al, 1977, p 388).

(ii) More knowledge about the depth of the mobile sediment layer is needed.

(iii) To obtain quantitative estimates, there is a limitation to smaller surf conditions; large surf conditions result in excessive sand being transported offshore; in addition sampling in the surf zone will become hazardous in these conditions.

(iv) Since tracer studies of this type are conducted for a period of only a few days at most, the above estimates of the sediment transport rate, Q, represent only short term littoral transport phenomena. For the estimation of longer term littoral transport, repeated studies are required over a long period.

(d) Deep water analysis technique

If the likely direction of sediment movement is not known, then samples can be taken on concentric circles around the injection point. The concentrations of tracer grains obtained on these circles can be displayed as illustrated in Fig. 4.3 . In the figure, the plotted lines represent concentrations found at concentric circles of particular radii, in various directions. From such a diagram the resultant direction and rate of sediment movement can be estimated, provided that the depth of the mobile sediment layer is estimated (dealt with in part (a) above) (Bratteland and Bruun, 1974, p 988).

(e) Qualitative techniques

From spatial sampling, and processing samples, a grid of sample concentrations results. From this grid, contours of fixed concen-

trations can be drawn manually or with a computer plotter. This provides qualitative information; for example, the dominant direction of sand movement is easily interpreted from the contours.

Fluorescent tracer techniques can be used to determine the destination of sand which is being removed from a beach. Tracer may be injected at the site of sand loss; surveys for tracer along the shore on either side of the site will establish whether the removal is due to littoral drift, and also the direction of the drift. If no tracer can be found, then the loss is presumed to be offshore.

Alternatively, if sand is accumulating at a site (e.g. in a harbour), the source of sand may be determined. Different colours of tracer can be placed at the sites of possible sand sources. Tracer surveys at the sand accumulation area will indicate the source/s by the presence of a particular colour. If several colours occur, their relative concentration indicate the relative significance of the sources of supply (Kilner, 1988).

4.1.2 Sediment transport measurement with radioactive tracers

4.1.2.1 Introduction

Sediments can be labelled, or tagged with radioactive substances, and injected onto the sea bottom at the site of interest. Movements of sediment can then be detected easily by measuring the radioactivity level surrounding the injection site, by means of mobile detectors which are towed across the ocean floor. Samples can be taken for laboratory radioactivity measurements, to obtain the concentration and the depth of burial of tracer sands, necessary for sand transport estimation.

Since minute quantities of radioactive material have a significant radioactivity, it is possible to label very small sediment particles, including those which are transported as suspended load in the ocean. This method is therefore suitable for measurements where sediments of a smaller size are likely to be found e.g. beyond the surf zone, and in estuaries. In particular, the easy detection of radioactive tracers facilitates measure-

ment in deep water. Techniques of analysis are similar to those for fluorescent tracers, and quantitative estimates of sediment transport can be found.

(a) Applications of radioactive tracer techniques

Radioactive tracers are useful in dredging applications, for example:

(i) In the assessment of dredging economy; this is governed by the distance to the dumping site, and the amount of dredged material returning to the dredging site.

(ii) In assessments of the impact of dredging on the environment. Two important environmental effects of dredging are (a) change in the sea bottom contours which affect the direction of waves through refraction; waves with altered directions may cause harmful erosion; (b) removal of material which serves as a source of beach material.

Another application of radioactive tracers is the assessment of sediment movements at proposed sites of harbours, or navigation channels; for example, radioactive tracer studies were conducted at Brisbane, Australia, to determine whether a proposed channel would cut across a sand migration route; this would cause an undesirable accumulation of sediment in the channel.

Theoretical calculations and hydraulic models can also be used to determine sediment movements. However, these involve a wide range of parameters, complex liquid-solid interactions, and difficulties due to the cohesion of bed material; therefore calibration with in situ measurements are necessary - radioactive tracer measurements are useful for this purpose (Tola et al, 1984, p 2042).

(b) Advantages and disadvantages of the technique

Radioactive tracer techniques have the following major advantages:

(i) They are easy to detect in situ, with sensitive equipment; as a result, an almost immediate indication of sediment movement trends is obtained, which facilitates the planning of further sampling.

TABLE 4.2 RADIOACTIVE TRACER SAND

ISOTOPE	HALF-LIFE (days)	REFERENCE
Scandium - 46	84	Heathershaw & Carr (1977) Rohde (1976) Waters (1987)
Chromium - 51	27	Davison (1984) Rohde (1976)
Iridium - 192	74	Tola et al (1984) Ecker et al (1976)
Gold - 198	2,7	Tola et al (1984)
Silver - 110	253	Crickmore et al (1984)
Cobalt - 60	105 months	Sato (1962)

(ii) High sensitivity equipment facilitates the measurement of very dilute tracer quantities; allowing accurate measurements of tracer concentration over large areas.

Disadvantages are:

(i) Objections to the use of radioactive tracers by environmentalists.

(ii) Radioactive materials are hazardous, and many require protective measures.

(iii) A shortage of facilities for producing radioactive materials, and of expertise for handling them, especially in developing countries (Waters, 1987, p 34).

4.1.2.2 Technique

(a) Preparation of tracer sand

For a radioactive tracer study, the selection of a radioactive isotope depends on:

(i) The amount of radioactivity required. This is affected by factors such as the area over which the sediment is likely to be transported, and the sensitivity of detection equipment.

(ii) The duration of the study. The radioactive half life (i.e. the period of time required for the radioactive isotope to lose fifty percent of its activity) must be long enough to provide sufficient activity for the duration of the study. Examples of isotopes used in tracer studies and their half lives are given in table 4.2 .

(iii) Safety factors; some high activity isotopes will require lead shielding; others can be handled without any bulky shielding (e.g. chromium-51).

To manufacture tracer sand, the selected tracer element is generally incorporated in the manufacture of glass. Irradiation of the glass then causes the formation of the required radioactive isotope, from the tracer element. The glass is crushed, and graded with sieves so that its particle size distribution corresponds to the natural sediment. This is achieved before irradiation (Heathershaw and Carr, 1977, p 401) or afterward (Sato, 1962, p 85).

In a tracer study for shingle, radioactive material may be placed in a hole in each pebble, then filling each hole with epoxy resin (Crickmore et al, 1972, p 1009).

(b) Tracer injection

Relatively small quantities of tracer are injected onto the sea floor at the site of interest; this must be done carefully, to avoid unnatural dispersion. Injection may be achieved with a long tube extending down to the sea bottom (Heathershaw and Carr, 1977, p 401). Alternatively, tracer can be lowered in containers; at the sea bottom these are opened, for example, by a falling weight (Svasek and Engel, 1960, p 447), or by electrically-operated detonators (Davison, 1984, p 2067). Since this is a delicate operation, injection is generally limited to favourable conditions.

Another approach, for determining the movements of dredged spoil, is to introduce tracer into the hoppers of dredgers before dumping.

(c) Detection and sampling

Sensors

In order to detect radioactivity, scintillation and Geiger-Muller sensors are used (the scintillation detector is more sensitive). These sensors may be lowered to the ocean bottom on cables (Heathershaw and Carr, 1977, p402; Sato, 1962, p 85). Alternatively, sensors mounted on sledges are commonly used; these are dragged behind a vessel (Svasek and Engel, 1960, p 448; Davison, 1984, p 2068; Rohde, 1976, p 2031). Wheeled vehicles can also be used; Crickmore et al (1972, p 1010) use 5 scintillation detectors mounted on a 3-wheeled vehicle. Acree et al

(1970, p 815) use a single wheeled ball-shaped detector vehicle which, when towed behind an amphibious vehicle, can be used on the beach, in the surf zone, and offshore. For accurate measurements, which are used to determine the depth of tracer burial, portable radioactivity detectors, held by divers, may be used (Crickmore et al, 1972, p 1010).

(d) Background measurement

Before the injection of tracer, the natural background radioactivity at the site is measured, for the following reasons: (i) to ensure that radioactivity levels are not excessive, thereby affecting the accuracy of measurements; (ii) to facilitate the subtraction of background radioactivity from subsequent radioactivity measurements, in order to estimate the tracer concentrations.

(e) Radioactivity measurements

After a time interval, following injection of tracer (to allow mixing of the tracer with the sediment in situ), the radioactivity is measured. Measurements are usually taken along straight, parallel lines; the result is a grid of radioactivity values. The location of these grid radioactivity values is determined, during measurement, with various radio systems such as Decca HiFix, HIFAR, and Hydrodist MRB2. These systems fix the position of a vessel; however, the position of a towed detector behind a vessel must be estimated, by assuming it to be on the line of the boats course. The distance of the detector behind the boat is determined from the length of the tow cable, although errors are likely in strong crosswinds and currents.

(f) Sediment samples

Sediment samples are generally not necessary in this technique. Nevertheless, core samples may be obtained for determining the depth of the mobile sediment layer, for estimating sediment transport rates. In addition, samples may be taken from dredger hoppers (after an adequate time lapse after tracer injection), if the amount of dredged spoil collecting in a dredged channel is of interest.

4.1.2.3 Analysis and Interpretation

The analysis is similar to that for fluorescent tracers. Values of measured radioactivity must be corrected for decay of the radioactive isotope. In addition, the background radiation, which is measured separately before injection (Sec. 4.1.3.2(c)), must be subtracted. The resulting radioactivity values, which correspond to tracer concentration, can be plotted on a grid (interpolation may be necessary for values which do not occur at grid points). From these grid values, contours of constant radioactivity values (i.e. isoactivity lines) may be drawn, manually or with a computer plotter. Trends of sediment movement are easily observed from these contours.

Provided that a sufficiently high proportion of injected tracer is detected, a quantitative estimate of the rate of sediment transport, Q_r , per metre width across the flow direction, can be obtained from the formula (Heathershaw and Carr, 1977, p 406):

$$Q_r = \rho V.D. \quad (\text{tonnes. day}^{-1} .\text{m}^{-1}) \qquad (4.7)$$

where V = the centroid velocity
D = the depth of burial of tracer (i.e. the approximate depth of the mobile layer)
ρ = the bulk density of the sediment.

The centroid velocity, or advection rate, may be calculated in the manner described for fluorescent tracers, in Sec. 4.1.1.3(a).

The depth of burial, D, may be found from core samples, analysed in the laboratory. Alternatively, it may be found using the tracer balance method. This method is based on the assumption that a reduction in tracer recovery is caused by the burial of material in the sea bed, rather than by dispersion to a region beyond that covered (Heathershaw and Carr, 1977, p 405; Davison, 1984, p 2071).

4.1.3 Alternative techniques of tracing sediment movement

A number of alternative techniques exist for tracing sediments. These are described briefly below:

4.1.3.1 A semi-radioactive technique

Sediment representative of the site is labelled with a tracer element (Iridium may be used; it is attached to the sediment by adsorption (Ecker et al, 1976, p 2010)). This tracer sand is injected at the desired location. Samples taken after an interval are irradiated; the tracer element then becomes radioactive. Radioactivities are then measured to determine concentrations of the tracer element, which yield information on sediment movement, using analysis techniques such as those outlined in Sec. 4.1.1.3.

The advantage of this technique is that radioactivity is only involved after sampling; until then, no protection is required and there is no danger to the environment. However, the tracer cannot be detected in situ. Nevertheless, the technique has been successfully used in San Francisco Bay (Ecker et al, 1976, pp 2009-2026).

4.1.3.2 Naturally radioactive minerals

Radioactive materials such as thorium, and some heavy minerals, can be found in coastal sediment. The sources of these materials are generally rivers, or a region having a particular rock type. If a predominant direction of littoral drift occurs, the concentration of these materials will decrease with distance from the source area. Thus, sand samples may be taken on beaches along the coast, and analysed for their radioactive content, to reveal qualitative information about the littoral drift.

4.1.3.3 Metal tracer technique

This technique is suitable for determining the movements of shingle (pebbles). Metal "pebbles" are made to reproduce the size, shape and specific gravity of the shingle in situ; with the use of metal detectors, these can easily be subsequently recovered, even if they are beneath the surface. Once recovered, analyses mentioned in Sec 4.1.1.3, for fluorescent tracers, can be employed.

These tracer pebbles provide no health risk (unlike radioactive tracers) and are unobtrusive (unlike fluorescent tracers, which are susceptible to public interference). However, due to the limited sensitivity of metal detectors, this technique is limited to larger sediment sizes (i.e. shingle).

4.1.3.4 Thermoluminescent tracer technique

Thermoluminescence is the property of certain substances e.g. fluorite, to absorb radiation and to release it, on application of heat, in the form of optical radiation. Development of the following technique is in progress (Waters, 1987, p 36): Fluorite ore is injected as a tracer material; samples of sediment taken subsequently are irradiated. Thereafter, while applying heat, the optical radiation emitted (due to thermoluminescence) is measured; this signal is interpreted to indicate the concentration of fluorite tracer; this will reveal sediment movement information.

4.2 POINT MEASUREMENTS

The sediment transport rate, or the sediment concentration, can be measured at selected points in the ocean, particularly in and near the surf zone, where most sediment transport occurs. These point measurements are used to improve the understanding of the processes of sediment transport, and to develop empirical relationships to predict sediment transport. This type of measurement is achieved with sampling techniques, and with sensing devices.

Common problems with point measurement are:

(i) Measurement instruments influence the water flow; this may change the sediment concentration.

(ii) Scour (i.e. disturbance of the sea bed) may occur around the instrument and its supporting structure; this can produce either an artificially high or low concentration near the bed.

(iii) Calibration of sensing devices is very difficult.

(iv) Both the bedload and the suspended load quantities are needed in order to determine the total sediment transport, however many devices measure only one of these.

(v) Instruments are not always robust enough to withstand forces in the surf zone.

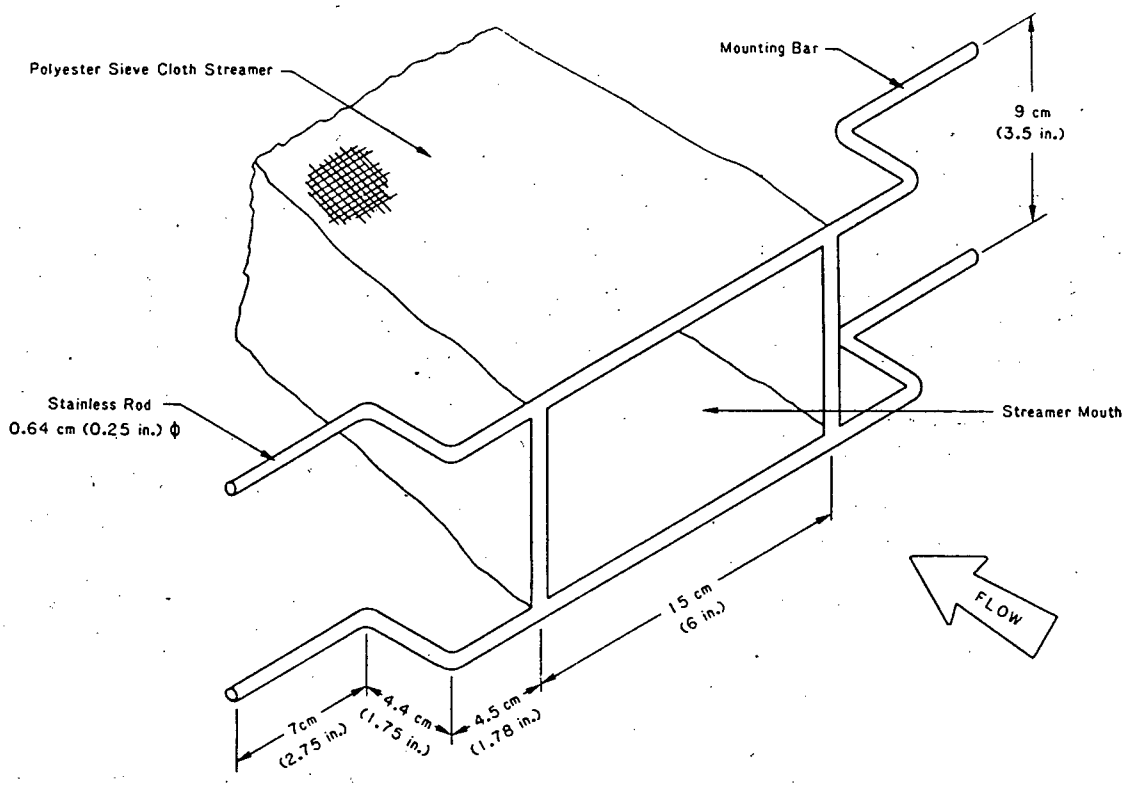

Figure 4.4 : Streamer trap mouth.

Kraus (1987)

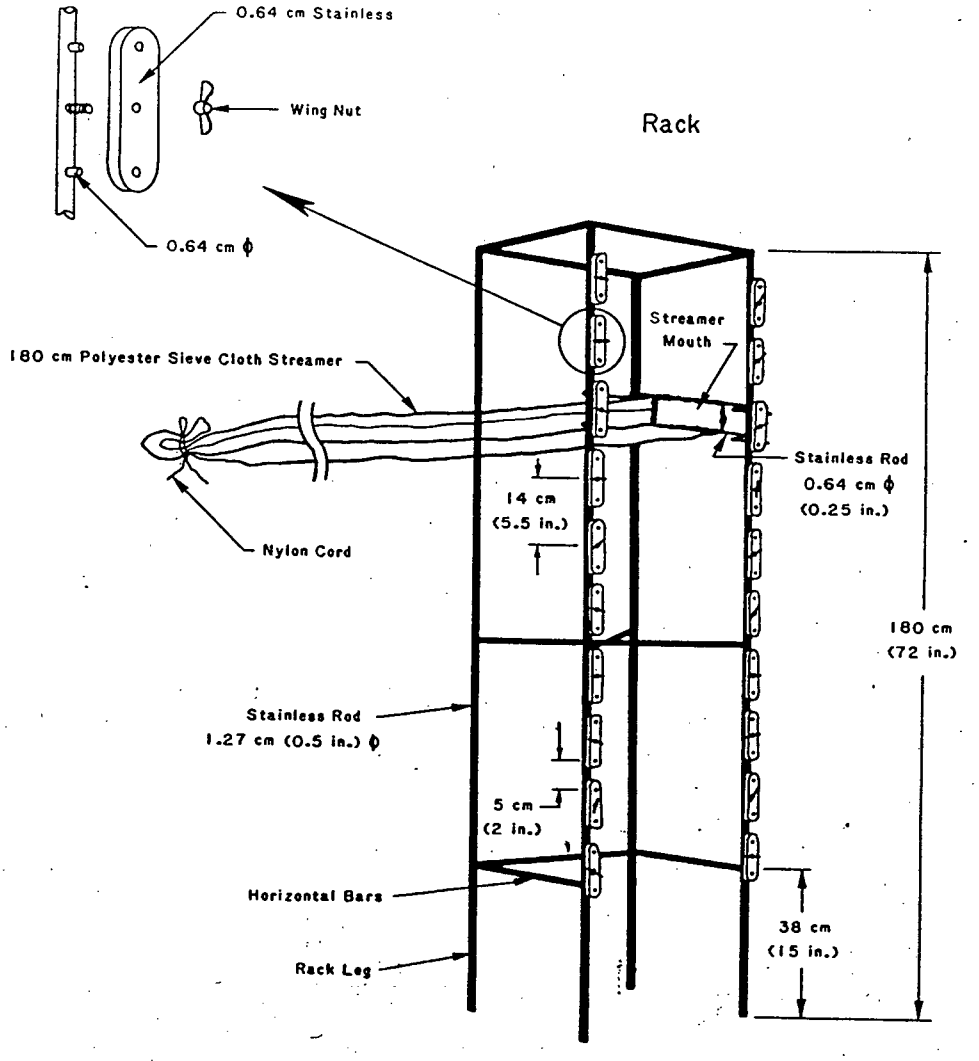

Figure 4.5 : Streamer trap rack.

Kraus (1987)

The most successful sampling and sensing devices are those which eliminate and minimize problems such as these.

4.2.1 Sediment sampling techniques

4.2.1.1 The streamer trap

Principle of operation

Water entering the mouth of the streamer trap, flows through the stocking-like sieve-cloth streamer (Fig 4.4), which filters out sand. The mass of the retained sand, divided by the duration of sampling, yields the rate of sediment transport, corresponding to the location and orientation of the streamer trap mouth (Kraus, 1987, pp 139-151). By mounting several streamer traps on a rack (Fig. 4.5), the vertical distribution of the suspended sediment transport rate can be measured. In addition, since the bottom-most trap is at bed level, it will measure the bedload transport.

Measurement

The rack of sand traps is portable and is deployed in the surf zone by thrusting the legs of the rack into the sand. After the sampling interval of 5-10 minutes, the rack is removed. Sand retained in the traps is then weighed.

Analysis:

As mentioned above, the mass of sediment trapped at a point, divided by the time of sampling, yields the sediment transport rate at that point. Thus, from measurements taken at various depths, along a cross-section of the surf zone, vertical and horizontal profiles of the sediment transport rate can be obtained. These are useful for the development of sediment transport theory. In addition, the average sediment transport across the surf zone can be calculated.

Advantages:

The streamer trap has several favourable features :

(i) Since it is slender in construction, it produces minor scour, provided that the sampling interval is sufficiently short.

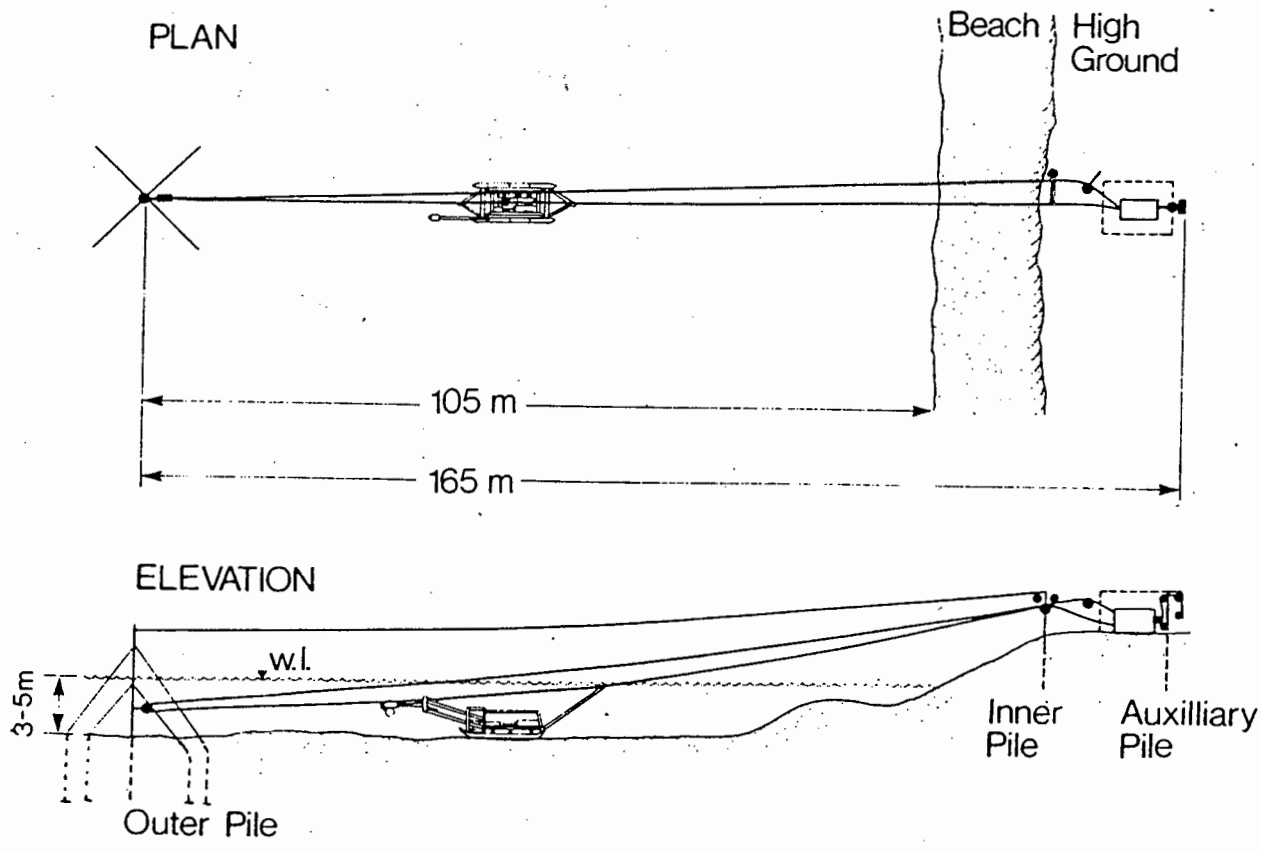

Figure 4.6 : Littoral drift sledway, general arrangement.

Coakley and Savile (1979)

(ii) It does not significantly disturb the flow, to influence measurements.

(iii) A vertical array of streamer traps can measure both suspended load and bedload transport.

(iv) It is light and easy to handle, and the time between successive deployments is short.

4.2.1.2 Concentration samplers

The sediment transport rate can be estimated with theoretical relationships (CERC, 1977 p 4-88). Due to complex liquid-solid interactions and complex flow characteristics (Thornton and Morris, 1977, p 656), these theoretical relationships cannot be derived from basic physical principles; they must therefore be derived from empirical data. The empirical data required includes wave heights and directions (Chapter 1), current velocities (Chapter 3), beach profiles (Sec 4.3), and sediment concentrations at various locations in the surf zone, which are discussed in this section.

Seawater is sometimes required for industrial uses (e.g. cooling purposes). In relation to this, sediment concentration data is sometimes required for the design of seawater intake structures, since excessive sediment in suspension can have an adverse effect on intake structures by causing abrasion, or by blocking conduits.

Sediment concentration is measured with pump-operated samplers, or with portable samplers operated by swimmers in the surf zone.

(a) Pump-operated samplers

Seawater can be sampled from various locations in the sea by pumps. The pumped seawater may be stored in containers e.g. jars or plastic bags. The sediment in the containers can be filtered out, dried, and weighed; its mass divided by the sampled water volume yields the concentration. There are several types of pump-operated samplers:

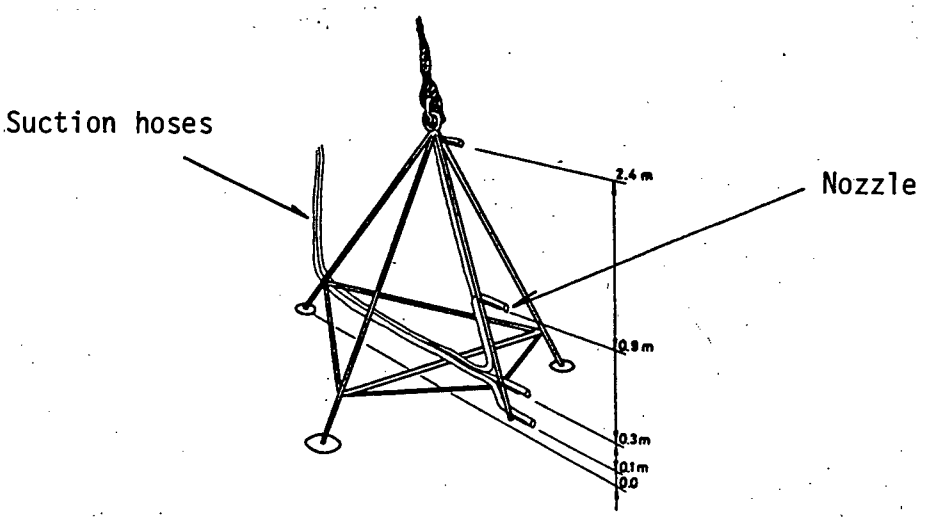

Figure 4.7 : Sampling structure.

Jensen and Sorenson (1972)

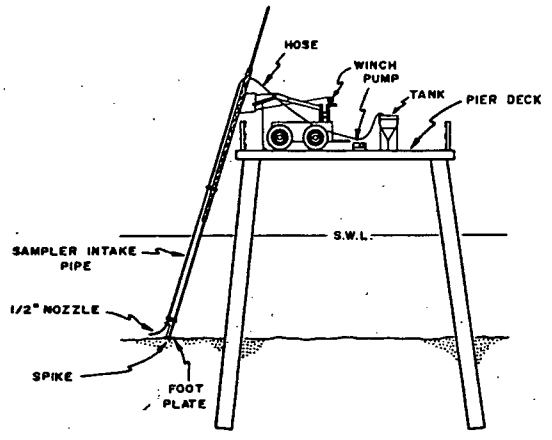

Figure 4.8 : Schematic view of a tractor-mounted suspended sand sampler on a pier.

Fairchild (1972)

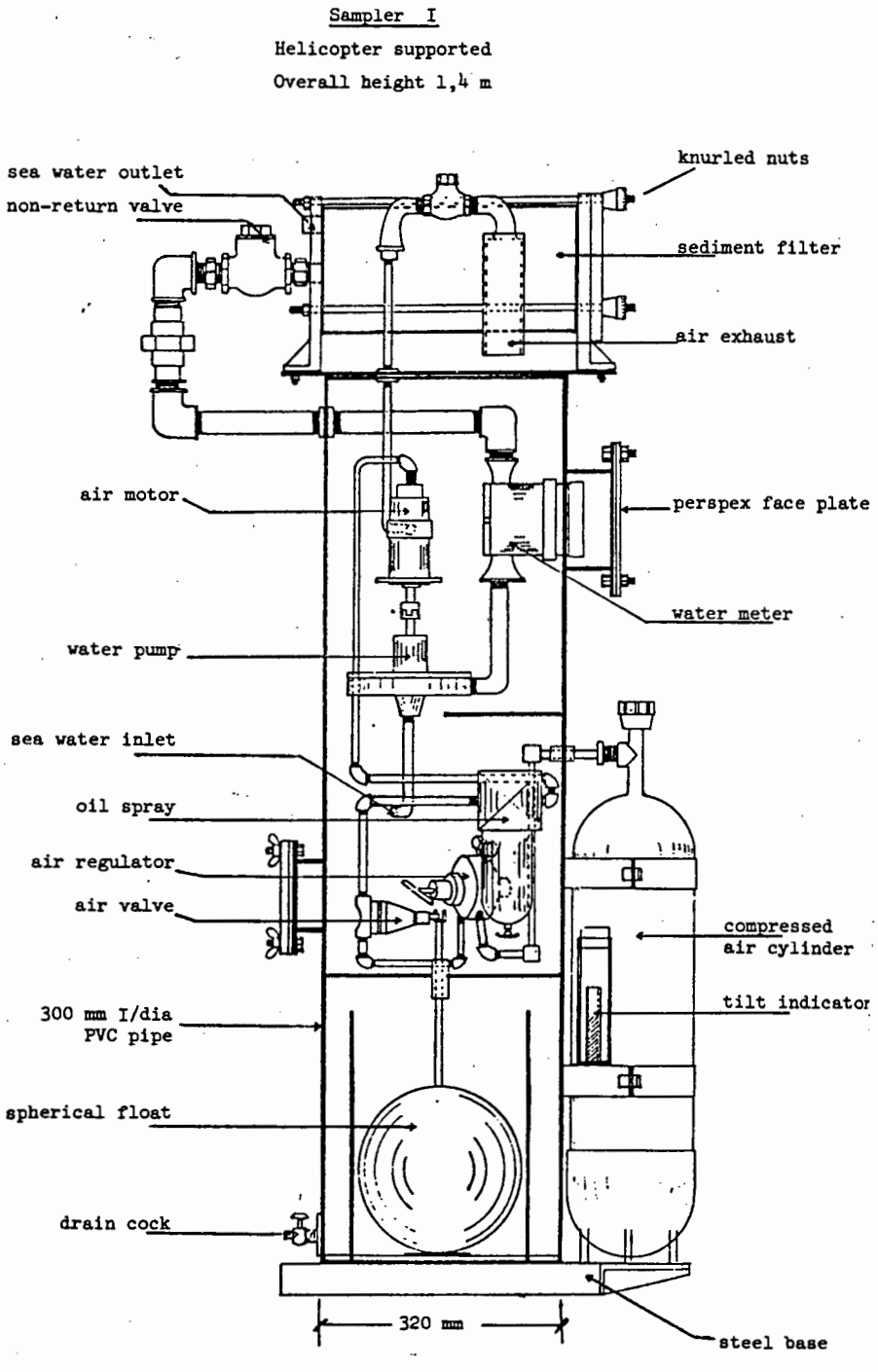

Figure 4.9 : The Helicopter-borne sampler.

Kilner (1976)

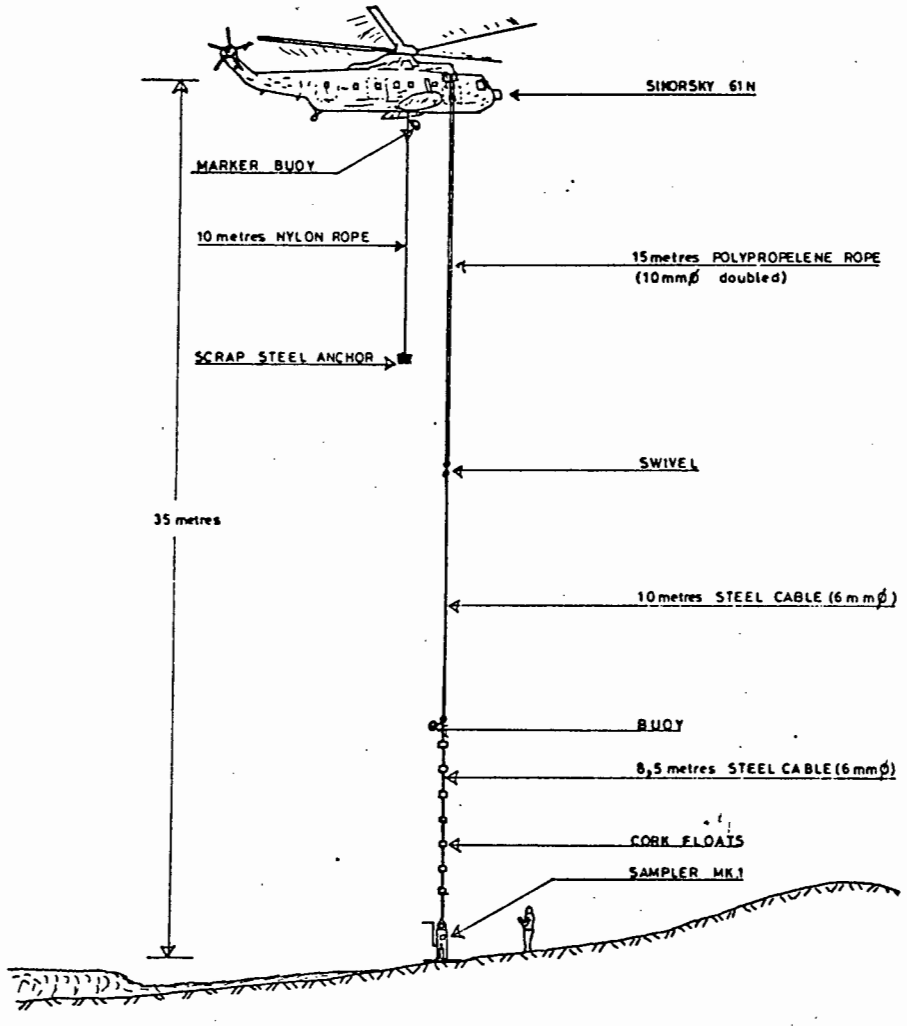

Figure 4.10 : Helicopter sampler being prepared on the bench.

Kilner (1976)

Helicopter sampler (no I)
on sea bed

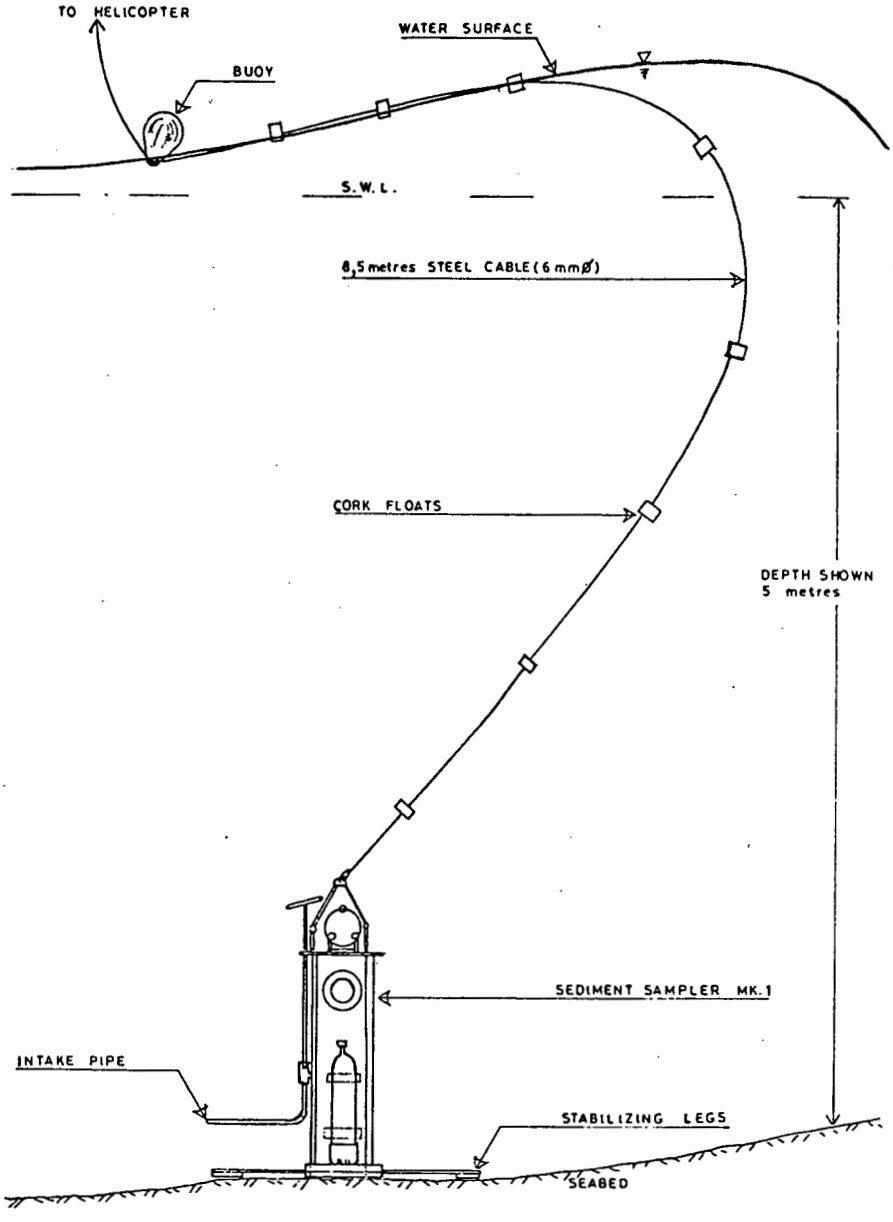

Figure 4.11 : Helicopter sampler on the sea bed.

Kilner (1976)

(i) A sledge-mounted sampler

A sledge can be towed out through the surf zone and back by means of a winch and cable system extending out to an offshore pile (Fig 4.6). At desired locations the sledge is stopped; samples are pumped into bags through an intake nozzle mounted on a boom, which is programmed for sampling at three predetermined depths. The bag contents are subsequently processed for sediment concentration (Coakley and Savile, 1979, p 176).

A problem is that drag forces acting on the cable are integrated along its length; therefore the system is likely to fail in locations where the longshore currents are significant.

(ii) Fixed samplers

Several sample intake nozzles may be situated at various depths on a fixed structure, as illustrated in Fig. 4.7. Suction hoses are attached to the nozzles, and litre samples are pumped (separately) from these points (Jensen and Sorenson, 1972, pp 1097-1104).

Another sampler of this type is described by Nielson (1984, p 52). In this case, samples are sucked into sampling jars by means of a simple pressure difference, between subsurface intake points, and the jars, which are connected to the surface (i.e. to atmospheric pressure) by a tube.

(iii) A pier operated sampler

Samples may be taken at any location adjacent to a pier using the apparatus illustrated in Fig 4.8; this tractor-mounted sampler is completely mobile. Samples of a 40 gallon capacity are obtained; after allowing sand to settle, excess water is decanted on site, leaving a manageable sample of wet sand, to be dried and weighed. (Fairchild, 1972, p 1070).

(iv) A helicopter-borne sampler

A sampler which is positioned in the desired location by a helicopter (Fig 4.9) has been developed at the University of Cape Town (Kilner, 1976, pp 2045-2059). The sampler operates as follows:

The sampler is transported by a helicopter to the desired location, where it is lowered to the sea bed (Figs. 4.10 and 4.11). Water inflow activates an air-driven centrifugal pump, which is powered by compressed air from a cylinder. About 100 litres of water is pumped through an inlet pipe, fixed at a predetermined elevation from the sea bed. The water is pumped through a meter, and through a nylon mesh filter which retains the sand, and back into the sea. After the sampling duration of a few minutes, the sampler is returned to shore; the compressed air cylinder is replaced, the sand sample retained in the filter is removed, and the volume of water sampled is read off from a meter. The dry mass of the sand, divided by the water volume (i.e. the meter reading) yields the concentration. This tech-nique has the advantage that a large quantity of water is sampled; this allows the measurement of very small concen-trations. In addition, the sampling duration, of about five minutes, ensures that short term fluctuations in sediment concentration (e.g. due to wave action) are averaged out.

Unfortunately, due to strain on the helicopter pilot, "not more than eight readings have been taken in one day." For this reason another sampler was developed, to avoid the use of a helicopter. This sampler is positioned in the nearshore zone by means of rope and an offshore anchor. However, the forces of longshore currents on the sampler and the rope were found to be excessive.

(b) Portable samplers

If waves breaking in the surf zone are less than about 2 m high, then portable samplers can be operated by swimmers. These samplers are generally simple and inexpensive.

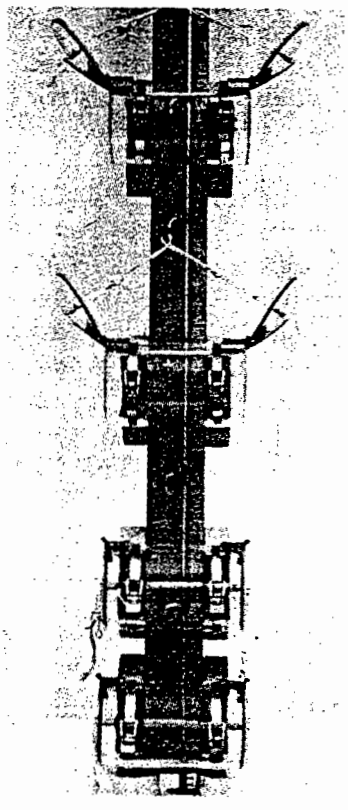

Figure 4.12 : Apparatus used to collect water samples in the surf zone. A 2 m-long pole supporting several 2 l. bottles is emplaced vertically in the surf zone. When thrust into the bed, a foot pad moves the trigger assembly up, simultaneously tripping each bottle. Top two bottles are rigged for sampling. Bottom bottles are in the tripped position.

Kana (1978)

(i) Jar samplers

Commercially available preserving jars, which are able to withstand a total internal vacuum, can be used for sampling. With a portable generator and a vacuum pump, the jars are vacuumised. Thereafter, they are opened at the desired location in the surf zone; a water sample replaces the vacuum in about two seconds (Kilner, 1976, p 2048).

This technique is simple and effective for concentrations of the order of thousands of ppm (parts per million) or more.

(ii) The "Kana" sampler

This portable sampler is useful for obtaining a vertical array of samples, virtually instantaneously (Kana, 1977, p 371). The sampler consists of several acrylic tubes mounted on a wooden pole (Fig 4.12). When this apparatus is thrust into the sand in the surf zone, the doors at the ends of all the tubes spring shut. The sediment in each sample is subsequently filtered out and weighed, to yield the concentration corresponding to the sample elevation above the sea bed. The apparatus is quick and easy to use, and allows the collection of many samples in a short time. Since samples are taken virtually instantaneously, concentration can be measured in different phases of wave motion (e.g. at the crest, or at the trough); this information assists in gaining an understanding of sediment processes, to develope theoretical relationships.

(c) Analysis

The following analysis technique is one of several which can be used to determine the longshore sediment tranport rate, from concentration data, as well as other data measured in the nearshore zone:

The cross-section of the surf zone may be determined from a measured beach profile (Sec. 4.3). The cross-section area may be divided into elements of area A_i, which correspond to measured concentrations C_i. Assuming that the seaward limit of littoral transport is at the breaker line, a formula for estimating the longshore sediment transport, Q , is (Kana, 1977, p 374):

$$Q = \frac{k_s}{n} \sum_{i=1}^{n} C_i . A_i . V_i \qquad (4.8)$$

where V_i = the current velocity corresponding to each area element A. In practice, an average velocity for the whole cross-section area can be used (the measurement of current velocity is dealt with in Chapter 3)

k_s = a conversion factor to yield Q in tonnes/day.

n = the number of elements of area, A (corresponding to the number of concentration measurements)

In this type of calculation, it is important to note that in order to obtain the total sediment transport rate, the suspended load concentration, and the bedload concentration must be obtained; often samplers do not sample both of these adequately (Kraus, 1987, p 141).

4.2.1.3 Bamboo-type samplers

One of the original sediment samplers is the bamboo sampler; this is a bamboo pole arranged vertically in the sea. The bamboo has openings in every alternate bamboo segment; these face different directions. Sand in suspension enters these openings and settles. Several samplers have been modelled on the bamboo instrument e.g. Basinski and Lewandowski (1974, p 1100), and Swart (1984) use modernised 'bamboo' samplers, made of perspex and PVC respectively. Sediment quantities trapped in the segments of the sampler indicate the relative rate of movement of suspended sediment (or the relative concentrations), with respect to height and direction. In addition, the sampler can be calibrated to relate the mass of trapped sediment to sediment concentration (Swart, 1984). This type of measurement is very simple, and inexpensive.

4.2.2 Sediment concentration sensors

The concentration of sediment suspended in water can be detected with various sensing devices. A unique feature of measurement with sensors is that a continuous record of concentration versus time can be obtained. This is extremely useful in gaining understanding of sediment transport processes (Brenninkmeyer, 1974, pp 812-827) to develop empirical relationships.

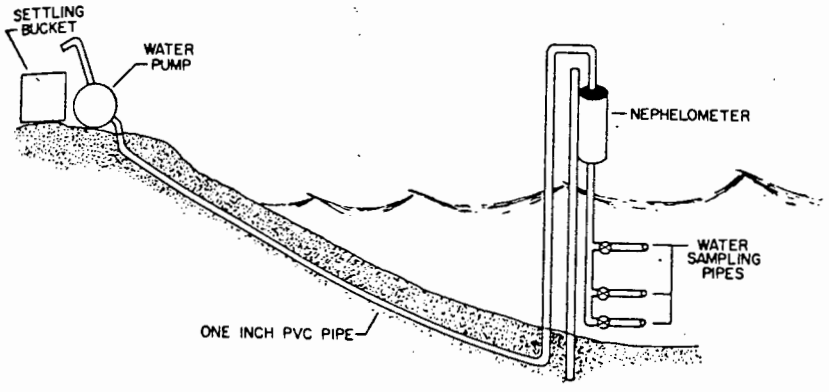

Figure 4.13 : The Nephelometer sampling system.

Thornton and Morris (1977)

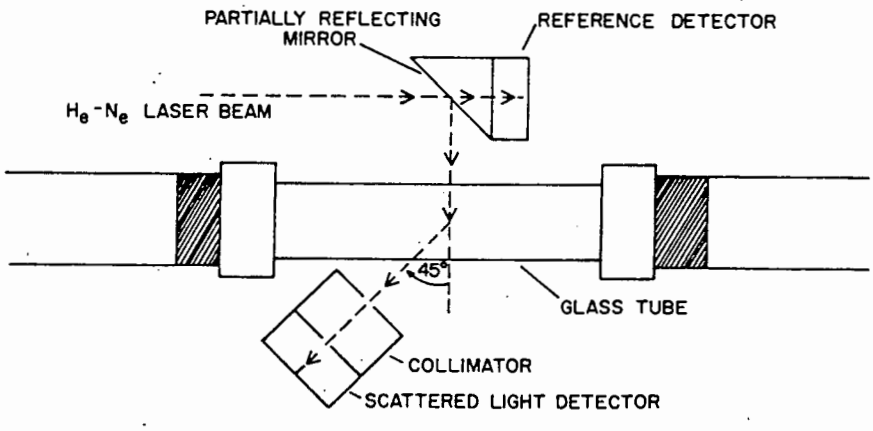

Figure 4.14 : The Nephelometer.

Thornton and Morris (1977)

4.2.2.1 Photoelectric devices

Suspended sediment in water can cause the attenuation and scattering of light. Either of these two properties can be measured and correlated to the concentration of the suspension.

(i) Light attenuation technique

The almometer is an example of a device which measures the sediment concentration by means of light attenuation. It consists of two metal poles embedded vertically in the sea floor. One pole holds a high intensity fluorescent lamp; the other holds a vertical series of photoelectric cells, at 1 cm intervals, from the sea bed to a height of 1,2 m. Water flows freely between the two poles; the concentration of sediment in the water affects the intensity of light received by each photocell, which thereby generates a recordable voltage. Thus, using a calibration, a continuous record of the sediment concentration (in grams/litre), at 1 cm height intervals , is measured. (Brenninkmeyer, 1974, p 812)

Unfortunately the attenuation of light intensity is affected by:

- the ambient light (which is affected by the cloud cover);
- the size and form of the particles in suspension;
- the amount of organic matter in suspension;
- the amount of air entrainment.

These factors therefore affect the accuracy of the device.

(ii) Light scattering technique

The amount of light scattered by suspended sediment is a function of the sediment concentration. Thornton and Morris (1977, p 658) describe an instrument (called a nephelometer) which measures the sediment concentration in this fashion:

The sampling system is illustrated in Fig 4.13; water is sampled from any one of three intake pipes; the water passes the nephelometer, which is illustrated in Fig 4.14. As shown in the figure, the source of light intensity is first detected by a reference photocell detector, which produces a voltage X.

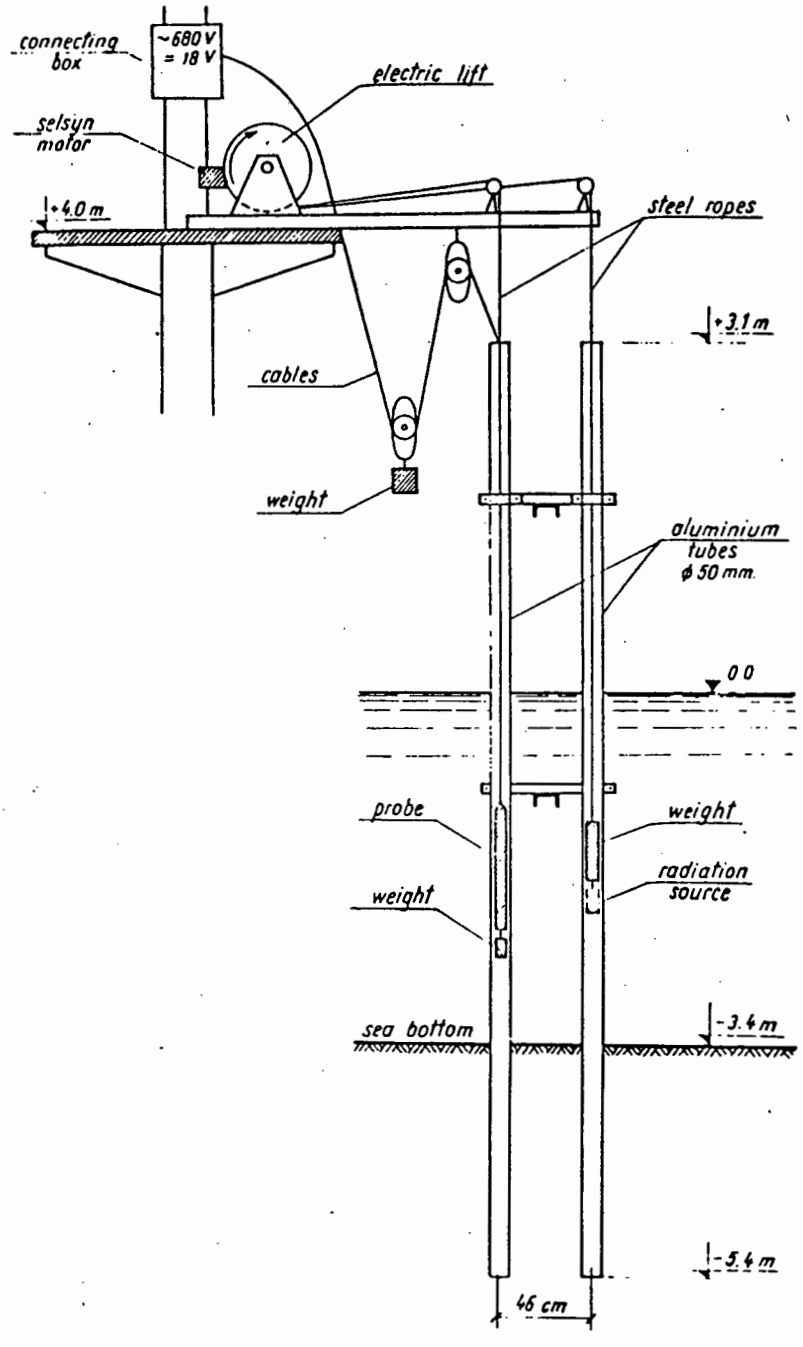

Figure 4.15 : The radiometric probe installation.

Basinski and Lewandowski (1974)

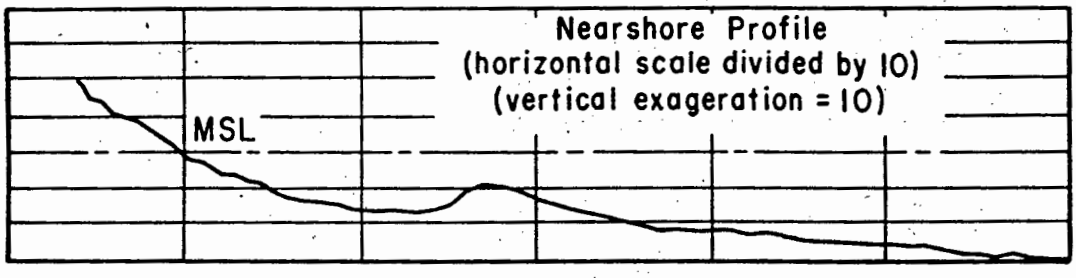

Figure 4.16 : Nearshore profile.

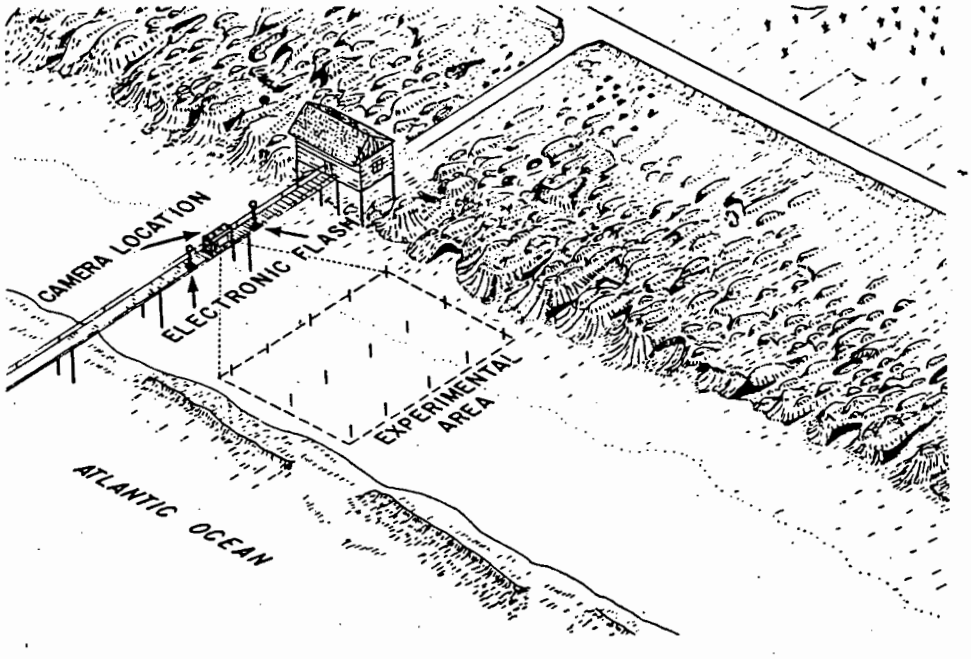

Figure 4.17 : Photographic arrangement to measure sand elevation.

Dolan (1967)

Light scattered at 45 degrees by sediment in the water is then detected by a second photocell, to produce a voltage Z. The ratio X/Z is then determined; this is related, through calibration, to the sediment concentration. The advantage of including the reference voltage, X, in the ratio, X/Z, is that fluctuations in the light source are compensated.

After passing the nephelometer, sediment samples can be taken, in a settling bucket (Fig 4.13). From the samples, the mean concentration for the sampling period can be obtained. This is facilitates an *in situ* calibration of the nephelometer (This useful, since calibration is normally difficult, due to unknown scattering characteristics)

4.2.2.2 Acoustic technigue

Wenzel (1974, pp 741-755) describes the development of a device which measures the absorption of ultrasound, at 0,6 m from a source, in the vertical plane. The measurement is related, by means of calibration, to the average sediment concentration for a 0,6 m layer. Thus, a time series of the sediment concentration is obtained.

4.2.2.3 Radiometric technique

The intensity of gamma radiation, at a small distance from a source in the sea, is attenuated due to absorbtion. This absorbtion varies with the concentration of the sediment in the water; therefore, by means of a calibration, the intensity of radiation is related to the concentration.

A radioactive isotope can be used as the source of radiation. Basinski and Lewandowski (1974, p 1098) use a Co^{60} source, and a scintillation counter 46 cm away, to record the gamma radiation intensity, continuously. This probe installation is illustrated in Fig 4.15. As shown, the radiation source and probe can be raised and lowered with an electric lift, in order to measure the sediment concentration at various depths.

4.3 NEARSHORE PROFILES

4.3.1 Introduction

A nearshore profile is a two-dimensional vertical section which shows the variation of elevation of the ground with distance, extending seawards from the beach to depths of about 10 m (Fig 4.16). They are usually measured perpendicular to the shoreline.

Nearshore profiles measured over successive time intervals may reveal sea bed elevation changes, which can be related to volumes of sediment gained or lost. This information, averaged over time, can reveal the rate of sediment transport, however errors occur because:

(i) sediment erosion, followed by an equal amount of sediment accretion, will not be detected ;
(ii) the accuracy of profile measurements is limited.

Nevertheless, qualitative measurements are feasible. For example, from several closely spaced nearshore profiles, a contour map of the nearshore zone can be constructed; by comparing successive maps of this type, the formation and movement of sandbars along the coastline can be studied (Zwamborn et al, 1972, p 93).

Nearshore profiles generally change seasonally. Therefore, for design purposes, envelopes of profiles occuring throughout at least a year are required,for:

(i) the design of shore protection structures, such as sea walls, and breakwaters. The bathymetry data is particularly important in determining whether a structure will be affected by unbroken, breaking or broken waves; this affects the forces impinging on the structure (Sec. 2.4.1.1) ;
(ii) pipeline design; it may be desirable to ensure that a pipeline remains buried beneath the sand surface in order to avoid forces due to wave action, particularly in the surf zone; the depth of pipeline burial necessary can be determined from profile data ;

(iii) the estimation of dredging quantities necessary for navigation channels.

This section deals with techniques of profile measurement,including direct surveying techniques, echo sounding, and other indirect techniques.

4.3.2 Direct surveying techniques

4.3.2.1 Survey stakes

Stakes can be driven firmly in the sand between the low water and the high water level, in a line perpendicular to the shoreline.

Measurements from the top of the stakes to the beach level yield the nearshore profile, provided that the elevation of the tops of stake is predetermined. (Alternatively, measurements of sand elevation at the stakes can be taken with conventional levelling techniques). This measurement is usually carried out at low tide, to the low water level.

The technique facilitates quick and easy measurement at successive intervals, to determine changes in sand elevation. If necessary, these measurements can be obtained in the surf zone by divers, however this can prove costly (Rukavina and Lewis, 1979, p 61). It is very accurate (± 10 mm); however it is practical only for a short length of coastline, and only in shallow water.

If several measurements are necessary, a automatic photographic technique can be used, since the sand elevation can be determined from oblique photographs of graduated stakes (Fig 4.17). Dolan (1967, pp. 77-80) describes such a system, in which frequent measurements are required for a study equating surf zone processes to short interval beach changes. However, the technique is restricted to the intertidal zone.

4.3.2.2 Conventional land surveying techniques

Conventional survey, using levelling techniques, can be used to measure nearshore profiles. However, it is difficult to manually hold the graduated survey staff in position in breakers over 1 m high (Seymour et al, 1978,

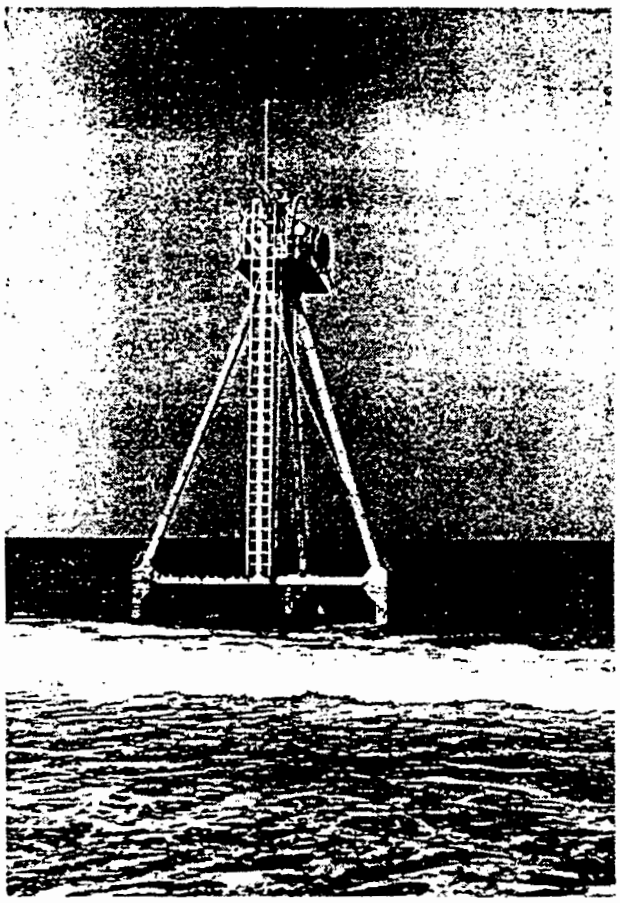

CERC's Coastal Research Amphibious Buggy (CRAB)

Figure 4.18 : The CRAB.

Gable and Wanetick (1984)

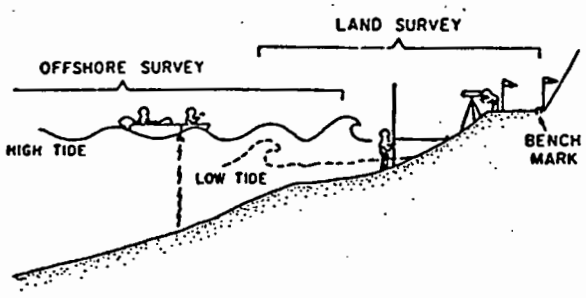

Figure 4.19 : Survey overlapping procedure.

Gable and Wanetick (1984)

p 1542), and in deep water; therefore various devices and techniques have been developed to overcome this problem, such as a survey sled, and an amphibious vehicle.

4.3.2.3 A survey sled

A sled with a high mast was developed by the CSIR, to substitute for the survey staff in the nearshore zone. The sled has a 3 x 3 m tabular base and a 9 m aluminium mast. It is towed out to sea by a ski-boat and winched to shore from the beach. Depth information and position can be obtained by surveying with two theodolites, taking readings simultaneously, and recording the horizontal and vertical angles to the top of the mast. This method yields satisfactory results for coastal design; however, it is time consuming.

4.3.2.4 The Coastal Research Amphibious Buggy (CRAB)

CERC has developed a vehicle for obtaining nearshore profiles. It is 10.6 m high and uses three hydraulically driven tyres on the legs of a tall tripod (Fig. 4.18). The vehicle, which can operate in depths up to 9 m, supports a prism cluster above water. An electronic instrument, the Zeiss Elta-2, is set up at a known elevation on the shore. It is aimed at the prism cluster; the distance to the CRAB, and the horizontal and vertical angles are measured automatically in a few seconds; a micro-processor then calculates the x,y and z co-ordinates of the position on the sea bed directly under CRAB, and stores them into memory. In addition, a direct readout of the co-ordinates allows the surveyor on shore to guide the CRAB operator along the desired course.

Advantages of the system are:

(i) Profiles can be measured from deep water and through the surf zone.

(ii) The ability to operate in high wind and strong longshore current conditions.

(iii) The technique requires a minimum of manpower.

(iv) The technique has a high accuracy of ± 5 cm.

(v) Profiles can be obtained quickly (in about 45 minutes).

Disadvantages are:

(i) CRAB may be caught on obstructions on the sea bottom e.g. debris or isolated rocks.

(ii) High initial expenses in CRAB construction and instrument purchase (although the long term cost is cheaper).

(iii) The size of CRAB, and cost of transportation, make it highly immobile.

(iv) Small bottom profile features are not always detected, due to a wide wheel base.

4.3.3 Boat Echo sounding techniques

Nearshore profiles can be obtained from measurements of depth with an echo sounder mounted on a boat; with highly manoeuverable ski-boats, this is possible in the surf zone, in water of a minimum depth of only 0,5 m depth. Echo sounding is the most common form of profile measurement.

4.3.3.1 Principle of operation

The echo sounder operates on the following principle: the time interval between the transmission of a sound pulse and the reception of the reflected echo from the bottom is measured; if the velocity of sound is known, the distance to the bottom can be simply calculated. A trace of depth versus time is produced. The position of the boat, corresponding to the depth measurement, is usually obtained by conventional survey methods from two shorebased stations.

4.3.3.2 Method

As mentioned above, the speed of sound must be known, in order to relate the time interval between transmission and echo, to the depth. The speed of sound is a function of temperature; therefore, from temperature measurements, it can be determined (from tables). Alternatively, direct calibration can be achieved in situ by lowering a bar to specific depths, and adjusting equipment to obtain a readout corresponding to those depths (Gable and Wanetick, 1984, p 1880).

In order to obtain a profile, the boat may align itself with two targets placed on the desired line perpendicular to the shoreline. The position of the boat may be periodically fixed by using two theodolites, and radio communications; one theodolite sights along the profile line and guides the boat; the other is situated further along the beach. At a pre-arranged signal the position of the boat is fixed (by the intersection technique) and the echo sounding trace is marked. Alternatively, automatic navigation systems can be used (Gable and Wanetick, 1984, p 1880).

If the technique is carried out at high tide, then profiles can be obtained close to the shore. In this fashion, echo sounding surveys can be overlapped with conventional land surveys taken at low tide, as shown in Fig. 4.19. This overlapping serves as a check.

The best result is obtained when the ski-boat travels shoreward at the same speed as the dominant waves; by remaining at the same position in a wave trough throughout the journey, the reference level of the echo sounder is kept as constant as possible. In addition, if the vessel speed is constant, then the time scale of the depth trace can easily be converted into a distance scale, without distortion.

4.3.3.3 Analysis

The result of a single profile survey is an echo sounder trace of depth versus time, with marks corresponding to position fixes. The distance between the marks on the time scale can be determined from the position co-ordinates; thus, the time scale is substituted by a distance scale, to yield a profile.

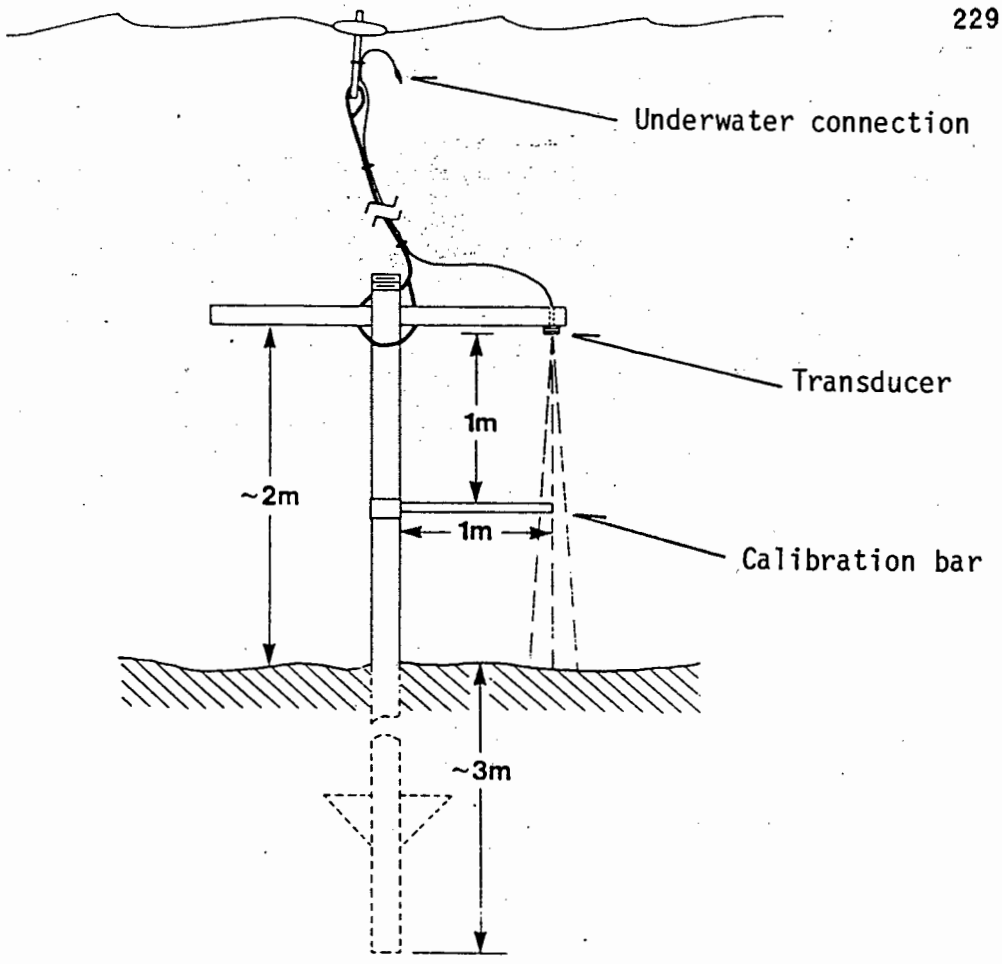

Figure 4.20 : FIXED TRANSDUCER SITE

after Rukavina and Lewis (1979)

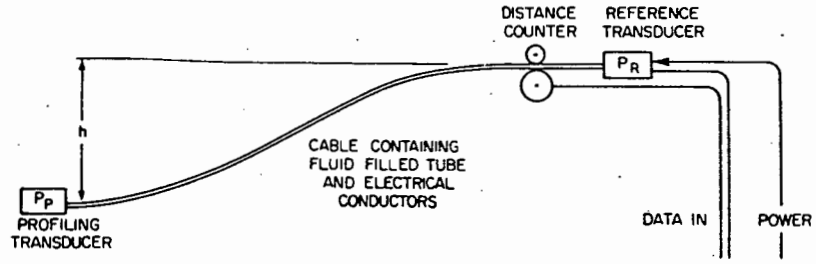

Figure 4.21 : The hydrostatic profiler.

The variance of the depth, due to the rise and fall of waves of different frequencies, affects the accuracy. A running-mean filter can be used to smooth the profile (i.e. reduce the variance) if the data is digital. This is achieved, for example, by averaging every consecutive 20 digital depth values (Gable and Wanetick, 1984, p 1884). Unfortunately small bottom features may be "smoothed out" by this technique. Alternatively, the variance can be reduced by simply averaging depth measurements over equal intervals (e.g. by averaging the depth values in every 5 m interval)

4.3.3.4 Accuracy

Echo sounding surveys have low precision (±10 to ±20 cm).(Rukavina and Lewis, 1979, p 61). This is even more so in high-energy surf zones (occurring on the South African coast), where an accuracy of only 0,5 m is possible (Zwamborn et al, 1972, p 93).

Accuracy can be checked by repeating measurements on a profile. In addition, the depth at a point can be checked using a leadline (a line, wire, or chain weighted at one end with a plummet; the line may have distance marked on it). Furthermore, overlap with conventional land surveying serves as a check on accuracy (Fig. 4.19).

In particular, uncertainties in the reference level occur, due to the fact that:

(i) tide measurements are often taken several kilometres away (and may not be representative of the site of measurement);
(ii) wave set-up and set-down effects (Kilner, 1988) cause variations in the sea level;
(iii) storm surge affects the water level.

4.3.3.5 Advantages of the technique

The technique is not limited by obstructions on the bottom such as debris or isolated rocks. In addition, profiles can be measured rapidly. However, it has the disadvantage that it is error-prone and less accurate than other techniques.

4.3.4 Other indirect techniques

4.3.4.1 A fixed echo-sounder

As discussed above, the accuracy of echo-sounding from the sea surface is adversely affected by the movement of the sea; the problem is eliminated by using echo-sounders at fixed positions. With several fixed echo-sounders spaced out along a perpendicular to the shoreline, a profile can be measured.

Rukavina and Lewis (1979, p 62) describe this type of system; an acoustic transducer is mounted on a T-frame which is embedded in the bottom sediment (Fig. 4.20). The transducer is connected to a cable and an underwater connection, which are connected to a surface buoy, as shown in the Fig. 4.20.

Measurements are obtained from a small craft; the underwater connection is retrieved at the buoy, and attached to a sounder-digitizer, to form a complete echo-sounding unit. A bar, fixed at a depth of 1 metre, facilitates in situ calibration. This is achieved by adjusting a calibration control, so that the delay of sound energy returning from the bar corresponds to one metre. The complete measuring operation takes less than 5 minutes per site and can be managed only in small wave heights (up to 0,5 m).

The technique is very accurate (± 1 cm). This system is durable, and has the potential for automatic operation, whereby results could be stored automatically.

4.3.4.2 Pressure-operated profiling instruments

Using the water level as a reference, the depth can be found by measuring the pressure head at the sea bed. This can be achieved with a pressure transducer mounted on a mobile sled, which traverses the surf zone. Coakley and Saville (1979, p 177) use the sled and cableway system described in Sec. 4.2.1.2.(a) for this purpose.

The disadvantage of this measurement is that the fluctuating water surface makes accurate depth measurement difficult, in spite of filtering techniques (such as those described in Sec. 4.3.3.3). In addition, the uncertainties in using the sea level as a reference level can cause erroneous depth measurement (as outlined in Sec. 4.3.3.4). These problems can be solved by using an another type of instrument which measures hydrostatic pressure only: two pressure sensors or transducers are connected by a fluid-filled tube (Fig. 4.22); the reference transducer is placed at a known elevation on shore; and the profiling transducer is fixed to a sled which traverses the surf zone. The difference in pressure between the two transducers is due to the pressure head of water: i.e.:

$$P_P - P_R = \rho g h \qquad (4.9)$$

where P_P = the pressure at the profiling transducer
P_R = the pressure at the reference transducer
ρ = the density of the fluid
g = the gravitational acceleration
h = the difference in elevation between the two sensors

rearranging, to determine the desired elevation difference:

$$h = \frac{P_P - P_R}{\rho g}$$

The distance of the profiling transducer offshore is determined by measuring the extension of a cable (which contains the fluid-filled tube), by a system which counts the rotations of a wheel which is held tightly against the cable.

A small boat is used to transport the sled (and the connected cable) to the desired distance offshore, on a perpendicular to the coast line, which is marked with flags, to allow the boat to align itself. The sled is then winched to shore with its cable, by a winch mounted on a four-wheel drive truck; every 5 m pressure measurements are taken. Pressure measurements with the transducers must be corrected for temperature effects; therefore the temperature is measured at both transducers with thermistors.

Some advantages of the system are:

(i) It is highly mobile and can be operated by two people.

(ii) The distance measurement is accurate to ± 1 m, and the elevation is accurate to ± 5 cm.

(iii) Unlike many other techniques, small relief features (e.g. small sand bars) are detected.

However, the system has some disadvantages:

(i) The longshore position of the sled depends on the accuracy of deployment with the small boat; this is dependent on the surf conditions and the skill of the boat driver;

(ii) The profiler sled and cable can get caught up on obstructions;

(iii) The quality of data is affected by high waves and strong currents, which disturb the cable excessively;

(iv) The surveying time for a profile is long (a minimum of two hours).

4.3.4.3 A slope-and-distance measuring vehicle

A tractor, with bulldozer-type treads, can be guided underwater by signals transmitted through a cable attached to a shore station. The horizontal position and vertical elevation of the tractor are obtained from instruments mounted on it: a two-axis vertical gyroscope, a compass, and an odometer for each tractor tread. Every second, these instruments measure the pitch angle, ϕ, the compass direction, θ, and the distance, ℓ, respectively, and transmit the data to shore via the cable. The change in co-ordinates Δx, Δy and Δz, for every second, can be obtained from:

$$\Delta x = \ell \cos\theta \cos\phi$$
$$\Delta y = \ell \cos\theta \sin\phi$$
$$\Delta z = \ell \sin\phi$$

By summing these increments over progressively longer intervals, the co-ordinates of the nearshore profile, corresponding to the path of the tractor, are obtained. This information can be used periodically in situ, to aid navigation.

This technique is found to be as accurate as conventional levelling techniques (Seymour et al, 1978, p 1549).

4.4 CONCLUSION

The following significant conclusions are drawn from this chapter:

(i) Fluorescent tracer techniques are best suited to beach sediment transport studies; radioactive tracers are more suitable for deep water sediment transport studies.

(ii) Quantitative analysis methods have been devised for tracer studies, but an investigation of the shortcomings of the method reveals that these are unreliable. Nevertheless, tracer studies produce useful qualitative information.

(iii) There are many types of sensors and samplers for sediment measurements at a point, but most of these suffer from problems associated with the dynamic surf zone; a device which overcomes most of these problems, and directly measures the sediment transport rate at a point, is the streamer trap.

(iv) There are several effective techniques of measuring the nearshore profile, however all are limited by high surf conditions. In addition, nearshore profiles yield only limited information about sediment transport.

BIBLIOGRAPHY : CHAPTER 4

Acree, E.H., Brashear, H.R. and Case, F.N. 1970 "Underwater Survey System for Radionuclide-tagged Sediment Tracing", Proc. of the 12th Coastal Eng. Conf., Vol.2, pp.821-830.

Basinski, T. and Lewandowski, A. 1974 "Field Investigations of Suspended Sediment", Proc. of the 14th Coastal Eng. Conf., Vol.2, pp.1096-1108.

Boon, J.D. 1969 "Quantitative Analysis of Beach Sand Movement, Virginia Beach, Virginia", Sedimentology, Vol.13, pp.85-103.

Bratteland, E. and Bruun, P. 1974 "Tracer Tests in the Middle North Sea", Proc. of the 14th Coastal Eng. Conf., Vol.2, pp.978-990

Brenninkmeyer, B.M. 1974 "Mode and Period of Sand Transport in the Surf Zone", Proc. of the 14th Coastal Eng. Conf., Vol.2, pp.812-827.

Coakley, J.P. and Savile, H. 1979 "Field Measurments of Littoral Transport Transport Processes in Lake Ontario", Proc Workshop on Instrumentation for Currents and Sediments in the Nearshore Zone, October 1979, pp.176-182.

Coastal Engineering Research Centre (CERC), U.S. Army 1977 Shore Protection Manual, Washington, D.C., U.S. Government Printing Office, 1977.

Crickmore, M.J., Waters, C.B. and Price, W.A. 1972 "Measurement of Offshore Shingle Movement", Proc. of the 13th Coastal Eng. Conf., Vol.2, pp.1005-1026.

Davison, A. 1984 "A Pre-dredging Sand Mobility Study using a Radioisotope Tracer", Proc. of the 19th Coastal Eng. Conf., Vol.2, pp.2063-2075.

Dolan, R. 1967 "Photographic Beach Measurements", Sedimentology, Vol.8, No.1, pp.77-80.

Ecker, R.M. Sustar, J.F. and 1976 "Tracing Estuarine Sediments by Neutron Neutron Activation", Proc. of the Harvey 19th Coastal Eng. Conf., Vol 2, pp 2009-2029.

Fairchild	1972	"Longshore Transport of Suspended Sediment", Proc. of the 13th Coastal Eng. Conf., Vol.2, pp.1069-1088.
Gable, C.G. and Wanetick, J.R.	1984	"Survey Techniques used to Measure Nearshore Profiles", Proc. of the 19th Coastal Eng. Conf., Vol 2, pp.1879-1895.
Greenwood, B., Hale, P.B. and Mittler, P.R.	1979	"Sediment Flux Determination in the Nearshore Zone : Prototype Measurements, Proc Workshop on Instrumentation for Currents and Sediments in the Nearshore Zone, October 1979, pp.99-119.
Heathershaw, A.D. and Carr, A.P.	1977	"Measurements of Sediment Transport Rates using Radioactive Tracers", Coastal Sediments '77, November 1977, pp.399-416.
Horler, V.	1989	"Pollution Trapped by the Waves", Weekend Argus, August 12, 1989, p.22.
Inman, D.L., Zampol, J.A., White, T.E., Walton Waldorf B., Hanes, D.M. and Kastens, K.A.	1980	"Field Measurements of Sand Motion in the Surf Zone", Proc. of the 17th Coastal Eng. Conf., Vol.2, pp 1215-1234.
Kadib, Abdel-Latif A.	1972	"Rate of Sediment Motion using Fluorescent Tracer", Proc. of the 13th Coastal Eng. Conf., Vol.2, pp.985-1004.
Kana, T.W.	1978	"Surf Zone Measurement of Suspended Sediment" Proc of the 16th Coastal Eng. Conf., Vol 2, pp.1725-1743.
Kana, T.W.	1977	"Suspended Sediment Transport at Price Inlet, S.C.", Coastal Sediments '77, November 1977, pp.366-382.
Kilner, F.A.	1988	Sediment Movement and Measurement, Lecture notes, Dept of Civil Engineering, UCT.
Kilner, F.A.	1976	"Measurement of Suspended Sediment in the Surf Zone", Proc. of the 15th Coastal Eng. Conf., Vol.2, pp.2045-2059.
Knoth, J.S. and Nummedal, D.	1977	"Longshore Sediment Transport using Fluorescent Tracer", Coastal Sediments '77, November 1977, pp.383-398.

Kraus, N.C. 1987 "Application of Portable Traps for Obtaining Point Measurements of Sediment Transport Rates in the Surf Zone", Journal of Coastal Research, Vol.3, No.2, pp.139-152.

Jensen, J.K. and Sorenson, T. 1972 "Measurement of Sediment Suspension in in Combinations of Waves and Currents", Proc. of the 13th Coastal Eng. Conf., p 1097

Jensen, J.K. and Sorenson, T. 1979 Measurement of Sediment Suspension in Combinations of Waves and Currents", Proc. of the 13th Coastal Eng. Conf., Vol.2, pp.1097-1104.

Nielson, P. 1984 "Field Measurements of Time-averaged Suspended Sediment Concentrations under Waves", Coastal Engineering, Vol.8, pp.51-72.

Readshaw, J.S. 1979 "Analysis of Fluorescent Tracer Sand", Proc. Workshop on Instrumentation for Currents and Sediments in the Nearshore Zone, October 1979, pp.141-160.

Rohde, H. 1976 "Sand Movement Investigations by means of Radioactive Tracers in a Hydraulic Model and in the Field", Proc. of the 15th Coastal Eng. Conf., Vol.2, pp.2027-2044.

Rukavina, N.A. and Lewis, E.O. 1979 "A Fixed Transducer System for Recording Nearshore Profile Change", Proc. Workshop on Instrumentation for Currents and Sediments in the Nearshore Zone, November 1979, pp.61-74.

Russel, R.C.H. 1960 "The Use of Fluorescent Tracers for the Measurement of Littoral Drift", Proc. of the 7th Coastal Eng. Conf., pp.418-443.

Sato, S. 1962 "Sand Movement at Fukue Coast in Atsumi Bay, Japan, and its Observation by Radioactive Glass Sand", Coastal Eng. in Japan, Vol.5, pp.81-92.

Seymour, R.J., A.L. and Bothman, D.P. 1978 "Tracked Vehicle for Continuous Higgins, Nearshore Profiles", Proc. of the 16th Coastal Eng. Conf., Vol 2, pp.1542-1554.

Svasek, J.N. and Engel, H.	1960	"Use of a Radioactive Tracer for the Measurement of Sediment Transport in the Netherlands", Proc. of the 7th Coastal Eng. Conf., pp.445-454.
Thornton, E.B. and Morris, W.D.	1977	"Suspended Sediments measured within the Surf Zone", Coastal Sediments 77, November, pp.655-668.
Thornton, E.B.	1970	"Variation of Longshore Current across the Surf Zone", Proc. of the 12th Coastal Eng. Conf., Vol.1, pp.291-308.
Tola, F., Caillot, A., Courtois, G., P., Hoslin, R., Massais, J., Quesney, M. and Sauzay, G.	1984	"Study of the Evolution of Dredged Material Discharges by Means of Gourlez, Radioactive Tracers", Proc. of the 19th Coastal Eng. Conf., Vol 2, pp 2042-2061.
Waters, C.B.	1987	"Field Sediment Studies - Some Recent Developments and Techniques", Bulletin of the Permanent International Association of Navigation Congresses, No.56, pp.29-38.
Wenzel, D.	1974	"Measuring Sand Discharge near the Sea-bottom", Proc. of the 14th Coastal Eng. Conf., Vol.2, pp.741-755.
Wright, P., Cross, J.S. and Webber, N.B.	1978	"Shingle Tracing by a New Technique", Proc. of the 16th Coastal Eng. Conf., Vol.2, pp.1705-1714.
Zwamborn, J.A., Russel, K.S. and Nicholson, J.	1972	"Coastal Engineering Measurements". Proc. of the 13th Coastal Eng. Conf., Vol.1, pp.75-94.

APPENDIX 1

```
*************************************************************************
*    DEPT. OF CIVIL ENGINEERING                                         *
*    UNIVERSITY OF CAPE TOWN                                            *
*                                                                       *
*    This program calculates the wave energy spectrum by obtaining the  *
*    Fourier transform of the autocorrelation estimate.                 *
*                                                                       *
*************************************************************************

*-----------------------------------------------------------------------
*    Dimension statement. Open data files 'datafile.1' for data input and
*    'plotdata.1' for storage of the spectral density values u(i) and
*    corresponding frequencies f(i). Set variables. Sampling interval, h, is
*    set to 0.5 seconds here.
*-----------------------------------------------------------------------

          dimension x(4000),c(1200),v(1200),u(1200),f(1200)
          open (unit=8,file='datafile.1')
          open (unit=4,file='plotdata.1')
          pi = 3.1415926536
          h = 0.5

*-----------------------------------------------------------------------
*   Read from 'datafile.1': n, the number of data points, and m, the maximum
*   lag number. Thereafter read in the digitised wave record, wherein the
    mean
*   water level is at approximately 10 m.
*-----------------------------------------------------------------------

          read (8,*) n,m
          read (8,5) (x(i),i=1,n)
5         format(20f4.2)

*-----------------------------------------------------------------------
*   Find the mean water level and set it to zero. Water surface elevations,
*   x(i) are referenced to this zero mean water level.
*-----------------------------------------------------------------------

          sumx = 0
          do 6 i=1,n
6         sumx = sumx + x(i)
          do 7 i=1,n
7         x(i) = x(i) - sumx/n

*-----------------------------------------------------------------------
*   Calculate the estimate of autocorrelation for maximum lag numbers 0 to m
*-----------------------------------------------------------------------

          do 50 ir = 0,m
          nr = n - ir
          sumxx = 0
          nr = n - ir
          do 40 i = 1,nr
40        sumxx = sumxx + x(i) * x(i+ir)
50        c(ir+1) = sumxx/nr
```

```
*-----------------------------------------------------------------------
*   Calculate values of the raw energy spectrum, v(i), for harmonic numbers
*   (ir) from 0 to m.
*-----------------------------------------------------------------------

          mm = m - 1
          do 60 ir = 0,m
          sumc = 0
          do 65 i=1,mm
65        sumc = sumc + c(i+1) * cos(i*ir*pi/m)
60        v(ir+1)=(c(1)+2.*sumc + c(m+1) * cos(ir*pi))*2.*h

*-----------------------------------------------------------------------
*   The area under the spectrum = the autocorrelation at zero lag. This is
*   tested here.
*-----------------------------------------------------------------------

          sumv = 0.
          do 67 j = 2 , m
67        sumv = sumv + v(j)
          sumchk = (1/(2 * h * m)) * (0.5 * v(1) + sumv + 0.5 * v(m))
          print *,c(1)
          print *,sumchk

*-----------------------------------------------------------------------
*   Apply the Hanning spectral window to the raw energy spectrum estimates,
*   v(i), to reduce leakage. Smoothed values, u(i), result.
*-----------------------------------------------------------------------
*
          u(1) = (v(1) + v(2)) / 2.
          do 70 i = 2,m
          u(i) = v(i-1)/4 + v(i+1)/4 + v(i)/2
70        continue
          u(m+1) = (v(m) + v(m+1)) / 2.

*-----------------------------------------------------------------------
*   Calculate the Nyquist frequency, which is the highest frequency plotted.
*   Store this value together with the maximum lag number, m, which
indicates
*   the number of spectral estimates, u(i), to plot.
*-----------------------------------------------------------------------

          fmax = 1/(2*h)
          write (4,*) m,fmax

*-----------------------------------------------------------------------
*   Round off the spectral estimates, u(i), for plotting convenience. Find
*   the peak spectral estimate (for plotting purposes) and find the index,
*    npeak, of the corresponding frequency.
*-----------------------------------------------------------------------

          xmax = 0.0
          do 75 i = 1,m
          round1 = u(i) * 1000.
          round2 = anint(round1)
          round3 = round2/1000.
          if( u(i).gt.xmax) go to 71
```

```
          go to 75
71        xmax = u(i)
          npeak = i
75        write (4,*) round3

*-------------------------------------------------------------------------
*   Calculate and store the frequency values, f(i), corresponding to the
*   spectral estimates.
*-------------------------------------------------------------------------

          fc=1/(2*h)
          do 80 i=1,m
          k = i-1
          f(i) = (k * fc)/m
          write (4,*) f(i)
80        continue

*-------------------------------------------------------------------------
*   Calculate and store the significant wave height, hmo, and the peak
period,
*   tpeak
*-------------------------------------------------------------------------
          sum = 0.0
          do 90 i=1,m+1
          sum = sum + u(i)
90        continue
          firstm = sum * fc/m
          hmo = 4.0 * sqrt(firstm)
          print * , 'hmo =',hmo
          write (4,*) hmo
          tpeak =1/((npeak * fc)/m)
          write (4,*) xmax,tpeak
          stop
          end
```

APPENDIX 2

```
*******************************************************************************
*   DEPT. OF CIVIL ENGINEERING
*
*   UNIVERSITY OF CAPE TOWN            G.G.SMITH
*
*
*
*   This program calculates estimates of the energy spectrum by means of
*
*   the fast Fourier transform
*
*
*
*******************************************************************************

*-------------------------------------------------------------------------------
*   Dimension statement. Open data files: 'datafile.1' for data input and
*   'plotdata.1' for storage of the smoothed spectral density values u(i)
and
*   corresponding frequencies f(i). Set parameters.
*-------------------------------------------------------------------------------

          dimension x(2048)
          dimension smth(210)
          real f(210)
          complex a(2048),u,w,t
          open (unit=8,file='datafile.1')
          open (unit=4,file='plotdata.1')
          pi = 3.1415926536
          m=10
          n=1024

*-------------------------------------------------------------------------------
*   Read from 'datafile.1', the sampling interval, h. Then read in the
*   digitised wave record, wherein the mean water level is at approximately
*   10 m.
*-------------------------------------------------------------------------------

          read (8,*) h
          print *, n,h
          delf = 1 / (float(n)*h)
          d5 = 5. * delf
          print *,delf,d5
          read(8,5) (x(i),i=1,n)
5         format(20f4.2)

*-------------------------------------------------------------------------------
*   Find the mean water level and set it to zero. Water surface elevations,
*   x(i), are referenced to this zero mean water level.
*-------------------------------------------------------------------------------
```

```
          xsum = 0.
          do 6 i = 1,n
6         xsum = xsum + x(i)
          xmean = xsum / n
          print * ,xmean
          do 10 i=1,n
          x(i) = x(i) - xmean
10        continue

*-------------------------------------------------------------------------
*   Apply the Cosine Taper window to the one tenth of the data at the begin-
*   ning and at the end.
*-------------------------------------------------------------------------

          tr = n * h
          n10 = ifix(0.1 * n)
          n910 = ifix(0.9 * n)
          do 15 i = 1,n10
          tn = i * h
          fu = 0.5 * (1.-cos(10.*pi*tn/tr))
          x(i) = x(i) * fu
15        continue
          do 16 i = n910,n
          tn = i * h
          fu = 0.5 * (1.-cos(10.*pi*tn/tr))
          x(i) = x(i) * fu
16        continue

*-------------------------------------------------------------------------
*   Fast Fourier Transform. Reference:  program "WAVES", C.S.I.R., South
*   Africa
*-------------------------------------------------------------------------

          do 20 i=1,n
          a(i) = cmplx(x(i),0.0)
20        print *,a(i)
          nv2 = n/2
          nm1 = n-1
          j = 1

          do 50 i = 1,nm1
          if (i .ge. j) go to 30
          t = a(j)
          a(j) = a (i)
          a(i) = t
30        k = nv2
40        if(k .ge. j) go to 50
          j = j-k
          k = k/2
          go to 40
```

```
50        j = j+k
          do 70 l =1,m
          le = 2 ** l
          le1 = le/2
          u = (1.,0.)
          ang = pi/le1
          w = cmplx(cos(ang),-sin(ang))
          do 70 j=1,le1
          do 60 i=j,n,le
          ip = i+le1
          t = a(ip) * u
          a(ip) = a(i) - t
60        a(i) = a(i) + t
          u = u * w
70        continue
          z2 = 2./n
          do 80 i = 1,n

*-------------------------------------------------------------------------
*   Calculate values of the raw energy spectrum, x(i), for index i = 1 to n
*   Also divide by 0.9 to compensate for cosine taper window.
*-------------------------------------------------------------------------

          x(i) = z2 * cabs (a(i))
          print *, x(i)
80        continue
          do 90 i = 1,n
          x(i) = (x(i) * x(i) / 2.)/0.9
          print *, x(i)
90        continue

*-------------------------------------------------------------------------
*   Smooth 4 adjacent values of the raw energy spectrum, x(i), to obtain
*   smth(i). Round of these values, and store them. Find the value of peak
*   energy density, xmax, and the corresponding frequency, fpeak.
*-------------------------------------------------------------------------

          delf = 1. / (float(n)*h)
          d4 = 4.0 * delf
          ismh2 = n/(2*4)
          fmax = ((4*ismh2)-1.5) * delf
          write (4,*) ismh2,fmax
          xmax = 0.0
          do 100 i=1,ismh2
          k = i * 4 + 1
          smth(i) = (x(k) + x(k-1) + x(k-2) + x(k-3))/d4
          f(i) = (4*i-1.5) * delf
          round1 = smth(i) * 1000
          round2 = anint(round1)
          round3 = round2/1000
          if (smth(i).gt.xmax) go to 95
          go to 100
95        xmax = smth(i)
          fpeak = f(i)
100       write (4,*) round3
```

```
*-----------------------------------------------------------------------
*   Store the frequency values corresponding to the spectral densities
    stored,
*   f(i). Find the significant wave height, hmo, and store it.
*-----------------------------------------------------------------------
          do 110 i=1,ismh2
          write (4,*) f(i)
110       continue
          sum = 0.0
          do 120 i=1,ismh2
          sum = sum + smth(i)
120       continue
          firstm = sum * d4
          print * ,'moment =',firstm
          hmo = 4.0 * sqrt(firstm)
          print * ,'hmo =',hmo
          tpeak = 1/fpeak
          write (4,*) hmo,xmax,tpeak
          print * ,'peak period =',tpeak
          close (unit=4)
          stop
          end
```

APPENDIX 3 : THE FOURIER TRANSFORM OF AN EVEN FUNCTION

According to Bracewell (1965), any function x(t) can be split into even and odd parts, i.e.

$$x(t) = E(t) + O(t) \quad , \tag{1}$$

where E(t) is an even function, and
O(t) is an odd function.

The Fourier transform of this is :

$$F(f) = \int_{-\infty}^{+\infty} x(t)\, e^{-j\,2\pi ft}\, dt$$

$$= \int_{-\infty}^{+\infty} \Big(E(t) + O(t)\Big)\Big(\cos 2\pi tf - j \sin 2\pi ft\Big) dt \quad . \tag{2}$$

Now considering the following:

1. the product of the two even functions is an even function ;
2. the product of two odd functions is an even function ;
3. the product of an even function with an odd function is an odd function ;
4. $\int_{-\infty}^{+\infty} E(x)dx = 2\int_{0}^{+\infty} E(x)\, dx$;
5. $\int_{-\infty}^{+\infty} O(x)dx = 0$
6. cosines are even functions and sines are odd functions.

Applying the above properties, equation (2) becomes :

$$F(f) = 2\int_{0}^{\infty} E(t)\cos(2\pi ft)dt - 2j\int_{0}^{\infty} O(t)\sin(2\pi ft)dt \quad .$$

If $x(t)$ is an even (and real) function, then :

$$x(t) = E(t)$$

and $$O(t) = 0 \ .$$

Therefore

$$F(f) = 2 \int_{0}^{+\infty} x(t) \cos (2\pi ft) dt \ .$$

This is the case with the autocorrelation function (where $x(t) = R(\tau)$ in the above).

APPENDIX 4: Typical Input Data for Spectral Analysis

```
1058108111081124111310731019 980 977 986 970 926 898 920 955 960 943 933 948
 958 956 966 985101010371057107710981108110410971087104l 954 850 795 804 837
 886 949 993101710491086110310951081105610261026 997 99710121007 961 901 858 842
 844 875 937 998104110791113112511201087104910211021 987 949 921 899 895 908 932
 949 955 950 974101810601112116211651120105810001000 965 963 973 966 949 911 890
 875 841 822 850 919 994105410891106111211071083104910461050102410241024 979 965 977
 977 935 870 847 849 845 855 904 977102910531083113211711155109310291003101710171017
1014 972 953 98610251013 933 859 827 823 831 851 890 948100210341050107911051105 
1126113311241113109510541001 964 946 955 98710011007 979 910 848 823 843 874
 899 941100410571084108110591050104210321038106611021114109610591014 959 914
 888 859 856 870 867 853 862 911 967102110651111114811581127108310551047103910391039
1000 962 951 965 974 936 899 902 936 952 956 947 935 934 960 970 965 9721008
106311091122110810811033 974 958 999102910271012 996 973 933 905 901 893 885
 897 930 964 982 990 988 993101810391046107411181146114511121074104210191019 989
 947 908 876 834 799 814 854 899 943 984102110511055105610801118114811691173
11461083 994 898 839 801 774 804 871 931 972 995101710501076109010881073103710371037
 996 989101310301016 980 950 932 903 883 892 892 886 917 963 988101310441049
1047105910701087109810861064105410281028 991 952 932 924 913 914 931 929 916 941
 98510111006 971 959 968100010311047107511181155114911051044 987 935 886 841
 828 837 855 874 883 906 929 961101110661111114611571165118111641094100510251025
 871 867 889 921 933 939 947 947 964101010591074104510081008 974 917 881 862 848
 857 946103510801097113311651165114711161063101010101010 971 946 921 898 876 839 819
 836 863
```

This wave data was recorded with a waverider buoy offshore from Slangkop on the Cape Peninsula, South Africa, at 08h00 hours on 25 October 1988.

The following points are relevant:

1. The values are in units of cm; they are corrected to units of m during input, by means of a format statement in the spectral analysis computer programs of appendix 1 and 2.

2. The average value of this data is approximately 910 cm; this represents the mean water level.

3. Since the spectral analysis of the wave record requires a mean water level of 0, this must be corrected - this is achieved in the spectral analysis computer programs of appendix 1 and 2.

APPENDIX 5

COURSES ATTENDED AND EXAMINATIONS COMPLETED
TOWARDS THE REQUIREMENTS OF THE
M.Sc (Eng.) DEGREE

Course Code	Title	Credit Rating
CIV 509F	Structural Loading	3
CIV 516F	Coastal Hydraulics	5
CIV 536F	Coastal Engineering Practice	5
AMA 363F	Numerical Analysis	3
SEA 200F	Physical Oceanography	4
	Dissertation	
CIV 500Z	"A critical review of measurement techniques in coastal hydraulics:	20
		40
	Credit requirements for the degree	40

UNIVERSITY OF CAPE TOWN

DEPARTMENT OF CIVIL ENGINEERING

CIV 509F - STRUCTURAL LOADING

Time : 3 hours Date: 18 June 1988

Answers should be concise, but must show understanding of the subject. Approximately equal marks will be awarded for each question.

1.(a) List the probability functions best suited to each of the following loads : dead, imposed office floor, wind, flood, earthquake.

(b) Explain how the overall probability of failure of a structural element is derived from the probability functions of load effect and of resistance.

2.(a) For imposed loading on floors of buildings, describe the relationship between load intensity and floor area.

(b) For multi-storey buildings, describe the relationship between floor loading magnitude and the number of storeys.

3. List the most likely combinations of loads on a steel railway bridge according to BS 5400. Discuss the relevance of each combination.

4. Explain the need for specifying three different types of road bridge traffic loadings : NA, NB and NC in TMH 7, instead of just one single loading system.

5. Describe the procedure for obtaining the displacement spectrum for a flexible tower from records of the wind gust velocity.

6. Describe one example of a restraint action responsible for structural failure, that was discussed in the seminars in this course - other than the one that you might have submitted as a project.

7. Discuss how each relevant property of a structural system can contribute to minimize earthquake damage.

8. Discuss the major factors influencing the pressure distribution inside a tall circular grain silo filled from the top and emptied at the bottom.

9. Sliding formwork is used to construct a tall concrete chimney. Discuss all the factors likely to affect the loading on the formwork and on the concrete just below the formwork.

UNIVERSITY OF CAPE TOWN

DEPARTMENT OF CIVIL ENGINEERING

CIV 509F - STRUCTURAL LOADING

Time : 3 hours

Date: 18 June 1988

Answers should be concise, but must show understanding of the subject. Approximately equal marks will be awarded for each question.

1.(a) List the probability functions best suited to each of the following loads : dead, imposed office floor, wind, flood, earthquake.

(b) Explain how the overall probability of failure of a structural element is derived from the probability functions of load effect and of resistance.

2.(a) For imposed loading on floors of buildings, describe the relationship between load intensity and floor area.

(b) For multi-storey buildings, describe the relationship between floor loading magnitude and the number of storeys.

3. List the most likely combinations of loads on a steel railway bridge according to BS 5400. Discuss the relevance of each combination.

4. Explain the need for specifying three different types of road bridge traffic loadings : NA, NB and NC in TMH 7, instead of just one single loading system.

5. Describe the procedure for obtaining the displacement spectrum for a flexible tower from records of the wind gust velocity.

6. Describe one example of a restraint action responsible for structural failure, that was discussed in the seminars in this course - other than the one that you might have submitted as a project.

7. Discuss how each relevant property of a structural system can contribute to minimize earthquake damage.

8. Discuss the major factors influencing the pressure distribution inside a tall circular grain silo filled from the top and emptied at the bottom.

9. Sliding formwork is used to construct a tall concrete chimney. Discuss all the factors likely to affect the loading on the formwork and on the concrete just below the formwork.

[4 PAGES]

UNIVERSITY OF CAPE TOWN

DEPARTMENT OF CIVIL ENGINEERING

M.Sc. in CIVIL ENGINEERING

CIV 516F : COASTAL HYDRAULICS

UNIVERSITY EXAMINATION : JULY 1988

ALL question may be attempted. TIME: 4 hours +

(OPEN BOOK EXAMINATION)

Constants

Sea water density = 1025 kg/m^3

Sea water weight = 10 kN/m^3

QUESTION 1

The standard alignment chart is attached and a new blank line has been inserted at the bottom of the page. This line is to be used for determining values of U_{max}, the maximum horizontal orbital velocity at the water surface, according to the Airy theory. If $U^*_{max} = \frac{U_{max}}{\pi H/T}$ is to be the dimensionless form of the variable on this line, mark off the correct positions of the $\overset{*}{U}_{max}$ values given in the following list.

$\overset{*}{U}_{max}$ = 1,01 2 6
1,10 3
1,40 4

Note that H is the local wave height throughout. Suggest a small change in the line label which would permit the scale to be used for maximum horizontal surface acceleration values. Use the new line to solve the following problem.

A swell of 10 second period with a deep water wave height H_o = 1,59 m approaches a beach with the wave crests parallel to the shore. Plot the value of u_{max} at the water surface for the following selected water depths.

65 m ; 34,4 m ; 15,9 m ; 6,8 m ; 2,86 m .

Use these calculations to estimate the water depth when the U_{max} value first reaches 1,5 m/s and check that the wave has not broken.

QUESTION 2

A sea platform consists of a square concrete slab positioned horizontally on four cylindrical vertical piles, each placed at a corner, the slab side being parallel to the local wave crest. The pile diameter is 1 m, the total pile height above sea bed is 6,4 m, and the slab dimensions are sides of 5 m with a thickness of 200 mm. The local wave characteristics are height 2 m, length 100 m, and period 12 s, the local water depth being 8 m.

(a) Considering the central 1 m high slice of any pile, calculate the horizontal forces per metre due to velocity and acceleration and by plotting these throughout one wave period or otherwise, identify the maximum force and the timing of its occurrence. Check that the velocity and acceleration distributions over the height of the pile are reasonably constant and thus estimate the total force on one pile.

Take C_D = 1,2 and C_M = 2,0 .

QUESTION 2 (continued)

(b) Estimate the maximum vertical force on the slab due to wave action.

Take $C_D = 1,0$ and $C_M = 1,8$.

QUESTION 3

In a study of wave penetration into a bay, the 10 m, 9 m and 8 m sea bed contours are approximated by three straight lines with contained angles of 12 degrees as shown on the attached page. An incoming wave orthogonal, 10 second period, impinges on the 10 m contour at an angle of 50 degrees as shown. With the usual approximations obtain by trial the angle at whch the emerging orthogonal cuts the 8 m contour. Take the step lines on the 9,5 m and 8,5 m lines.

[1 diagram attached]

QUESTION 4

A train of waves is approaching a shore line, of regular bed slope 1 in 80, the wave crests being essentially parallel to the shore. Two aerial still photographs are taken 8 seconds apart. On the first photograph, two successive crests are identified as being 247 m apart. A comparison between the two photographs indicates that the trough between the two crests has advanced forward a distance of 153 m. Further, stereo photographs taken at the same time as the first exposure indicate that the wave height in the vicinity of the trough is close to 3 m. Retrace the history of this wave as it came in from deep water, and further trace the progress of the wave as it moves towards the beach, including the following calculations:

(i) the wave length and celerity in deep water ;

(ii) the wave length, celerity and height for water depths at 20 m intervals from deep to the 10 m depth, and at 1 m intervals inshore from this to a depth of 3 m ;

(iii) the depth of water in which the wave breaks, the type of breaker, and the wave height at breaking. Set up and down may be ignored ;

(iv) the energy flow in W/m in two water depths outside the breakers, and one depth in the breaker zone (depths at your choice) and compare.

QUESTION 5

(a) A storm at sea generates waves with a period range of 6 to 12 seconds. The resulting swell travels towards a harbour 400 km away. Estimate the time interval between the arrival of the shortest and longest waves, assuming deep water throughout.

(b) A refraction diagram is constructed for a bay, and the spacing between a particular pair of adjacent orthogonals doubles in travelling from deep water to the 10 m depth zone, the wave period being 7 seconds. Estimate the percentage change in wave height occurring between these two zones on the assumption that no breaking waves are present in-between.

(c) In a zero damage design calculation for the armour protection of a rubble mound breakwater, 3 tonne and 5 tonne dolosse are specified for the trunk and head respectively, the slope of the breakwater face being cot α = 2. Estimate the block masses and block heights if tetrapods had been used in the same design. If the design wave height was 3 m, and a storm causes damage of the order 20 - 30 per cent to the tetrapod scheme, estimate the storm wave height (concrete density 2245 kg/m^3).

(d) An incoming swell has crests parallel to a straight beach with a deep water wave height of 2 m. Estimate the horizontal force (per metre along the beach) acting on the beach inside the refraction zone, due to the dynamic action of the waves.

(e) In an area where the sea bed is horizontal, and the water depth is 3 m, a wave has a period of 7 s, a wave length of 38 m, and a wave height of 1,5 m. Estimate the drift velocity at bed level, and indicate the direction. Compare this velocity with the maximum orbital velocity at the same level, and indicate the influence on bed drift of a strong onshore wind.

(f) A coastal model is to be constructed to explore wave action in a sea area 1 km offshore by 2 km along shore. The laboratory area available is 20 m wide and of considerable length. Suggest a linear scale suitable for this and calculate the wave period of the model paddles to duplicate a 12 second wave in nature. Discuss which of the following characteristics are accurately modelled in the laboratory:

(i) wave refraction pattern ;
(ii) wave heights before breaking ;
(iii) wave heights after breaking ;
(iv) settlement of fine sands.

* * * * * * * * *

Name: .....

QUESTION 1

Briefly explain, in words and by means of annotated sketches, the meaning of the following terms:

1.1 Cope level [2]

1.2 Pendant fender [2]

1.3 Tidal prism [2]

1.4 Seiche [2]

1.5 Clinometer [2]

1.6 Show on a sketch plan of Hout Bay where you would expect to observe the effects of wave diffraction and refraction. Clearly indicate the physical cause of each effect and the form of the wave orthogonals and crests. [2]

1.7 Explain, by means of a sketch, the basic physical elements of airborne (single channel) linescan apparatus that could be used for remote sensing of the ground. [2]

1.8 Explain by means of a sketch how a dredger may be positioned using sextant resection. [2]

1.9 Explain the principle of subtense ranging using a sextant. Indicate the practical distance limit.

[2]

1.10 Explain by means of a sketch the principle of echo sounding for seabed profiling.

[2]

1.11 Give a sketch of the components and the arrangement that is used for tide recording at Granger Bay.

[2]

1.12 Explain the term "tidal residual". What is the cause of tidal residuals?

(2)

1.13 Explain the principle of the "Wave rider" accelerometer buoy. [2]

1.14 Show by means of simple sketches how field measurements of the following may be graphically presented in reports :

wind speed and direction [2]

Radioactive tracers [2]

Beach profiles [2]

1.15(a) Give a typical section of a rubble mound breakwater (annotate). [2]

1.15(b) Show the sequence of how this would be constructed in an exposed situation. [2]

1.16 Comment very briefly (<u>with a simple sketch</u>) on the adequacy or inadequacy of the following :

position of the slipway at Granger Bay [2]

boat "access" situation at harbour entrance in Hout Bay [2]

boat "access" situation at Kalk Bay harbour entrance [2]

a boat ramp at 1:6 [2]

a boat ramp at 1:15 [2]

1.17 Explain what you would look for in an aerial photograph of the coast to discern the direction of littoral drift. [2]

Total for SECTION 1 = 48 marks.

SECTION 2 - OPEN BOOK

2.1 Assuming that you are a Consulting Engineer specialising in coastal matters, reporting to the local authority responsible for the coast, write advisory notes to the responsible Committee on the following :

(a) It is September and the beach has steepened and eroded sufficiently for an adjacent parking area to appear to be in danger of being totally eroded.

Outline your proposed method of investigation, your preliminary advice as to what the Council should instruct you or Contractors to do, what alternatives measures are likely to be appropriate after completing the investigation. Give a staged breakdown of costs with time/construction expense justification. Assume the total beach length is 1 km and that the situation is as occurs at Fish Hoek.

[15]

(b) It is proposed that the harbour at Granger Bay be improved. Write a memorandum to the responsible Committee outlining the problems that occur at present and the approach you would take to improve the situation. Provide an approximate cost for the investigation and the development of a new construction plan. Give a breakdown of the work required. (Give sketch plans as needed).

[15]

(c) Describe the present situation and outline the approach you would take to investigate the cause of the tilt on the breakwater at Hermanus. Indicate two possible alternative causes, and how you would remedy the situation for each case. (In a sketch show the type of construction).

[10]

(d) Briefly explain how you would determine the directions of nett littoral drift and how you would estimate the littoral drift quantity at Hout Bay beach.

[10]

(e) Hout Bay harbour is to be extended to provide for an additional 500 floating berths for small craft. Present a breakwater and mooring layout, and show in plan details of boat ramps, harbour control and other infrastructure requirements that should be considered at a preliminary stage. State all assumptions.

[60]

Total for SECTION 2 = 110 marks

UNIVERSITY OF CAPE TOWN
UNIVERSITY EXAMINATION : JUNE 1988

APPLIED MATHEMATICS AMA 300W, 301W

PAPER 2 : AMA 363F

Numerical Analysis

Time : 2hr 30 min

Answer ALL questions

Full marks = 100
Marks available = 105

Hand held battery powered calculators may be used

---

1. a) Give two iterative forms which could be used to solve a square root problem.

(2)

b) Using a Taylor series expansion derive the Newton-Raphson method for the iterative solution of nonlinear equations.

(5)

c) State the definition of "order of iteration" and show that the Newton-Raphson method is a second order method.

(3)

d) State the condition which the iterative form must satisfy for a scheme to be convergent. With the aid of diagrams show the conditions which lead to (i) oscillating convergence and (ii) monotonic divergence.

(5)

e) Solve $e^x - 3x = 0$ using the Newton-Raphson method.

(5)

[20]

2. a) Derive the Newton forward difference formula (below) for a polynomial approximation of a function $y(x)$ through a set of evenly spaced data points

$$y(x) \approx P_n(x) = y_o + \Delta y_o s + \frac{\Delta^2 y}{2!} s(s-1) + \ldots$$

$$+ \frac{\Delta^n y_o}{n!} s(s-1)(s-2)(s-3) \ldots (s-n+1) .$$

where $s = (x-x_o)/h$, h is the interval between data point and Δ is the forward difference operator.

What is the most significant difference between an interpolation of this type and a least squares approximation to a function?

(10)

b) In the attached difference table one of the data points has an error in it. It is suspected that this error arose by obtaining the data at an incorrect value of x ; find out the value of x at which the data was collected.

First complete the table, once the error has been found indicate the corrected values. Detach the page with the difference table on it and hand it in with your answer book.

(10)

[20]

University of Cape Town, University Examination, June 1988
AMA300W, 301W Paper 2: AMA 363F, Numerical Analysis (continued)

Difference table for question 2(b)

Detach and hand in with your answer book.

NAME : .....

x	y	Δy	$\Delta^2 y$	$\Delta^3 y$	$\Delta^4 y$	etc
-2.5	15.50					
		6.50				
-2.0	22.00		-2.75			
		3.75				
-1.5	25.75		-2.00			
		1.75				
-1.0	27.50		-1.25			
		0.50				
-0.5	28.00		-0.50			
		0.00				
0.0	28.00		0.25			
		0.25				
0.5	28.25		0.50			
		0.75				
1.0	29.00		2.75			
		3.50				
1.5	32.50		2.00			
		5.50				
2.0	38.00		3.25			
		8.75				
2.5	46.75					

University of Cape Town, University Examination, June 1988
AMA300W, 301W Paper 2: AMA 363F, Numerical Analysis (continued)

3. a) The general form for a Numerical integration or Quadrature rule is that the error $\int_a^b f(x)\,dx - \sum_{i=1}^{n} w_i f(x_i)$ at a given point is proportional to the step length. Why doesn't reducing the step size always result in an improvement in solutions computed with this method? (5)

c) The trapezoidal rule and Simpsons rule are of this type. What is the maximum order of $f(x)$ which can be integrated exactly using each of these rules and what is the minimum number of points required to achieve this in each case? For n point Gaussian quadrature what is the maximum order of $f(x)$ which is integrated exactly? How many points must be used to integrate exactly a 4th order function?

d) Use 5 point Gaussian quadrature to obtain an approximation to $\int_{+1}^{3} e^{x^2}\,dx$ (7)

b) Derive Simpson's rule from Stirling's formula (5)

c) Solve $y'' = 8x^2y' + 3xy - 4x^2$ $y(0) = 0$, $y'(0) = 0.5$ using an Euler predictor and a trapezoidal corrector. Write down the expressions for both the predictor and the corrector. Show that the method may be considered an explicit method when only one application of the predictor is made. Rewriting the method in the form generally used for Runge-Kutta formulae. [0,2] (7)

5. a) Solve the boundary problem $y'' = 2y' - 3x^{-1}$ (3)
where δ is the central difference operator $\delta f_o = f(\tfrac{1}{2}) - f(-\tfrac{1}{2})$
$\mu\delta$ is the averaging operator $\mu\delta^n f_o = \frac{1}{2}(\delta^n f(\tfrac{1}{2}) + \delta^n f(-\tfrac{1}{2}))$
using a finite difference scheme with 3 interior mesh points. Use the following central difference approximations (7)

c) Use Chebyshev polynomials $T_n(x)$ to economise a 5 term Maclaurin expansion of e^x (below) to only 4 terms.

$$e^x = 1 + x + \frac{x^2}{2!} + \frac{x^3}{3!} + \frac{x^4}{4!}$$

$$y'(x_i) = \frac{y_{i+1} - y_{i-1}}{2h} \qquad y''(x_i) = \frac{y_{i+1} - 2y_i + y_{i-1}}{h^2}$$

Calculate the maximum error on the interval $[-1,1]$ before and after economization.

$$T_0(x) = 1 \quad T_1(x) = x \quad T_{n+1}(x) = 2x\,T_n(x) - T_{n-1}(x)$$ (6)

to obtain the largest eigenvalue λ and its corresponding (7)
for the eigenvalue problem using an iterative method. [21]

4. a) Classify the following differential equations for the purpose of applying numerical methods to solve them.

i) $y'' = xe^x y' + y^2$

ii) $x^3y''' + ye^x = 0$

iii) $\dot{y} = (t+e^t)y + e^t$ $y(0) =$ (6)

order partial differential equations. (3)
ple class of problem. (9)

Question 4, continued/...

Table

Abscissae and Weight Coefficients of the Gaussian Quadrature Formula

$$\int_{-1}^{1} f(x)\,dx = \sum_{j=1}^{n} H_j f(a_j),$$

$\pm a$	H
$n = 1$	
0	2·00000 00000 00000
$n = 2$	
0·57735 02691 89626	1·00000 00000 00000
$n = 3$	
0·77459 66692 41483	0·55555 55555 55556
0·00000 00000 00000	0·88888 88888 88889
$n = 4$	
0·86113 63115 94053	0·34785 48451 37454
0·33998 10435 84856	0·65214 51548 62546
$n = 5$	
0·90617 98459 38664	0·23692 68850 56189
0·53846 93101 05683	0·47862 86704 99366
0·00000 00000 00000	0·56888 88888 88889
$n = 6$	
0·93246 95142 03152	0·17132 44923 79170
0·66120 93864 66265	0·36076 15730 48139
0·23861 91860 83197	0·46791 39345 72691
$n = 7$	
0·94910 79123 42759	0·12948 49661 68870
0·74153 11855 99394	0·27970 53914 89277
0·40584 51513 77397	0·38183 00505 05119
0·00000 00000 00000	0·41795 91836 73469
$n = 8$	
0·96028 98564 97536	0·10122 85362 90376
0·79666 64774 13627	0·22238 10344 53374
0·52553 24099 16329	0·31370 66458 77887
0·18343 46424 95650	0·36268 37833 78362
$n = 9$	
0·96816 02395 07626	0·08127 43883 61574
0·83603 11073 26636	0·18064 81606 94857
0·61337 14327 00590	0·26061 06964 02935
0·32425 34234 03809	0·31234 70770 40003
0·00000 00000 00000	0·33023 93550 01260
$n = 10$	
0·97390 65285 17172	0·06667 13443 08688
0·86506 33666 88985	0·14945 13491 50581
0·67940 95682 99024	0·21908 63625 15982
0·43339 53941 29247	0·26926 67193 09996
0·14887 43389 81631	0·29552 42247 14753

UNIVERSITY OF CAPE TOWN - JUNE EXAMINATION 1988

OCEANOGRAPHY SEA 200F

TIME: 3 HOURS TOTAL MARKS: 150

Answer ALL questions in SECTION A
Answer ONE question from SECTION B and THREE questions from SECTION C

SECTION A

Answer ALL questions in this section

1. Sketch the oxygen distribution in the deep ocean (4 km deep), at mid-latitude. (2)
2. What variables does the seawater density depend on? (2)
3. Define the "potential temperature". When should this be used in place of the "in situ" temperature? (2)
4. Is the ocean well stratified in the vertical? (2)
5. Give a labelled t,s diagram for the Atlantic ocean at 35^{o} S. (2)
6. Define "sigma-t" and the "standard ocean". (2)
7. Explain how a CTD works and what it measures. (2)
8. What is the "solar constant"? (2)
9. What is Group velocity and how is it related to the phase velocity of "deep water" waves? (2)
10. What is a "tsunami"? (2)
11. Define the terms "geopotential" and "dynamic metre". (2)
12. When does the diurnal inequality of the tide vanish? (2)
13. Sketch and describe the main elements of a Kelvin wave. (2)
14. Describe the terms "amphidromic point", "co-range lines". (2)
15. Give a simple definition of Salinity. (2)

TOTAL (30)

SECTION B

Answer EITHER OF the following questions:

(a) Describe with the aid of suitable diagrams, the characteristics of the major ocean current systems and the major bathymetric features around southern Africa. Include details of current speeds and surface temperatures. (30)

OR

(b) Write an essay on the phenomenon of El Nino - Southern Oscillation (ENSO) in the Pacific Ocean. (30)

SECTION C

ANSWER ANY THREE FULL QUESTIONS

(A) Discuss the main elements of the heat budget in the atmosphere and ocean, and give an indication of the relative importance of the terms in the heat budget equation.

Using the concept that a windstress in the y direction causes an Ekman flux or transport in the upper ocean in the x direction, describe how it is possible to set up an anticyclonic gyre in the South Atlantic ocean. (Hint: let y be positive north, and x positive west) (30)

(B) Discuss the method of dynamic sections to obtain the baroclinic, geostrophic velocity structure in the vertical in the Agulhas current. How can these relative velocities be converted into absolute currents?

If the surface slope on the current is 1 m in 100 km, up away from the coast, calculate the barotropic current speed and direction at 30^{o} S. (Use g=10 m s^{-2}, $f=2\Omega\sin(\theta)$, $\Omega = 7.29\ 10^{-5}\ s^{-1}$) (30)

(C) The dispersion of surface wind waves in the ocean is given by

$$\sigma^2 = gk \tanh(kd),$$

where $\sigma = 2\pi f = 2\pi/T$ is the radian frequency and
$k = 2\pi/L$ is the wave number, g = 10 ms^{-2}, d is depth.

Discuss the terms "deep water" and "shallow water" waves, and derive the phase velocities in these cases. What is the "deep water" wavelength of waves with a period of 15 s? What is the phase speed of these waves in 5m deep water?

Given that the approximate average power of the waves off the Cape coast is 40 Kw per metre of wave crest, calculate how many kilometres of wave crest must be harnessed by a wave absorbing device which is 50% efficient at extracting energy from the waves, to equal the power from a Power station producing 2 000 Mega watts. (30)

(D) Write short notes on:
The Phillips-Miles theories of wind wave generation,
South African tides,
Waves entering shoaling water,
Different types of breaking waves,
Fronts and convergences. (30)